UNIVERSITY OF CALIFORNIA
RIVERSIDE

A Characterization of Quiescent Behavior and Profiling of the Brain Transcriptome During Larval Development of the Holometabolous Insect, *Manduca sexta*

A Dissertation submitted in partial satisfaction
of the requirements for the degree of

Doctor of Philosophy

in

Neuroscience

by

Dyan MacWilliam

June 2011

Dissertation Committee:
Dr. Michael E. Adams, Chairperson
Dr. Anandasankar Ray
Dr. Scott N. Currie

The Dissertation of Dyan MacWilliam is approved:

_____

_____

_____

Committee Chairperson

University of California, Riverside

Acknowledgements

I am grateful to Dr. Michael Adams for providing resources and financing necessary for the carrying out of this project and for supporting my graduate studies at UCR. Other contributors are here acknowledged: Transcriptome sequencing was performed by the wonderful team at Illumina-FastTrack Sequencing Services (Hayward, CA). Dr. Peter Arensburger contributed to the analysis of the Illumina RNA-seq data. Jason Higa designed many of the primers used for qPCR, and also provided his invaluable assistance in the rearing of the *Manduca sexta* colony. I would also like to acknowledge Rob Hice and Dr. Anand Ray for their intellectual contributions to both the design and carrying out of the Illumina sequencing project, and Dr. Crystal Pontrello for her advice and consultation on the manuscript.

Dedication

I would like to thank my advisor Dr. Michael Adams for going far beyond the call of duty both in the support of this project and in the facilitation of my progress towards a degree. I would also like to thank Dr. Scott Currie, and Dr. Anand Ray for taking the time to serve on my committee, and for their valuable guidance. Thank you to Dr. Curras-Collazo and Dr. Dave Eastmond for serving on my qualifying exam committee. Special thanks should go out to Dr. Eastmond for the confidence he showed in my abilities that led to a much appreciated teaching opportunity.

Many individuals have contributed both intellectually and personally to my progress here at UCR. Included among them are Dr. Chris Banks, Leslie Hasegawa, Jason Higa, Rob Hice, Dr. Glenn Hicks, Dr. Do-Hyoung Kim, Sonali Deshpande, Dr. Dusan Zitnan, Dr. Glenn Stanley, Dr. Todd Fiacco, Dr. Ed Korzus, Amy Sage, Perla Fabelo, Jenny Donovan, and the MacWilliam and Smith families. I should also thank the thousands of undergraduates from whom I have learned so much over the years. I owe very much, both personally and professionally to Mark Van Oene, and to my cherished friends, Dr. Mary Nolan, and Dr. Chris Riegle.

Last but certainly not least, I would like to thank Dr. Crystal Pontrello, who has never failed to support me, both intellectually and emotionally throughout a graduate school experience that could sometimes be described as rather strange and rocky. Thank you Crystal, for your talent, grace and humor. I am very lucky to have you in my life.

ABSTRACT OF THE DISSERTION

A Characterization of Quiescent Behavior and Profiling of the Brain Transcriptome During Larval Development of the Holometabolous Insect, *Manduca sexta*

by

Dyan MacWilliam

Doctor of Philosophy, Graduate Program in Neuroscience
University of California, Riverside, June 2011
Dr. Michael E. Adams, Chairperson

The holometabolous insect *Manduca sexta* has served as one of the primary model systems for the study of the neuroendocrine regulation of the insect molt. It has long been observed that during the molting period prior to cuticle shedding during its larval-larval stage transitions, *M. sexta* displays an extended period of quiescent behavior. This behavior has been called the "molt-sleep", and has been described anecdotally as a non-moving, non-feeding state; but it has never been characterized. We observed that molting larvae respond to gentle handling and noxious stimuli with behavior resembling that observed for inter-molt larvae, and hypothesized that the quiescent behavior of larvae is similar to the sleep-like behavior observed for many adult insects, and for molting *C. elegans*. We used time-lapse digital recordings to profile the rest-activity patterns of *M. sexta* across several larval stages, and found that larval quiescent behavior shows developmental rhythms that are reproducible both across individuals and across larval stages. Quiescent behavior is reversible both during the inter-molt and molting periods.

Once aroused, molting larvae can locomote at rates comparable to inter-molt larvae. Larvae that are quiescent also have increased response latencies following exposure to a noxious stimulus, resembling (in both stages) the sleep-like states of other invertebrates. However, there are differences between inter-molt and molting quiescence, in that both feeding and quiescence seem to be homeostatically regulated during the inter-molt, but not the molting period. We propose that molting larvae engage in an adaptive quiescent state that promotes energy conservation while retaining the ability to respond to a changing environment. The correlation between the timing of molt-sleep onset with the estimated peak of the steroid molting hormones suggests that molting hormones might act directly or indirectly on the nervous system to bring about changes in gene expression that alter general arousal state. To investigate possible gene products that might be involved in the induction and maintenance of the molt-sleep, we used Illumina RNA-seq to profile the brain transcriptome at several developmental time points both during and surrounding the onset of the molt-sleep. This study is the first to profile the transcriptome of any *M. sexta* nervous tissue. We developed a novel method for identifying transcripts, which entailed the mapping of translated reads onto the proteome of *Bombyx mori*, the most closely related species for which a genome is known. 10,664 unique proteins were mapped by Illumina reads during at least one stage of development. Between 2.8%-7.8% of all genes were differentially-expressed in the brain at a given stage when compared to mid-inter-molt reference levels. Cluster and enrichment analysis reveals a dominance of processes related to trachea cuticle synthesis and degradation. In addition, many of the differentially-expressed transcripts encode neuropeptides, enzymes

involved in the synthesis of small neurotransmitters, ligand-gated ion channels, G-protein-coupled receptors, ion channels and other products associated with neural activity. Possible roles for these gene products in the modulation of larval arousal-state are described.

Table of Contents

List of Figures

Chapter 1: Introduction

Hormones target both the central nervous system (CNS) and peripheral tissues to bring about a coordination of animal behavior and physiology. Imagine an animal without such coordination. In mammals, sex hormones act peripherally to ready the body for the bearing of offspring, but male advances are unlikely to be successful without a concomitant central activation of mating behaviors. The detection of a predatorial threat might engage neural circuitry underlying escape behavior, but without peripheral changes such as those that promote cardiovascular, respiratory and muscle function, the animal would surely be eaten. The hormonal coordination of physiology and behavior is observed for many processes essential to animal fitness, including (to name a few) feeding, drinking, mating, caring for offspring, fighting, and development (Pfaff et al 2004).

The coordination of behavior with physiology is common across animal phyla, and "simpler" invertebrate organisms have served as model systems to study basic principles. The insect *molt* has proved useful as a model process. During the non-reproductive post-embryonic stages, insects feed and increase in size. Because insects have an exoskeleton (cuticle), the multiple larval or nymphal feeding stages that lead eventually to the attainment of the final adult size are separated by a molting process, which consists of the synthesis of a new larger cuticle, and the digestion and shedding of the old confining one. The success of the molting process depends on a tight coordination between physiology (cuticle synthesis/digestion) and behavior (cuticle

shedding). Insect molting is regulated by the neuroendocrine system (Nijhout 1994). Studies of the steroid molting hormones led to the first evidence (in any animal) that steroid hormones can act directly on the genome to alter gene expression (Ashburner 1973; 1974; Clever 1964; Clever & Karlson 1960). The effects of molting hormones on gene expression are both tissue and stage-specific (Li & White 2003; Thummel 1990). During larval development, the rise and fall of molting hormones act on cells of the epidermis to program successive bouts of gene expression necessary for the synthesis of the new cuticle, and the break-down and digestion of the old cuticle (Riddiford 1981). In addition, molting hormones also target the central nervous system and endocrine glands to program ecdysis behavior—the complex centrally generated stereotyped behavioral sequence that leads to the shedding of undigested cuticle at the end of the molt (Zitnan et al 2007). As failure to perform ecdysis results in the confinement of the animal in the old cuticle and prevention of further growth, this behavioral sequence is essential to the fitness and survival of developing insects.

The *absence* of motor behavior at the appropriate time is also an important component of an animal's behavioral repertoire. The activation of one motor behavior is often accompanied by the suppression of another, conflicting behavior (Kandel 1976). Behavioral *quiescence*—defined here as periods of inactivity during which there is an absence of any motor behavior in terms of an animal's interaction with or movement through the environment—also contributes to animal fitness. For example, brief periods of inactivity accompanied by vigilance can help a predator to catch its prey (or if expressed by the latter, may allow the prey to go unnoticed). Resting states that follow

periods of intense motor activity can be important for the recovery of neuromuscular function. Sleep-like states, which are often more prolonged periods of quiescence, differ from rest and quiet vigilance in that they are accompanied by a reduced sensory responsiveness (Campbell & Tobler 1984). The possible function(s) of such a state is (are) under debate, but the importance of sleep is suggested by the universality of its presence across animal phyla, and also by observations that prolonged periods of sleep-deprivation can lead to cognitive and motor impairments, and even death (Rechtschaffen et al 1989; Shaw et al 2002; Tobler 2000).

Adult *Drosophila melanogaster* has quickly become an important invertebrate model system for the study of sleep-like and other arousal states following the finding that the fly's period of consolidated quiescence which occurs during the nighttime exhibits sleep-like properties (Hendricks et al 2000a; Shaw et al 2000). Although the search for molecular correlates of insect sleep-states has largely focused on factors generated in the central nervous system, a recent study has demonstrated that the insect steroid molting hormones play a sleep-promoting role in the adult fly (Ishimoto & Kitamoto 2010). The presence of sleep-like states during the larval stages of insects has not been investigated, but in the developing nematode *C. elegans*, consolidated periods of behavioral quiescence that occur during the molting periods between its larval stages were found to exhibit sleep-like properties (Raizen et al 2008). As the endocrine factors that (presumably) regulate the nematode molt have yet to be identified, an understanding of the coordination of this quiescent state in relation to the molting process awaits further clarification.

It has long been observed that larvae of the holometabolous insect, *Manduca sexta* (*M. sexta*), exhibit prolonged periods of consolidated quiescence around the time of its molting periods. This quiescent period immediately precedes ecdysis behavior, and its duration can last for over a day during the molt to the 5th and final larval stage (Reinecke et al 1980). While rearing a *M. sexta* colony, I noticed that molting larvae respond to gentle handling with behaviors resembling those observed for inter-molt larvae, and that these behaviors far outlasted the application of the stimulus. In addition, the molting larvae responded to noxious stimuli with robust defensive strikes, followed by a period of feeding-stage-like behaviors. The rapid-reversibility of molting-quiescence suggested a resemblance to the sleep-like states found in molting *C. elegans* and adult flies. *M. sexta* has long served as one of the primary model systems for the study of the neuroendocrine regulation of molting and metamorphosis, and both the identity of endocrine factors that regulate the molt and levels of these hormones relative to major developmental events have been carefully studied in this species. As the reported timing of this quiescent behavior places the onset of the molt-sleep sometime during or following the surge of molting hormone, it is likely that in addition to their peripheral actions on the epidermis and central actions that program the ecdysis behavior, molting hormones may also effect the nervous system—either directly or indirectly—to cause the onset and maintenance of the molt-sleep. If this is so, then the larval molt would be an excellent model system with which to study the neuroendocrine regulation of quiescent "arousal states", including possibly sleep-like states. The characterization of *M. sexta* larval quiescence and an examination on a molecular level of changes that occur in the larval brain during the

transition into the molt-sleep are the main subjects of this thesis. This introductory chapter summarizes our current understanding of invertebrate sleep-like states and addresses the use of *M. sexta* as a model system to study quiescent behavior.

Invertebrate sleep-like states

Sleep-states are loosely defined.

The definition of sleep is not well-defined currently. Because the characteristics of the quiescent behaviors that are "identified" as sleep-states can vary across species and lifespan, it may be more appropriate to call this behavior (or these behaviors), sleep-*like* state(s). An early survey of sleep literature identified over 150 species for which authors claimed the presence of a sleep-state, but in many cases, the assignment of such a state was made without use of strictly defined criteria (Campbell & Tobler 1984). The presence of an extended period of immobility is not in itself sufficient evidence of sleep, as it does not distinguish sleep-states from other quiescent behaviors such as quiet wakefulness. There seems to be agreement that at a bare minimum, in order for a quiescent state to be defined as sleep-like, it must be accompanied by a rapidly-reversible reduced responsiveness to environmental stimuli (Siegel 2008). In many mammalian and avian species, reduced sensory responsiveness is also accompanied by characteristic electroencephalographic (EEG) signals, and these patterns of activity have been long used as the defining feature of sleep. This has tended to slow progress in the field of comparative sleep research, because many animals do not have the functional

neuroanatomy required for the generation of these same EEG patterns (Neckelmann & Ursin 1993). Even in higher vertebrates, there are some exceptions to the co-occurrence of immobility, reduced sensory-responsiveness, and characteristic cortical patterns.

A functional definition of sleep might greatly simply the identification of this state both across species and phyla, but at present, the function of sleep is not known. There are many hypotheses, mostly generated from the adverse behavioral and physiological effects that follow deprivation of quiescence, but also from large scale genetic screenings and functional transcriptome profiling in genetically-tractable organisms. The most commonly proposed functions include processes related to healing (removal of toxic substances), energy replenishment, and cognition (synaptic plasticity), and evidence to support these hypotheses are summarized in several reviews (Cirelli 2009; Crocker & Sehgal 2010; Mackiewicz et al 2008). It is possible that there is no "one" function of the sleep-like state, just as there seems to be no "one" set of behavioral and physiological requirements used to define sleep. Although sleep-researchers are actively engaged in the search for sleep-functions, it is important to remember that this search is usually based on an initial identification of a sleep-state in the model organism, and as we can see, this state is itself not clearly defined. In this section, we will discuss the various criteria that have been used to identify sleep-like states in invertebrate animals, and then we will describe the results obtained from the handful of invertebrate model systems for which a sleep-like state has been described using one or more of these criteria.

Criteria used to identify invertebrate sleep-like states.

Most criteria used to identify invertebrate sleep-like states are behavioral (Campbell & Tobler 1984; Hendricks et al 2000b). Identification usually begins with the observation of an extended ***period of quiescence*** (general immobility), during which time many animals display a species-specific, ***characteristic positioning of the body***. Movements associated with basic autonomic functions, such as respiration and circulation of vital fluids, are excluded from the definition of behavioral immobility so that quiescent behavior is contrasted from purposeful movements through or interactions with the environment. In many species, behavioral quiescence is concentrated during a particular portion of the 24 hr cycle, and it is this observation that has led to the proposal that lists of sleep-criteria should include a regulation by endogenous circadian clocks (Hendricks et al 2000b; Zimmerman et al 2008). Although the timing of sleep is often controlled, or at least influenced, by clock mechanisms, sleep can persist in species for which changes have occurred that abolish clock function (Hendricks et al 2000a; Hendricks et al 2003; Shaw et al 2000). Even in species that do show an uneven distribution of sleep across the 24 hr cycle, sleep can still occur at a time outside of the normal period of consolidation, usually occurring in short "naps". Although a periodic consolidation of quiescence seems to be most common, and probably confers a selective advantage, this clock-controlled criterion does not seem to be applicable.

Sleeping animals are also thought to have a reduced responsiveness to sensory stimuli, otherwise referred to as ***increased arousal thresholds***. This criterion helps to distinguish sleep-like states from simple rest or vigilance. A stimulus of greater

magnitude is needed to obtain the same behavioral response from a sleeping animal than from one that is awake. It is important that the requirement of a behavioral response is not substituted with a measure of responsiveness at the level of the sensory receptor, as there are several cases in which peripheral sensory response is inversely related an animal's behavioral responsiveness (Chen et al 1992; Kaiser & Steiner-Kaiser 1983; Krishnan et al 1999).

There is a rich body of literature surrounding the concept of "arousal state". In mammals, there is evidence for a *general* arousal system that drives (and is necessary for) the activation of the various forms of specific arousal (or specific motivational states) such as sex or feeding (Pfaff et al 2008). Building on work that clarified the neural circuitry underlying the estrogen-depended *lordosis* behavior in mammals (a female sexual response that aids in copulation), Donald Pfaff and co-workers at Rockefeller University made the first pioneering attempts to operationally define this generalized arousal state. *Generalized* CNS arousal was defined operationally as a state which, when increased, results in greater sensory responsiveness to sensory stimuli across sensory modalities, and the occurrence of more motor activity and emotional reactivity (Garey et al 2003; Pfaff et al 2008). *Drosophila* researchers have relied heavily on the first two criteria in studies that require a measure of the fly's general arousal state. In flies, changes in activity levels correlate well with changes in sensory responsiveness to a variety of exogenous stimuli (Hendricks et al 2000a; Huber et al 2004; Shaw et al 2000). Like mammals, insects have a variety of motivational states (specific arousal states) expressed as escape behaviors, aggression, courtship behavior, and feeding behavior.

Although transitions from sleep to wakefulness (or wakefulness to sleep) seem to be co-regulated with many of these specific arousal states in the same direction, there may be exceptions (Lebestky et al 2009). So although invertebrates such as *Drosophila* can become aroused from quiescence following exposure to a variety of sensory stimuli (Nitz et al 2002), the specific type of behavior that is monitored following these arousals may or may not serve as a good measure of generalized arousal state.

Another common criterion is that both the behavioral immobility and the accompanying elevation of arousal threshold be ***rapidly reversible***, which distinguishes sleep-states from quiescent behaviors that might occur as a result of motor depletion, or perhaps damage to the nervous system. This does not refer only to spontaneous, endogenously driven awakenings, but also to the ability of the animal to rapidly resume normal waking activity following exposure to a strong stimulus applied to an animal that is in the proposed sleep-state.

The presence of a ***homeostatic regulation*** is also a criteria used to distinguish sleep-like states from simple resting states. It is expected that deprivation of sleep is followed by recovery sleep (sleep-rebound), which is characterized by both a relatively longer duration and/or deeper sleep. Often, deficits in behavioral performance (learning and memory, and complex behaviors such as courtship) following sleep-deprivation are also used as evidence of this homeostatic regulatory mechanism. The regulation of the "amount" of sleep obtained suggests that sleep-states perform some vital function.

One non-behavioral criterion that has been used to identify invertebrate sleep-states is the presence of ***distinct patterns of neural activity*** recorded during the putative

sleep-state. Some attempts have been made to identify neural activity that is correlated with the onset and maintenance of the invertebrate sleep-state (discussed below). Changes in arousal state that accompany sleeping are thought to be the direct consequence of altered CNS activity. Identifying neural circuitries that can drive or maintain the sleep-state, or that are shut-down during such a state, is one of the goals of invertebrate sleep research.

A survey of invertebrate sleep-studies

Using some or all of the above-mentioned behavioral criteria, sleep-like states have been identified for several invertebrates, namely octopi, scorpions, crayfish, cockroaches, honey bees, fruit flies and roundworms. This section provides a description of the sleep-like states identified for each of these organisms, and highlights the types of behavioral and physiological criteria used as evidence for the presence of such a state.

Octopus. Evidence for a sleep-like state in the octopus comes from a single study (Brown et al 2006). Time-lapse recordings in the cephalopod *Octopus vulgaris* under a 12L:12D light cycle show daily rest-activity patterns. The animal is nocturnal, and quiescence was more concentrated during the light period. Periods of quiescence were associated with "eye closures" and a decreased responsiveness to tank-taps and light-flashes, as well as increased attack latency. 12 hrs of rest-deprivation during the day was accomplished using a manually applied, mild tactile stimulation, and this

procedure was followed by rest-rebound. In this study, surface electrodes where placed above the brain ganglion, and monitoring of electrical activity in behaving animals demonstrated that spike activity intensifies mainly during quiescent periods. This latter result is surprising because it contrasts with recordings from other invertebrates which show decreased brain activity during the sleeping state (discussed below).

Crayfish. Video recordings (12L:12D) made simultaneously with recordings of spontaneous brain activity were used to describe a sleep-like state for the crayfish *Procambarus clarkii* (Ramon et al 2004). Crayfish exhibit periods of immobility that are accompanied by a stereotyped posture described as "lying-on-one-side", and while in this position, responses to mechanical stimuli and light flashes were attenuated (Ramon et al 2004). The "lying-on-one-side" behavior occurred more often during the lights-off period. Following 24 hrs of rest-disturbance via continuous exposure to bubbling air, the occurrence of the putative sleep-position increased significantly. The transition to the putative sleep-like state was also accompanied by a transition from spiking activity (100-300 Hz) to slow wave electrical activity (15-20 Hz) at surface regions of the proto- and deutocerebrum (Agosto et al 2008; Mendoza-Angeles et al 2007; Mendoza-Angeles et al 2010; Ramon et al 2004). This is the first invertebrate system for which sleep-related slow-waves have been identified.

Scorpion. In a single study, the presence of a sleep-like state was tested for several species of tropical scorpions (Tobler & Stalder 1988). Time-lapse recordings

revealed a nocturnal activity pattern (quiescence was most consolidated during the light phase). One of the resting postures described as a "relaxed immobility" was accompanied by a reduced responsiveness to disturbances of the housing cages. Implanted electrodes were used to monitor heart rate, and a decreased beat frequency correlated well with occurrences of the identified sleep-posture. When scorpions were partially deprived for 12 hr (during the light period) of relaxed immobility using cage tapping and air-puffs, they showed an increased occurrence of relaxed immobility for at least 24 hrs following deprivation. A large individual variability, in terms of activity level (spontaneous and following deprivation) and activity patterns may have prevented further use of the scorpion as a model system.

Cockroach. Sleep-like behavior has been investigated in 3 species of cockroach. Time-lapse video recordings (12L:12D) of *Leucophea maderae* were used to characterize spontaneous behavior, as well as effects on behavior that resulted from forced activity (Tobler 1983). Cockroaches were more active during dark periods. Forced locomotion (via the periodic disturbance of the dishes in which they were housed) during the last 3 hrs of the light period did *not* result in significant rest-rebound that could be measured during the 12 or 24 hr recording period following treatment. The rest-activity profile of the cockroach *Blaberus giganteus* was similar to the later profile, but descriptions of the behavior of this species were more detailed (Tobler & Neuner-Jehle 1992). The most predominant form of immobility (named "state 1") in *Blaberus* was characterized by a resting posture where both the body and antennae touched the substrate. Cockroaches

exhibiting state 1 immobility showed attenuated responses to a vibration stimulus. For this species, 6 hrs of rest-deprivation also did not result in an overall compensatory rest-rebound. The cockroach *Diplotera punctata* exhibits behaviors and rest-activity profiles similar to that found for the above-mentioned species (Stephenson et al 2007). In *Diplotera*, prolonged, continuous deprivation of quiescent behavior led to a significant increase in metabolic rate and increased mortality rates following 16 days of deprivation (Stephenson et al 2007).

Honey bee. An early study of the honey bee, *Apis mellifera,* involved the use of extracellular, single unit recordings from the interneurons of the forager bee's optic lobe to demonstrate a circadian rhythm in their responsiveness to moving stimuli (Kaiser & Steiner-Kaiser 1983). Decreased responsiveness was correlated with troughs of daily (diurnal) activity-patterns and was reversible following application of arousing stimuli. When honey bees are observed in the hive or under isolated laboratory conditions, periods of immobility are accompanied by decreased body temperature and muscle tone, reduced responsiveness to light and thermal stimuli, and a characteristic resting posture (away from the brood), which involves a "sinking down" to the substrate and a unique positioning of the antennae (Kaiser 1988). Bee antennal movements have received special attention because their movements and positioning were shown to be predictive of the animal's arousal state, with highest arousal thresholds occurring during periods of complete antennal immobility (Kaiser 1988; Sauer et al 2003). When forager bees were deprived of antennal immobility for 12 hrs during the nighttime (12L:12D conditions) by

periodically "rolling" the glass cylinders in which they were contained, bees showed a significant rebound in the amount of antennal immobility during the subsequent dark period (Sauer et al 2004). Interestingly, deprivation of the identified sleep-state has also been shown to lead to impairments in *Apis mellifera's* "waggle dances", which are behaviors used to communicate directional and distance information about food sources (Klein et al 2010).

Apis mellifera has also been used to study age- and caste-related differences in sleep architecture. Interestingly, very young bees (~3 days old) do not show strong circadian rest-activity rhythms as do the older forager bees; in contrast, these young bees are described as being active in the hive "around-the-clock", and resting periods are distributed evenly across the 24 day (Eban-Rothschild & Bloch 2008). It was found that quiescent behaviors of young and old bees are characterized by the same sleep-postures. However, there were differences in the way that young and old bees transitioned through the different quiescent behaviors, suggesting at least some age-dependant plasticity in sleep behavior (Eban-Rothschild & Bloch 2008). *Apis mellifera* exhibit age polyethism; they change casts (sets of behavioral tasks) as they age. An investigation of sleep-differences across four worker castes revealed that as bees change castes, daily rhythmicity becomes more pronounced, and older castes (especially foragers) sleep more when outside of hive cells, while younger castes (especially cell cleaners) slept more when inside cells; and although the evidence is not conclusive, there is data to suggest that the youngest adult bees sleep more than bees from older castes (Klein et al 2008).

Fruit fly. Of all the identified invertebrate sleep-states, *Drosophila melanogaster's* has been the most studied. There are numerous articles dedicated to reviewing the abundance of fly sleep and arousal-state literature that has accumulated over the past decade following initial characterizations of the *Drosophila* sleep-like state (Birman 2005; Cirelli 2009; Cirelli & Bushey 2008; Crocker & Sehgal 2010; Foltenyi et al 2007a; Harbison et al 2009b; Sehgal et al 2007; Shaw 2003). Here we will describe the initial characterizations of the fruit fly's sleep-like state, and highlight some important findings that followed from these observations.

In 2000, two separate groups published articles that provided the initial characterizations of the sleep-like state of *Drosophila melanogaster* (Hendricks et al 2000a; Shaw et al 2000). Prior to these studies, it was already known that the fruit fly exhibited robust circadian rhythms (under L:D cycles, or free-running under D:D conditions), and the fly was already a well-established model system for the study of the molecular clock mechanisms (Dunlap 1999). Video, ultrasound and infrared analysis were used to monitor rest-activity cycles, and to further characterize rest parameters (Hendricks et al 2000a; Shaw et al 2000). Observations of individual flies showed that prior to resting periods (relatively immobile periods devoid of purposeful movement), flies move away from food and areas where social interactions predominate, and adopt a "prone" position (Hendricks et al 2000a). Flies rest for close to half of the total amount of time in a 24 hr period, with rest being most consolidated during the night, during which time, most rest bouts exceed 30 min (Hendricks et al 2000a). Quiescent flies showed reduced responsiveness to both vibratory and mechanical stimuli, and resting

flies were also less responsive to social interactions (Hendricks et al 2000a; Shaw et al 2000). Manual and automated application of mechanical stimuli applied during the subjective night is followed by robust rest-rebounds during the following subjective day, providing evidence for the presence of homeostatic control mechanisms underlying the regulation of the fly sleep-like state (Hendricks et al 2000a; Huber et al 2004; Shaw et al 2000). Interestingly, although mutants for the circadian clock gene *period* abolished circadian activity-rhythms (rest-activity levels in these mutants were evenly distributed throughout the 24 hr cycle), deprivation of rest was still followed by rest-rebound, indicating that homeostatic regulation of the sleep-like state can be dissociated from circadian control mechanisms (Shaw et al 2000).

From a comparative standpoint, studies that followed the initial characterizations of fly sleep demonstrated many features that are conserved across phylogeny. Flies respond similarly to many of the same drugs as do humans, including cocaine, methamphetamine, caffeine, antihistamines and general anesthesia, suggesting a conservation of neurotransmitter systems involved in sleep-regulation (Andretic et al 2005; Hendricks et al 2000a; Ho & Sehgal 2005; Lebestky et al 2009; Shaw et al 2000; van Swinderen 2006; Weber et al 2009; Wu et al 2009). Sleep is important for early-adult fly development, and flies sleep less and sleep becomes progressively more fragmented with age (Koh et al 2006; Seugnet et al 2011). Sleep duration and depth is influenced by nutritional status, as well as immune response following infection (Agosto et al 2008; Catterson et al 2010; McDonald & Keene 2010; Williams et al 2007). Although fly brains do not show electrophysiological correlates similar to mammalian

patterns, surface recordings of the medial protocerebrum demonstrated that the sleep-like state was associated with distinct neural patterns in that during sleep, there is a generalized decrease in brain activity (Nitz et al 2002).

By observing the behavioral and physiological effects of sleep-deprivation, many *Drosophila* researchers have provided evidence to support the hypothesis that sleep is important for processes related to synaptic plasticity, such as learning and memory and nervous system development. Sleep-deprivation during early adult development leads to learning deficits in the adult stages, and adults deprived of sleep show impairments in the acquisition of olfactory memories (Li et al 2009; Seugnet et al 2011). Flies exposed to enriched social environments sleep more than flies reared in isolation, demonstrating an experience-dependent plasticity in sleep need (Ganguly-Fitzgerald et al 2006). The mushroom bodies have been identified as a brain region that mediates experience-dependent sleep need; this region has been shown to regulate both sleep duration and architecture, and to be essential for certain types of memory formation (Foltenyi et al 2007a; Joiner et al 2006; Pitman et al 2006). It seems though, that this proposed plasticity function for sleep may apply more generally across the nervous system, and that sleep may be necessary to maintain synaptic homeostasis. When levels of synaptic markers in the *Drosophila* brain were tracked, synaptic markers increased progressively with increasing wake-time, and sleep was necessary for their decline (a synaptic "pruning") (Gilestro et al 2009). This synaptic downscaling is thought to underlie the beneficial effects of sleep on cognition and performance (Tononi & Cirelli 2003).

Several microarray analyses have been performed to examine differences in gene expression in brains or whole fly heads between sleep, sleep deprived and waking states, and across populations with naturally varying sleep-phenotypes (Cirelli & Bushey 2008; Harbison et al 2009a; Seugnet et al 2009; Zimmerman et al 2006). It is evident that brains of sleeping and awake flies differ on a molecular level independent of time of day. Stringent cut-offs used during analysis coupled with microarrays low sensitivity for the detection of genes that might be expressed at very low levels may obscure the identification of transcripts related to specific neurotransmitter and neuropeptide systems. Also, sampling of tissues is often limited to two time-points (subjective day and night) so that the differential expression of many arousal-related transcripts is likely to be missed. Future studies that include more sensitive methods such as RNA-seq, coupled with a higher sampling rate (especially around times of behavioral transitions) should facilitate the discovery of more sleep- and wake-related transcripts. At present, comparisons across fly studies, as well as microarray studies performed on rat and mice brain tissue, reveal that sleep- and wake-related transcripts belong to several different functional categories: transcripts related to wake and sleep-deprived states are involved in carbohydrate metabolism, cellular stress and synaptic potentiation, while sleep-related transcripts are associated with protein synthesis, synaptic depression and lipid metabolism (Cirelli 2009).

Just as there is evidence for multiple sleep-functions, there is also evidence of multiple neurotransmitter and hormonal systems involved in the regulation of sleep-like states, even in the tiny *Drosophila*. Many of these systems are conserved across species

and phyla, and in insects they form the equivalent of the mammalian diffuse modulatory systems that are thought to act as the core regulators of general arousal state. The use of high-throughput forward genetic screenings, and targeted gene manipulations has led to the identification of several neurotransmitter systems, ion channels, hormones and other protein products putatively involved in sleep-regulation. Many of these candidate sleep-regulators are involved in the modulation of other, more specific forms of arousal, such as mating and foraging. Whether these systems regulate the different forms of arousal separately or together awaits further characterization of the neurocircuitry. Brain dopaminergic signaling, however, is now known to differentially regulate different forms of arousal, depending on the site of action (Lebestky et al 2009). In terms of sleep-wake-type arousal, the actions of dopamine (DA) seem to be straightforward; DA is generally wake-promoting, and its effects on sleep-wake regulation are thought to be mediated through its actions on the mushroom bodies (Andretic et al 2005; Kume et al 2005; Van Swinderen & Andretic 2011). Octopamine is also wake-promoting via its actions on insulin-producing cells of the pars intercerebralis (Crocker & Sehgal 2008; Crocker et al 2010). Another arousal-promoting factor in the brain is the peptide pigment dispersing factor (PDF). PDF is expressed in a set of brain clock neurons that regulate the timing of the sleep-wake cycle, and disruption of PDF signaling increases sleep, although the downstream targets that mediate this effect are still unknown (Chung et al 2009). The role of potassium channels will be discussed in detail in Chapter Three.

Gamma-aminobutyric acid (GABA) is one of several *somnogens*, or sleep-promoting agents identified in the *Drosophila* brain, and its effects have been found to be

mediated via its inhibitory actions on PDF-expressing clock neurons (Chung et al 2009; Parisky et al 2008). Other sleep-promoting factors include epidermal growth factor (EGF), serotonin and ecdysone signaling. The sleep-promoting effects of these somnogenes are thought to be mediated through their actions on the brain. Sleep-promoting EGF neurons were identified as the subset of the neurons in the pars intercerebralis that project to regions of the tritocerebrum (Foltenyi et al 2007b). Sleep-promoting roles of serotonin and ecdysone are both thought to be mediated through actions on the mushroom bodies (Ishimoto & Kitamoto 2010; Yuan et al 2006).

Roundworm. In contrast to the other above-described invertebrate systems, studies of quiescent behavior in the roundworm *Caenorhabditis elegans* (*C. elegans*) have concentrated on the period of development that *precedes* the adult stage. Like insects such as *Drosophila* and *M. sexta*, *C. elegans* post-embryonic development consists of a series of larval feeding stages that are separated by a molting period. There are four molts separating each of the four larval stages and the adult stage, and these relatively brief periods—called *lethargus*—were described some time ago as periods of behavioral quiescence (Cassada & Russell 1975). But it was not until 2008 that *lethargus* behavior was characterized, and it was then demonstrated that quiescence during the *C. elegans* molt resembles the sleep-like states in other adult invertebrates (Raizen et al 2008). During lethargus, animals showed a reduced responsiveness to olfactory stimuli, but this reduction was reversible when preceded by an arousing mechanical stimulus. Following arousal by exogenous stimuli, behaviors exhibited by molting larvae

resembled those observed for inter-molt larvae. Deprivation of quiescence during the molting period resulted in a subsequent increase in quiescence-bout duration, a further reduction in sensory responsiveness and a reduced latency to quiescent behavior following arousal, which suggested that the level of quiescence during lethargus is under homeostatic control.

Like *Drosophila*, *C. elegans* is a genetically-tractable model system. So far, genetic manipulations have allowed for identification of a wake-promoting function for cAMP signaling, and have also pointed to sleep-promoting factors, including a cGMP dependant protein kinase (sleep-promoting when expressed in a subset of sensory neurons), and the epidermal growth factor signaling pathway (Raizen et al 2008; Van Buskirk & Sternberg 2007).

Another interesting finding is that rest-activity during *C. elegans* post-embryonic development shows developmental, but not circadian rhythms. Although levels of adult insect sleep are regulated by homeostatic control mechanisms, the *timing* of insect (and our own mammalian) diurnal rest-activity cycles is largely regulated by brain "clock neurons", which are themselves driven endogenously by transcription/translation regulatory feedback loops (Bell-Pedersen et al 2005; Hardin 2006; Taghert & Shafer 2006). *C. elegans* rest-activity cycles during the larval stages do not occur with a 24-hour periodicity; rather, they show much shorter rhythms corresponding to developmental events. Homologs to the *Drosophila* core clock genes have been identified in *C. elegans* larvae, and expression patterns also display developmental, but not circadian rhythms; and although their connection to molt-sleep behavior has not been

explored, these genes are known to be important in control of the timing of developmental events, such as timing of tissue differentiation (Banerjee et al 2005; Jeon et al 1999). Even though *Drosophila* larvae do not exhibit circadian locomotor rhythms, clock neurons are functional during the larval stages, where they are known to play a role in setting the timing of adult emergence (Kaneko et al 1997).

Manduca sexta **as a model system for the study of quiescent behavior.**

Manduca sexta is a moth of the family Sphingidae (order Lepidopteran) that can be found throughout much of the American continent. The larvae of this species feed on the foliage of various solanaceous plants such as tobacco plants; hence, one of its common names is "Tobacco Hornworm". *M. sexta* is a holometabolous insect, meaning that it undergoes *complete* metamorphosis. The larval and adult stages of *M. sexta* exhibit remarkable differences in their morphology and behavior. Larvae are designed for crawling and feeding, while the adult is a winged moth, designed for reproduction. A series of immature larval (worm-like) feeding stages are separated from the winged adult reproductive stage by a non-feeding pupal stage, during which the complete change in body form occurs. Under optimal conditions, *M. sexta* develops through 5 larval stages (instars). *M. sexta* can increase its body weight from ~1-2 grams to over 10 grams during the fifth instar. The large size of these larvae, coupled with their relatively short life-cycle, has led to the use of *M. sexta* as a model system for the study of various physiological processes and behaviors.

Approximately half of *M. sexta's* larval mass is attributable to its hemolymph volume, and this has facilitated the profiling of several hormones in relation to key developmental events. There are many excellent reviews detailing the identities and roles of these hormones in *M. sexta* development (Bollenbacher et al 1987; Nijhout 1994; Nijhout & Williams 1974; Riddiford et al 2001; Truman JW & Riddiford LM 2002). Key hormones that initiate and program insect developmental transitions are the steroid molting hormones "ecdysteroids", the sesquiterpenoid "juvenile hormones" (JH), and the peptide hormone "prothoracicotropic hormone" (PTTH). During each stage of larval development, feeding and growth leads to the release of PTTH from brain neurosecretory cells, where it then acts on the prothoracic glands to initiate the synthesis and secretion of molting hormones (Nijhout 1980; 1981). The actual mechanism that triggers PTTH release is unknown, but its release is known to be photoperiodically gated (Truman 1972). Larvae that do not reach a critical period within a given temporal gate must wait until the gate on the following day; hence the terms "gate I" and "gate II" larvae (Truman 1972). The steroid molting hormones are collectively termed *ecdysteroids*. In *Manduca*, 3-dehydroecdysone is synthesized and secreted by the prothoracic glands, and is converted into α-ecdysone (usually a pro-hormone) in the hemolymph, which is then converted into an active form in peripheral tissues (Feyereisen 1999; Sakurai et al 1989). Depending on species and developmental stage, numerous metabolites (as well as the α-ecdysone itself) can have biological actions, but 20-hydroxyecdysone is considered the active hormone in larval *M. sexta*. Whether molting hormones can influence gene expression in a cell depends on the presence of a receptor. Unlike the molting hormones, JHs are secreted

(from the corpora allata) throughout much of a larval stage, and although its receptors are not yet identified, these hormones are known to influence the actions of molting hormones (Fain & Riddiford 1975; Riddiford 1996). The presence of JH during the ecdysteroid surge promotes a molt to the same "juvenile" stage. Four or five days into the 5th and final instar, the small surge of ecdysteroids that occurs in the absence of JH triggers the onset of metamorphosis.

The larval molt of *M. sexta* has been used as a model system to study ecdysteroid-mediated changes in gene expression occurring in epidermal cells of the body wall (Hiruma & Riddiford 2001; 2009; 2010). In contrast to their sensitivities during metamorphic processes, neurons and glia of the CNS are thought to be relatively insensitive to the hormone surges that occur during larval-larval transitions. The canonical ecdysteroid receptor is a heterodimer composed of the ecdysteroid nuclear receptor EcR (there are two isoforms in *Manduca*) and another member of the nuclear receptor family, ultraspiracle (USP) (Yao et al 1993; Yao et al 1992). Larval neurons and glial cells show very low levels of EcR throughout much of larval life, and prior to the late 5th instar, surges of molting hormones (in the presence of JH) do not lead to the dramatic changes in neuronal morphology that are observed during metamorphosis (Truman et al 1994). But the idea that the larval CNS is not influenced by molting hormones conflicts with observations that exposure of the larval CNS to ecdyseroids leads to changes in gene expression that's confers sensitivity of the CNS to ecdysis triggering hormone. (Zitnanova et al 2001). Just how ecdysteroids act to confer CNS sensitivity to ecdysis triggering hormone has not been addressed. Autoradiographic

localization of EcR's has been used to map the location ecdysteroid receptors in the brains of *M. sexta* larvae during larval-pupal development, but only one time-point was sampled during the larval molt, and that was following the decline of ecdysteroids during the late molt; in this study, EcR's were localized to neurons of the brain, but the identities of these neurons have not yet been investigated and EcR expression at earlier times during the molt was not examined (Bidmon et al 1991). A later immunohistochemistry study demonstrated a transient expression of EcR's in abdominal neurons late during the larval molt (Truman et al 1994). EcR's have not been localized to the neurons that are known to respond to ecdysteroids by expressing receptors to ecdysis triggering hormone (*personal communication*). It is possible that during the larval molt, ecdysteroids are acting through EcR-independent pathways. USP can heterodimerize with other members of the nuclear receptor family, such as hormone receptor 38, and unlike EcR, USP is expressed ubiquitously in the larval tissues (Asahina et al 1997; Baker et al 2003). In *Drosophila*, an ecdysteroid-sensitive G-protein coupled receptor also has been identified, so another possibility is that ecdysteroids are acting on other currently unidentified membrane-bound receptors (Srivastava et al 2005). Regardless of the receptor identity, ecdysteroid actions on the CNS toward the end of the molt seem to influence behavioral, but not morphological changes. This is also true during the final instar, when exposure of the brain to ecdysteroids is both necessary and sufficient to induce wandering behavior, which consists of a cessation of feeding behavior, followed by the induction of a series of behaviors that leads relocation of the larvae to its underground pupation site (Dominick & Truman 1986). Wandering behavior is triggered by the "commitment peak" of

ecdysteroids that occurs in the absence of JH's (Dominick & Truman 1985). The correlation of the onset of molting quiescence (described below) with the larval peak of ecdysteroids suggests that ecdysteroid surges that occur in the presence of JH might be acting on the nervous system to induce the early-molt quiescent behaviors.

The central nervous system of *M. sexta* consists of a dorsally-located brain (also known as the supraesophageal ganglion), and a series of separate ventral ganglia, which includes the subesophageal ganglia, three thoracic and eight abdominal ganglia (fused abdominal ganglia 7 and 8 are called the "terminal abdominal ganglion"). Although the brain is made up of the three major protocerbral, deutocerebral, and tritocerebral regions, the larval brain differs from the adult in that regions that process visual and olfactory information are less well-developed. The *Manduca* brain does, however, receive information from larvae antennae and from stemmata, which in Lepidopteran larvae are sensitive to green, blue and UV light (Gilbert 1994; Kent & Hildebrand 1987). Sites of multimodal sensory integration that are known to influence sleep-wake arousal in adult insects are also present (although less well-developed) in the brain during the larval stages. Mushroom bodies, the protocerebral bridge, and a small division of the central complex are all present at the first instar (Homberg & Hildebrand 1994; Yack JE & Homberg U 2003). Neurotransmitter systems that regulate arousal state in the adult, including dopamine, serotonin, octopamine, acetylcholine, GABA, and multiple neuropeptides are also synthesized/expressed in the larval brain and ventral nerve cord, and it is likely that these systems share some conserved function across developmental stages.

During larval development, cells of the *M. sexta* nervous system increase in size, and cell number also increases through divisions of neuroblasts, the progeny of which are destined for differentiation into neurons of the adult brain during metamorphosis (Booker & Truman 1987). But between hatching and metamorphosis, these new cells do not mature into functional neurons, and across the feeding stages, there seem to be no changes in the functional larval circuitry in terms of cell number and neurotransmitter identity (Booker & Truman 1987; Granger et al 1989; Homberg & Hildebrand 1994). Since behavioral changes that coincide with the periodic surges of molting hormones during transitions between larval stages are not likely to be due to large scale structural changes, the behavioral transitions from feeding to molting, and then from molting to feeding, can be attributed solely to changes in neural activity and/or neurotransmitter and receptor synthesis. These larval-larval transitions may be excellent models in which to study the coordination of centrally- generated behaviors with peripheral developmental events, and the predictability of the timing of these developmental events may facilitate investigations into circuitries and systems that underlie behaviors both during the feeding and the molting stages.

M. sexta larvae do not transition directly from feeding to ecdysis behavior. It has long been reported (anecdotally) that *Manduca's* ecdysis behavior is first preceded by an extended period of quiescence during which the animal does not feed. This non-feeding and reportedly non-moving state has been dubbed the "molt-sleep". The onset of the molt-sleep has been associated with apolysis of the head capsule (head capsule slippage; HCS), a morphological change that coincides with peak levels of molting hormones in

the hemolymph (Curtis et al 1984; Langelan et al 2000; Reinecke et al 1980). The molt-sleep has been reported to occur during all of *M. sexta's* larval stage transitions, with durations estimated at ~ 15 hrs for the first three transitions and ~ 25 hrs during the transition to the 5th and final larval stage (Reinecke et al 1980). Prior to HCS, larval are actively feeding, so the onset of the molt-sleep represents a dramatic shift in behavior, and its coincidence with HCS suggests either direct or indirect neuroendocrine regulation. Surprisingly, quiescent behavior during the molt has not been characterized. Our observations that molt-sleep larvae retain reflex and motor behavior suggests that molting quiescence is not due to the inability to behave, but that it is likely due to either a decreased motivation to behave, an increased drive toward quiescence, or a combination of both. The presence of a sleep-like state during the larval-larval transitions of *C. elegans* begs the question as to whether the presence of a sleep-like state is conserved across phyla. Because the morphological changes that accompany apolysis of the cuticle prevent larvae from feeding, and as this inability to feed can persist for up to a day, the programming of a concomitant decrease in arousal state during the molting period would be beneficial, both in terms of energy conservation and predator avoidance. A rapidly-reversible "sleep-like" state would also be beneficial as it would allow the animal to retain some level of response to a changing environment.

Quiescent behavior also takes place during the inter-molt feeding stages, occurring in short inter-feeding bouts. Larvae of *M. sexta* have long been used as a model system to study the architecture of lepidopteran larval feeding behavior, as well as the relationship between nutritional status and the regulation of post-embryonic

development. *M. sexta* larval behavior has been monitored both in the wild and under laboratory conditions, and there is an across-study consensus that *M. sexta* has a robust feeding homeostat that is largely influenced by nutritional content, so that although larvae spend ~half of their time in a quiescent state, that amount of time can vary depending upon whether they are fed on high nutrient laboratory diet or lower nutrient food such as tobacco leaves (Timmins et al 1988). Apart from feeding and quiescence, larva display locomotion, grooming, and robust defensive behaviors when disturbed by noxious stimuli such as attack from predators (birds) or parasitic wasps (Bernays 2000; Walters et al 2001). Although the predominant behavior during the larval feeding stages is quiescent behavior, this behavior has also not been characterized, so it is not known if this state represents a simple resting behavior or some other form of quiescence. The feeding period between molts can last for several days. As it is hypothesized that sleep is somehow important to nervous system function, one would expect that sleep-behavior would occur at some time across these long-duration larval stages, and *M. sexta* provides an excellent opportunity to test that hypothesis.

Although moths have not served as a primary model system for the study of sleep-like states, investigations into feed-back mechanisms regulating moth population densities led to the observation and description of a sleep-like behavior in the adult Mediterranean flour moth, *Anagasta kuehniella* (Andersen 1968). Anderson (1968) described several "sleeping" postures displayed by quiescent moths that differ from active adults, and that could be described based on antennal position. While in sleeping postures, moths were less responsive when the investigator disturbed their wings using a

fine brush. Although moths have not been used in any other sleep-studies, a 1945 study that used seven species of Lepidopteran to study caterpillar responsiveness to mechanical and thermal stimuli described a "between-feeding" resting posture, during which responses to mechanical stimuli were difficult to elicit (Frings 1945). Once aroused, the animals' responses were observed to resemble those of feeding larvae, and the author hypothesized that caterpillar resting behavior might resemble a sleep-like state.

Investigating the molecular correlates of a sleep-like state in a non-genetically tractable system.

Identifying neurotransmitter systems and brain structures involved in the modulation of larval arousal states could aid in the understanding of these processes in the adult stages. Although metamorphosis involves a massive remodeling of larval neurons, as well as the addition of large numbers of new adult-specific neurons to the nervous system, many of the larval neurons and neurotransmitter systems may be conserved during this process (Truman 1990). Neurotransmitter systems involved in the regulation of arousal state during larval development also are likely to be relevant to quiescence during metamorphosis, and to the environmentally-induced *diapause* state, which is a period of arrested development that is also accompanied by quiescence and changes in the hormonal milieu.

The successful identification in *Drosophila* and *C. elegans* of genes, gene products, and specific circuitries that are important to arousal state regulation can be

largely attributed to the genetic tractability of these organisms. Its large size, short life cycle, and the predictability of changes in key hormones relative to developmental and morphological events makes *M. sexta* an excellent candidate to study the neuroendocrine coordination of behavior and physiology, but its genome is not yet available. Electrophysiological recordings, *in situ* hybridization and immunochemistry are often used successfully in this organism, but these techniques require the targeting of *specific* transcripts or proteins. But in general, there are many systems known to be involved in the modulation of insect arousal state, and these systems in turn can be regulated at multiple levels (from the synthesis of a neurotransmitter, to ion channels and membrane proteins that affect transmission, for example). If molting hormones are acting either directly or indirectly on the larval nervous system to bring about changes in arousal state through the induction or suppression of gene expression, how do we identify the system(s) and processes(s) involved?

The use of techniques that survey the expression changes of thousands of genes simultaneously would greatly facilitate hypothesis generation. Microarray technology is often used for this purpose, but this method uses a hybridization-based approach, which again requires an *a priori* knowledge of an organism's mRNA sequences. Recently, new technologies have become available that utilize sequencing-based (non-hybridization-based) approaches. *RNA-seq* technologies can now be used to rapidly profile entire transcriptomes from non-model organisms (Wang et al 2009). Illumina mRNA sequencing is one of several newly-developed sequencing technologies; it is based on the parallel sequencing of millions of cDNA fragments using reversible terminator-based

sequencing (www.illumina.com). The technology allows for a *direct* sequencing of transcripts, and also an absolute quantification of transcript level, thereby enabling the detection of differential expression across tissues or developmental time-points. In Chapter 2 of this dissertation, *M. sexta* is used as a model system to characterize larval quiescent behavior, and in Chapter 3 of this dissertation, we take advantage of Illumina sequencing to profile the *M. sexta* brain transcriptome during the transition from larval feeding to molting quiescence.

References

Agosto J, Choi JC, Parisky KM, Stilwell G, Rosbash M, Griffith LC. 2008. Modulation of GABAA receptor desensitization uncouples sleep onset and maintenance in Drosophila. *Nat Neurosci* 11:354-9

Andersen F. 1968. Sleep in moths and its dependence on the frequency of stimulation in *Anagast kuehniella. Opuscula entomologica* 33:15-24

Andretic R, van Swinderen B, Greenspan RJ. 2005. Dopaminergic modulation of arousal in Drosophila. *Curr Biol* 15:1165-75

Asahina M, Jindra M, Riddiford LM. 1997. Developmental expression of Ultraspiracle proteins in the epidermis of the tobacco hornworm, Manduca sexta, during larval life and the onset of metamorphosis. *Dev Genes Evol* 207:381-8

Ashburner M. 1973. Sequential gene activation by ecdysone in polytene chromosomes of Drosophila melanogaster. I. Dependence upon ecdysone concentration. *Dev Biol* 35:47-61

Ashburner M. 1974. Sequential gene activation by ecdysone in polytene chromosomes of Drosophila melanogaster. II. The effects of inhibitors of protein synthesis. *Dev Biol* 39:141-57

Baker KD, Shewchuk LM, Kozlova T, Makishima M, Hassell A, et al. 2003. The Drosophila orphan nuclear receptor DHR38 mediates an atypical ecdysteroid signaling pathway. *Cell* 113:731-42

Banerjee D, Kwok A, Lin SY, Slack FJ. 2005. Developmental timing in C-elegans is regulated by kin-20 and tim-1, homologs of core circadian clock genes. *Dev Cell* 8:287-95

Bell-Pedersen D, Cassone VM, Earnest DJ, Golden SS, Hardin PE, et al. 2005. Circadian rhythms from multiple oscillators: lessons from diverse organisms. *Nat Rev Genet* 6:544-56

Bernays EA. 2000. Foraging in nature by larvae of Manduca sexta-influenced by an endogenous oscillation. *Journal of Insect Physiology* 46:825-36

Bidmon HJ, Granger NA, Cherbas P, Maroy P, Stumpf WE. 1991. Ecdysteroid receptors in the central nervous system of Manduca sexta: their changes in distribution and quantity during larval-pupal development. *J Comp Neurol* 310:337-55

Birman S. 2005. Arousal mechanisms: speedy flies don't sleep at night. *Curr Biol* 15:R511-3

Bollenbacher WE, Granger NA, Katahira EJ, Obrien MA. 1987. Developmental Endocrinology of Larval Molting in the Tobacco Hornworm, Manduca-Sexta. *Journal of Experimental Biology* 128:175-92

Booker R, Truman JW. 1987. Postembryonic neurogenesis in the CNS of the tobacco hornworm, Manduca sexta. I. Neuroblast arrays and the fate of their progeny during metamorphosis. *J Comp Neurol* 255:548-59

Brown ER, Piscopo S, De Stefano R, Giuditta A. 2006. Brain and behavioural evidence for rest-activity cycles in Octopus vulgaris. *Behav Brain Res* 172:355-9

Campbell SS, Tobler I. 1984. Animal sleep: a review of sleep duration across phylogeny. *Neurosci Biobehav Rev* 8:269-300

Cassada RC, Russell RL. 1975. Dauerlarva, a Post-Embryonic Developmental Variant of Nematode Caenorhabditis-Elegans. *Dev Biol* 46:326-42

Catterson JH, Knowles-Barley S, James K, Heck MM, Harmar AJ, Hartley PS. 2010. Dietary modulation of Drosophila sleep-wake behaviour. *PLoS One* 5:e12062

Chen DM, Christianson JS, Sapp RJ, Stark WS. 1992. Visual receptor cycle in normal and period mutant Drosophila: microspectrophotometry, electrophysiology, and ultrastructural morphometry. *Vis Neurosci* 9:125-35

Chung BY, Kilman VL, Keath JR, Pitman JL, Allada R. 2009. The GABA(A) receptor RDL acts in peptidergic PDF neurons to promote sleep in Drosophila. *Curr Biol* 19:386-90

Cirelli C. 2009. The genetic and molecular regulation of sleep: from fruit flies to humans. *Nat Rev Neurosci* 10:549-60

Cirelli C, Bushey D. 2008. Sleep and wakefulness in Drosophila melanogaster. *Ann N Y Acad Sci* 1129:323-9

Clever U. 1964. Actinomycin and Puromycin: Effects on Sequential Gene Activation by Ecdysone. *Science* 146:794-5

Clever U, Karlson P. 1960. Induction of puff alterations in the salivary gland chromosomes of Chironomus tentans by Ecdysorie. *Exptl Cell Res* 20:623-6

Crocker A, Sehgal A. 2008. Octopamine regulates sleep in drosophila through protein kinase A-dependent mechanisms. *J Neurosci* 28:9377-85

Crocker A, Sehgal A. 2010. Genetic analysis of sleep. *Gene Dev* 24:1220-35

Crocker A, Shahidullah M, Levitan IB, Sehgal A. 2010. Identification of a neural circuit that underlies the effects of octopamine on sleep:wake behavior. *Neuron* 65:670-81

Curtis AT, Hori M, Green JM, Wolfgang WJ, Hiruma K, Riddiford LM. 1984. Ecdysteroid Regulation of the Onset of Cuticular Melanization in Allatectomized and Black Mutant Manduca-Sexta Larvae. *Journal of Insect Physiology* 30:597-&

Dominick OS, Truman JW. 1985. The physiology of wandering behaviour in Manduca sexta. II. The endocrine control of wandering behaviour. *J Exp Biol* 117:45-68

Dominick OS, Truman JW. 1986. The physiology of wandering behaviour in Manduca sexta. IV. Hormonal induction of wandering behaviour from the isolated nervous system. *J Exp Biol* 121:133-51

Dunlap JC. 1999. Molecular bases for circadian clocks. *Cell* 96:271-90

Eban-Rothschild AD, Bloch G. 2008. Differences in the sleep architecture of forager and young honeybees (Apis mellifera). *J Exp Biol* 211:2408-16

Fain MJ, Riddiford LM. 1975. Juvenile hormone titers in the hemolymph during late larval development of the tobacco hornworm, Manduca sexta (L.). *Biol Bull* 149:506-21

Feyereisen R. 1999. Insect P450 enzymes. *Annu Rev Entomol* 44:507-33

Foltenyi K, Andretic R, Newport JW, Greenspan RJ. 2007a. Neurohormonal and neuromodulatory control of sleep in Drosophila. *Cold Spring Harb Symp Quant Biol* 72:565-71

Foltenyi K, Greenspan RJ, Newport JW. 2007b. Activation of EGFR and ERK by rhomboid signaling regulates the consolidation and maintenance of sleep in Drosophila. *Nat Neurosci* 10:1160-7

Frings H. 1945. The reception of mechanical and thermal stimuli by caterpillars. *The Journal of Experimental Zoology* 99:115-40

Ganguly-Fitzgerald I, Donlea J, Shaw PJ. 2006. Waking experience affects sleep need in Drosophila. *Science* 313:1775-81

Garey J, Goodwillie A, Frohlich J, Morgan M, Gustafsson JA, et al. 2003. Genetic contributions to generalized arousal of brain and behavior. *Proc Natl Acad Sci U S A* 100:11019-22

Gilbert C. 1994. Form and Function of Stemmata in Larvae of Holometabolous Insects. *Annual Review of Entomology* 39:323-49

Gilestro GF, Tononi G, Cirelli C. 2009. Widespread changes in synaptic markers as a function of sleep and wakefulness in Drosophila. *Science* 324:109-12

Granger NA, Homberg U, Henderson P, Towle A, Lauder JM. 1989. Serotonin-immunoreactive neurons in the brain of Manduca sexta during larval development and larval-pupal metamorphosis. *Int J Dev Neurosci* 7:55-72

Harbison ST, Carbone MA, Ayroles JF, Stone EA, Lyman RF, Mackay TF. 2009a. Co-regulated transcriptional networks contribute to natural genetic variation in Drosophila sleep. *Nat Genet* 41:371-5

Harbison ST, Mackay TF, Anholt RR. 2009b. Understanding the neurogenetics of sleep: progress from Drosophila. *Trends Genet* 25:262-9

Hardin PE. 2006. Essential and expendable features of the circadian timekeeping mechanism. *Curr Opin Neurobiol* 16:686-92

Hendricks JC, Finn SM, Panckeri KA, Chavkin J, Williams JA, et al. 2000a. Rest in Drosophila is a sleep-like state. *Neuron* 25:129-38

Hendricks JC, Lu S, Kume K, Yin JC, Yang Z, Sehgal A. 2003. Gender dimorphism in the role of cycle (BMAL1) in rest, rest regulation, and longevity in Drosophila melanogaster. *J Biol Rhythms* 18:12-25

Hendricks JC, Sehgal A, Pack AI. 2000b. The need for a simple animal model to understand sleep. *Prog Neurobiol* 61:339-51

Hiruma K, Riddiford LM. 2001. Regulation of transcription factors MHR4 and betaFTZ-F1 by 20-hydroxyecdysone during a larval molt in the tobacco hornworm, Manduca sexta. *Dev Biol* 232:265-74

Hiruma K, Riddiford LM. 2009. The molecular mechanisms of cuticular melanization: the ecdysone cascade leading to dopa decarboxylase expression in Manduca sexta. *Insect Biochem Mol Biol* 39:245-53

Hiruma K, Riddiford LM. 2010. Developmental expression of mRNAs for epidermal and fat body proteins and hormonally regulated transcription factors in the tobacco hornworm, Manduca sexta. *J Insect Physiol* 56:1390-5

Ho KS, Sehgal A. 2005. Drosophila melanogaster: an insect model for fundamental studies of sleep. *Methods Enzymol* 393:772-93

Homberg U, Hildebrand JG. 1994. Postembryonic development of gamma-aminobutyric acid-like immunoreactivity in the brain of the sphinx moth Manduca sexta. *J Comp Neurol* 339:132-49

Huber R, Hill SL, Holladay C, Biesiadecki M, Tononi G, Cirelli C. 2004. Sleep homeostasis in Drosophila melanogaster. *Sleep* 27:628-39

Ishimoto H, Kitamoto T. 2010. The steroid molting hormone Ecdysone regulates sleep in adult Drosophila melanogaster. *Genetics* 185:269-81

Jeon M, Gardner HF, Miller EA, Deshler J, Rougvie AE. 1999. Similarity of the C-elegans developmental timing protein LIN-42 to circadian rhythm proteins. *Science* 286:1141-6

Joiner WJ, Crocker A, White BH, Sehgal A. 2006. Sleep in Drosophila is regulated by adult mushroom bodies. *Nature* 441:757-60

Kaiser W. 1988. Busy Bees Need Rest, Too - Behavioral and Electromyographical Sleep Signs in Honeybees. *Journal of Comparative Physiology a-Sensory Neural and Behavioral Physiology* 163:565-84

Kaiser W, Steiner-Kaiser J. 1983. Neuronal correlates of sleep, wakefulness and arousal in a diurnal insect. *Nature* 301:707-9

Kandel ER. 1976. *Cellular basis of behavior : an introduction to behavioral neurobiology*. San Francisco: W. H. Freeman. xx, 727 p. pp.

Kaneko M, HelfrichForster C, Hall JC. 1997. Spatial and temporal expression of the period and timeless genes in the developing nervous system of Drosophila: Newly identified pacemaker candidates and novel features of clock gene product cycling. *J Neurosci* 17:6745-60

Kent KS, Hildebrand JG. 1987. Cephalic sensory pathways in the central nervous system of larval Manduca sexta (Lepidoptera : Sphingidae). *Philos Trans R Soc Lond B Biol Sci* 315:1-36

Klein BA, Klein A, Wray MK, Mueller UG, Seeley TD. 2010. Sleep deprivation impairs precision of waggle dance signaling in honey bees. *Proc Natl Acad Sci U S A* 107:22705-9

Klein BA, Olzsowy KM, Klein A, Saunders KM, Seeley TD. 2008. Caste-dependent sleep of worker honey bees. *J Exp Biol* 211:3028-40

Koh K, Evans JM, Hendricks JC, Sehgal A. 2006. A Drosophila model for age-associated changes in sleep:wake cycles. *Proc Natl Acad Sci U S A* 103:13843-7

Krishnan B, Dryer SE, Hardin PE. 1999. Circadian rhythms in olfactory responses of Drosophila melanogaster. *Nature* 400:375-8

Kume K, Kume S, Park SK, Hirsh J, Jackson FR. 2005. Dopamine is a regulator of arousal in the fruit fly. *J Neurosci* 25:7377-84

Langelan RE, Fisher JE, Hiruma K, Palli SR, Riddiford LM. 2000. Patterns of MHR3 expression in the epidermis during a larval molt of the tobacco hornworm Manduca sexta. *Dev Biol* 227:481-94

Lebestky T, Chang JS, Dankert H, Zelnik L, Kim YC, et al. 2009. Two different forms of arousal in Drosophila are oppositely regulated by the dopamine D1 receptor ortholog DopR via distinct neural circuits. *Neuron* 64:522-36

Li TR, White KP. 2003. Tissue-specific gene expression and ecdysone-regulated genomic networks in Drosophila. *Dev Cell* 5:59-72

Li X, Yu F, Guo A. 2009. Sleep deprivation specifically impairs short-term olfactory memory in Drosophila. *Sleep* 32:1417-24

Mackiewicz M, Naidoo N, Zimmerman JE, Pack AI. 2008. Molecular mechanisms of sleep and wakefulness. *Ann N Y Acad Sci* 1129:335-49

McDonald DM, Keene AC. 2010. The sleep-feeding conflict: Understanding behavioral integration through genetic analysis in Drosophila. *Aging (Albany NY)* 2:519-22

Mendoza-Angeles K, Cabrera A, Hernandez-Falcon J, Ramon F. 2007. Slow waves during sleep in crayfish: a time-frequency analysis. *J Neurosci Methods* 162:264-71

Mendoza-Angeles K, Hernandez-Falcon J, Ramon F. 2010. Slow waves during sleep in crayfish. Origin and spread. *J Exp Biol* 213:2154-64

Neckelmann D, Ursin R. 1993. Sleep stages and EEG power spectrum in relation to acoustical stimulus arousal threshold in the rat. *Sleep* 16:467-77

Nijhout HF. 1980. Physiological Control of Prothoracicotropic Hormone-Secretion. *Am Zool* 20:760-

Nijhout HF. 1981. Physiological Control of Molting in Insects. *Am Zool* 21:631-40

Nijhout HF. 1994. *Insect hormones*. Princeton, N.J.: Princeton University Press. xi, 267 p. pp.

Nijhout HF, Williams CM. 1974. Control of Molting and Metamorphosis in Tobacco Hornworm, Manduca-Sexta (L) - Growth of Last-Instar Larva and Decision to Pupate. *Journal of Experimental Biology* 61:481-91

Nitz DA, van Swinderen B, Tononi G, Greenspan RJ. 2002. Electrophysiological correlates of rest and activity in Drosophila melanogaster. *Curr Biol* 12:1934-40

Parisky KM, Agosto J, Pulver SR, Shang Y, Kuklin E, et al. 2008. PDF cells are a GABA-responsive wake-promoting component of the Drosophila sleep circuit. *Neuron* 60:672-82

Pfaff D, Ribeiro A, Matthews J, Kow LM. 2008. Concepts and mechanisms of generalized central nervous system arousal. *Ann N Y Acad Sci* 1129:11-25

Pfaff DW, Phillips IM, Rubin RT. 2004. *Principles of hormone behavior relations*. Amsterdam ; Boston, MA: Elsevier Academic Press. xviii, 335 p. pp.

Pitman JL, McGill JJ, Keegan KP, Allada R. 2006. A dynamic role for the mushroom bodies in promoting sleep in Drosophila. *Nature* 441:753-6

Raizen DM, Zimmerman JE, Maycock MH, Ta UD, You YJ, et al. 2008. Lethargus is a Caenorhabditis elegans sleep-like state. *Nature* 451:569-72

Ramon F, Hernandez-Falcon J, Nguyen B, Bullock TH. 2004. Slow wave sleep in crayfish. *Proc Natl Acad Sci U S A* 101:11857-61

Rechtschaffen A, Bergmann BM, Everson CA, Kushida CA, Gilliland MA. 1989. Sleep deprivation in the rat: X. Integration and discussion of the findings. *Sleep* 12:68-87

Reinecke JP, Buckner JS, Grugel SR. 1980. Life-Cycle of Laboratory-Reared Tobacco Hornworms, Manduca-Sexta - Study of Development and Behavior, Using Time-Lapse Cinematography. *Biol Bull* 158:129-40

Riddiford LM. 1981. Hormonal-Control of Epidermal-Cell Development. *Am Zool* 21:751-62

Riddiford LM. 1996. Juvenile hormone: the status of its "status quo" action. *Arch Insect Biochem Physiol* 32:271-86

Riddiford LM, Cherbas P, Truman JW. 2001. Ecdysone receptors and their biological actions. *Vitam Horm* 60:1-73

Sakurai S, Warren JT, Gilbert LI. 1989. Mediation of Ecdysone Synthesis in Manduca-Sexta by a Hemolymph Enzyme. *Arch Insect Biochem* 10:179-97

Sauer S, Herrmann E, Kaiser W. 2004. Sleep deprivation in honey bees. *J Sleep Res* 13:145-52

Sauer S, Kinkelin M, Herrmann E, Kaiser W. 2003. The dynamics of sleep-like behaviour in honey bees. *J Comp Physiol A Neuroethol Sens Neural Behav Physiol* 189:599-607

Sehgal A, Joiner W, Crocker A, Koh K, Sathyanarayanan S, et al. 2007. Molecular analysis of sleep: wake cycles in Drosophila. *Cold Spring Harb Symp Quant Biol* 72:557-64

Seugnet L, Suzuki Y, Donlea JM, Gottschalk L, Shaw PJ. 2011. Sleep deprivation during early-adult development results in long-lasting learning deficits in adult Drosophila. *Sleep* 34:137-46

Seugnet L, Suzuki Y, Thimgan M, Donlea J, Gimbel SI, et al. 2009. Identifying sleep regulatory genes using a Drosophila model of insomnia. *J Neurosci* 29:7148-57

Shaw P. 2003. Awakening to the behavioral analysis of sleep in Drosophila. *J Biol Rhythms* 18:4-11

Shaw PJ, Cirelli C, Greenspan RJ, Tononi G. 2000. Correlates of sleep and waking in Drosophila melanogaster. *Science* 287:1834-7

Shaw PJ, Tononi G, Greenspan RJ, Robinson DF. 2002. Stress response genes protect against lethal effects of sleep deprivation in Drosophila. *Nature* 417:287-91

Siegel JM. 2008. Do all animals sleep? *Trends Neurosci* 31:208-13

Srivastava DP, Yu EJ, Kennedy K, Chatwin H, Reale V, et al. 2005. Rapid, nongenomic responses to ecdysteroids and catecholamines mediated by a novel Drosophila G-protein-coupled receptor. *J Neurosci* 25:6145-55

Stephenson R, Chu KM, Lee J. 2007. Prolonged deprivation of sleep-like rest raises metabolic rate in the Pacific beetle cockroach, Diploptera punctata (Eschscholtz). *J Exp Biol* 210:2540-7

Taghert PH, Shafer OT. 2006. Mechanisms of clock output in the Drosophila circadian pacemaker system. *J Biol Rhythms* 21:445-57

Thummel CS. 1990. Puffs and gene regulation--molecular insights into the Drosophila ecdysone regulatory hierarchy. *Bioessays* 12:561-8

Timmins WA, Bellward K, Stamp AJ, Reynolds SE. 1988. Food Intake Conversion Efficiency and Feeding Behavior of Tobacco Hornworm Caterpillars Given Artificial Diet of Varying Nutrient and Water Content. *Physiological Entomology* 13:303-14

Tobler I. 1983. Effect of forced locomotion on the rest-activity cycle of the cockroach. *Behav Brain Res* 8:351-60

Tobler I. 2000. Phylogeny of sleep regulation. In *Principles and Practices of Sleep Medicine*, ed. RT Kryger MH, Dement WC, pp. 72-81. Philadelphia: WB Saunders

Tobler I, Stalder J. 1988. Rest in the Scorpion - a Sleep-Like State. *Journal of Comparative Physiology a-Sensory Neural and Behavioral Physiology* 163:227-35

Tobler II, Neuner-Jehle M. 1992. 24-h variation of vigilance in the cockroach Blaberus giganteus. *J Sleep Res* 1:231-9

Tononi G, Cirelli C. 2003. Sleep and synaptic homeostasis: a hypothesis. *Brain Res Bull* 62:143-50

Truman JW. 1972. Physiology of Insect Rhythms .1. Circadian Organization of Endocrine Events Underlying Molting Cycle of Larval Tobacco Hornworms. *Journal of Experimental Biology* 57:805-&

Truman JW. 1990. Metamorphosis of the central nervous system of Drosophila. *J Neurobiol* 21:1072-84

Truman JW & Riddiford LM. 2002. Insect Developmental Hormones and Their Mechanism of Action. In *Hormones Brain and Behavior*, ed. DPe al., pp. 841-73: Elsevier Science (USA)

Truman JW, Talbot WS, Fahrbach SE, Hogness DS. 1994. Ecdysone receptor expression in the CNS correlates with stage-specific responses to ecdysteroids during Drosophila and Manduca development. *Development* 120:219-34

Van Buskirk C, Sternberg PW. 2007. Epidermal growth factor signaling induces behavioral quiescence in Caenorhabditis elegans. *Nat Neurosci* 10:1300-7

van Swinderen B. 2006. A succession of anesthetic endpoints in the Drosophila brain. *J Neurobiol* 66:1195-211

Van Swinderen B, Andretic R. 2011. Dopamine in Drosophila: setting arousal thresholds in a miniature brain. *Proc Biol Sci*

Walters ET, Illich PA, Weeks JC, Lewin MR. 2001. Defensive responses of larval Manduca sexta and their sensitization by noxious stimuli in the laboratory and field. *J Exp Biol* 204:457-69

Wang Z, Gerstein M, Snyder M. 2009. RNA-Seq: a revolutionary tool for transcriptomics. *Nat Rev Genet* 10:57-63

Weber B, Schaper C, Bushey D, Rohlfs M, Steinfath M, et al. 2009. Increased volatile anesthetic requirement in short-sleeping Drosophila mutants. *Anesthesiology* 110:313-6

Williams JA, Sathyanarayanan S, Hendricks JC, Sehgal A. 2007. Interaction between sleep and the immune response in Drosophila: a role for the NFkappaB relish. *Sleep* 30:389-400

Wu MN, Ho K, Crocker A, Yue Z, Koh K, Sehgal A. 2009. The effects of caffeine on sleep in Drosophila require PKA activity, but not the adenosine receptor. *J Neurosci* 29:11029-37

Yack JE & Homberg U. 2003. Nervous System. In *Lepidoptera, Moths and Butterflies: Morphology, Physiology and Development*, ed. N Kristensen. NY: Walter de Gruyter, Inc.

Yao TP, Forman BM, Jiang Z, Cherbas L, Chen JD, et al. 1993. Functional ecdysone receptor is the product of EcR and Ultraspiracle genes. *Nature* 366:476-9

Yao TP, Segraves WA, Oro AE, McKeown M, Evans RM. 1992. Drosophila ultraspiracle modulates ecdysone receptor function via heterodimer formation. *Cell* 71:63-72

Yuan Q, Joiner WJ, Sehgal A. 2006. A sleep-promoting role for the Drosophila serotonin receptor 1A. *Curr Biol* 16:1051-62

Zimmerman JE, Naidoo N, Raizen DM, Pack AI. 2008. Conservation of sleep: insights from non-mammalian model systems. *Trends Neurosci* 31:371-6

Zimmerman JE, Rizzo W, Shockley KR, Raizen DM, Naidoo N, et al. 2006. Multiple mechanisms limit the duration of wakefulness in Drosophila brain. *Physiol Genomics* 27:337-50

Zitnan D, Kim YJ, Zitnanova I, Roller L, Adams ME. 2007. Complex steroid-peptide-receptor cascade controls insect ecdysis. *Gen Comp Endocrinol* 153:88-96

Zitnanova I, Adams ME, Zitnan D. 2001. Dual ecdysteroid action on the epitracheal glands and central nervous system preceding ecdysis of Manduca sexta. *J Exp Biol* 204:3483-95

Chapter 2: Characterization of Quiescent States in *Manduca Sexta*

Abstract

During the past decade, the adult fruit fly *Drosophila melanogaster* has provided a model system for elucidation of neural mechanisms underlying various forms of arousal. In contrast, arousal states that occur during immature larval stages have not received much attention. In the developing nematode *C. elegans*, quiescent behavior that occurs around the time of the molt has sleep-like properties resembling the night-time sleep-state identified for adult Drosophila. It has long been recognized that larvae of the tobacco hornworm *Manduca sexta* exhibit prolonged quiescence during their molt. This behavior, dubbed the "molt-sleep", has been described anecdotally as a non-feeding, non-moving state, but it has not been well characterized. The molting process is controlled by the neuroendocrine system, so it is likely that changes in arousal state during the molt are also programmed by molting hormones. Using time-lapse digital recordings, we have generated rest-activity profiles across several larval stages. Rest-activity patterns do not show circadian rhythms, but do display developmental rhythms. Deprivation of quiescence or nutrition results in compensatory rebounds during the inter-molt, but not during the molting periods, suggesting a neuroendocrine-mediated “shut-down” of homeostatic control mechanisms during the molting period. Using both mildly-arousing and noxious stimuli, we discovered that quiescent behavior, both in and outside of the molt-sleep, is characterized by an increased arousal threshold and is rapidly reversible. Although spontaneous activity is low, molting larvae maintain the ability to locomote and

to escape from noxious stimuli at a rate similar to that observed for intermolt larvae. We propose that molting larvae engage in an adaptive sleep-like state that promotes energy conservation (one of many possible functions of sleep during this non-feeding state) while retaining the ability to respond to a changing environment. The correlation of these changes in quiescent levels with the known hormone profiles suggests that insect larvae may provide an excellent model system for studies of interactions between steroid hormones, central modulatory systems, and quiescent behaviors.

Introduction

The use of "simpler" organisms—organisms with fewer cells in their nervous systems—as model systems, has provided the field of neuroscience with general principles, and has led to insights into the neural basis of our own human behavior. Locomotion, mating, foraging, predation and predator avoidance are among the list of behaviors, the neural correlates of which we can claim at least a partial knowledge in one, or several model systems.

An *absence* of motor behavior at the appropriate time can also be important to the survival of an animal. "Quiescent behavior" is a term that can be used to describe an animal in a non-feeding, non-mating, generally non-moving state. Types of quiescence include short-term states of vigilance and quiet wakefulness (rest)—brief interludes between waking-state activities. Other states of quiescence, such as mammalian hibernation and insect diapause, can last for many months. Many animals also experience a daily rhythm in their overall level of activity, quiescence being most

concentrated during a particular fraction of the day. For diurnal animals such as humans, quiescent behavior is consolidated during the nighttime, and the type of quiescent behavior during this time is called “sleep.”

Over the past decade, the study of quiescent behavior in invertebrate organisms has gained momentum due to findings that the quiescent behavior of adult *Drosophila melanogaster* resembles sleep-like states found in mammals (Hendricks et al 2000; Shaw et al 2000). Investigations into endogenously-generated sleep-wake transitions, as well as arousal states evoked by environmental stimuli, demonstrate a conservation of neurotransmitter systems involved in the modulation of both mammalian and insect arousal. Sleep in the adult fly can be modulated by pharmacological agents, its timing is regulated by circadian clocks, and its onset is accompanied by the expression of distinct neural genetic markers, as well as characteristic electrophysiological signatures in the brain (Andretic et al 2005; Cirelli et al 2005; Hendricks et al 2000; Kume et al 2005; Nitz et al 2002; Shaw et al 2000). The use of adult insects as model systems to gain insights into basic principles underlying the neural regulation of quiescent behaviors such as sleep is promising.

In contrast to the adult stage, quiescent behaviors that accompany the immature larval stages of insects have not received as much attention. In the developing nematode *Caenorhabditis elegans*, quiescent behavior that occurs during the molting period (the transitions between larval stages) has sleep-like properties resembling the nighttime sleep-state identified for adult *Drosophila* (Raizen et al 2008). Molting is common to all ecdysozoan animals, including arthropods and nemotodes (Ewer 2005). For many

insects, the adult form is preceded by a larval stage, when the animal feeds and increases its size prior to metamorphosis into the adult, reproductive stage. Because the cuticle (the outer covering of the insect) does not increase in size, larval stages are separated by a molting period, whereby the animal synthesizes a new larger cuticle and sheds the old.

Molting physiology and behavior are under the control the neuroendocrine system. The lepidopteran insect *Manduca sexta* has long served as a useful model system to study the neuroendocrine regulation of physiology and behavior associated with the molt. In *Manduca*, the larval molt can be divided behaviorally into an extended period of quiescence (up to 30 hrs during its molt to the 5^{th} and final larval stage), during which the animal breaks down the old cuticle and synthesizes the new one, and a brief period of activity called ecdysis—a stereotypic centrally-patterned behavior that results in the shedding of the old cuticle. The relatively large size of *Manduca's* nervous system and hemolymph volume has aided the discovery and characterization of hormones that govern the molt, as well as behavioral and electrophysiological studies that have helped to define ecdysis behavior.

Although ecdysis behavior has been well-characterized in *Manduca* and other insects, the period during the molt that precedes ecdysis has not received similar attention; it has only been described through casual observations as a period of inactivity, and has been dubbed the "molt-sleep" (Reinecke et al 1980). In a recent study, it was demonstrated that the active form of the insect steroid molting hormone ecdysone has sleep-promoting effects in the adult fly (Ishimoto & Kitamoto 2010). Steroid molting hormones also coordinate transitions between developmental stages, including the larval

molts. Because levels of molting hormones in relation to several developmental markers are known for *Manduca sexta* during its transition from the 4th to 5th larval stage, this model system can be used to examine possible correlations between neuroendocrine events and early-molt behavioral transitions. Also, the long duration of *Manduca's* intermolt and molting period, along with its large size and easy accessibility (unlike *Drosophila* larvae, it does not burrow), makes *Manduca* an excellent model system for the characterization of quiescent behavior, in developing holometabolous larvae.

In this study, we have profiled rest-activity patterns of *Manduca sexta* across multiple larval stages, and provide the first characterization of larval quiescent behavior both within and outside of the molting period. Rest-activity patterns do not show circadian rhythms, but do display a "molting pattern." Levels of quiescence decrease with increasing time within a larval stage until the predicted peak of the molting hormone 20-hydroxyecdysone (the active molting hormone in larval staged *Manduca*), at which time quiescent levels increase dramatically, and remain elevated until ecdysis to the next larval stage. Using both mildly arousing and noxious stimuli, we discovered that quiescent behavior, both within and outside of the molting period, is characterized by an increased arousal threshold and is rapidly reversible. Although spontaneous activity is low, molting larvae maintain the ability to locomote and to escape from noxious stimuli at rates similar to those observed for intermolt larvae. Also, although we observe a robust homeostatic regulation of both feeding and quiescence during the intermolt period, the homeostatic regulation of these behaviors seems to be shut down following the onset of molting-quiescence. We propose that molting larvae engage in an adaptive quiescent

state that promotes energy conservation (one of the many possible functions of quiescence during this non-feeding state) while retaining the ability to respond to a changing environment. The correlation of changes in quiescent level with known hormone profiles suggests that insect larvae may be excellent model systems for studies of interactions between steroid hormones, central modulatory systems and quiescent states. That molting-quiescence is also accompanied by changes in the way larvae regulate both foraging and quiescent behavior also suggests that this system might prove to be an excellent model system for the study of mechanisms underlying the homeostatic control of sleep and feeding in insects.

Materials and Methods

Insect rearing conditions. *Manduca sexta* were reared at the University of California, Riverside. Adults were maintained in a rearing room at 27^{o}C +/-1^{o}C under a 16 hr light: 8 hr dark (16L:8D) photoperiod and fed 40% sugar water *ad libitum*. Eggs were transferred to incubators set at a temperature of 25^{o}C +/-1^{o}C under a 17L:7D photoperiod (Lights on at 8:30AM), and all larval stages were reared under these conditions. Hatched 1st instar larvae were transferred to individual 1oz disposal plastic cups, where they were maintained until transferred as late 4th or early 5^{ths} to individual 5 oz cups. Larvae were fed *ad libitum* on a modified artificial diet (Bell & Joachim 1976).

Quiescence levels. ***Setup and analysis*.** All behavior was monitored in an isolated dark-room (under various photoperiods) at 25 +/-1°C. Behavior was monitored using time-

lapse digital recordings. A webcam (Logitech QuickCam Deluxe for Notebooks; Logitech, Freemont CA) and time-lapse recording software (Flix version 3.3; Nimisis) was used to acquire images onto a desktop computer. Images were viewed and scored using an imaging capturing/processing utility (Virtualdub v1.9.7). Frames were captured every 10 sec for the duration of each recording session. Behavior was scored by visually monitoring shifts in position between frames. Each frame was scored based on a comparison to the previous frame. For frames that showed no change in larval position when compared to the previous frame, that frame was assigned a score of "1" (quiescent between frames); a score of "0" was assigned to frames for which a change in position was detected when compared to the previous frame (active between frames). The fraction of quiescence was then calculated for selected time-blocks.

***Long quiescence profiles*.** For long quiescence profiles, each larval stage was recorded independently, and individual larvae were used for the recording of only one larval stage. For 2nd instar recordings, animals were staged so that by 10AM on the day prior to recording, all animals showed fluid-filled head capsules and an absence of mandible tanning. Recording sessions then began the day following ecdysis to the 2nd instar, and continued uninterrupted until ecdysis to the 3rd instar had been completed. For recordings of the 3rd and 4th larval stages, larvae with fluid filled head capsules were selected, and recording sessions began prior to ecdysis to the stage of interest, and continued without interruption until ecdysis to the following larval stage was completed. Behavioral arenas were constructed using polystyrene Petri dishes (Falcon #351008 and #351005; Becton Dickinson, Franklin Lakes, NJ). Arena sizes varied as follows: (1) A depth of 1 cm and

diameter of 3.5 cm for 2nd instar recordings, (2) A depth of 1.5 cm and a diameter of 3.5 cm for 3rd instar larvae, and (3) A depth of 4 cm and a diameter of 8.5 cm for 4th instar larvae. Larval diet formed the base of all arenas, and air holes were formed on the upper edges of the arena using the tip of a hot soldering iron. For maximal resolution, only 3 larvae (each in their respective, individual arenas) were monitored during each recording session. Arenas were placed on a vibration isolation table and shielded from air currents. For recordings under continuous light conditions (L:L), arenas were illuminated continuously by white light (Energy Smart Soft White 13 Watt bulbs #72466, 870 lumens; General Electric). For larvae that were recorded under a light cycle (L:D conditions), the photoperiod was set to a 16L:8D cycle (lights "ON" at 9AM) using an automated timer, and infrared lighting (wavelength=850 nm) was used to monitor larvae during the scotophase period. For L:D recordings, camera resolution allowed for the recording of only one larvae per session.

Starved controls. Larvae were reared under 17L:7D (colony) conditions. Developmental markers and larval weights were used to ensure the selection of only Gate II larvae approximately 24 hours prior to the onset of natural head capsule slippage (*see staging methods for qPCR*). Larvae were recorded under constant light conditions, and quiescent profiles were monitored using the same method that was used for *long quiescent profiles,* except that no food was provided during the recording sessions, and arenas were composed of 5 1/2 ounce translucent plastic souffle cups (#P550; Solo Cup Company, Urbana IL) and covered with a 100x20 mm style Petri dish lid (Falcon #351005). Air

holes were made in the upper portions of the cup using forceps. Recording sessions were terminated after 17 hours.

Bout duration. Quiescent-bout durations were calculated using Clampfit 10.2 software (pClamp 10.2; Molecular Devices). Bouts were calculated using scores obtained from long quiescence profile analyses. Prior to analysis, all values were set relative the time of ecdysis to the next larval instar. Quiescent-bout initiation was defined as the beginning of any period of inactivity $\geq$ 10 sec. The termination of a quiescent bout was defined as the beginning of any period of activity > 30 sec.

Arousal Thresholds. ***Behavior.*** A water bath was constructed using a hot plate and an 8 in x 8 in aluminum baking pan. The temperature of the water bath was set to room (25°C) temperature, 40°C, or 50°C. Temperature of the water bath was monitored continuously with a digital cooking thermometer. Behavior "arenas" were constructed using 23 cm diameter (d) foam plates (Stater Bros; Colton, CA) with 12.5 cm d holes cut out of the middle. Filter paper (15 cm d; Whatman #1005150) was stapled to the surface of the plates so as to cover the opening and form the base of the arena. For control (DRY) conditions, filter paper was stapled to the surface of uncut plates. A plastic, two-tiered circular ledge formed an exterior rim around the circumference of the arena. Prior to testing, animals were placed in the center of their arenas under 1 ½ oz plastic cups for a $\geq$ 15 minute (min) equilibrium period. Animals (and arenas) were used only once.

During each recording session, arenas were placed gently, one at a time, on the water bath. Placement on the bath coincided with an almost immediate "wetting" of the filter paper. The response of each animal was recorded for 10 min, or until such time as the animal was able to escape water contact by climbing over the plastic ledge. Behavior was monitored using the same setup used to monitor quiescent levels, except that time-lapse recordings were set to a 0.2 sec delay between frames (5 frames/ sec).

Scoring and analysis. Images were viewed and scored using an imaging capturing/processing utility (Virtualdub v1.9.7). The time of stimulus onset was defined as the frame during which the wetting of the filter paper encompassed an area that completely surrounded the larva. Locomotion onset was defined as the frame corresponding to initiation of peristaltic contractions that led to a shift in larval position. Time of edge contact was defined as the frame where the anterior tip of the larvae made contact with the peripheral ledge. Larvae were considered to have escaped the arena if at any time all portions of the larval body were lifted from the wet filter paper. For those larvae that did not escape under DRY and 25°C conditions, quiescence levels were calculated using the methods outlined in *quiescence levels*.

Staging. All animals were staged so that developmental timing could be estimated just prior to testing. Following testing, time-lapse digital recordings (1 min between frames) were used to monitor development, and the time of the completion of ecdysis to the next instar was noted. Developmental categories were based on the time of testing, relative to completion of ecdysis. The following categories were used: Late 4^{th} (~40 hrs prior to ecdysis), Middle-molt (~15 hrs prior to ecdysis), Late-molt (~6 hrs prior to ecdysis), and

Late-molt (~3 hours prior to ecdysis). All animals were reared under colony conditions (17L:7D photoperiod, 25 +/-1°C) and were moved to the behavior room just prior to testing.

Quiescence deprivation. ***Set-up.*** In order to deprive larvae of behavioral quiescence, a semi-automated deprivation system was devised. A cardboard box lid with dimensions 27 cm x 27 cm was secured upside-down to a test tube mixer/rocker (Thermolyne Vari Mix; #M48725). Within the lid, 3 separate "tracks" were constructed using 2 ml polystyrene disposable pipets that spanned the area of the lid. Each track was constructed to allow for the unimpeded movement of a toy car (2010 Ford Mustang GT Hot Wheels; Mattel). Petri dish lids (Falcon #351007) were secured to the roof of each car to cradle the 5 1/2 ounce plastic cups containing an individual larva. Larval diet formed the base of each cup.

Rocker speed was set to 1 rock for every 12-14 sec. The toy cars bumped into *Drosophila* vial plugs (Flugs; Genesee Scientific) that had been secured to the box-lid at the ends of the tracts. Impact did not result in any visible injury to the larvae. In most cases, larvae were either dislodged from their position on the food, or rolled so that they were forced into a righting reflex. Larvae were visually monitored during the recording session. If larvae were able to secure themselves against periodic rolling, they were gently dislodged from their position using either blunt forceps or by tapping the base/sides of the arena. During the deprivation sessions, control larvae were kept in the same room and in the same type of behavioral arena, but on a table away from the deprivation set-up. Immediately following the deprivation sessions, the 3 deprived and 3

control animals were weighed and then transferred to new arenas composed of 1.5 ounce plastic cups containing 15g of larval diet that formed the arena base. Post-deprivation quiescence behavior was recorded for 24 hrs under L:L conditions. Behavior was monitored and analyzed using the same setup outlined for *quiescent levels*.

Intermolt larvae were deprived of quiescence for 3, 6 or 12 continuous hours. For all inter-molt groups, larvae were staged so that deprivation was terminated at 9 PM, ~27 hrs following larval ecdysis to the 4th instar. Molting larvae were deprived of quiescence during either the last 6-9 hrs of the molt to the 4th instar, or during the molt to the 5th instar for the first 6 hrs following HCS.

Profiling *period* (*per*) gene expression. ***Isolation of total RNA from nerve cord and peripheral tissues.*** Late 4th instar larvae were selected randomly from a colony reared at 25 +/-1°C, under a 17L:7D photoperiod. For isolation of the full nerve cord, a single larva was anesthetized on ice for 5 min, and a small incision was made through the body wall by snipping the base of the dorsal horn with scissors. The larva was then submerged in ice-cold saline made to the specifications outlined in Zitnan (1999). The body wall was cut dorsally along the midline, and gut and fat body were removed to expose the ventral nerve cord. Peripheral nerves were trimmed close to the ganglia, and the entire nerve cord (terminal abdominal ganglia to brain) was removed. Peripheral epidermis and fat body were isolated from a separate larva by cutting a small square of tissue from the body wall and scraping the adhering tissues with a sharp scalpel. Tissues were immediately placed in tubes on try ice, and then stored at -80°C until further use.

Total RNA was extracted from ground samples using TRIzol (guanidinium thiocyanate/phenol solution for RNA extraction) (Invitrogen, Carlsbad, CA) according to the manufacturer's guidelines. Each sample was DNase treated using TURBO DNA-*free* (Applied Biosystems/Ambion), and total volumes (8 ul/sample) of total RNA were reverse-transcribed into cDNA using the Superscript First Strand Synthesis System for RT-PCR kit (Invitrogen) according to the manufacturer's protocols.

Primers were designed from a 1062 bp partial clone of a *Manduca sexta period* gene, (NCBI Accession #U12773) (Reppert et al 1994). The following primers were used for amplification of an expected 976 bp amplicon: Forward 5'-CAGATCGTTCATCGACTTCGTTCATCC-3', Reverse 5'- GCTAGACTTACTGTCGT TGTAGTCGTGGTGC (Integrated DNA Technologies; San Diego, CA). PCR was performed as follows: 94 °C for 2 min for 1 cycle, 94°C for 20 s, 58°C for 20 s, 72°C for 1 min for 35 cycles, and a final extension at 72°C for 10 min using Accupower PCR PreMix (Bioneer; Alameda, CA). Portions of the PCR products were run on a 1.2% agarose gel w/ ethidium bromide and compared to standards (1kb plus; Invitrogen). The remaining PCR product was purified using QuickClean 5M PCR Purification Kit (GenScript; USA) and submitted for Sanger (BigDye) sequencing (Applied Biosystems) at the Genomics Core of the University of California, Riverside.

Per gene expression profiles from 4th stage whole brains using Quantitative PCR (qPCR). Larvae were reared under a 17L:7D photoperiod at 25°C, with lights-on at 8:30AM. The timeline below outlines the developmental timing of larvae used for qPCR experiments.

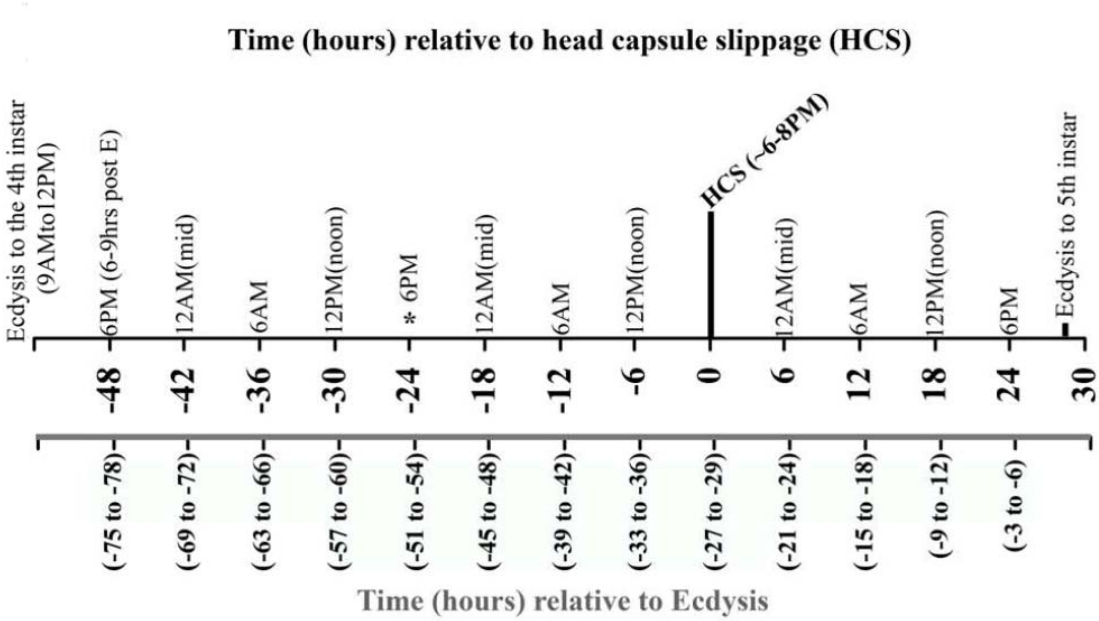

Figure 2-1. Timeline: Gate II 4th /Gate I 5th larval development. All insects were reared under a 17L:7D (lights on at 8:30 AM) photoperiod at 25°C. Developmental timing is displayed in 6 hr intervals. On the upper scale, time relative to HCS is show along with the corresponding time-of-day. On the lower scale is shown the time of development relative to ecdysis to the 5th instar. For these larvae, ecdysis is estimated to occur between ~27 and 29 hrs following HCS. The entire larval stage, from ecdysis to ecdysis, is estimated to be ~84 to 87 hrs in duration.

Larvae were staged relative to the time of the HCS that occurs during the molt to the 5th instar. Only gate II, 4th/gate I, 5th instar larvae were used for these experiments, as these larvae were found to be highly synchronous when staged using weight indicators and developmental markers. Larvae were selected during the late 3rd instar if HCS occurred after 4PM, and weights were measured to be over 200 mg following HCS during the molt to the 4th instar. Larvae that ecdysed, or showed air-filled HC with

blackened mandibles by 9AM the next morning, were selected for further staging; these animals undergo HCS (molting to the 5th instar) ~54 to 57 hrs following ecdysis to the 4th instar. Animals dissected prior to 24 hrs before HCS were staged based on pharate 4th weights and developmental markers. For animals dissected between -24 and -6 hrs relative to HCS, developmental time was further ensured by using an additional weight marker at -22 hrs; only larvae over 600mg by -22 hrs (~4PM) were selected. All larvae from 0 to 30 hrs following HCS were staged by visually monitoring the time of HCS. Brains were harvested from animals at the following developmental times relative to HCS: -48 hrs (n=24, n=20, n=17); -36 hrs (n=20, n=20, n=19); -24 hrs (n=17, n=19, n=17); -18 hrs (n=17, n=17, n=10); -12 hrs (n=12, n=12, n=12); -6 hrs (n=10, n=12, n=11); 0 hrs (n=12, n=10, n=10); +6hrs (n=12, n=12, n=11); +12 hrs (n=12, n=12, n=10); +18 hrs (n=9, n=12, n=10); +24 hrs (n=12, n=12, n=11). Brains were dissected by first chilling larvae on ice for 5 min (or until immobile), and then decapitating and pinning heads on a dissection dish filled with ice cold saline. For all larvae at developmental stages prior to HCS, brains were exposed by cutting a window through the head capsule using a sharp scalpel. Prior to HCS, the brain lies just ventral to the head capsule. For all larvae at developmental stages following HCS, brains are easily exposed by pinning the decapitated head head-capsule-side-down. Once exposed, nerves and trachea were carefully trimmed as close to the ganglia as possible, and the brain was placed in a tube on dry ice. Pooled brain samples were stored at -80°C until further processing.

Total RNA was extracted and cDNA was synthesized using the same techniques as stated above for whole ganglia, with some adjustments. For these samples, the

quantity of total RNA extracted was assessed using a spectrophotometer (Nanodrop ND-1000 Spectrophotometer). For each sample, 1µg of total RNA was used in the reverse transcription reaction. To control for possible genomic DNA contamination, 1µg of total RNA was also used for a no-RT control reaction, and contamination was checked for using PCR followed by gel electrophoresis.

Primers were designed from the period gene sequence verified as present with the CNS of *Manduca* larvae (NCBI Accession #U12773). Primers were also optimized for *Manduca* non-muscle actin (act) (NCBI Accession #AJ519536) to be used as the reference gene. Gradient PCRs followed by electrophoresis on 2% agarose w/ ethidium bromide gels were first used to check for specificities of primers and optimal annealing temperatures. Sequence identity of the amplicon was verified using Sanger (BigDye) sequencing (see above). Serial dilutions of cDNA were then used with qPCR to generate standard curves to evaluate amplification efficiency and to further check the specificity of primers. QPCR was carried out in 25µl reaction volumes containing 12.5µl of IQ SYBR Green Supermix (Bio-Rad, USA), 2µl of cDNA template, primers at the appropriate concentrations, and water. The Bio-Rad iQ5 Real Time PCR Detection System (Bio-Rad, USA) was used according to the manufacturer's specifications. The optimized period gene primers used for qPCR analysis were as follows: Forward 5´-TCTAATCCCGACGTGTTCC-3´, Reverse 5´-TCATCTGCTGTTTGGCTACC-3´ used at a concentration of 500 nM with an expected amplicon size of 154bp. The optimized act primers were Forward 5´-GTATGGAAGCCAACGGTATTCACG-3´, Reverse 5´-TGTCGAAGGAGCAAGAGCTGTG-3´ at a concentration of 200 nM with an expected

amplicon of 170bp. For each experimental replicate, cDNA (diluted 10-fold) from every developmental time-point sampled was run in triplicate on the same plate. All control reactions were also run in triplicate on the same plate with experimental reactions. The cycling parameters were 1x 3 min @95°C, 40x (20 sec @95°C, 20 sec @50°C, 20 sec @72°C), 1x 1 min @95°C, 1x 1 min @55°C, followed by a melt curve from 55 to 95°C at 0.5°C steps (10 sec/step) to verify amplification specificity. The results were analyzed using the iCycler iQ Optical System Software v2.0 (Bio-Rad Laboratories). The threshold was set manually within the linear amplification range for all expression data. The crossing point of an amplification curve with the threshold represents the cycle threshold (Ct). Ct values were exported to Microsoft Excel for further analysis. Relative expression ratios were calculated by the Pfaffl equation (Pfaffl 2001).

Results

Larval quiescence profiles show developmental rhythms. Rest-activity patterns of larval-staged *Manduca sexta* have been studied in the past using a variety of direct and indirect techniques geared mostly toward the elucidation of inter-molt feeding behavior (Bernays 2000; Bowdan 1988; Heinrich 1971; Reynolds et al 1986; Stewart & Nelson 1977; Timmins et al 1988). Research into the determinants of molt-initiation has examined the relationship between nutritional state, growth rate and the timing of the release of molt-initiating hormones, but for these studies, changes in behavioral state were largely ignored (Nijhout & Williams 1974; Safranek & Williams 1984). Observations of *Manduca* larval behavior have been limited to individual studies of either

the inter-molt period or the end of the molting period (around the time of ecdysis), so behavioral studies have excluded the transitional period between feeding and molting behaviors, a time when molting hormones are known to be fluctuating (Langelan et al 2000). In order to investigate the possible relationship between changes in levels of developmental hormones and the initiation of the increased quiescence reported for molting larvae, rest-activity profiles (also referred to in this study as *quiescence* profiles) were constructed for the entirety of a larval stage, from ecdysis to ecdysis.

To determine the distribution of quiescence across a larval stage, time-lapse digital recordings were used to monitor larvae for the duration of the 4^{th} instar under constant light conditions. Snapshots were taken every 10 sec beginning late during the molt to the 4^{th} stage, and ending after the completion of ecdysis to the 5^{th} stage. *M. sexta* exhibits a variety of behaviors during its larval stages, including subtle head movements associated with feeding and searching, locomotion, and robust defensive responses (Bernays & Woods 2000; Miles & Booker 2000; Walters et al 2001). The purpose of this quiescence profiling was not to asses the distribution and frequency of every behavior in the larval behavioral repertoire, but rather to examine the tendency at any given time during a developmental stage of the animal to exhibit any type of motor behavior. In this case, the only behavior that was accurately measured was "quiescent behavior," defined here simply as a state of inactivity. Movement then, was used as a gross, indirect measure of a *generalized* arousal state, the increase of which can be associated with a subsequent increase in the probability of the occurrence of some behavior (Pfaff et al 2008). Regardless of the subtlety of the movement, the animals were considered to be

active if there was any indication of movement, and behavioral quiescence was defined as a period during which movement could not be detected.

Fractions of quiescence in 1 hr bins were calculated for 8 individual larvae across the entire duration of their 4th stage. The duration of the 4th stage (from ecdysis to ecdysis) varied within a range between 90 to 110 hrs, indicating that both Gate I and Gate II larvae were used for these initial observations of quiescent behavior (Truman 1972).

Circadian rest-activity patterns are commonly observed for insects in the adult stage. Direct and indirect measurements have indicated a lack of influence of either time-of-day or photoperiod on levels of feeding behavior during the larval stages of *Manduca*, both in the field and under controlled laboratory conditions (Bernays & Woods 2000; Reynolds et al 1986; Stewart & Nelson 1977). In these studies, detailed behavioral observations were limited to discrete portions of the larval cycle, focused mainly on feeding behavior during the 5th and often final larval stage. To examine whether quiescent behavior across an entire larval stage might fluctuate with respect to a 24 hr cycle, all 1 hr fractions of quiescence, and all average 1 hr fractions of quiescence were plotted against time-of-day (Figure 2-2A and 2-2B, respectively). Average levels of quiescence during each hr of the 24 hr day are shown in Figure 2-2B. The average of all average 1 hr quiescence fractions for larvae within the 4th instar is 0.73 (+/- 0.005 s.e.m.). Although the level of quiescence for an individual larva can vary from moment to moment, no significant differences in average quiescence values were observed for any particular hour across the entire 24 hr daily cycle, which supports previous reports that larval behavior is not influenced by an endogenously-driven circadian rhythm

Previous studies have demonstrated that the timing of ecdysis to the 5th instar occurs at a fixed time interval following the initiation of endocrine events that lead to the onset of molting (Truman 1972). To test whether there is a relationship between quiescence levels and changes in hormone levels associated with the onset of molting, individual fractions of quiescence were set relative to the time of ecdysis to the 5th instar (Figure 2-2C). For these analyses, the duration of the developmental time from which fractions were calculated was limited to 90 hrs because the minimum larval stage duration was slightly more than 90 hrs. When all individual fractions are set relative to ecdysis, quiescence levels do fluctuate across developmental time (Figure 2-2C). Average quiescence levels show a pattern of declining gradually from maximum values between 0.7 and 0.8, to the minimum fraction of quiescence of 0.38 (+/- 0.06 s.e.m.) occurring at 37 hrs prior to the completion of ecdysis (Figure 2-2D). Comparisons between quiescence levels during early, middle and late inter-molt (feeding) stages were made by calculating the fraction of quiescence in 10 hr bins between -90 and -80 (early) (Ave=0.73 +/-0.01 s.e.m.), -70 and -60 (middle) (Ave=0.67 +/-0.02 s.e.m.), -50 and -40 (late) (0.55 +/-0.03 s.e.m.) hours prior to ecdysis. At the -36 hr mark, quiescence levels begin to rise dramatically, with average values exceeding 0.8 by -31 hrs. For the remainder of the molt (excluding ecdysis events that occur within the final 2 hrs), 86% of all fractions fall between 0.9 and 1, exceeding any levels observed during the intermolt feeding stage. The average fraction of quiescence for molting larvae between -20 and -10 hrs was 0.97 +/- 0.004 s.e.m. Significant differences were found between all intermolt and molting 10 hr average fractions of quiescence.

The sudden change in quiescence level correlates well with developmental events associated with the rise and fall of the molting hormone 20-hydroxyecdysone (20-HE) (Langelan et al 2000). At ~27-30 hrs prior to the completion of ecdysis, the larvae used for these long quiescent profiles undergo apolysis of the head capsule, or head capsule slippage (HCS), which is the movement of the head capsule downwards to allow for the formation of the new 5th instar capsule. HCS is a well-known developmental marker used to stage for neuroendocrine events occurring during the late molt, and previous reports on the timing of this event relative to ecdysis agree well with the timing presented here (Bollenbacher et al 1987; Langelan et al 2000; Zitnan et al 1999). According to studies that have examined ecdysteroid levels at time-points *prior* to HCS, 20-HE levels in the hemolymph begin to rise at least ~18 hrs prior to HCS, and peak at ~5-6 hrs prior to HCS onset (Langelan et al 2000). The onset of the sudden and dramatic rise in quiescent level coincides with the timing of the putative 20-HE peak. This correlative relationship suggests the possibility that molting hormones can influence arousal state during the larval stages.

Although circadian rhythms of activity were not observed in the previously-described 4th stage larvae, it is possible that continuous light conditions disrupted the function of circadian clocks, thus obscuring a possible natural endogenous rhythm (Aschoff 1960). Also, it was not known whether photoperiod itself might act exogenously to influence arousal state across the developmental stage. In order to test for these possibilities, 4th stage larval activity was monitored under a 16L:8D photoperiod. As with larvae recorded under continuous light conditions, there were no significant

differences between average quiescence level when plotted against time-of-day (Figure 2-3A). Interestingly, the overall average level of quiescence was slightly lower for larvae recorded under the L:D photoperiod than for larvae recorded under continuous light. A previous study of feeding behavior suggests that, although feeding rate as measured by fecal evacuations is not influenced by photoperiod, larvae reared under continuous darkness or under a photoperiod develop at slightly faster rates when compared to larvae reared under continuous light conditions (Stewart & Nelson 1977). How continuous light might lead to an increase in baseline quiescence level is not known. It is also possible that the lowered baseline level of quiescence is an artifact of the low sample size. In any case, an overlay of L:L and L:D quiescence profiles shows that the *patterning* of rest-activity matches that observed under continuous light conditions (Figure 2-3B). Quiescence decreases with increasing time within an instar, and then increases to levels above 90% following the predicted time of the ecdysteroid peak. An example of an individual quiescence profile of a larva recorded under 16L:8D photoperiod is provided in Figure 2-3D. When average quiescence levels recorded during the first photophase were compared to average quiescence levels recorded during the first two (surrounding) scotophases, no significance difference in average quiescence levels were detected (Figure 2-3C); which demonstrates that although baseline quiescence is slightly lower in larvae recorded under the L:D cycle, this increase in activity is distributed evenly across both light conditions, and the events of “lights on” or “lights off” does not influence a change in overall activity during the 24 hour cycle. In summary, the L:D cycle did not

alter the overall pattern of rest-activity across the 4th larval stage, which follows a developmental pattern that is repeatable across individuals of the same stage.

Prior to its 5th and final larval stage, *Manduca sexta* develops through a successive series of larval stages during which the rise and fall of molting hormones show a repeated pattern. To test if the pattern of quiescent behavior observed for individuals during the 4th larval stage is repeatable across larval stages, quiescence profiles were also recorded for the entire 3rd instar and the latter half of the 2nd larval stage. When fractions of quiescence are set relative to the time of ecdysis, a developmental pattern emerges for both 2nd and 3rd instar larvae, showing a decrease in quiescence with increasing time within the instar, followed by a rapid rise in quiescence level, leading to a prolonged elevated quiescent level that persists until the onset of ecdysis behavior (Figure 2-4). This developmental pattern, then, is repeatable both across individuals within an instar and across instars, demonstrating that prior to the final larval stage, larval staged *Manduca sexta* show a characteristic rest-activity pattern that is well-correlated with changes in molting hormones.

Quiescence during the molt is characterized by an increase in maximal bout duration. During both the intermolt and molting periods, *Manduca* larvae are quiescent (and active) in bouts. A typical 4th instar quiescence profile is illustrated in Figure 2-5A. Shown is the fraction of quiescence in 10 min time-windows, shifted 10 sec for each data-point. Note that each deflection represents an increase in activity. When quiescence levels begin to rise at ~36 hrs prior to the completion of ecdysis, there is a corresponding

change in typical bout parameters. A comparison of typical inter-molt and molting activity is provided (Figure 2-5B, 2-5C). Interestingly, although larvae spend much of their time in a quiescent state following HCS, spontaneous activity bouts do still occur, suggesting that larvae retain the ability to move during the molting period.

The duration of all quiescent bouts was calculated for the 8 larvae recorded under L:L conditions and sorted in 5 hr bins according to occurrence relative to the time of ecdysis. As with quiescence levels, average quiescent bout durations decrease with increasing time within the feeding period of the 4^{th} instar (Figure 2-6). This supports previous investigations into feeding behavior of 5^{th} instar *Manduca sexta* that showed increases in the duration of feeding bouts as the 5^{th} instar proceeds; in those studies, feeding duration also increased at the expense of the duration of inter-feeding intervals (Bowdan 1988; Reynolds et al 1986). Between 25 and 30 hrs prior to ecdysis, peak bout durations increase to levels that exceed all intermolt values. Only during the molting period do quiescent bouts exceed 80 min, the maximum value reaching 183 min mid-way through the molting period. The percentage of bouts falling within different ranges of bout durations was compared for early/late inter-molt and molting periods. During early feeding periods, the majority of quiescent bouts fall within the 10 to 30 min range, whereas a higher percentage of bouts during the late feeding stage fall between 1 to 5 min (Figures 2-7A, 2-7B). During the molting period, the duration of most bouts fall within a range between 10 and 30 min, but in contrast to inter-molt values, over half of all bouts are above 30 min, and 29% of quiescent bouts are over 1 hr (Figure 2-7C). Only 1% of all bouts extend beyond one hr during the inter-molt period examined.

The increased consolidation of quiescence during the molting period could be due to a decrease in the drive to initiate and maintain behaviors such as feeding, an increased drive toward quiescence behavior, or a combination of both. It is also possible that arousal states are not at all altered, but that anatomical changes during the molting period serve to inhibit movement, (although the presence of spontaneous activity during the molting period suggests otherwise). That average quiescence level and bout duration show a rapid increase at the developmental time-point that corresponds to the predicted ecdysteroid peak suggests that the onset and maintenance of molting quiescence may be programmed by molting hormones. The rise and the fall of ecdysteroids programs successive bouts of gene expression that affect both anatomy and behavior. In addition to directing the synthesis and absorption of cuticle, molting hormones directly and indirectly affect the nervous system to organize the ecdysis behavior that terminates the molt; perhaps molting hormones also affect the larval nervous system earlier during the molt to bring about a decreased general arousal state. However, as mentioned previously, the peak of ecdsyteroids is also followed by apolysis of the old head capsule, which effectively blocks the larval mouthparts, rendering larvae incapable of feeding until after ecdysis is complete. Although quiescence begins to increase prior to the time when slippage of the old head capsule is noticeable, it is not known exactly when the old mouthparts become dysfunctional. The increase in quiescence levels that starts ~5-7 hrs prior to the onset of HCS might be the result of a sudden inability to feed. It is possible that the elevated quiescence levels observed during the molting period are due either to a

lack of nutrition, or to a lack of feeding-related sensory input that might normally drive larval activity.

Starvation does not trigger molting quiescence. To determine whether food-deprivation can lead to a sudden increase in quiescent behavior similar to that observed for larvae ~35-37 hrs prior to ecdysis, time-lapse digital recordings were used to monitor the quiescence levels of late 4th intermolt food-deprived larvae. Larvae were staged so that deprivation commenced an estimated 24 hrs prior to HCS. Results show that larval quiescence decreased immediately following the onset of starvation, and fractions of quiescence are maintained on average below 30% for the first 7 hrs, and for the remainder of the 17 hr recording sessions, average quiescence levels do not rise to values characteristic of molting levels, with the maximum average reaching only 61% at 15 hrs post-deprivation (Figure 2-8A). A typical quiescence profile for an individual deprived larvae is shown in Figure 2-8B, where average fractions of quiescence were calculated for 10 minute time-windows, and shifted 10 sec for each data point. No larvae showed quiescence bouts with durations exceeding 1 hr, and the maximum bout duration for any larvae was 44.5 min at 15 hrs post deprivation onset (data not shown). For all larvae, an average of only 3.7% of all bouts extended beyond 30 min, and the average bout duration was 9.6 min. These results indicate that both quiescent level and bout durations do not resemble those measured for molting larvae, suggesting that food deprivation does not lead to the onset of molting quiescence, at least within the 17 hrs of deprivation for late intermolt larvae. This result was expected based on previous reports that *Manduca sexta*

larvae have a robust feeding homeostat. Decreasing nutritional content of larval diet results in a compensatory increase in feeding behavior to maintain constant growth rates (Nijhout & Williams 1974). In flies and mammals, starvation results in a suppression of quiescent behaviors, such as sleep (McDonald & Keene 2010). It is evident that the feeding homeostat is intact in the late 4th instar larvae used for this study, which suggests that increased quiescence observed during the molt may also be accompanied by an uncoupling of the feeding homeostat.

* * *

That the onset of molting quiescence is correlated with the reported peak levels of ecdysteroids suggests the possibility that in addition to the multiple physiological changes that occur during a larval molt, molting hormones might also program an accompanying increase in quiescent behavior. In many mammalian systems, the physiological effect of a hormone is often coupled to synergistic behavioral effects through its actions on the central nervous system (Pfaff et al 2004). Although it is evident that the molting period is accompanied by an increase in quiescence, "quiescence" is a general description that can apply equally well to many very different types of arousal state, including comatose states, sleep-like and resting states, or even to states of intense vigilance. Here, the prolonged consolidation of quiescence coupled with brief spontaneous activity during the molt, along with preliminary observations that molting larvae retain the ability to perform robust defensive responses when elicited by rough handling (personal observations), suggests a resemblance to the sleep-like states

observed for other invertebrate model systems. A recent study demonstrated that ecdysteroids may act to regulate sleep-like behavior in the adult stage of *Drosophila melanogaster* (Ishimoto & Kitamoto 2010). In the nematode *Caenorhabditis elegans*, *lethargus* behavior—the molting quiescence between the worm's larval stages—has been characterized as a sleep-like state (although the hormonal trigger for nematode molting remains illusive) (Raizen et al 2008). In adult *Drosophila*, sleep is most consolidated during the scotophase, during which time, sleep-bouts are characteristically long in duration (Hendricks et al 2000). In the fly, the timing of sleep consolidation is regulated by endogenous circadian clocks, but sleep itself is a process that is not dependant on a functional clock (Hendricks et al 2000; Shaw et al 2000). In *Caenorhabditis elegans* larvae, sleep periods do not follow circadian rhythms, but do follow developmental rhythms. Interestingly, the lethargus periods maintain a temporal relationship with the *C. elegans period* gene homologue LIN-42, which functions in the larval heterochronic pathway to regulate tissue differentiation (Jeon et al 1999).

As a result of the genetic and molecular studies undertaken during the past decade, several possible functions for sleep have been proposed. Among these are processes related to protein synthesis, synaptic plasticity, immune response, metabolism, and a general replenishment and repairing (Crocker & Sehgal 2010). In addition to the potential benefits related to physiological and cellular processes, sleep-like states also confer behavioral benefits. Many animals sleep during a period of the light cycle when feeding and mating does not occur, which both saves energy and limits exposure to predators. During the larval molts of *Manduca sexta*, molting quiescence precedes and

extends throughout a period when the animal has lost the ability to feed, a period that can last for up to 30 hrs during the molt to the 5th instar. The characteristic rapid reversibility of sleep-like states that follow exposure to strong or noxious stimuli would allow the animal to maintain some level of response to a changing environment.

Taken together, our present (and preliminary) observations of *M. sexta* larval quiescence, the occurrence of a sleep-like state during the transitions between nematode larval stages, and the link between ecdysteroids and sleep in adult insects suggests the possibility that molting hormones might be involved in the programming of a sleep-like state during the transitions between *M. sexta* larval stages. The following experiments were designed to compare the quiescent behavior of *M. sexta* larva to the sleep-like behavior characterized in other invertebrates.

Larval quiescence is a rapidly-reversible state. A key feature of sleep is rapid reversibility. That molting larvae show brief periods of spontaneous activity, demonstrates that they do exhibit some type of endogenously-driven motor behavior during the molt. In addition, molting larvae are able to right themselves when flipped onto their dorsal surface, and touching the tip of a hot soldering iron to the base of their dorsal horns leads to a robust defensive strike (personal observations). The latter observations indicate that, at least in terms of reflexive behavior, some response to exogenous stimuli remains intact during molting quiescence. In order to test whether this reversal of molting quiescence can last for a more extended period of time, we measured

quiescence levels of larvae during a prolonged (10 min) exposure to a mildly-arousing stimulus.

Each behavioral arena was constructed with a filter paper base so that placement of arenas on a water bath resulted in an immediate and persistent "wetting" of the base (see "Materials and Methods"). A two-tiered ledge surrounded the periphery of the arena, enabling the possibility of complete escape from contact with the wet base. To avoid behavioral differences due to variations in size and weight, only late inter-molt larvae (late 4^{th}) were used for comparison with larvae molting (mid-molt ~15 hrs prior to ecdysis) to the 5^{th} instar. Inter-molt and molting larvae were monitored for 30 sec prior to testing, and categorized as either inter-molt quiescent (IMQ), inter-molt active (IMA), mid-molting quiescent (MMQ), or mid-molting active (MMA). Larvae were considered "quiescent" if no movements were observed for the entire 30 sec monitoring period, and "active" if they exhibited movements during the entire 30 sec monitoring period. (Larvae that initiated locomotion during monitoring were excluded).

Following placement on the bath, larvae were monitored using time-lapse recordings (0.2 sec between frames). Larvae exhibit several behaviors following exposure to a wet surface, including searching, locomotion, and sometimes brief anterior and/or posterior thrashing movements. Similar to the long quiescence profiles, larvae were considered to be aroused if they were exhibiting any type of motor behavior.

Under control (DRY) conditions, intermolt larvae that were quiescent for at least 30 sec prior to testing (IMQ) showed a significantly higher average fraction of quiescence (0.78 +/- 0.08 s.e.m.) during the 10 min recording session when compared to

inter-molt larvae that were active (IMA) prior to testing (0.37 +/- 0.01 s.e.m.) (Figure 2-9A). This demonstrates that the methods used to categorize these larvae are sufficient to predict the level of larval quiescence during the 10 min testing period following categorization. When IMQ larvae are continuously exposed to a wet surface, the average fraction of quiescence decreases to levels previously observed for IMA larvae under DRY conditions (Figure 2-9A). There were no significant differences between average quiescence levels recorded for IMA larvae on a dry surface, and IMQ and IMA larvae on the wet surface. This shows that exposure to a wet surface arouses larvae to levels that are comparable to those observed for inter-molt larvae that are spontaneously active, but not beyond. That none of the larvae escaped from the arena suggests that contact with room temperature water is arousing, but not noxious.

Interestingly, the average fraction of quiescence was not significantly different for IMQ and MMQ larvae under dry conditions (Figure 2-9A, 2-9B, respectively). This suggests the possibility that the quiescent state experienced by larvae during the molt is not in itself unique to the molting period, rather, that the molt-sleep might represent a period of increased consolidation of a quiescent state that is also present during the inter-molt period.

Spontaneous activity is rare for molting larvae. To test responses of aroused molting larvae, quiescent larvae were forced to perform a single righting reflex. Following this righting-reflex, larvae were monitored for 30 sec. After righting themselves, larvae exhibit brief twitches of the body wall musculature, followed by movements of the head that resemble movements observed for spontaneously active

inter-molt larvae. Larvae that showed indications of these movements during the 30 seconds following the completion of a righting reflex were categorized as aroused molting larvae (MMA). Under dry conditions, average fractions of quiescence for MMQ larvae are above 0.9, similar to the levels of molting quiescence observed in previous experiments (Figure 2-9B). Quiescence fractions of MM larvae are significantly decreased when larvae are aroused prior to testing under DRY conditions, but average quiescence levels are still significantly higher that those recorded for IMA larvae. This suggests that, although molting larvae are aroused immediately following a righting reflex, the level of arousal is either not equivalent to IMA arousal, or that it is equivalent following the reflex, but is not maintained throughout the entire 10 min recording period. This might indicate either increased arousal thresholds, an inability to become aroused to inter-molt levels, or an increased quiescence-drive (reduced latency to quiescence).

When MMQ and MMA larvae are exposed continuously to the wet surface, average quiescence levels decrease significantly compared to those observed for larvae recorded under DRY conditions (Figure 2-9B). Under WET conditions, levels of quiescence exhibited by molting larvae are not significantly different from quiescence levels recorded for intermolt larvae of the same initial behavioral state, and are comparable to those observed for spontaneously active inter-molt larvae (IM/DRY) (Figure 2-9C). These results demonstrate that quiescence during the molting period and the inter-molt period is a reversible state, and that molting larvae can maintain levels of activity similar to those exhibited by inter-molt larvae when exposed to an arousing stimulus.

It is interesting that although almost all larvae did not escape from the wet surface, (thus allowing for the 10 min measure of quiescence level), 1 out of the 10 MMA larvae did locate the ledge and escape (escape was not rapid, and occurred towards the end of the allotted recording period), which might suggest that wet surfaces are more repulsive to molting larvae (Figure 2-10). A possible function of a reversible quiescent state during the larval stages might have to do with escape from inappropriate substrates following changes in the environment such as falling from a leaf onto wet soil. To test if larvae retain the ability to reverse their behavioral state throughout the molt, their response to a wet surface was also tested for molting larvae ~ 5-6 and ~ 2-3 hrs prior to their predicted time of ecdysis. There was no significant difference between quiescence levels measured during mid and late molting periods, which indicates that larvae maintain the ability to be aroused until late in the molt (Figure 2-9D).

Quiescent larvae have increased arousal thresholds that are rapidly reversible. The reversibility of sleep-like states is adaptive in that it allows animals to respond to sudden, sometimes potentially threatening changes in the environment, or to quickly renew normal behavior, such as feeding, when the sleep state is naturally terminated. In addition to reversibility, sleep-like states are also associated with increased arousal thresholds. To test for a reduced sensory responsiveness, as well as the ability of molting larvae to respond appropriately to sudden changes in the environment, larvae were exposed to a sudden, noxious heat stimulus. During preliminary observations, it was observed that larvae begin to respond to focal application of a heat stimulus with

defensive strikes at temperatures above 36°C (data not shown). Water baths were set to either room temperature (~25°C), 40°C or 50°C. Larvae placed on dry arenas do not attempt to escape the arena. When arenas are placed on room temperature water baths; almost all larvae did not attempt escape; quiescent and aroused inter-molt larvae, and quiescent molting larvae do not escape the arena, and as mentioned above, only 10% of aroused molting larvae escape the arena (Figure 2-10). When inter-molt larvae are placed on water baths set to 40°C, or 50°C, larvae respond by escaping the arena within the allotted 10 min recording time. Escape was characterized by rapid locomotion towards the outer ledge. This behavior differed from spontaneous locomotion generated by larvae on dry and room-temperature baths in that once initiated, locomotion on the hot-water baths resulted in a rapid, linear displacement of larvae towards the outer ledge. Spontaneous locomotion on the dry and room-temperature baths is often brief, non-linear and does not usually culminate in contact with the outer ledge. All locomotion that resulted in a rapid, linear displacement that resulted in contact with the ledge and subsequent attempt at removal of the body from contact with the arena was considered in this study to represent an escape behavior elicited by the thermal stimulus. At 40°C and 50°C, following contact with the ledge, larvae either climb on top and cling to the ledge, or they climb over the ledge and remain on the dry, elevated portion of the foam plate

All inter-molt larvae rapidly removed themselves from contact with the hot baths, which suggests that water at these temperatures represent a noxious stimulus (Figure 2-10). At 50°C, all molting larvae also escape from contact with the water. At 40°C, all MMA larvae escape from the water bath, but only 70% of MMQ larvae escape within the

allotted 10 min recording session. That some molting larvae do not escape suggests that 40°C may fall in the threshold range for the elicitation of an escape response from molting larvae. That all inter-molt larvae escape at the lower temperature suggests that quiescent molting larvae have comparatively higher arousal thresholds, or a reduced sensory responsiveness. The observation that MMA larvae all escape the 40°C water bath suggests that the increased arousal threshold or reduced sensory responsiveness is reversible. The behavioral response of molting larvae to contact with the 40°C and 50°C water baths shows that molting larvae are capable of responding appropriately when exposed suddenly to a noxious stimulus.

In order to further assess differences in sensory responsiveness between quiescent and active larvae during intermolt and molting periods, latencies to the onset of locomotion following exposure to 40°C and 50°C water baths were measured. Forward locomotion in *Manduca sexta* larvae involves waves of contractions that move anteriorly through the abdominal segments, resulting in displacement of the animal (Trimmer & Issberner 2007). Locomotion onset was defined as the time of contraction of the first abdominal segment involved in a peristaltic wave that leads to a displacement of the animal. Stimulus onset was defined as the time that coincides with wetting of the filter-paper situated directly beneath the animal. Latency to locomotion onset was defined as the time from stimulus onset to the initiation of locomotion.

When placed on the 40°C bath, IMQ larvae initiate locomotion within an average of 55.25 (+/- 6.3 s.e.m.) sec (Figure 2-11A). IMA larvae showed significantly shorter latencies (35.9 +/- 3.2 s.e.m. sec), suggesting that arousal thresholds are elevated during

the quiescent bouts of inter-molt larvae. Response-latencies decrease with increasing intensity of stimulus. At 50°C, IMQ and IMA response latencies decline to averages of 16.1 (+/-1.3 s.e.m.) and 15.7 (+/-1.4 s.e.m.) sec, respectively. That there is no significant difference between IMQ and IMA latencies at 50°C indicates that this temperature represents a very intense stimulus for inter-molt larvae.

MMQ larvae respond to 40°C water baths with an average latency of 74.3 (+/- 7.9 s.e.m.) sec (Figure 2-11B). This latency is higher but not significantly different from latencies shown by IMQ larvae, indicating that although there is a trend towards longer latencies, larvae respond similarly when quiescent prior to testing, regardless of developmental state. Again, this suggests that quiescence in molting and inter-molt larvae might represent similar physiological states, but it is more consolidated during the molting periods. MMA larvae respond with significantly shortened latencies (50.7 +/- 4.2 s.e.m. sec) compared to MMQ larvae, which demonstrates that molting larvae that are quiescent prior to testing have reduced responsiveness compared to aroused larvae. As with inter-molt larvae, response-latencies decrease when tested on the 50°C bath, but in contrast to IM larvae, MMA larvae respond with significantly shorter latencies at 50°C (14.0 +/-1.1 s.e.m. sec) compared to MMQ larvae (27.9 +/-2.6 s.e.m. sec), suggesting that molting larvae have a reduced sensitivity, or an increased threshold compared to late inter-molt larvae. At 50°C, MMA latencies are not significantly different from latencies observed for IM larvae at the same temperature, which shows that once aroused, molting larvae retain the ability to respond to a noxious stimulus with a robustness that is similar to inter-molt larvae.

To assess the extent of reversibility, the ability of larvae to respond to a noxious stimulus was further assessed by measuring the amount of time it took for them to reach the ledge following the initiation of locomotion. A larva was considered to have reached the ledge when the most anterior portion of its body made contact with the ledge. If quiescence during larval stages is a reversible state, the rate of locomotion should be similar for animals regardless of whether they were quiescent or aroused prior to placement on the bath, and this was the case for all animals tested. Following the onset of locomotion, there were no significant differences in the time taken to locomote towards the edge when IMQ larvae were compared to IMA larvae, or when MMQ larvae were compared to MMA larvae, and this was true following exposure to both 40°C and 50°C water baths (Figure 2-11C/D). For both molting and inter-molt larvae, rates of locomotion increased with increasing stimulus. Most surprisingly, molting larvae were able to locomote at rates comparable to those measured for inter-molt larvae, demonstrating that although molting larvae rarely move, the ability to behave is not impaired, and strong stimuli can induce escape behaviors similar to those observed for feeding stage larvae.

Quiescence-deprivation during the inter-molt, but not the molt, results in a quiescent rebound. In addition to changes in arousal thresholds and increased consolidation, another feature that is often characteristic of sleep-states is that they can be homeostatically regulated (the *amount* of sleep is tightly regulated). This homeostatic property is manifest following a period of forced wakefulness, which in mammals, flies

and worms, is followed by a recovery sleep or "sleep-rebound," consisting of increased sleep-consolidation and duration, elevated arousal-thresholds and deficits in vigilance and performance (Huber et al 2004; Raizen et al 2008). In the adult fly, ecdysone signaling has been shown to influence the homeostatic regulation of sleep; sleep-deprived flies show increased endogenous levels of ecdysteroids, and impairment of ecdysteroid signaling decreases the magnitude of sleep-rebound. Since both intermolt and molting quiescence are states of reversible, increased arousal threshold, the homeostatic regulation of sleep was also tested for 4th stage feeding and molting larvae.

A semi-automatic deprivation device was constructed using a test-tube rocker, a box lid and cups secured to the tops of "Hot Wheels" cars (Figure 2-12A; see "Materials and Methods"). In brief, individual larvae were placed in 5 oz plastic cups, and larval diet formed the base of the arena so that larvae could feed *ad libitum*. Each individual cup was secured to the top of a toy car so that for each "rock", arenas would run back and forth along a track. At the termination of each rock, the toy cars bump into the sides of the lid, and the impact results in the disturbance of the animal. Most impacts result in a "flipping" of the animal so that it is forced into a righting-reflex, a behavior that is followed by locomotion and/or feeding. Animals were observed continuously for the entire deprivation session, and those that were able to secure themselves against disturbance were dislodged manually with blunt forceps, or by tapping the container. The rocker was set to the minimum rate, which resulted in 1 rock/ every 12-14 sec. A maximum of 3 animals could be tested during each session. Animals were deprived for 3, 6, 6-9, or 12 continuous hrs, and time-lapse digital recordings were used to monitor

behavior following the termination of deprivation. For deprivation during the inter-molt, all deprivation was terminated at the same time, at 9 PM (~24-30 hrs following ecdysis to the 4th instar). For deprivation during the late molt to the 4th instar, deprivation of each individual larva was terminated at the time it completed ecdysis to the 4th instar, which occurred between 3 and 6 PM, resulting in 6 to 9 hrs of deprivation during the late-molt. Larvae deprived during the early molting period were deprived for 6 hrs at the start of the molt to the 5th instar, and deprivation was terminated at ~12 AM (midnight).

When animals were deprived of quiescence for 3 hrs during the 4th instar feeding stage, larvae showed significantly elevated fractions of quiescence during the first 4 hrs following the termination of deprivation protocols (Figure 2-12B). The highest average fraction of quiescence occurred during the first hr following deprivation offset, with a value of 0.82 (+/-0.03 s.e.m.), a 44% increase over control animals. Average quiescence levels during the first 6 hrs after the termination of deprivation were 0.70 +/-0.04 s.e.m. for deprived animals and 0.52 +/-0.01 s.e.m. for controls (a 34.6% increase). There was no significant difference between deprived and control fractions during the final 6 hrs of recording, which suggests that animals are able to fully recover from the effects of quiescence deprivation.

After 6 hrs of deprivation, inter-molt larvae show significantly higher 1 hr average fractions of quiescence during post-deprivation hrs (0-1), (2-3), (3-4), (5-6) and (11-12) (Figure 2-12C). The highest average fraction of quiescence occurred during the first post-deprivation hr, with a value of 0.86 +/-0.03 s.e.m., a 51.6% increase compared to controls. Total average quiescence levels during the first 6 hrs following deprivation

were significantly higher for deprived larvae (Average=0.72 +/-0.04 s.e.m.) compared to controls (Average=0.55 +/-0.03 s.e.m.). Larvae deprived for 6 hrs showed a 28.5% increase in quiescence levels during the first 6 hrs following deprivation. As with the 3 hr deprivations, there were no significant differences between deprived and control levels during the last 6 hrs of recording.

After 12 hrs of quiescence deprivation, inter-molt larvae show significantly higher 1 hr average fractions of quiescence during post-deprivation hrs (0-1), (1-2), (2-3), (4-5), (5-6), and (6-7), with the highest average 1 hr fraction of quiescence occurring during the 1st hour (Average=0.92 +/-0.02 s.e.m.) (Figure 2-12D). Although this fraction is higher than the maximum value calculated for larvae deprived for 6 hrs, the % change in quiescence during the first hour following 12 hrs deprivation was 40%, which is a smaller change when compared with larvae deprived for 6 hrs. The average fraction of quiescence during the first 6 hrs of the recording session was 0.80 +/-0.025 s.e.m. for deprived larvae and 0.62 +/-0.018 s.e.m. for control larvae, an overall increase of 29%, similar to that seen for larvae following 6 hrs of deprivation. This suggests the possibility that there is a maximum level of deprivation, beyond which larvae are able to habituate. Larvae deprived for 12 hrs also recover; compared with controls, there are no significant differences between deprived and control 6 hr fractions of quiescence during the last part of the recording session.

These results suggest that the level of quiescence is homeostatically regulated during the inter-molt feeding period of 4th instar *Manduca sexta* larvae. When deprivation time is increased from 3 to 6 or 12 hrs, the peak level of quiescence increases

in proportion to the amount of prior time deprived. When larvae are deprived for 3 hrs instead of 6 or 12 hrs, the increase in quiescence level during the first 6 hrs following deprivation is more robust, showing on overall increase of 34.6% during that period, compared to the initial 28.5% and 29.0% increases observed following the longer deprivation protocols (Figure 2-12B, 2-12C, 2-12D). The % increase across the entire 24 hr recording session shows that 6 and 12 hr deprivations result in an overall increase of 13.5% and 12.8%, respectively, which is greater than the overall 6.5% increase observed following 3 hrs of deprivation. Although the rest rebound is initially more robust following 3 hrs of deprivation, a longer deprivation period results in an overall increase in recovery time. During the 3 and 6 hr deprivation sessions, animals gain weight at rates similar to those measured for control larvae, but weight-gain during deprivation is impaired when animals are deprived for 12 hrs. Based on weights recorded prior to and immediately following deprivation, larvae deprived for 12 hrs gained only ~21% of their morning weights, while control larvae gained ~46% of their weight within the same time period. It is possible that after prolonged deprivation, larvae are able to recover quiescence even when subjected to the periodic disturbances. It is also possible that the prolonged mechanical disturbances somehow impair the animal's ability to feed. In any case, since larvae are able to gain weight at normal levels for up to 6 hrs of deprivation, and because there is little difference between overall quiescence recovery following 6 hr and 12 hr deprivations, future studies can omit the longer (12 hr) deprivation protocols.

Since feeding behavior is also homeostatically regulated, and it is also known that starvation has a sleep-suppressing effect, it is possible that a conflict between the sleep

and feeding homeostats leads to a more attenuated rebound directly following the termination of deprivation after 12 hrs, compared to the 3 hr deprivation (Keene et al 2010). That deprivation for 6 and 12 hrs results in a more robust rebound than at 3 hrs over the total 24-hr recording session following deprivation suggests that the eventual recovery of lost quiescence is of some physiological importance to the inter-molt animal. As larval quiescence levels show no significant differences compared to controls during the last 6 hrs of the 24 hr recording session following termination of deprivation, quiescence rebound is not likely to be due to delayed development.

Although the robust quiescence-rebound suggests a central, homeostatic regulation of the level of quiescence, it is possible that the deprivation protocol, which forces a repetitive righting-reflex, results in depletion or impairment of the peripheral motor system. To test if larvae retain the ability to exhibit motor behavior following deprivation, larvae were continuously deprived for 3 hrs, and response to a thermal stimulus was tested using the 40°C water bath assay. Latency from the initiation of locomotion to the time larvae made contact with the peripheral ledge was used as the measure of motor function. Following the 3 hr deprivation sessions, the average rate of locomotion (23.8 +/-5.0 s.e.m. sec, n=6) was not significantly different from control rates (30.0 +/-6.3 s.e.m. sec, n=6), which suggests that motor function is not impaired by the deprivation protocol.

To assess the possible homeostatic regulation of quiescence level during the molting period, larvae were deprived of quiescence for 6 hrs during the early molt to the 5^{th} instar, and for 6-9 hrs during the late molt to the 4^{th} instar (Figure 2-12E, 2-12F). For

deprivation during the early molt, animals were staged so that HCS occurred between 4 and 5 PM, and deprivation of larvae lasted for 6 hrs, from ~6 to ~12AM (midnight). Following deprivation, behavior was monitored throughout the molting period until the time of ecdysis, which occurred ~20-23 hrs following the end of deprivation. Surprisingly, following deprivation, molting larvae showed no significant difference in quiescent levels when compared to controls (Figure 2-12E). Also, deprivation did not seem to affect developmental timing, as larvae ecdysed when expected, ~27 hrs following HCS. Because molting larvae already show high fractions of quiescence, it is possible that a rebound effect was obscured. Larvae were also deprived during the late molt to the 4^{th} instar so that behavior following deprivation would occur during the inter-molt period when average quiescence levels are lower. Larvae were staged so that HCS occurred in the evening between 6:30 and 7:30PM, and deprivation commenced the following day starting at 9AM. Deprivation continued until larvae completed ecdysis to the 4^{th} instar, and larval behavior was recorded immediately following ecdysis. Deprivation duration was between 6-9 hrs. Quiescence levels during the inter-molt immediately following deprivation of quiescence during the late molt did not show any significant changes when compared to controls (Figure 2-12F). Also, deprivation during the late molt did not alter time to ecdysis, or the ability of the animals to complete ecdysis.

These results suggest that quiescence is homeostatically regulated during the inter-molt, but not during the molting periods. This is surprising, given that in almost all animals tested, forced deprivation of quiescence leads to some level of rebound. In order to verify the lack of rebound following quiescence deprivation during the molt, we

manually deprived animals for 3 hrs following HCS during the early molt to the 5th instar (n=6). Animals were monitored continuously and when movement ceased for more than ~30 sec, animals were flipped or tapped in order to induce movement. Following deprivation, animals were allowed to equilibrate for 15 to 30 min, and their response to placement on a room temperature water bath was tested. Although the intention was to monitor the fraction of quiescence during a 10 min exposure to room temperature water (previously shown to arouse molting larvae), this was not possible, because in contrast to non-deprived larvae, all but one of the deprived larvae escaped the water bath prior to the termination of the recording session. These results suggest that in addition to the lack of a rest-rebound following deprivation, responses to arousing stimuli may actually be enhanced following deprivation.

That molting larvae do not show a rest-rebound suggests that quiescence is not a physiological necessity during the molt. The increased consolidation observed during the molting period may have evolved to provide the animal with a purely behavioral advantage during a time when feeding is impossible and locomotion is dangerous. That inter-molt larvae do show a robust quiescence-rebound following deprivation shows that quiescence plays an important role in the physiology of the inter-molt animal, and processes dependent upon these quiescence states may be somehow shut-down or altered during the molting process.

***Period* gene expression in the brain of 4th stage larvae.** In most animals, consolidation of quiescence is regulated by both homeostatic and circadian mechanisms. In adult

insects, a circadian clock determines the timing of consolidated periods of quiescence so that rest and activity cycles are synchronized with specific portions of the 24 hr light cycle. The basic clock mechanism involves feedback loops during which clock proteins rhythmically control the expression of their own mRNA. In *Drosophila*, a principle loop involves the cycling of period (PER) and timeless (TIM) proteins (Hall 2003). These and other clock components share homology with clock components in other insects and phyla, including mammals.

Clock cells that control the adult fly locomotor activity rhythm are located in the brain (Bollenbacher et al 1987; Ewer et al 1992; Frisch et al 1994; Konopka et al 1983). Within these cells, *period* (*per)* and *timeless* (*tim*) genes are actively transcribed during the day, leading to peak levels of mRNA during the early evening. During the middle of the night, high protein levels coupled with translocation of protein products into the nucleus results in the inhibition of *per* and *tim* transcription (Hardin 2005). The temporal variation of clock transcripts and proteins is thought to be responsible for the cycling transcription of putative clock output genes, resulting in rhythmic changes in physiology and behavior. The gene expression of clock components is less well-characterized for larval stage insects. Cycling *per* and *tim* expression has been located to brain neurons of fly larvae, and *per* expression occurs in larval heads of the lepidopteran, *Bombyx mori* (Iwai et al 2006; Kaneko et al 1997; Kostal et al 2009). In the hemimetabolous insect *Rhodnius prolixus*, synthesis of developmental hormones is thought to be influenced by activities of clock neurons (Steel & Vafopoulou 2006). The relationship between clock gene expression and the timing of developmental events in holometabolous insects has

not been explored. In *C. elegans* larvae, the PER homologue LIN-42 does not oscillate with a 24 hr rhythm, but instead, gene expression levels show a 6 hr period of oscillation, corresponding to the molting rhythm (Jeon et al 1999). LIN-42 is a member of the heterochronic pathway regulating developmental time, and has influence over a broad range of developmental events, from the differentiation of cell lineages to the negative regulation of diapause induction (Jeon et al 1999; Tennessen et al 2006; Tennessen et al 2010). Since *per* gene expression is known to occur in the brains of other holometabolous larvae, and since *Manduca* larval activity is not coupled to circadian rhythms, we set out to determine if changes in *per* gene expression in the brains of 4th stage larvae show correlations with developmental events associated with changes in quiescence level.

The *period* gene is expressed in the larval CNS and peripheral tissues. *Period* gene expression in the brains and antennae of adult stage *Manduca sexta* has been verified in previous studies using RT-PCR, *in situ* hybridization and immunohistochemistry (Schuckel et al 2007; Wise et al 2002). In order to test for *per* gene expression during the larval stages, primers were designed from a 1062 bp partial clone of a *Manduca sexta per* gene (Reppert et al 1994). Initial primer sets were aimed at amplifying a large portion of the known *per* sequence. Total RNA was extracted from the entire nerve cord (brain through terminal abdominal ganglion) of a late 4th instar feeding larvae. An additional sample was obtained from a small sampling of peripheral tissues that included epidermis, fat body and trachea. PCR with probes against *per* was performed on cDNA constructed

from total RNA, and a single PCR product of the expected size of 976bp was detected for both samples (Figure 2-13). Sequence identity was verified using Sanger-based sequencing methods (Sanger (BigDye) Sequencing Services; Genomics Core at the University of California, Riverside), confirming *per* gene expression in the central nervous system and peripheral tissue of 4th instar *Manduca sexta*.

A profile of *period* gene expression in the whole brain of 4th stage larvae using quantitative PCR (qPCR). To profile the expression of per mRNA across the 4th larval stage, pooled brain samples were collected from staged animals at the following time-points relative to HCS: -48 hrs, -36 hrs, -24 hrs, -18 hrs, -12 hrs, -6 hrs, 0 hrs, +6 hrs, +12 hrs, +18 hrs and +24 hrs. 3 sets (replicates) of such tissues were collected. Biological replicates were run independently, and each sample within a replicate was run in triplicate. Relative expression ratios were calculated by the Pfaffl equation (Pfaffl 2001). Values were normalized to cytoplasmic actin and all fold change is an expression of change relative to an arbitrarily selected stage, HCS -36 hrs.

Shown in Figure 2-14 are the relative fold changes of *per* mRNA plotted against time-of-day, and 4th stage developmental time. In contrast to that observed for adult-staged insects, expression of *per* in the larval brains of 4th instar *Manduca sexta* does not show a significant correlation with time-of-day (Figure 2-14A). When expression levels are plotted against time-of-development, no significant differences in per mRNA expression levels are found between any sampling across the 4th larval instar. Although

not statistically significant, all replicates showed increases in per expression levels at 18 hrs following HCS (Figure 2-14B). Previous studies have demonstrated co-localization of per expression with the neuropeptide corazonin in the adult brain of *Manduca sexta*. Corazonin is known to be expressed in the *Manduca* brain during the larval stages, when the peptide plays a role in the initiation of the ecdysis behavioral program (Kim et al 2004). HCS +18 hrs is a developmental time-point that follows the decline of ecdysteroids, and correlates with the timing of the coordination of complex peptidergic networks that drive behaviors unique to the latter part of the molt (Zitnan et al 2007). Expression in the brain of this clock gene does not seem to be coupled to changes in rest-activity levels across the molt, or to behavioral adaptations related to the light cycle, which leads to speculations as to what role a brain clock might play during larval development. It is possible that clock-gene expression during the larval stages only serves to set the timer for adult emergence, which does show a circadian rhythm. From this data, there does not seem to be any similarity between the *Manduca per* and the *C. elegans* LIN-42 expression profiles, as in the latter profile, LIN-42 expression peaks during the inter-molt, but not the molting periods (Jeon et al 1999). The hypothesis that endogenous clocks play a role in the orchestration of an innate behavior during the molt is enticing, but more detailed studies will be needed to localize gene-expression, verify the translation of clock-components, and test the behavioral consequences of clock-disruption.

Discussion

Monitoring of rest-activity patterns across multiple larval stages shows that larval *M. sexta* motor activity lacks circadian rhythms. This finding is in agreement with both field and laboratory studies that have examined the behavior of 5th instar *M. sexta* larvae during isolated periods of activity during the day and nighttime (Bernays & Woods 2000; Reynolds et al 1986). Our study provides the first detailed, uninterrupted monitoring of lepidopteran rest-activity levels across entire larval instars (from ecdysis to ecdysis) under controlled laboratory conditions. Across the entire 4th larval stage, there was no correlation between activity levels and time of day under either continuous light conditions or a 16L:8D photoperiod. The lack of circadian rhythmicity of larval rest-activity patterns may be the norm for holometabolous larvae. When the measurement of larval path length was used to monitor *D. melanogaster* larval activity over a 96 hr test period, daily rest-activity rhythms also were not observed (Sawin et al 1994). For holometabolous larvae, there may be no advantage gained by consolidation of rest or activity within a particular time of day. The behavioral repertoire of *M. sexta* larvae differs greatly from that of the adult-staged insect; they are solitary feeders that live on or within their food source, and prior to metamorphosis to the adult reproductive stage, little if any need exists for intra-specific behavioral coordination. Maximizing growth rate might outweigh any possible benefits gained by coordination of activity level with daily environment cycles.

We demonstrated that the *period* gene is expressed in peripheral tissues and central nervous system of larval *M. sexta*. Surprisingly, brain mRNA expression profiles showed neither circadian nor developmental rhythms. Following *Drosophila's* metamorphosis to the adult stage, the brain's endogenous circadian clocks become coupled to (and are necessary for) the daily locomotor activity rhythm (Ewer et al 1992; Frisch et al 1994; Konopka et al 1983). The *period* gene homolog has also been shown to cycle with a 24 hr rhythmicity in brain neurons and antennae of adult staged *M. sexta* and in other adult lepidoptera, such as *B. mori* (Iwai et al 2006; Schuckel et al 2007; Wise et al 2002). In *Drosophila*, even though clock gene expression is not thought to influence the pattern of larval motor activity, the core clock genes *period* and *timeless* are expressed rhythmically in the larval brain, where their expression is thought to be important for circadian gating of eclosion (Kaneko et al 1997).

In the developing nematode *C. elegans*, the mRNA of clock homologs oscillate with a periodicity that matches the larval molting cycles, a much faster rhythm than the 24 hr daily cycle (Banerjee et al 2005; Jeon et al 1999). In *C. elegans* larvae, these clock gene homologs are heterochronic genes that function as developmental timers for regulation of cell fate, but the period gene homolog LIN-42 also has been associated with the regulation of the larval dauer state (a long-term quiescent state similar to diapause in insects). These findings, along with the observation that cycling of LIN-42 is correlated with larval molting quiescence, suggest a possible role for clock genes in the regulation of insect larval quiescent behavior (Raizen et al 2008; Tennessen et al 2006; Tennessen et al 2010). That clock genes cycle with a 24 hr rhythmicity in *Drosophila* does not rule of

the possibility that these genes time larval developmental behavior, because the *Drosophila* larval molting cycles themselves show periods of 24 hrs. Since the duration of the gate II 4th larval stage of *M. sexta* is well over 3 days long, we had expected to see the clear emergence of either a developmental or a circadian rhythm. But neither rhythm occurred, so we cannot conclude anything about the possible function of the *period* gene in the larval brain of *M. sexta*. It is likely that some form of a functional circadian clock is present in the brain during the larval stages, because endocrine events that initiate the 4th to 5th instar larval molt are gated by photoperiod (Truman 1972). Although this data suggests that the canonical clock gene *period* is not a component of a putative larval central clock, (at least in the brain), it is possible that samplings of whole brains obscure circadian rhythms of expression in individual neurons. In *Drosophila* larvae, a sub-set of brain neurons expressed *period* and *timeless* in antiphase to other neurons, indicating that in contrast to adults, larval clock genes are regulated differently in different brain neurons (Kaneko et al 1997). To clarify possible roles of the *period* gene during the larval stages of *M. sexta*, *in situ* and/or immunohistochemistry should be used to examine expression at the level of individual neurons.

When larval quiescence levels are set relative to the time of ecdysis, a distinct developmental pattern emerges that is both reproducible across individuals within a larval stage and across larval stages. The timing of ecdysis is known to occur at a set time interval following the onset of neuroendocrine events that initiate the molt (Truman 1972). Here, we show that when larvae are reared under controlled nutritional and environmental conditions, quiescence level can be predicted relative to the expected time

of ecdysis. This suggests that similar neuroendocrine factors might influence arousal state during larval stages.

During the inter-molt feeding stage, quiescence level decreases with increasing time spent within an instar. In other studies that have examined 5th instar larvae feeding behavior, an increase in feeding rate was observed during the progression through that stage (Bowdan 1988; Reynolds et al 1986). While the total amount of food consumed within a larval stage increases as time progresses, the maximum rate at which larvae are able to consume food at any time within a given larval stage remains constant (Reynolds et al 1985). The reason for this limitation in ingestion rate is that as soft bodied larvae progress through a larval stage, much of the body grows in size, but sclerotized regions of the cuticle, such as the mouthparts, cannot. In order for the animal to increase food intake, either the duration or number of feeding bouts must increase. Although our study measures all activity (not feeding, specifically), it is likely that the progressive decrease in quiescence level across the inter-molt stage is largely attributable to increased feeding behavior. It is not known what factors influence this progressive and predictable increase in activity during the inter-molt. It is tempting to speculate that the gradual decrease in quiescence across the inter-molt period of the larval stage is driven by an ever-increasing endogenously generated foraging drive. In *Drosophila*, it is known that growth rate is directly proportional to the level of insulin signaling during larval development (Orme & Leevers 2005), but whether insulin-like peptides also act directly or indirectly on the nervous system to bring about a concomitant and progressive increase in foraging drive is not known. It is possible that increased foraging is also the result of a gradual decline of

some other conflicting drive, such as a drive toward quiescence. The onset of the feeding stage follows a prolonged period of molting quiescence, and since the neurochemical and/or hormonal factors that might underlie the induction and maintenance of the molt-sleep have yet to be investigated, nothing can yet be said about the possible duration of their influence, if any.

The hypothesis that *M. sexta* larvae optimize growth rate during the inter-molt period conflicts with the observation that larvae spend more than half of the feeding stage in a quiescent state. It is not likely that this quiescent behavior is a result of temporary motor depletion, because starved larvae are able to maintain a dramatic increase in average activity level for an extended period of time. Also, under conditions where nutritional content of *M. sexta* larval diet is depleted, the amount of time spent feeding increases so as to maintain a constant growth rate (Reynolds et al 1986; Timmins et al 1988). As the artificial diet used here is of high nutritional content, it is likely that the larvae used in this study are not feeding at maximal rates. There is indirect evidence that rates of feeding activity reflect a maximization of the rate of nutrient uptake from ingested food (Reynolds et al 1985), which would imply that the putative feeding homeostat is not influenced by the amount of ingested food so much as by the amount of nutritional uptake. As starvation leads to such dramatic, long-duration increases in activity in our animals, it is evident that our animals have a robust feeding homeostat. But molting quiescence does not seem to be merely the result of a "turning off" of feeding behavior. That deprivation of quiescence results in a robust quiescence-rebound suggests that quiescent behavior is also homeostatically regulated during the inter-molt

feeding stages, and that it is somehow important to this stage. We have shown that quiescence during the inter-molt is accompanied by increased arousal thresholds that are rapidly reversible, resembling the sleep-like states found for adult insects. This suggests that a sleep-like state occurs during the inter-molt period, and is likely to be under homeostatic control. Just what is the function of this sleep-like state during the intermolt period is not know. The function of sleep in any animal is not known. Most hypothesized functions point to an optimization of nervous system function, and this is supported by deprivation experiments that result in a myriad of behavioral deficits that can be traced to changes in the nervous system. The 4th instar feeding stage can last for over 3 days. If it is true, as a general principle, that waking activities lead to a progressive imbalance of nervous system function that can only be corrected by a sleep-state, then we would expect these animals to sleep and to show increased drive toward sleep when deprived of that behavioral state. Indeed, this is what we have observed in this study. Although this study does not demonstrate that sleep during the inter-molt is important for the larval nervous system specifically, it demonstrates that feeding-stage larvae, with their relatively simple nervous systems and limited behavioral repertoire, may potentially serve as an excellent model system with which to examine the functions of sleep-like states.

During the 4th larval stage, average levels of quiescence decrease with increasing time within the instar until ~36 hrs prior to ecdysis, at which time levels of quiescence begin to rise. At ~30 hrs prior to the completion of ecdysis, average quiescence levels reach values higher than any measured during the inter-molt, and remain high until the

onset of ecdysis behavior. This period of consolidated quiescence represents the so-called “molt-sleep” period. We have shown that quiescence during the molting period is accompanied by a rapidly-reversible increase in arousal threshold, thus resembling the sleep-like states observed for adult insects, and now also for our inter-molt feeding larvae. Surprisingly, molt-sleep larvae retain the ability to perform multiple behaviors. When molting larvae are exposed to a mildly arousing stimulus, levels of quiescence drop considerably, and larvae respond appropriately when exposed to a noxious stimulus. When exposed to a strongly noxious stimulus, larvae locomote at rates indistinguishable from inter-molt larvae. This data suggests that circuitry used for inter-molt behaviors remains intact during the molt, but that there is a decreased behavioral drive. We also found that the ability of larvae to respond to arousing stimuli persists until very late in the molting period, up to at least 3 hrs prior to completion of ecdysis behavior. Also, preliminary observations in our lab suggest that larvae retain the ability to escape from noxious stimuli even after the initiation of pre-ecdysis behavior (data not shown). We propose that molting larvae engage in an adaptive sleep-like state that promotes energy conservation, one of many possible functions of sleep during this non-feeding state, while retaining the ability to respond to a changing environment.

It is interesting that, although larvae are unable to feed during this ~30 hr molt-sleep period, starvation during the molt does not lead to the same increased activity that is observed following the starvation of larvae during the inter-molt. Either the feeding homeostat is entirely shut down, or the link between feeding motivation and activation of that behavior is shut down during the molting period. Also unexpected were results

obtained from depriving molt-sleep larvae of quiescence; in contrast to the inter-molt stage, deprivation during the molting period is not followed by a compensatory quiescence-rebound. Deprivation of quiescence during the molting period does not seem to influence developmental timing, nor does it impair the level of inter-molt larval activity following late-molt deprivation. (It is possible that deprivation of quiescence might have a long-term impact on behavior or development, but larvae were not monitored following the 24 hr post-deprivation recording session). In any case, as with feeding behavior, regulation of the level of quiescence also seems to be shut down following onset of the molt-sleep. In both flies and mammals, feeding and sleeping behavior seems to be functionally interconnected (McDonald & Keene 2010). Perhaps the shut-down during the molt of systems related to feeding behavior result in the impairment of sleep-drive. It is also possible that a sleep-homeostat remains intact, and that even though molting larvae are active during deprivation, differences in neural chemistry prevent activation or stressing of particular circuitries for which recovery sleep is important. But at this point, we can only speculate. In the future, *M. sexta* larvae, and perhaps larvae of other holometabolous insects may prove to be excellent models for investigation of mechanisms underlying the regulation of feeding and sleep homeostasis.

Quiescence during the molting period does not seem to be homeostatically regulated, but elevated arousal thresholds occur that are rapidly reversible. Molting-quiescence therefore seems to share some, but not all of the properties of adult fly and larval *C. elegans* sleep. Whether or not one calls *M. sexta* molting-quiescence a "sleep-like" state depends entirely on the strictness of the criteria used for definition. For now,

as it does exhibit some sleep-like properties, we will continue to call quiescence during the *M. sexta* molting period the "molt-sleep". This distinguishes quiescent behavior from the sleep-like state that occurs during the larval feeding stages.

One of the most interesting findings of this study is the predictability of larval quiescence behavior relative to the time of ecdysis to the next instar. The steady decrease in quiescence that we observe throughout most of the inter-molt period is halted ~36 hrs prior to ecdysis to the 5^{th} instar. What follows is a rapid increase in quiescence above values that are observed for inter-molt larvae, and these levels (>90%) are then maintained throughout the duration of the molt-sleep. The timing of this transition occurs at a set time-interval relative to ecdysis, just as the timing of ecdysis occurs at a set time-interval relative to the onset of endocrine events that initiate the molt. The endocrine events that initiate the molt involve brain neurosecretion of prothoracicotripic hormone (~50-56 hrs prior to the completion of ecdysis), which acts on the prothoracic glands to increase synthesis of the molting hormone ecdysone (Truman 1972). Levels of molting hormones have been assayed across the 4^{th} larval stage of *M. sexta*, particularly around the time of the molt. In larval *M. sexta*, the active form of molting hormone is thought to be 20-hydroxyecdysone (20E) (Hiruma et al 1997). Peak levels of this hormone are predicted to occur at ~5-6 hrs prior to HCS (at ~36 hrs prior to the completion of ecdysis), a time that correlates well with the abrupt increase in larval quiescent behavior (Langelan et al 2000). This correlation suggests that, in addition to acting on the larval nervous system to program the ecdysis behavioral sequence, molting hormones might be either directly or indirectly acting on the nervous system to program the onset and

maintenance of the molt-sleep. Molting hormones influence changes in behavior and physiology by changing gene expression. As the timing of molt-sleep onset in relation to certain developmental markers and neuroendocrine events are so predictable, this system provides an excellent opportunity to identify gene products that might be involved in the regulation of arousal state during the larval stages; and this is the topic of the next chapter.

References

Andretic R, van Swinderen B, Greenspan RJ. 2005. Dopaminergic modulation of arousal in Drosophila. *Curr Biol* 15:1165-75

Aschoff J. 1960. Exogenous and Endogenous Components in Circadian Rhythms. *Cold Spring Harb Sym* 25:11-28

Banerjee D, Kwok A, Lin SY, Slack FJ. 2005. Developmental timing in C-elegans is regulated by kin-20 and tim-1, homologs of core circadian clock genes. *Dev Cell* 8:287-95

Bell RA, Joachim FG. 1976. Techniques for Rearing Laboratory Colonies of Tobacco Hornworms and Pink Bollworms Lepidoptera-Sphingidae-Gelechiidae. *Ann Entomol Soc Am* 69:365-73

Bernays EA. 2000. Foraging in nature by larvae of Manduca sexta-influenced by an endogenous oscillation. *Journal of Insect Physiology* 46:825-36

Bernays EA, Woods HA. 2000. Foraging in nature by larvae of Manduca sexta-influenced by an endogenous oscillation. *J Insect Physiol* 46:825-36

Bollenbacher WE, Granger NA, Katahira EJ, Obrien MA. 1987. Developmental Endocrinology of Larval Molting in the Tobacco Hornworm, Manduca-Sexta. *Journal of Experimental Biology* 128:175-92

Bowdan E. 1988. Microstructure of Feeding by Tobacco Hornworm Caterpillars, Manduca-Sexta. *Entomol Exp Appl* 47:127-36

Cirelli C, LaVaute TM, Tononi G. 2005. Sleep and wakefulness modulate gene expression in Drosophila. *J Neurochem* 94:1411-9

Crocker A, Sehgal A. 2010. Genetic analysis of sleep. *Gene Dev* 24:1220-35

Ewer J. 2005. How the ecdysozoan changed its coat. *Plos Biol* 3:1696-9

Ewer J, Frisch B, Hamblencoyle MJ, Rosbash M, Hall JC. 1992. Expression of the Period Clock Gene within Different Cell-Types in the Brain of Drosophila Adults and Mosaic Analysis of These Cells Influence on Circadian Behavioral Rhythms. *J Neurosci* 12:3321-49

Frisch B, Hardin PE, Hamblencoyle MJ, Rosbash M, Hall JC. 1994. A Promoterless Period Gene Mediates Behavioral Rhythmicity and Cyclical Per Expression in a Restricted Subset of the Drosophila Nervous-System. *Neuron* 12:555-70

Hall JC. 2003. Untitled. *Adv Genet* 48:1-280

Hardin PE. 2005. The circadian timekeeping system of Drosophila. *Curr Biol* 15:R714-R22

Heinrich B. 1971. Effect of Leaf Geometry on Feeding Behaviour of Caterpillar of Manduca-Sexta (Sphingidae). *Anim Behav* 19:119-&

Hendricks JC, Finn SM, Panckeri KA, Chavkin J, Williams JA, et al. 2000. Rest in Drosophila is a sleep-like state. *Neuron* 25:129-38

Hiruma K, Bocking D, Lafont R, Riddiford LM. 1997. Action of different ecdysteroids on the regulation of mRNAs for the ecdysone receptor, MHR3, dopa decarboxylase, and a larval cuticle protein in the larval epidermis of the tobacco hornworm, Manduca sexta. *Gen Comp Endocrinol* 107:84-97

Huber R, Hill SL, Holladay C, Biesiadecki M, Tononi G, Cirelli C. 2004. Sleep homeostasis in Drosophila melanogaster. *Sleep* 27:628-39

Ishimoto H, Kitamoto T. 2010. The steroid molting hormone Ecdysone regulates sleep in adult Drosophila melanogaster. *Genetics* 185:269-81

Iwai S, Fukui Y, Fujiwara Y, Takeda M. 2006. Structure and expressions of two circadian clock genes, period and timeless in the commercial silkmoth, Bombyx mori. *Journal of Insect Physiology* 52:625-37

Jeon M, Gardner HF, Miller EA, Deshler J, Rougvie AE. 1999. Similarity of the C-elegans developmental timing protein LIN-42 to circadian rhythm proteins. *Science* 286:1141-6

Kaneko M, HelfrichForster C, Hall JC. 1997. Spatial and temporal expression of the period and timeless genes in the developing nervous system of Drosophila: Newly identified pacemaker candidates and novel features of clock gene product cycling. *J Neurosci* 17:6745-60

Keene AC, Duboue ER, McDonald DM, Dus M, Suh GSB, et al. 2010. Clock and cycle Limit Starvation-Induced Sleep Loss in Drosophila. *Curr Biol* 20:1209-15

Kim YJ, Spalovska-Valachova I, Cho KH, Zitnanova I, Park Y, et al. 2004. Corazonin receptor signaling in ecdysis initiation. *Proc Natl Acad Sci U S A* 101:6704-9

Konopka R, Wells S, Lee T. 1983. Mosaic Analysis of a Drosophila Clock Mutant. *Mol Gen Genet* 190:284-8

Kostal V, Zavodska R, Denlinger D. 2009. Clock genes period and timeless are rhythmically expressed in brains of newly hatched, photosensitive larvae of the fly, Sarcophaga crassipalpis. *Journal of Insect Physiology* 55:408-14

Kume K, Kume S, Park SK, Hirsh J, Jackson FR. 2005. Dopamine is a regulator of arousal in the fruit fly. *J Neurosci* 25:7377-84

Langelan RE, Fisher JE, Hiruma K, Palli SR, Riddiford LM. 2000. Patterns of MHR3 expression in the epidermis during a larval molt of the tobacco hornworm Manduca sexta. *Dev Biol* 227:481-94

McDonald DM, Keene AC. 2010. The sleep-feeding conflict: Understanding behavioral integration through genetic analysis in Drosophila. *Aging (Albany NY)* 2:519-22

Miles CI, Booker R. 2000. Octopamine mimics the effects of parasitism on the foregut of the tobacco hornworm Manduca sexta. *J Exp Biol* 203:1689-700

Nijhout HF, Williams CM. 1974. Control of Molting and Metamorphosis in Tobacco Hornworm, Manduca-Sexta (L) - Growth of Last-Instar Larva and Decision to Pupate. *Journal of Experimental Biology* 61:481-91

Nitz DA, van Swinderen B, Tononi G, Greenspan RJ. 2002. Electrophysiological correlates of rest and activity in Drosophila melanogaster. *Curr Biol* 12:1934-40

Orme MH, Leevers SJ. 2005. Flies on steroids: the interplay between ecdysone and insulin signaling. *Cell Metab* 2:277-8

Pfaff D, Ribeiro A, Matthews J, Kow LM. 2008. Concepts and mechanisms of generalized central nervous system arousal. *Ann N Y Acad Sci* 1129:11-25

Pfaff DW, Phillips IM, Rubin RT. 2004. *Principles of hormone behavior relations*. Amsterdam ; Boston, MA: Elsevier Academic Press. xviii, 335 p. pp.

Pfaffl MW. 2001. A new mathematical model for relative quantification in real-time RT-PCR. *Nucleic Acids Res* 29:-

Raizen DM, Zimmerman JE, Maycock MH, Ta UD, You YJ, et al. 2008. Lethargus is a Caenorhabditis elegans sleep-like state. *Nature* 451:569-72

Reppert SM, Tsai T, Roca AL, Sauman I. 1994. Cloning of a structural and functional homolog of the circadian clock gene period from the giant silkmoth Antheraea pernyi. *Neuron* 13:1167-76

Reynolds SE, Nottingham SF, Stephens AE. 1985. Food and Water Economy and Its Relation to Growth in 5th-Instar Larvae of the Tobacco Hornworm, Manduca-Sexta. *Journal of Insect Physiology* 31:119-27

Reynolds SE, Yeomans MR, Timmins WA. 1986. The Feeding-Behavior of Caterpillars (Manduca-Sexta) on Tobacco and on Artificial Diet. *Physiological Entomology* 11:39-51

Safranek L, Williams CM. 1984. Determinants of Larval Molt Initiation in the Tobacco Hornworm, Manduca-Sexta. *Biol Bull* 167:568-78

Sawin EP, Dowse HB, Hamblencoyle MJ, Hall JC, Sokolowski MB. 1994. A Lack of Locomotor-Activity Rhythms in Drosophila-Melanogaster Larvae (Diptera, Drosophilidae). *J Insect Behav* 7:249-62

Schuckel J, Siwicki KK, Stengl M. 2007. Putative circadian pacemaker cells in the antenna of the hawkmoth Manduca sexta. *Cell Tissue Res* 330:271-8

Shaw PJ, Cirelli C, Greenspan RJ, Tononi G. 2000. Correlates of sleep and waking in Drosophila melanogaster. *Science* 287:1834-7

Steel CGH, Vafopoulou X. 2006. Circadian orchestration of developmental hormones in the insect, Rhodnius prolixus. *Comp Biochem Phys A* 144:351-64

Stewart PA, Nelson LA. 1977. Feeding of Tobacco Hornworm Larvae under Different Light Conditions as Indicated by Fecal Evacuations. *Ohio Journal of Science* 77:81-3

Tennessen JM, Gardner HF, Volk ML, Rougvie AE. 2006. Novel heterochronic functions of the Caenorhabditis elegans period-related protein LIN-42. *Dev Biol* 289:30-43

Tennessen JM, Opperman KJ, Rougvie AE. 2010. The C. elegans developmental timing protein LIN-42 regulates diapause in response to environmental cues. *Development* 137:3501-11

Timmins WA, Bellward K, Stamp AJ, Reynolds SE. 1988. Food Intake Conversion Efficiency and Feeding Behavior of Tobacco Hornworm Caterpillars Given Artificial Diet of Varying Nutrient and Water Content. *Physiological Entomology* 13:303-14

Trimmer B, Issberner J. 2007. Kinematics of soft-bodied, legged locomotion in Manduca sexta larvae. *Biol Bull* 212:130-42

Truman JW. 1972. Physiology of Insect Rhythms .1. Circadian Organization of Endocrine Events Underlying Molting Cycle of Larval Tobacco Hornworms. *Journal of Experimental Biology* 57:805-&

Walters ET, Illich PA, Weeks JC, Lewin MR. 2001. Defensive responses of larval Manduca sexta and their sensitization by noxious stimuli in the laboratory and field. *J Exp Biol* 204:457-69

Wise S, Davis NT, Tyndale E, Noveral J, Folwell MG, et al. 2002. Neuroanatomical studies of period gene expression in the hawkmoth, Manduca sexta. *J Comp Neurol* 447:366-80

Zitnan D, Kim YJ, Zitnanova I, Roller L, Adams ME. 2007. Complex steroid-peptide-receptor cascade controls insect ecdysis. *Gen Comp Endocrinol* 153:88-96

Zitnan D, Ross LS, Zitnanova I, Hermesman JL, Gill SS, Adams ME. 1999. Steroid induction of a peptide hormone gene leads to orchestration of a defined behavioral sequence. *Neuron* 23:523-35

Figure 2-2. Rest-activity patterns of 4th instar larvae under constant light conditions show developmental, but not circadian rhythms. (A) Fractions of quiescence (FQ) in 1 hr bins were calculated for 4th instar larvae recorded under L:L conditions (n=8). All individual fractions were plotted against time-of-day. **(B)** The average (error bars, s.e.m.) of all 1 hr fractions plotted in *Figure 2-1A*. There are no significant differences between levels of quiescence at any time-of-day. Statistical analysis was performed using Kruskal-Wallis one way analysis of variance on Ranks with Dunn's post-test. The average of all average 1 hr quiescence fractions for larvae within the 4th instar is 0.73 (+/- 0.005 s.e.m.). **(C)** When all 1 hr fractions of quiescence are set relative to the time of ecdysis to the 5th instar, a developmental pattern emerges. **(D)** Each data point represents the average (error bars, s.e.m.) of all 1 hr quiescence fractions that occurred at a given time, relative to the completion of ecdysis to the next instar. Quiescence levels decrease with increasing time during the larval feeding period, and then rise to high levels just prior to the time of head capsule slippage (HCS). Comparisons between quiescence levels during early, middle and late inter-molt (feeding) stages were made by calculating the fraction of quiescence in 10 hr bins between -90 and -80 (early) (Ave=0.73 +/-0.01 s.e.m.), -70 and -60 (middle) (Ave=0.67 +/-0.02 s.e.m.), -50 and -40 (late) (0.55 +/-0.03 s.e.m.) hours prior to ecdysis. At the time of head capsule slippage (HCS), which is approximately 27 to 30 hrs prior to ecdysis, average levels of quiescence exceed any of those observed during the inter-molt period, and they remain elevated until the time of ecdysis onset. The average fraction of quiescence for molting larvae between -20 and -10 hrs was 0.97 +/-0.004 s.e.m. Significant differences were found between all 10 hr average fractions using Kruskal-Wallis one way analysis of variance on rank with Student-Newman-Keuls post-test. The lowest Average 1 hr fraction of quiescence (Average=0.38 +/-0.06 s.e.m) occurred at 37 hrs prior to ecdysis, a developmental time-point which is thought to coincide with peak levels of molting hormones, therefore the onset of the rise in quiescent levels correlates well with the predicted peak and subsequent decline of molting hormones.

Figure 2-2

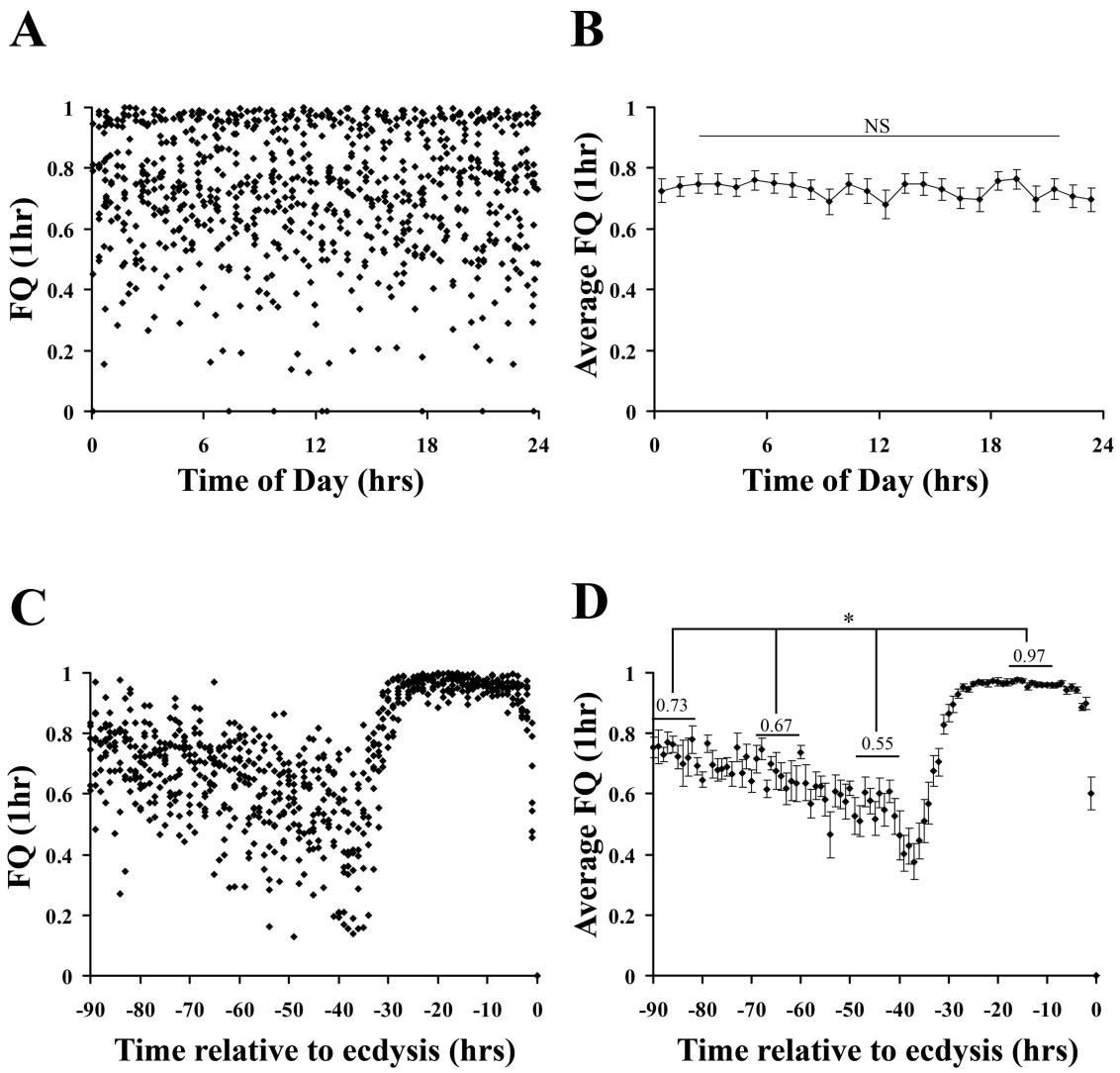
A
B
C
D
FQ (1hr)
Average FQ (1hr)
Time of Day (hrs)
Time relative to ecdysis (hrs)
NS
*
0.73
0.67
0.55
0.97
0
0.2
0.4
0.6
0.8
1
0
6
12
18
24
-90
-80
-70
-60
-50
-40
-30
-20
-10
0

Figure 2-3. Light cycle does not influence 4th instar rest-activity patterns. (A) Average fractions of quiescence in 1 hr bins were calculated for 4th stage larvae recorded under a 16L:8D photoperiod (n=3), and plotted against time-of-day (error bars, s.e.m.). There are no significant differences between average quiescence levels across time-of-day using Kruskal-Wallis one way analysis of variance on ranks. The average of all average 1 hr quiescence fractions under 16L:8D conditions, is 0.66 +/- 0.008 s.e.m. **(B)** All 1 hr fractions of quiescence were plotted relative to the time of ecdysis to the 5th instar. An overlay with values measured for larvae recorded under L:L conditions (*from Figure 2-1C*) demonstrates that the overall rest-activity patterns are the same for larvae under either L:L (grey diamonds) or 16L:8D conditions (black triangles). **(C)** There is no significant difference between quiescence levels when the average quiescence level during the first photophase is compared to behavior averaged from the scotophase, just prior to and following the first photophase (Student's t-test). **(D)** A typical 4th instar quiescence profile for an individual larva recorded under 16L:8D conditions is shown. Black bars in **(A)** and **(C)** represent the duration of lights-off.

Figure 2-3

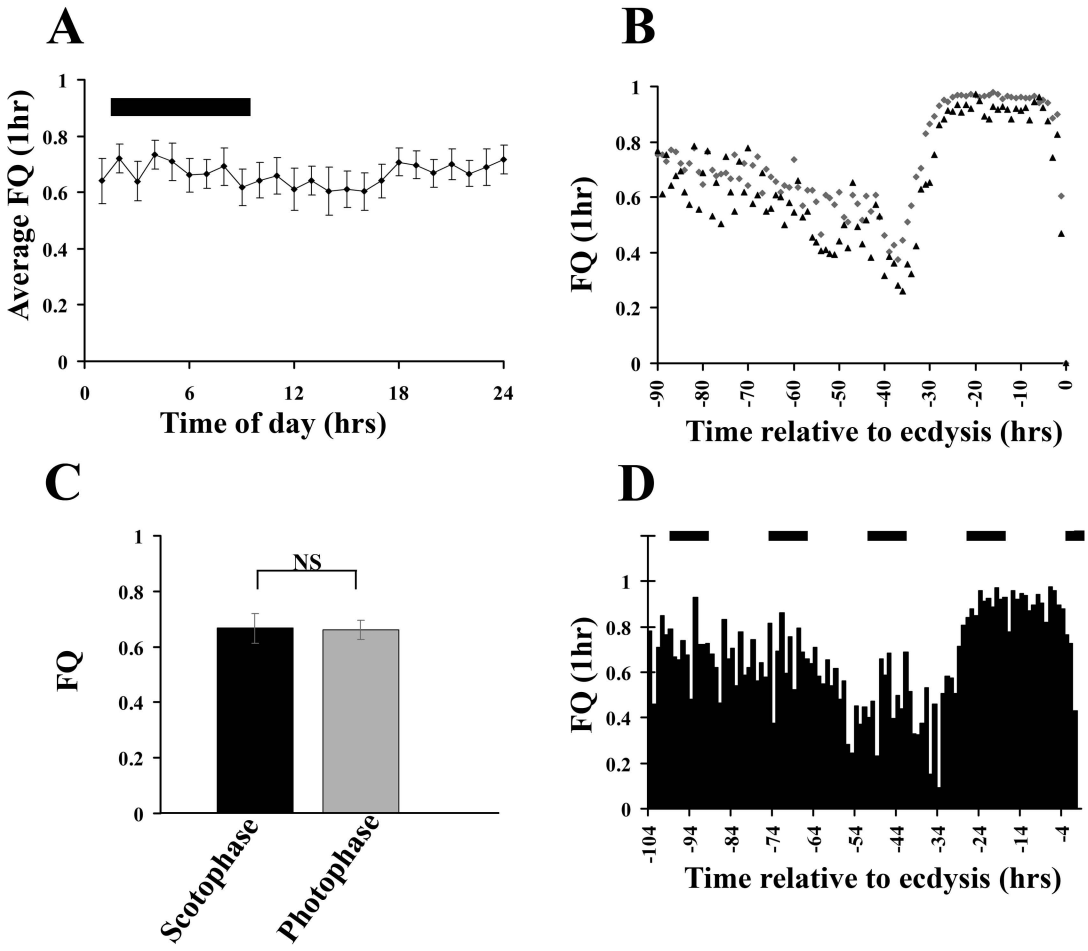
A
Average FQ (1hr)
Time of day (hrs)
B
FQ (1hr)
Time relative to ecdysis (hrs)
C
FQ
NS
Scotophase
Photophase
D
FQ (1hr)
Time relative to ecdysis (hrs)

Figure 2-4. Quiescence profiles across 3 larval stages. Average fractions of quiescence (in 1 hr bins) were calculated for larvae across the 4th (n=8), 3rd (n=6), and part of the 2nd (n=6) larval stages (L:L conditions). Individual values were set relative to time of ecdysis prior to the calculation of averages. Shown are the averages (error bars, s.e.m.). For all stages, behavioral quiescence is most concentrated during the molting periods. Quiescence levels decrease with increasing time within a larval stage, and then increase around the time the molt is initiated, where they remain elevated until the time of ecdysis. Quiescence patterns show distinct developmental rhythms, reproducible across individuals within a larval stage, and across larval stages.

Figure 2-4

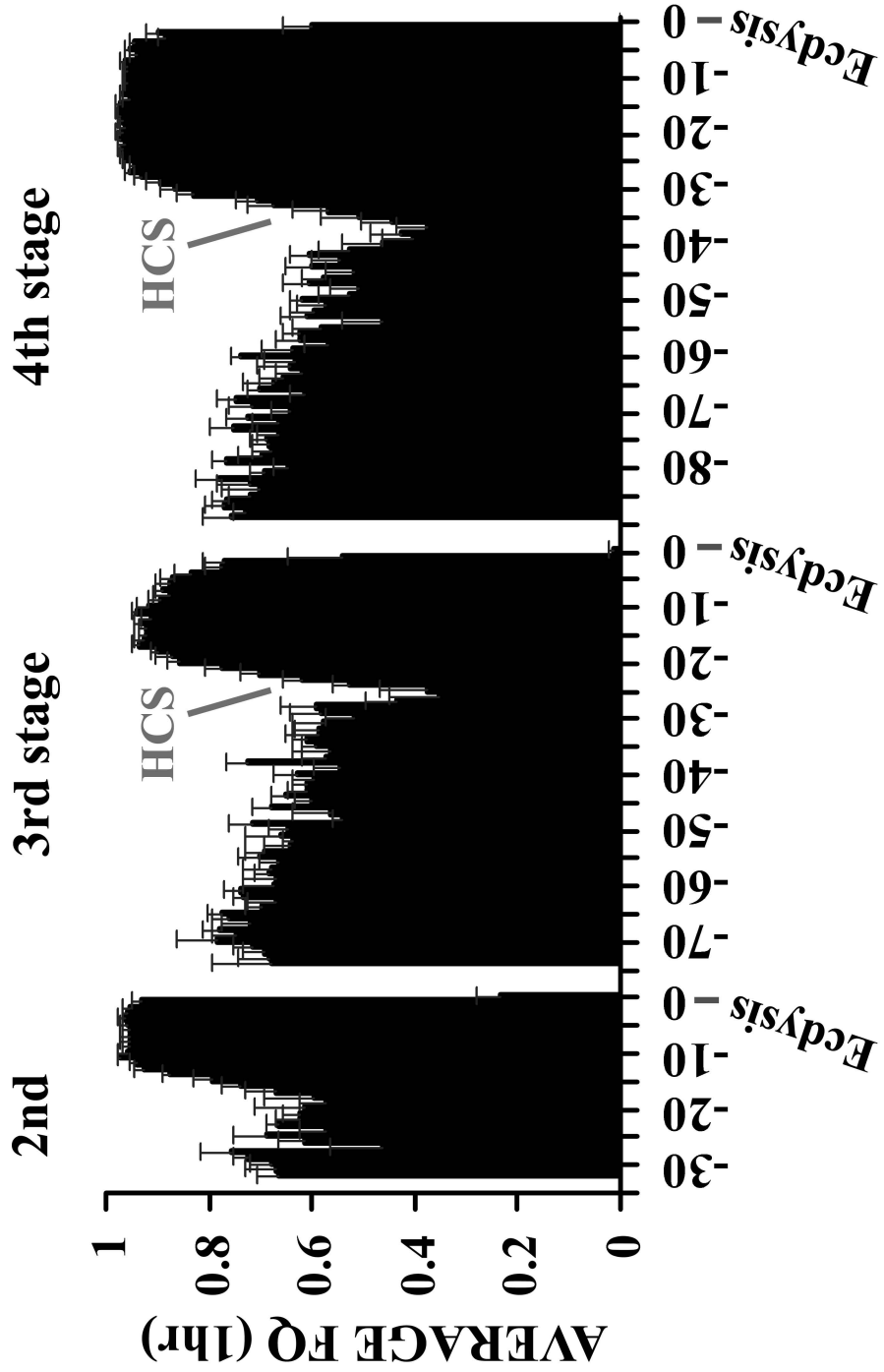
AVERAGE FQ (1hr)
1
0.8
0.6
0.4
0.2
0
2nd
3rd stage
4th stage
HCS
HCS
Ecdysis
Ecdysis
Ecdysis
-30
-20
-10
0
-70
-60
-50
-40
-30
-20
-10
0
-80
-70
-60
-50
-40
-30
-20
-10
0

Figure 2-5. Typical quiescence profile for an individual 4th instar larva. (A) Shown are the fractions of quiescence for an individual larvae in 10 min time windows, shifted 10 seconds for each data point. Each data point represents a 10 min fraction set relative to the time of ecdysis to the 5th instar. Each downward deflection represents increased activity over time. Activity is attenuated following the time of head capsule slippage, and quiescence values remain elevated until the time of ecdysis to the 5th larval stage. **(B)** A 10 hr time window from the inter-molt period (same individual as shown in *A*, time-frame is represented by the grey bar) shows that larvae are active and quiescent in distinct bouts. **(C)** A 10 hr time window from the molting period of the same animal shows that although activity decreases following head capsule slippage, activity bouts do still occur, demonstrating that larvae maintain the ability to behave during the molting period.

Figure 2-5

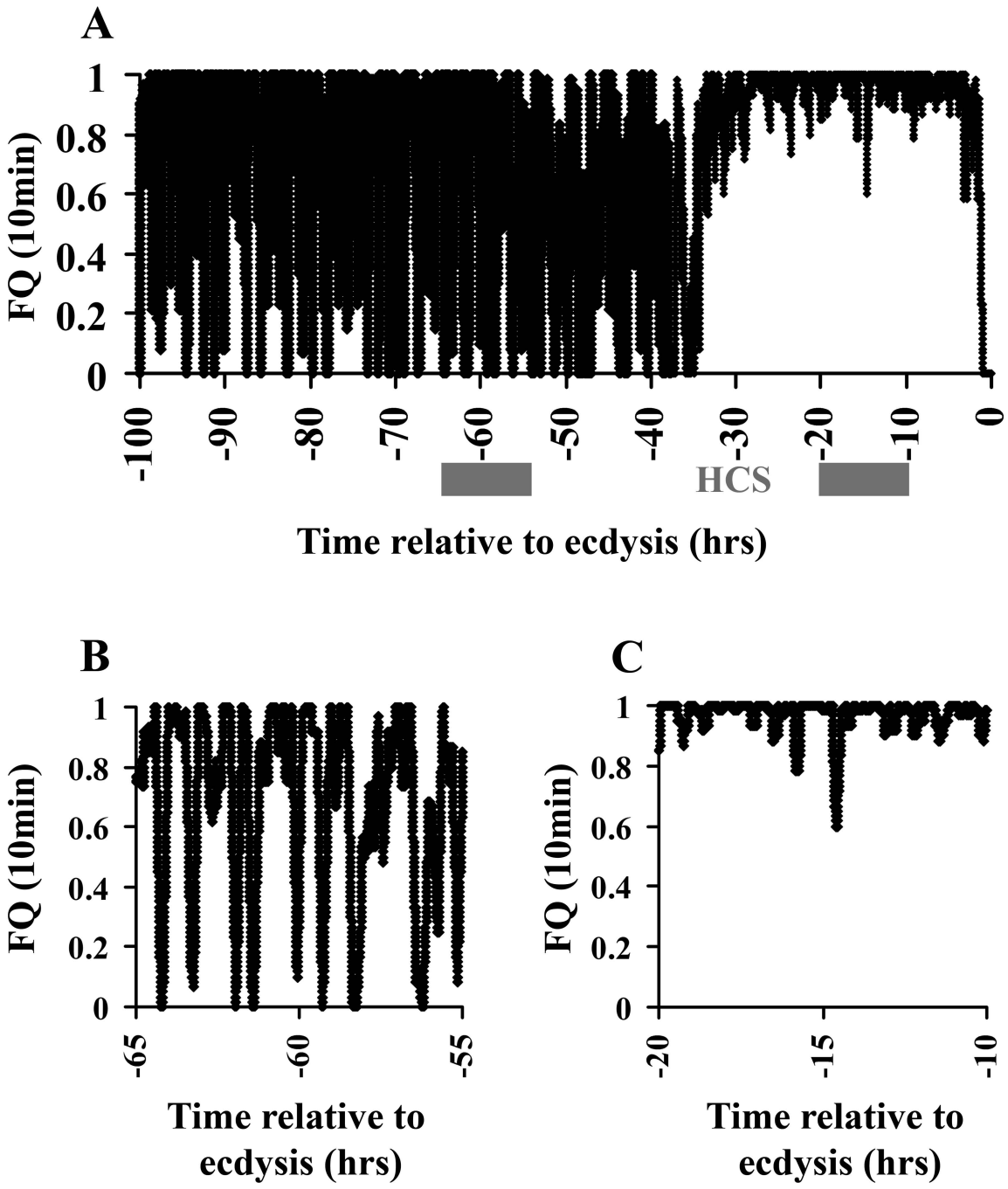
A
1
0.8
0.6
0.4
0.2
0
FQ (10min)
-100
-90
-80
-70
-60
-50
-40
-30
-20
-10
0
HCS
Time relative to ecdysis (hrs)
B
1
0.8
0.6
0.4
0.2
0
FQ (10min)
-65
-60
-55
Time relative to ecdysis (hrs)
C
1
0.8
0.6
0.4
0.2
0
FQ (10min)
-20
-15
-10
Time relative to ecdysis (hrs)

Figure 2-6. Quiescence-bout durations across the 4th larval stage. Prior to analysis, all values were set relative to time of ecdysis to the 5th larval stage. Each bin shows all bouts occurring within 5 hr bins for all larvae recorded under continuous light conditions (n=8). Maximal quiescent-bout duration decreases with increasing time within the inter-molt period. At the time of head capsule slippage, maximal bout duration increases above early and late inter-molt levels, indicating a more consolidated quiescence during the molting period. The peak quiescent bout duration is 183 min long, and occurs between 10 and 15 hrs prior to ecdysis.

Figure 2-6

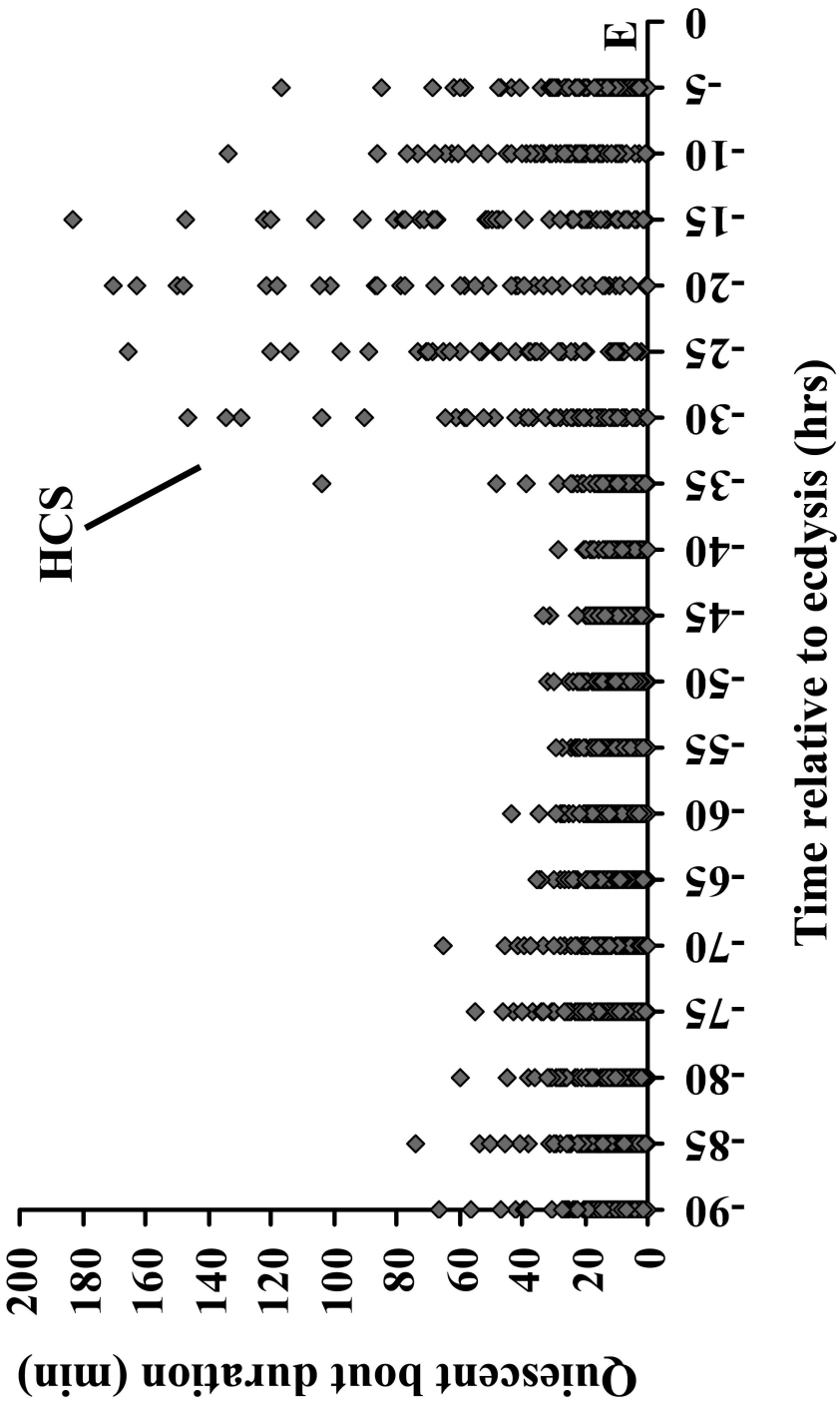
Quiescent bout duration (min)
200
180
160
140
120
100
80
60
40
20
0
Time relative to ecdysis (hrs)
-90
-85
-80
-75
-70
-65
-60
-55
-50
-45
-40
-35
-30
-25
-20
-15
-10
-5
E
0
HCS

Figure 2-7. Quiescence during the early and late inter-molt and mid-molting periods can be characterized based on bout duration. Bout duration from *figure 2-3* is divided into **(A)** early inter-molt (-80 to -90 hrs prior to ecdysis) **(B)** late inter-molt (-50 to -40 hrs prior to ecdysis), and **(C)** molting period (-20 to -10 hrs prior to ecdysis). For each stage is shown the percentages of quiescence bouts that fall into different duration categories. The categories are as follows: $\leq$1 min, >1 and up to 5 min, >5 and up to 10 min, >10 and up to 30 min, >30 and up to 1 hr, and >1 hr. Early and late inter-molt, and molting larvae can be characterized based on quiescent bout durations. Molting larvae show a high percentage of long-duration quiescent bouts with over half (54%) of all bouts showing a duration that is over 30 minutes. In contrast, only 1% of early inter-molt bouts and 0% of late inter-molt bouts show durations over 30 minutes.

Figure 2-7

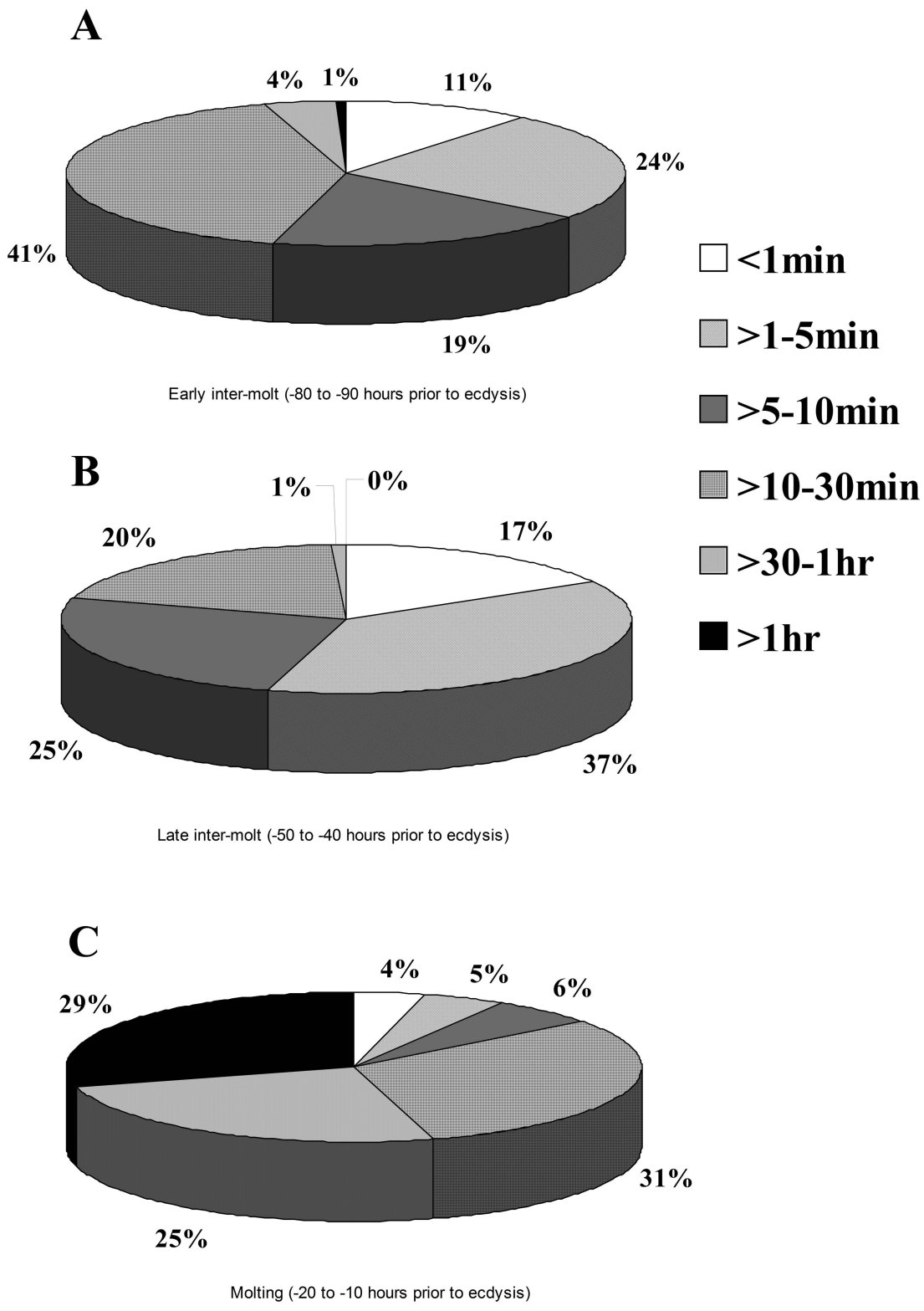
A
4%
1%
11%
24%
41%
19%
<1min
>1-5min
>5-10min
>10-30min
>30-1hr
>1hr
Early inter-molt (-80 to -90 hours prior to ecdysis)
B
1%
0%
20%
17%
25%
37%
Late inter-molt (-50 to -40 hours prior to ecdysis)
C
4%
5%
6%
29%
31%
25%
Molting (-20 to -10 hours prior to ecdysis)

Figure 2-8. Food-deprivation does not induce quiescent behaviors characteristic of molting larvae. Quiescent behavior was monitored for larvae deprived of food (n=6). All larvae were staged so that the 17-hr recording periods began ~24 hrs prior to the expected time of head capsule slippage. **(A)** All values are set relative to the onset of food-deprivation (recording start-time), and average fractions of quiescence were calculated for 1 hr bins (error bars, s.e.m.). During 17 hrs of food deprivation, average quiescence levels do not reach levels characteristic for molting larvae. The maximum average 1 hr fraction of quiescence reached only 0.61 at 15 hrs post-deprivation onset. **(B)** Shown is a typical rest/activity profile of an individual, food-deprived larva. Fractions of quiescence were calculated in 10 minute bins, and shifted 10 seconds for each data point. Extended activity bouts continued to occur throughout the entire 17 hr recording period. For all larvae, only 3.7% of all bouts extended beyond 30 minutes. The maximum bout duration for any larva was 44.5 minutes (at 15 hrs post-deprivation), and the average bout duration across the 17 hr recording period was between 9 and 10 min. At no time during 17 hrs of food deprivation does the behavior of starved late 4^{th} instar larvae resemble behavior observed during the molting period.

Figure 2-8

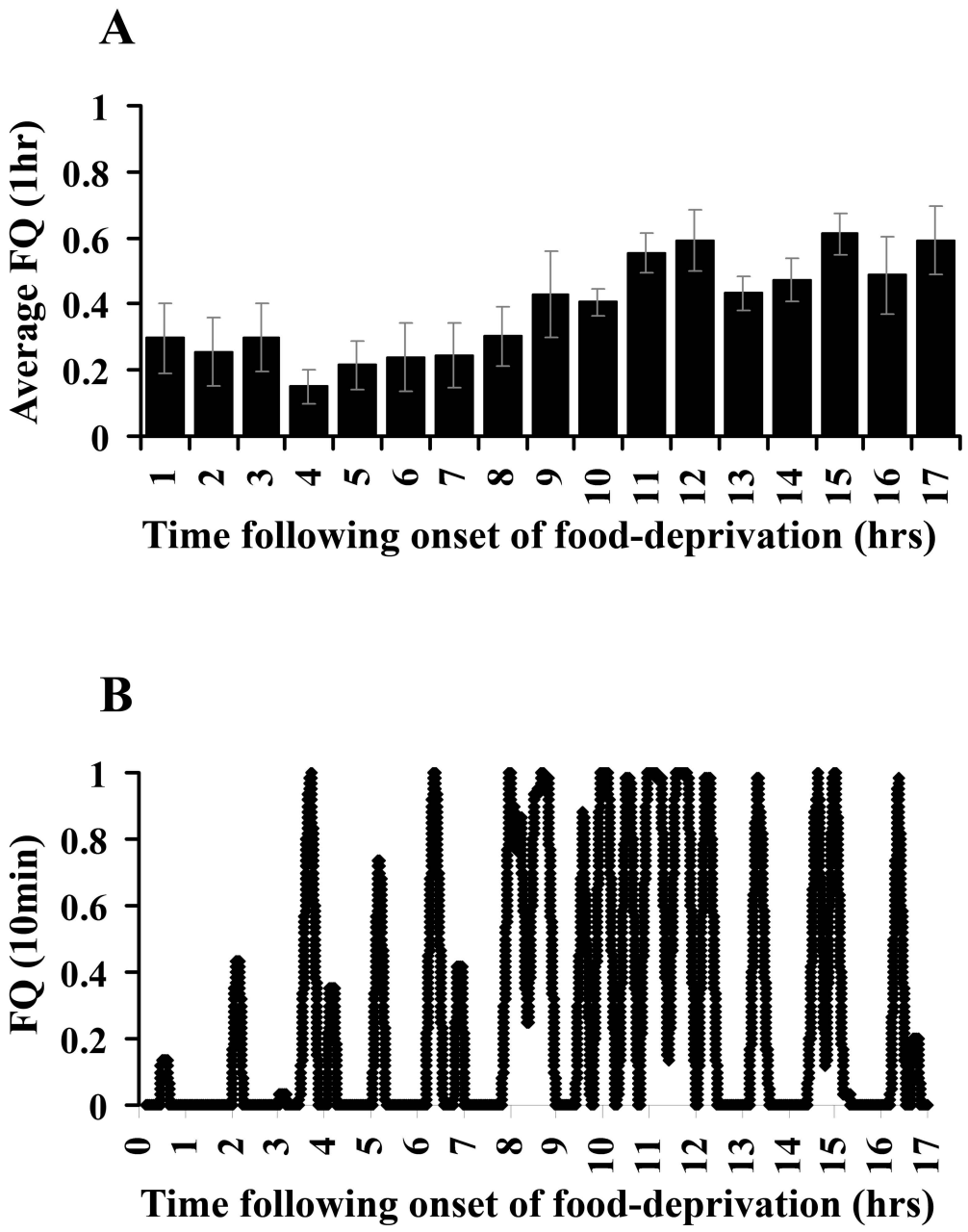
A
Average FQ (1hr)
1
0.8
0.6
0.4
0.2
0
1 2 3 4 5 6 7 8 9 10 11 12 13 14 15 16 17
Time following onset of food-deprivation (hrs)
B
FQ (10min)
1
0.8
0.6
0.4
0.2
0
0 1 2 3 4 5 6 7 8 9 10 11 12 13 14 15 16 17
Time following onset of food-deprivation (hrs)

Figure 2-9. Larval quiescence is a reversible state. Behavior was monitored for 10 min (0.2 sec between frames) while larvae were in continuous contact with either a DRY or a WET surface. **(A)** Under DRY conditions, inter-molt larvae (Late 4^{th}) that are quiescent for at least 30 sec prior to testing (IMQ) show significantly higher 10 min fractions of quiescence than inter-molt larvae that are active for at least 30 sec prior to testing (IMA) [Averages = 0.78 (+/-0.08 s.e.m.) and 0.37 (+/-0.1 s.e.m.), respectively. Students t-test, p=0.005]. There are no significant differences between quiescence levels measured for spontaneously active larvae in DRY conditions (IMA/DRY), and for inter-molt larvae tested under WET conditions [IMQ/WET average fraction of quiescence=0.34 (+/-0.09 s.e.m.), IMA/WET average=0.25 (+/-0.09 s.e.m.), Students t-test, no significance (NS)]. Quiescence during the inter-molt is reversed to levels observed for spontaneously active larvae during a 10 min exposure to a wet surface. **(B)** Mid-molting larvae (~15 hrs prior to ecdysis) that are quiescent for at least 30 sec prior to placement on the DRY bath (MMQ) are quiescent on average over 90% of the time [average 10 min fraction of quiescence = 0.91 (+/-0.03 s.e.m.)]. When molting larvae are aroused prior to placement on the bath (MMA) under DRY conditions, quiescence levels significantly decrease [ave=0.67 (+/-0.04 s.e.m.), Students t-test, p=<0.001], but do not drop to levels observed for spontaneously active IM larvae. When MMQ and MMA larvae are continuously exposed to the WET surface, 10 min fractions of quiescence do drop to levels observed for aroused inter-molt larvae [MMQ ave=0.42 (+/-0.06 s.e.m.), MMA ave=0.25 (+/-0.05 s.e.m.)]. Increased quiescence levels during the molt are rapidly reversible following exposure to an arousing stimulus, and increased activity levels can be maintained for at least 10 min under continuous exposure. **(C)** A comparison of molting and inter-molt quiescence levels under WET conditions. (Students t-test, NS). **(D)** 10 min fractions of quiescence under WET conditions were obtained for larvae at the time of air-filled head capsule [AF+0 = ~5-6 hrs prior to ecdysis; ave=0.42 (+/-0.08 s.e.m.)], and 3 hrs following air filling [AF+3 = 2-3 hrs prior to ecdysis; ave=0.46 (+/-0.10 s.e.m.)]. All larvae were quiescent for at least 30 sec prior to placement on the water bath. MMQ/DRY is shown for comparison. There are no significant differences between quiescence levels measured for any of the molting larvae exposed to wet conditions (ANOVA, NS). Molting larvae maintain the ability to respond to an arousing stimulus until late in the molt. (IMQ/DRY, n=10; IMA/DRY, n=10; IMQ/WET, n=10; IMA/WET, n=9; MMQ/DRY, n=10; MMA/DRY, n=10; MMQ/WET, n=10; MMA/WET, n=9; AF+0, n=5; AF+3, n=5). (Students t-test, ***p<0.001, **p<0.001, *p<0.05; error bars, s.e.m.).

Figure 2-9

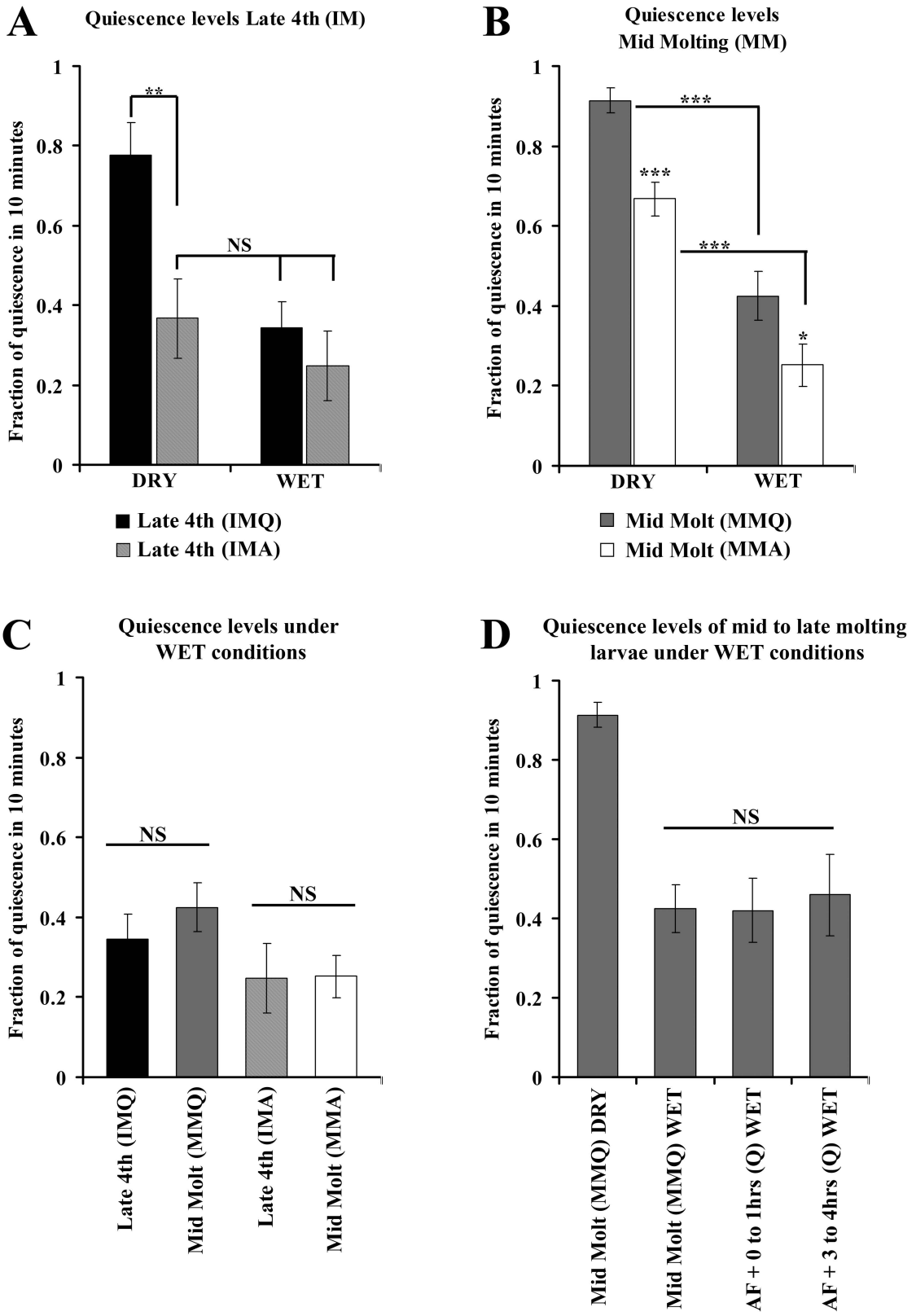
A
Quiescence levels Late 4th (IM)
Fraction of quiescence in 10 minutes
1
0.8
0.6
0.4
0.2
0
**
NS
DRY
WET
Late 4th (IMQ)
Late 4th (IMA)
B
Quiescence levels
Mid Molting (MM)
Fraction of quiescence in 10 minutes
***
***
***
*
DRY
WET
Mid Molt (MMQ)
Mid Molt (MMA)
C
Quiescence levels under
WET conditions
Fraction of quiescence in 10 minutes
NS
NS
Late 4th (IMQ)
Mid Molt (MMQ)
Late 4th (IMA)
Mid Molt (MMA)
D
Quiescence levels of mid to late molting
larvae under WET conditions
Fraction of quiescence in 10 minutes
NS
Mid Molt (MMQ) DRY
Mid Molt (MMQ) WET
AF + 0 to 1hrs (Q) WET
AF + 3 to 4hrs (Q) WET

Figure 2-10. The percentage of larvae that escape from the behavioral arena increases with increasing temperature of the water bath. When arenas are placed on the water bath, but contact with the water is prevented, no larvae escape from the arena within the 10 min recording period. When larvae are in contact with room temperature water, IMQ, IMA and MMQ larvae do not escape from the arena, but 10% of MMA do escape. All inter-molt larvae escape from 40 and 50°C water baths, which suggests that water at these temperatures, represents a noxious stimulus for inter-molt larvae. At 40°C, all MMA larvae escape from the arena, but only 70% of MMQ larvae escape from the arena, which suggests that molting quiescence is a state of reduced responsiveness compared to activity states and quiescence states during the inter-molt. At 50°C, all molting larvae escape from the arena. (IMQ/DRY, n=10; IMA/DRY, n=10; IMQ/25°C, n=10; IMA/25°C, n=9; IMQ/40°C, n=20; IMA/40°C, n=17; IMQ/50°C, n=24; IMA/50°C, n=19; MMQ/DRY, n=10; MMA/DRY, n=10; MMQ/25°C, n=10; MMA/25°C, n=9; MMQ/40°C, n=19; IMA/40°C, n=19; IMQ/50°C, n=16; IMA/50°C, n=18).

Figure 2-10

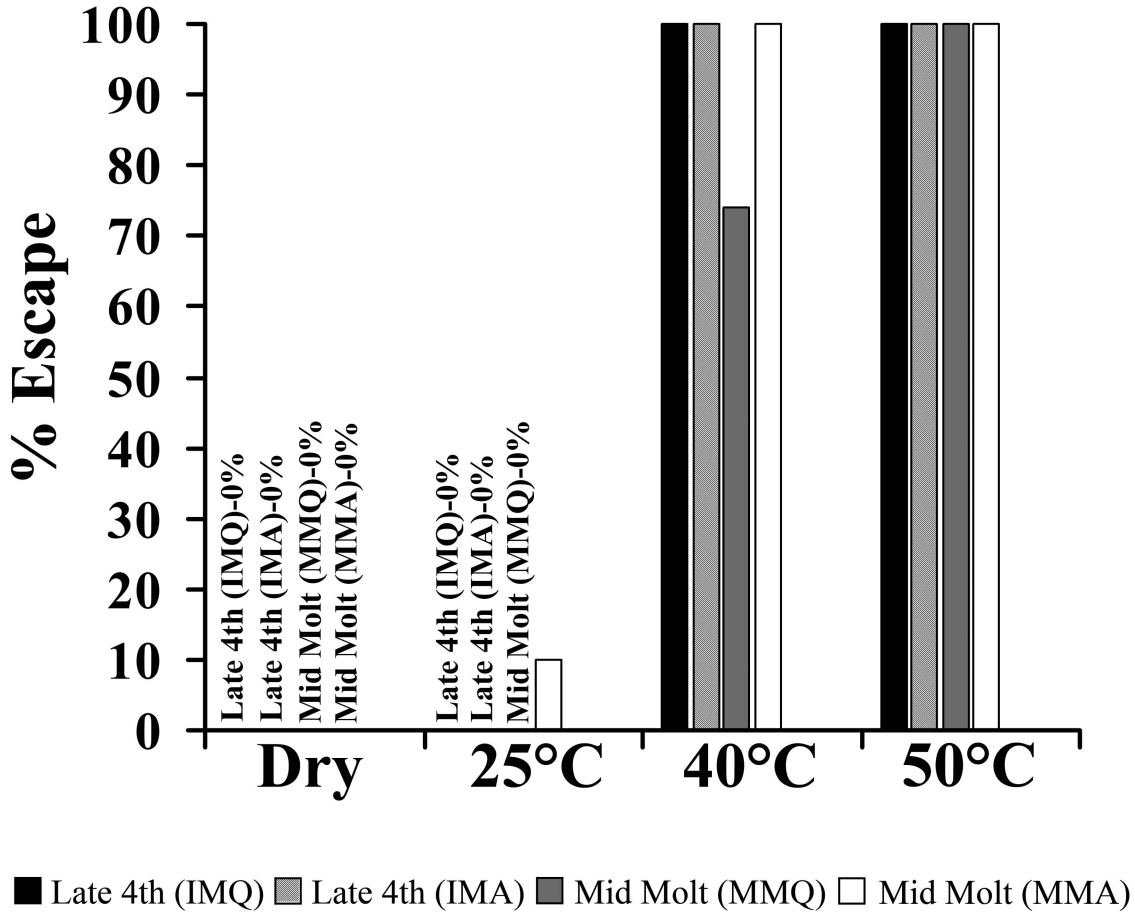
% Escape
100
90
80
70
60
50
40
30
20
10
0
Late 4th (IMQ)-0%
Late 4th (IMA)-0%
Mid Molt (MMQ)-0%
Mid Molt (MMA)-0%
Late 4th (IMQ)-0%
Late 4th (IMA)-0%
Mid Molt (MMQ)-0%
Dry
25°C
40°C
50°C
Late 4th (IMQ)
Late 4th (IMA)
Mid Molt (MMQ)
Mid Molt (MMA)

Figure 2-11. Larval quiescence is accompanied by a rapidly reversible increase in arousal threshold. (A) Shown are the response-latencies (time to the onset of locomotion following exposure to the water bath) for all inter-molt larval groups. The average latency of response to 40°C water for IMQ larvae is 55.25 (+/- 6.3 s.e.m.) sec. When larvae are spontaneously active (IMA) prior to placement on the 40°C bath, latency significantly declines to an average of 35.9 (+/- 3.2 s.e.m.) sec (Student's t-test, p=0.037). IMQ larvae show latencies that are reduced when larvae of the same stage are aroused prior to placement on the 40°C water bath. At 50°C, latency is reduced compared to larvae exposed to the lower temperature, but IMQ and IMA larvae respond with similar latencies, with average latencies of 16.1 (+/-1.3 s.e.m) and 15.7 (+/-1.4 s.e.m.) sec, respectively. **(B)** Shown are the response latencies of mid-molting larvae. At *both* temperatures, MMQ larvae show significantly increased latencies when compared to MMA larvae, and response latencies also decrease with increasing temperatures. Average latencies for MMQ and MMA larvae at 40°C are 74.3 (+/- 7.9 s.e.m.) and 50.7 (+/-4.2 s.e.m.) sec, respectively (Student's t-test, p=0.012). At 50°C, average response latencies are 27.9 (+/- 2.6 s.e.m.) sec for MMQ larvae, and 14.0 (+/- 1.1 s.e.m.) for MMA larvae (Student's t-test, p=<0.001). At 50°C, aroused molting larvae show latency values that are not significantly different from those observed for IMA and IMQ larvae (Student's t-test, NS). **(C, D)** Shown is the average time taken by IM and MM larvae to reach the edge of the arena following the initiation of locomotion. **(C)** At 40°C**,** IMQ and IMA larvae reach the edge in 62.8 (+/- 11.0 s.e.m.) and 50.02 (+/- 8.0 s.e.m.) sec, respectively. The rate of locomotion increases dramatically for IM larvae at 50°C [IMQ ave=7.1 (+/- 0.9 s.e.m.) and IMA ave=12.5 (+/- 2.6 s.e.m.)]. Once initiated, rate of locomotion is not significantly different for larvae that were quiescent or active prior to placement on the water bath. **(D)** Molting larvae locomote at rates that are comparable to those observed for inter-molt larvae. At 40°C, MMQ and MMA reach the edge in an average of 40.6 (+/- 6.0 s.e.m.) and 33.4 (+/- 4.2s.e.m.) sec, and at 50°C, MMA larvae reach the edge in 12.0 (+/- 1.4 s.e.m.) and 11.7 (+/- 1.2 s.e.m.) sec. These results demonstrate that locomotion is not impaired in molting larvae. (IMQ/40°C, n=20; IMA/40°C, n=17; IMQ/50°C, n=24; IMA/50°C, n=19; MMQ/40°C, n=19; IMA/40°C, n=19; IMQ/50°C, n=16; IMA/50°C, n=18). (Student's t-test, ***p<0.001, **p<0.001, *p<0.05; error bars, s.e.m.).

Figure 2-11

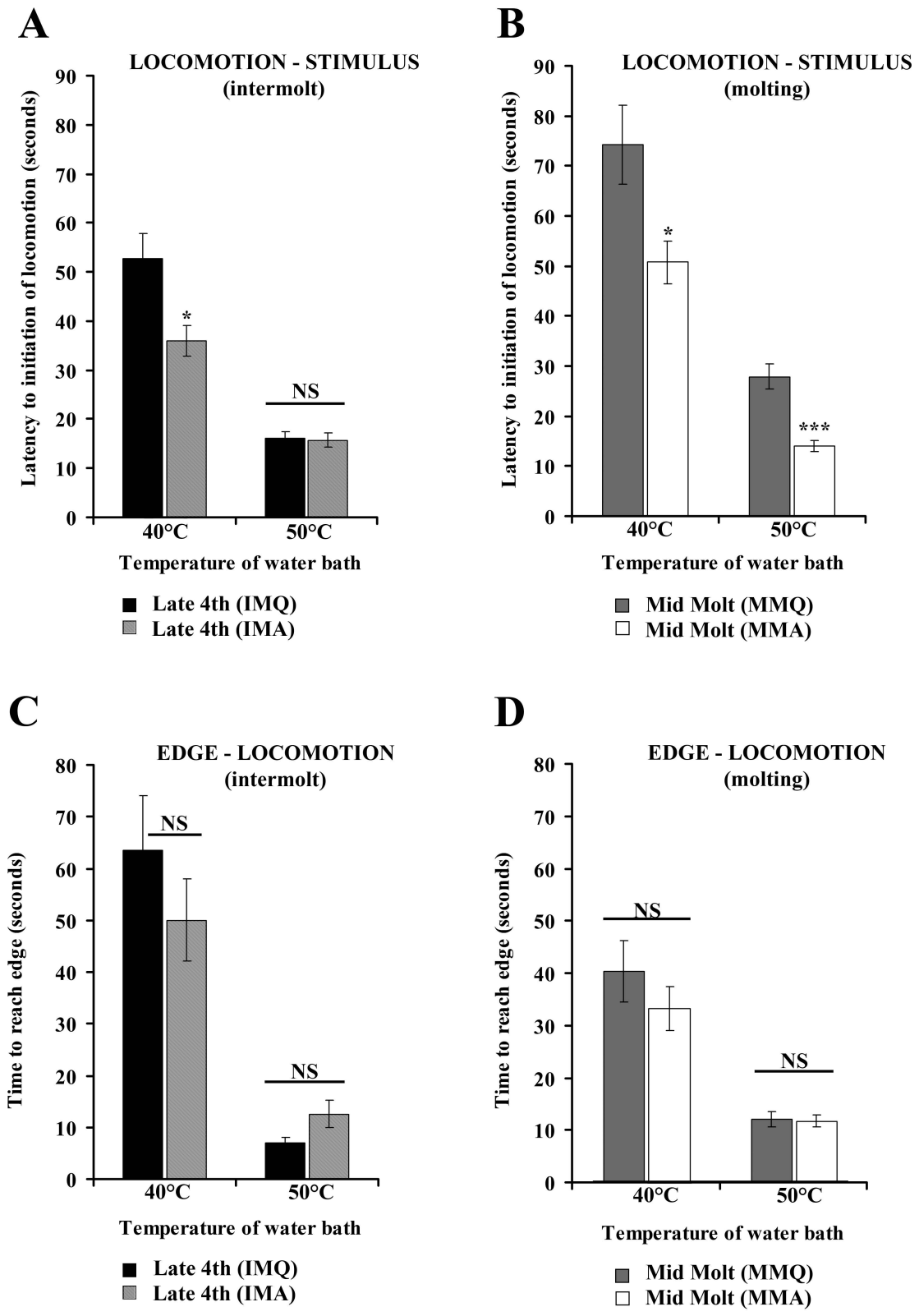
A
LOCOMOTION - STIMULUS
(intermolt)
Latency to initiation of locomotion (seconds)
90
80
70
60
50
40
30
20
10
0
*
NS
40°C
50°C
Temperature of water bath
Late 4th (IMQ)
Late 4th (IMA)
B
LOCOMOTION - STIMULUS
(molting)
Latency to initiation of locomotion (seconds)
*
***
40°C
50°C
Temperature of water bath
Mid Molt (MMQ)
Mid Molt (MMA)
C
EDGE - LOCOMOTION
(intermolt)
Time to reach edge (seconds)
80
70
60
50
40
30
20
10
0
NS
NS
40°C
50°C
Temperature of water bath
Late 4th (IMQ)
Late 4th (IMA)
D
EDGE - LOCOMOTION
(molting)
Time to reach edge (seconds)
NS
NS
40°C
50°C
Temperature of water bath
Mid Molt (MMQ)
Mid Molt (MMA)

Figure 2-12. Deprivation of quiescence during the intermolt, but not during the molting periods, is followed by quiescence-rebound. (A) A semi-automatic deprivation protocol was used to deprive larvae of quiescence (See "Materials and Methods"). **(B)** Shown are the average (error bars, s.e.m.) 1 hr fractions of quiescence (FQ) across a 24 hr recording session (10 sec delay between frames) following the termination of deprivation, and the % change in 1 hr average FQ compared to controls. Intermolt larvae deprived of quiescence for 3 hrs (n=9) show a significant quiescence rebound compared to control animals (n=9) during the first 4 hrs following the termination of deprivation. During the first 6 hrs of recording, average quiescence levels are increased by 34.6% compared to controls, and there is an overall increase of 6.5% across the entire 24 hr recording session. Peak quiescence levels occur during the first hour of recording (FQ=0.82 +/- 0.03 s.e.m.). When additional animals were deprived for 3 hrs (n=6) and then tested on a 40°C water bath, rates of locomotion (time to edge following the initiation of locomotion=23.8 +/-5.0 sec, s.e.m.) were not significantly different from controls (n=6) (time to edge=30.0 +/-6.3 sec, s.e.m.) (data not shown). **(C)** Following 6 hrs of deprivation (n=8), intermolt larvae show a significant increase in quiescence levels over controls (n=8) during hrs 1, 3-4, 6 and 12 following the termination of deprivation. During the first 6 hrs following deprivation, average quiescence are increased over controls by 28.5%, and levels are increased by 13.5% over the duration of the entire 24 hr recording session. Peak fraction of quiescence occurred at hr 1 (Average 1 hr FQ=0.86 +/- 0.03 s.e.m.). **(D)** Following 12 hrs of deprivation during the intermolt (n=9), average quiescence is significantly increased compared to controls (n=9) during hrs 1-3 and 5-7 of the recording session. During the first 6 hrs, average quiescence is increased by 29.0% and levels are increased over the total 24 hr recording session by 12.9%, similar to larvae deprived for 6 hrs. Peak average quiescence level was 0.92 (+/- 0.02 s.em.) and occurred during the first hr of recording. **(B-D)** For inter-molt larvae deprived of quiescence for 3, 6 or 12 hrs, average quiescence levels at the end of the recording session are not significantly different from control levels. **(E)** When larvae are deprived of quiescence for 6 hrs during the early molt (Emolt) to 5th instar (n=6), subsequent quiescence levels show no significant changes compared to controls (n=6). **(F)** Deprivation of quiescence for 6-9 hrs during the molting period just prior to ecdysis to the 4th instar (n=6) has no significant effect on quiescence levels of larvae during the early 4th intermolt stage that follows ecdysis (control, n=6). [*** indicates $p<0.001$, ** $p<0.01$, * $p<0.05$; Average fractions of quiescence were compared using Student's t-test for parametric and the Mann-Whitney Rank Sum Test for non-parametric data. NS=not significant].

Figure 2-12

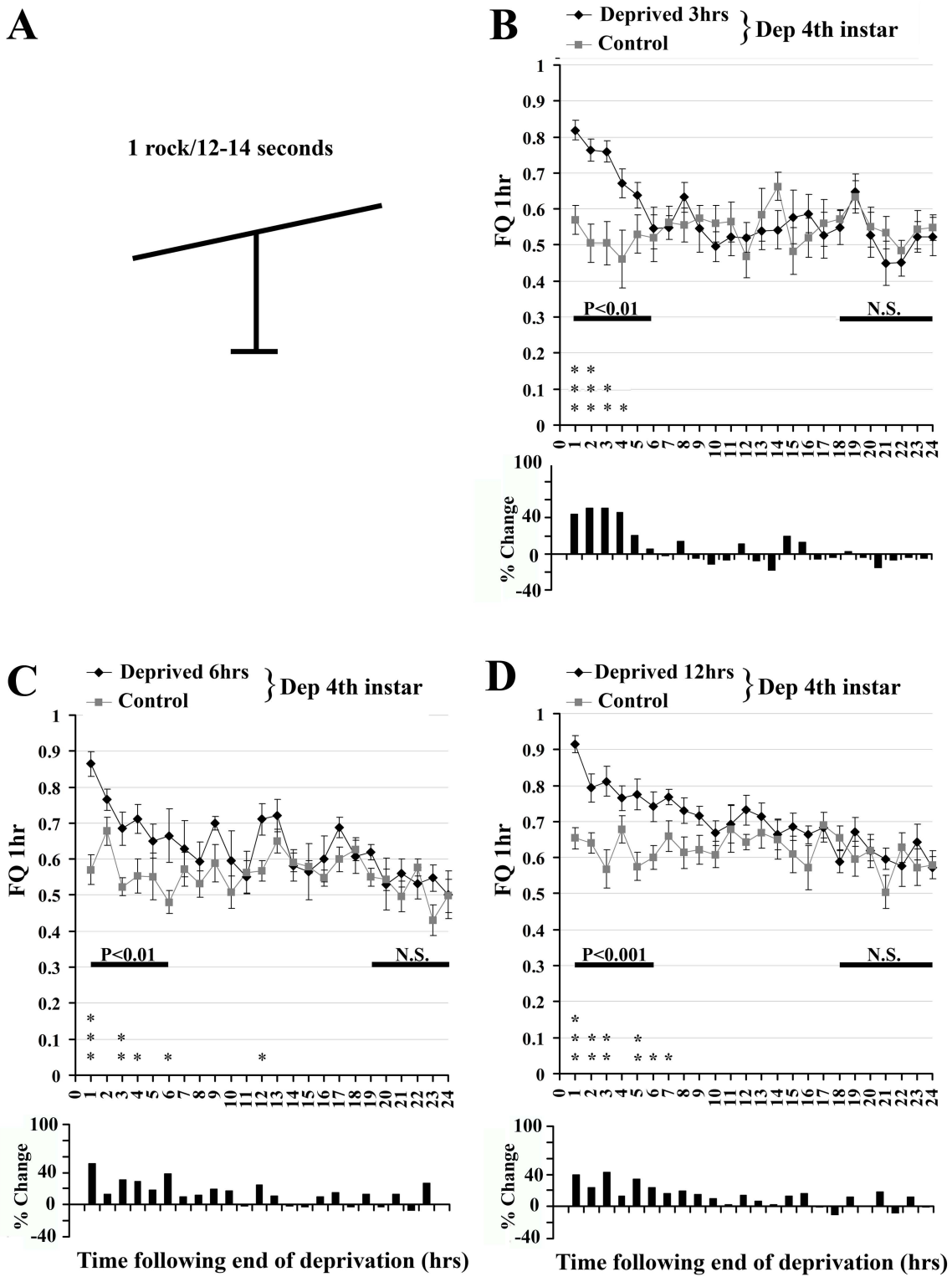
A
1 rock/12-14 seconds
B
Deprived 3hrs
Control
Dep 4th instar
FQ 1hr
P<0.01
N.S.
% Change
C
Deprived 6hrs
Control
Dep 4th instar
FQ 1hr
P<0.01
N.S.
% Change
Time following end of deprivation (hrs)
D
Deprived 12hrs
Control
Dep 4th instar
FQ 1hr
P<0.001
N.S.
% Change
Time following end of deprivation (hrs)

Figure 2-12 (Cont'd)

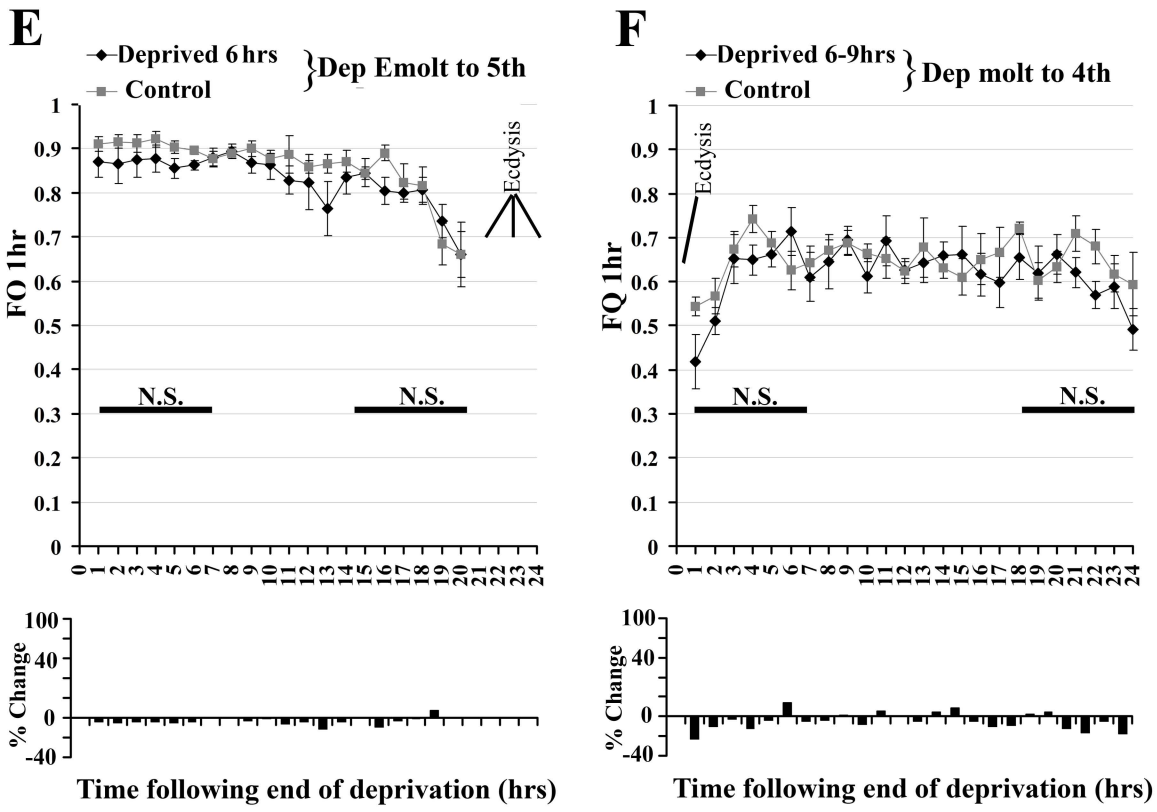

Figure 2-13. The *period* gene is expressed in peripheral and central nervous system tissues of 4th instar *Manduca sexta* larvae. A single PCR product of the expected size of 976bp was detected in samples representative of both peripheral and central nervous tissues. In lane 2 is shown PCR products from ventral nerve cord cDNA, and lane 3 shows the products from a sample that combined epidermis, fat body and trachea cDNA. Bands were compared to the 1Kb Plus DNA Ladder (Invitrogen) shown in lane 3. PCR products were run on a 1.2% agarose gel stained with ethidium bromide.

Figure 2-13

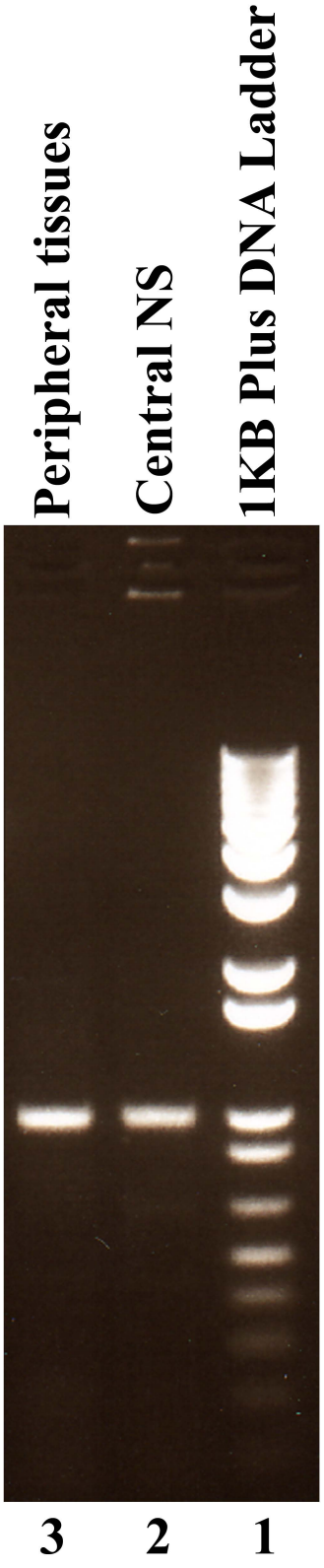

Figure 2-14. *Period* gene expression in the brains of 4th instar larvae does not show circadian or developmental rhythms. Quantitative PCR was used to profile per mRNA expression across 11 developmental stages spanning the 4th larval instar. Three biological replicates were run independently, and within each replicate, samples were run in triplicate. All fold-change is relative to developmental stage HCS -36 hrs, and cytoplasmic actin was used as the internal reference gene. **(A)** Shown is the average relative-fold change for each of the 11 developmental stages plotted against time of day (6=6AM, 24=midnight). There is no correlation between per expression and time-of-day (Pearson Product Moment Correlation, correlation coefficient= -0.0115, p=0.973). **(B)** When samples are plotted relative to the time of head capsule slippage (HCS), no significant difference is observed between samples at any time across development (Kruskal-Wallis One Way Analysis of Variance on Ranks, p=0.141).

Figure 2-14

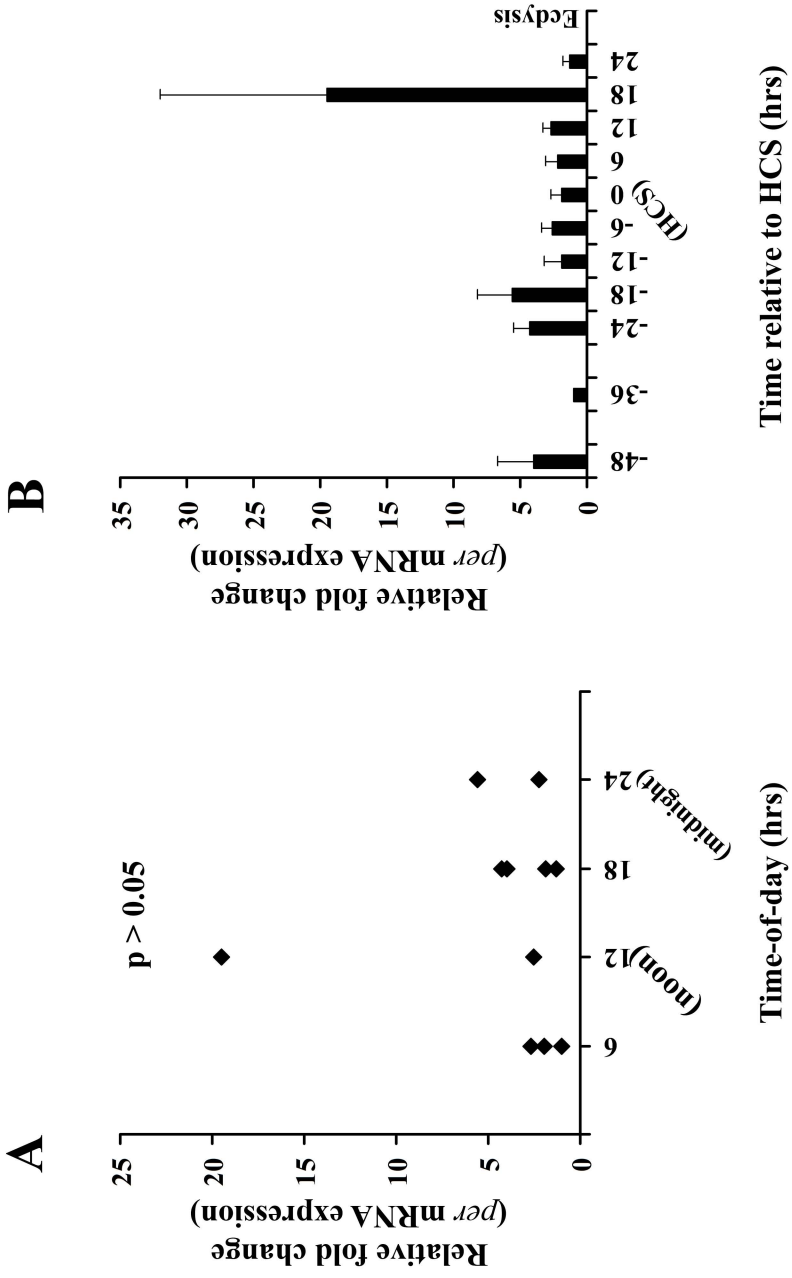
A
Relative fold change
(per mRNA expression)
25
20
15
10
5
0
p > 0.05
6
(noon)12
18
(midnight)24
Time-of-day (hrs)
B
Relative fold change
(per mRNA expression)
35
30
25
20
15
10
5
0
-48
-36
-24
-18
-12
-6
(HCS) 0
6
12
18
24
Ecdysis
Time relative to HCS (hrs)

Chapter 3: Profile and Analysis of the Brain Transcriptome During Larval Development of *Manduca Sexta*

Abstract

Larval molts of the holometabolous insect *Manduca sexta* have long been used as a model system to investigate the neuroendocrine coordination of insect physiology and behavior. The rise and fall of molting hormones program the successive bouts of gene expression in the epidermis that lead to synthesis and digestion of cuticle, as well as to the termination of the molt brought about by ecdysis—a centrally-generated behavior that leads to shedding of the old cuticle. During the molting period prior to ecdysis, *M. sexta* exhibits a prolonged period of quiescence characterized by low levels of spontaneous activity and increased arousal thresholds, but these quiescent larvae maintain the ability to respond to mildly arousing and noxious stimuli. The onset of molting-quiescence (known as "molt-sleep") correlates well with the predicted peak of molting hormones, which suggests that in addition to ecdysis, molting hormones also (either directly or indirectly) act on the nervous system to program a quiescent state. To investigate changes in gene expression that might underlie the induction and maintenance of the molt-sleep, Illumina RNA-seq was used to profile the *M. sexta* brain transcriptome at several developmental time points surrounding and during the onset of the 4^{th} to 5^{th} stage molt-sleep. Identification of expressed genes was achieved using a novel method that involved alignment of translated reads onto the proteome of *Bombyx mori*, which is the most closely-related species for which a genome is known. This study provides the first

description of any *M. sexta* nervous tissue transcriptome. 10,664 unique proteins were mapped during at least one developmental stage and between 2.8% and 7.8% of all corresponding genes were differentially-expressed during at least one stage when compared to mid-intermolt reference levels. Enrichment analyses of differentially-expressed transcripts show dominance in the enrichment of processes related to tracheal cuticle synthesis and degradation, and a number of transcription factors were enriched in brains prior to and during the onset of the molt-sleep. Cluster analysis identified 11 clusters of transcripts that shared similar expression profiles, and 4 clusters showed enrichment of functional categories, which included processes related to detoxification, juvenile hormone catabolism, chitin metabolism, autophagy, protein secretion, and cGMP metabolism. In addition, we identified differentially-expressed transcripts that code for neuropeptides, enzymes involved in the synthesis of small neurotransmitters, ligand-gated ion channels, G-protein coupled receptors, ion channels and other products associated with neural activity. Possible roles for these products in the modulation of larval arousal-state are described.

Introduction

The holometabolous insect, *Manduca sexta* (*M. sexta*), has long served as a primary model system for the study of physiological and behavioral changes surrounding the insect molt. In order to grow, insects must molt—a process that consists of periodic synthesis and shedding of the exoskeleton (cuticle) (Ewer 2005). The elaborate sequence of events that occurs during a molting cycle is driven by molting hormones (Nijhout

1994). There are many examples in the mammalian literature of hormonally driven processes that involve concomitant peripheral and central hormone actions, which bring about synergistic changes in behavior and physiology (Pfaff et al 2004). This is also true for insects. During the insect larval molt, the rise and the fall of molting hormones leads to the induction of successive bouts of gene expression that prepare the epidermal cells for their role in cuticle synthesis and degradation; but molting hormones also effect changes in the central nervous system that underlie behaviors, such as the precisely orchestrated ecdysis behavioral sequence that results in the shedding of the old cuticle at the end of the molt (Zitnan et al 2007). Over many decades, the timing of endocrine events that accompany *M. sexta*'s molt to its 5th and final larval stage have been carefully worked out, and in the previous chapter we demonstrated a correlation between the predicted peak of the steroid molting hormone 20-hydroxyecdysone with the onset of a consolidated quiescent period that persists for up to 30 hrs (until onset of ecdysis). Molting quiescence is similar across individuals within a larval instar, is repeated across multiple instars, and exhibits the sleep-like properties of increased arousal threshold and rapid reversibility. But homeostatic mechanisms that regulate the amount of quiescence seem to be shut down during this period, as is the drive to forage. The coincidence of molt-sleep onset with the ecdysteroid peak suggests that molting hormones might act, either directly or indirectly, on the central nervous system to bring about changes in gene expression that alter general, sleep-wake type arousal state.

Interest in the quiescent behaviors of insects increased following the discovery that the quiescence in adult flies shares many properties in common with mammalian

sleep-like states (Hendricks et al 2000; Shaw et al 2000). The relative simplicity of the *Drosophila* nervous system coupled with its genetic tractability makes the fly an excellent candidate for investigations into the elusive function(s) of sleep, as well as for identification of neurotransmitter systems involved in the initiation, maintenance and termination of sleep-like states. In the adult fly, the brain has been identified as a major site of sleep-wake regulation; several brain regions and neurotransmitter systems important for that regulation have been identified (Crocker & Sehgal 2010). The involvement of the neuroendocrine system in adult sleep-wake type arousal also is becoming apparent; in the adult fly, ecdysteroids have been shown to be sleep-promoting (Ishimoto & Kitamoto 2010).

As in mammals, fly neurotransmitter systems that modulate general arousal state are also potent modulators of more specific forms of arousal. Dopamine (DA), for example, increases general activity levels, but also influences courtship behavior, startle behavior, and learning and memory, and the effects of DA on specific behaviors are concentration and receptor subtype-dependent (Lebestky et al 2009; Van Swinderen & Andretic 2011). It is interesting that DA also has been implicated as an important factor in induction of pupal and egg diapause of developing lepidoptera (Noguchi & Hayakawa 1997; 2001). Many small molecule neurotransmitters and neuropeptides present in adults also are present in the larval CNS, and although the structures are simpler in terms of cell number and complexity of connections, larval brains also contain sites of multimodal sensory integration, such as mushroom bodies and the central complex, which are sites known in adults to be important for regulation of both general and specific arousal states.

Regulation of arousal state is an important component of the insect behavioral repertoire, and in general is likely essential to the proper functioning of the nervous system. It is likely that mechanisms underlying modulation of arousal state are conserved across both species and developmental stages.

Given the stereotyped nature of molt-sleep behavior, along with its predictability relative to certain developmental markers and endocrine events, we were interested in using the larval molt of *M. sexta* to explore possible mechanisms underlying induction and maintenance of larval quiescent behavior. As onset of molt-sleep behavior is correlated well with the predicted peak of molting hormone and its duration is prolonged, it is likely that arousal-related changes in the CNS result from either direct or indirect steroid-induced changes in gene expression. As a first step to investigate this possibility, we sought to compare the brain transcriptome at several developmental time-points surrounding the ecdysteroid peak, to the brain transcriptomes of inter-molt feeding-stage larvae. Much of the progress gained by fly researchers is owed to the use of genetic approaches, such as massive screenings of mutants for arousal-related phenotypes, use of transgenic lines to investigate the role of specific genes or systems, and of course microarray studies that allow for the screening of thousands of genes in parallel; however, these techniques are not available for use with models such as *M. sexta*, for which a genome has yet to be sequenced.

To achieve our goal, we utilized the Illumina RNA-Seq method (http://www.illumina.com), which is a non-hybridization based approach. High-throughput deep-sequencing technologies now provide a strategy for the analysis of

transcriptomes belonging to organisms for which a sequenced genome is not available. RNA-seq technologies utilize fragments of complimentary DNAs generated from RNA for massive parallel sequencing that generates absolute gene expression measurements with a greater accuracy and sensitivity than microarray (Wang et al 2009). We have sequenced the brain transcriptome of *M. sexta* during the early- and mid-inter-molt 4th instar feeding period, during the approach and onset of 4th stage molt-sleep, and during the late molting period. Identification of expressed genes was achieved using a novel method that involves the alignment of sequence reads onto the genome of the closely-related species *Bombyx mori* (*B. mori*) (Duan et al 2010). This chapter provides the first description of the *M. sexta* brain transcriptome. 10,664 unique genes were mapped by at least one read during at least one stage, and between 2.8%-7.8% of all genes were differentially expressed at a given stage when compared to mid-inter-molt levels. Cluster and enrichment analyses reveal a dominance of processes related to trachea cuticle synthesis and degradation. In addition, many of the differentially expressed transcripts encode neuropeptides, enzymes involved in the synthesis of small neurotransmitters, ligand-gated ion channels, G-protein coupled receptors, ion channels and other products associated with the neural activity. Possible roles for these gene products in the modulation of larval arousal-state are here described.

Materials and Methods

Insect rearing conditions. *Manduca sexta* were reared at the University of California, Riverside. Adults were maintained in a rearing room at 27^{o}C +/-1^{o}C under a 16L:8D

photoperiod and fed 40% sugar water *ad libitum*. Eggs were transferred to incubators set at a temperature of 25^{o}C +/-1^{o}C and a 17L:7D photoperiod (lights on at 8:30AM), and all larval stages were reared under these conditions. Hatched 1st instar larvae were transferred to individual 1 oz disposal plastic cups, where they were maintained until moved as late 4th or early 5^{ths} to individual 5 oz cups. Larvae were fed *ad libitum* on a modified wheat germ-based artificial diet (Bell & Joachim 1976).

Staging and dissections. All larvae were staged relative to time of the head capsule slippage (HCS) during the molt to the 5th instar. Only gate II 4th/gate I 5th instar larvae were used for these experiments, as these larvae were found to be highly synchronous when staged using weight indicators and developmental markers. Larvae were selected during the late 3rd instar if apolysis of the head capsule (HCS) occurred after 4PM and weights were measured to be over 200 mg following HCS during the molt to the 4th instar. Larvae that ecdysed or showed an air-filled head capsule with blackened mandibles by 9AM the next morning were selected for further staging; these animals undergo HCS (molting to the 5th instar) ~54 to 57 hrs following ecdysis to the 4th instar. Animals dissected prior to 24 hrs before HCS were staged based on pharate 4th weights and developmental markers. For animals dissected between -24 and -6 hrs relative to HCS, developmental time was further validated by using an additional weight marker at -22 hrs; only larvae over 600 mg by -22 hrs (~4PM) were selected. All larvae from 0 to 30 hrs following HCS were staged by visually monitoring the time of HCS. The timeline below outlines the developmental timing of the larvae used for these experiments.

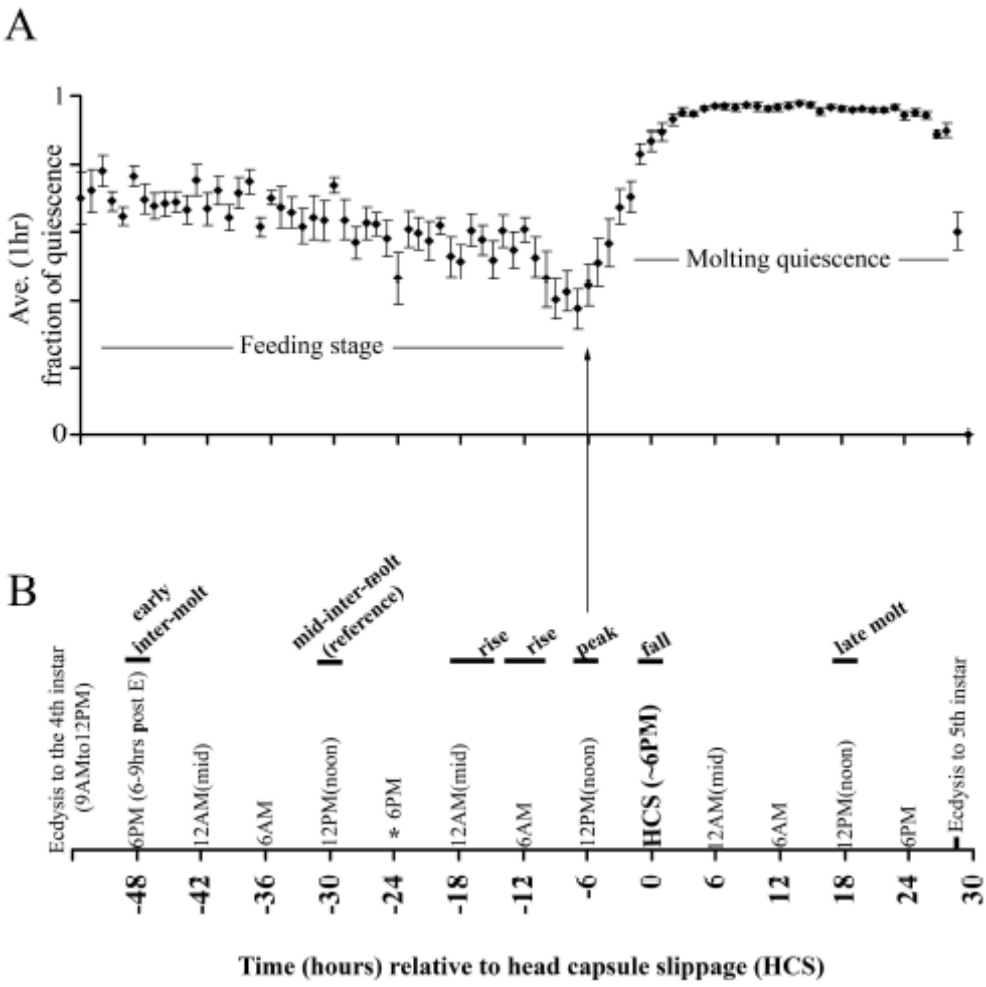

Figure 3-1. Gate II 4th /Gate I 5th instar larval development. All insects were reared under a 17L:7D (lights on at 8:30AM) photoperiod at 25°C (+/-1°C). Developmental timing is displayed in 6 hr intervals. Shown is time relative to HCS. Ecdysis occurs between ~27 to 30 hrs following HCS. The entire larval stage, from ecdysis to ecdysis, is estimated to be approximately 84 to 87 hrs in duration. (A) Average quiescence levels of 4th stage larvae (n=8). Error bars= s.e.m. (B) For Illumina sequencing, samples were selected during the early and mid-inter-molt feeding stages, during the predicted rise of ecdysteroids (at two time-points), during the predicted peak and fall of ecdysteroids, and during the late molting period.

Brains were dissected by first chilling larvae on ice for 5 minutes (or until immobile), and then decapitating and pinning whole heads onto a dissection dish filled with ice cold saline made to the specifications described previously (Zitnan et al 1999). Prior to HCS, the brain lies just ventral to the head capsule, but following HCS, brains shift progressively caudally relative to the old HC. For larvae dissected prior to HCS, brains were exposed by cutting a window through the head capsule using a sharp scalpel. For larvae dissected at developmental times following HCS, brains were exposed by pinning the decapitated head head-capsule-side-down. Once exposed, nerves and trachea were carefully trimmed close to the ganglia, and the brain was placed in a tube on dry ice. Individual brains were removed within 4 minutes of initiating surgery. Pooled brain samples were stored at -80°C until further processing.

For Illumina sequencing, two sets of pooled brain samples were each collected and total RNA was isolated for each of the selected developmental time-points. Prior to submission for sequencing, total RNA from both sets of the given stage was combined into one sample. Brains were collected at the following time-points relative to HCS: -48 hrs (total #brains n=41); -30 hrs (n=34); -18 hrs (n=24); -12 hrs (n=26); -6 hrs (n=23); 0 hrs (n=26); +18 hrs (n=26).

For quantitative PCR, brains were dissected from animals at the following time points relative to HCS: -48 hrs (n=17 to 24 brains/pooled brain sample); -30 hrs (n=20 to 21 brains/pooled brain sample); -18 hrs (n=10 to 17 brains/pooled brain sample); -12 hrs (n=12 brains/pooled brain sample); -6 hrs (n=10 to 12 brains/pooled brain sample); 0 hrs (n=10 to 12 brains/pooled brain sample); +18 hrs (n=9 to 12 brains/pooled brain sample).

Illumina RNA-Seq. Total RNA was extracted from pooled brain samples using TRIzol (guanidinium thiocyanate/phenol solution for RNA extraction) (Invitrogen, Carlsbad, CA). For each of the final 7 samples, the quantity and quality of extracted total RNA was assessed using a Nanodrop ND-1000 Spectrophotometer and an Agilent 2100 Bioanalyzer. An average of 9.8 +/-1.7 (s.d.) µg of high quality total RNA/sample was submitted to Illumina FastTrack Sequencing Services (Illumina, Inc., Hayward, CA) for further processing and sequencing. Samples were processed according to the Illumina RNA-Seq in-house protocol for the Genome Analyzer sequencing platform (http://www.illumina.com). cDNA fragment size selection was in the range of 150 bp-180 bp (insert size). Each sample was run on a single flow cell lane, and single read sequencing was used to sequence each sample to 75 bases. Each library generated an average of 1.9 +/-2.0 (s.d.) gigabases of sequence, and an average of 25,852,337 +/-2,662,408 (s.d.) sequences (reads) (Table 3-1).

Sequence mapping. Because a *Manduca sexta* genome is not yet available, sequenced libraries were mapped to proteins of the closely-related *Bombyx mori* genome available at http://www.silkdb.org/silkdb/. Mapping was performed using the program blastx (Altschul et al 1990) with an Expect value (E) of 10^{-6}. An average of 28% of all reads mapped to the *B. mori* proteome (Table 3-1). Only sequences that could be mapped to at least one *B. mori* protein were used in subsequent analyses. Using custom-written PERL scripts, sequences were assigned to individual *B. mori* genes based on the protein

sequences to which they mapped. In the few rare cases when a sequence mapped to two proteins of different genes, the sequence was assigned to the gene for which the protein mapping had the lowest E value. Data were summarized into a single table with the number of sequences mapping to each *B. mori* gene in each of the seven sequenced libraries. This table was used as input for differential gene expression analysis (described below).

In addition to the above-described sequence mapping to the *B. mori* genome, sequenced libraries were also mapped to 646 *M. sexta* gene sequences available at the National Center for Biotechnology Information database (NCBI) (http://www.ncbi.nlm.nih.gov/). Since both the libraries and the genes were from the same species, mapping could be performed using standard RNA-seq methods. The program TopHat with default parameters (Trapnell et al 2009) was used because of its ability to map across intron junctions. The number of sequences mapping to each *M. sexta* gene were summarized in a single table and used as input for differential gene expression analysis.

Sequence annotation. BLAST2GO v.2 (Gotz et al 2008) was used to perform several analyses on the resulting *B. mori* mapped gene sets. Sequence data for all 10,665 mapped genes were uploaded in FASTA format into the BLAST2GO application for annotation. Using default parameters, nucleotide sequences were blastx-searched against the NCBI nr protein database through QBLAST. For all BLAST hits, the mapping step was used to retrieve associated gene ontology (GO) terms, gene names or symbols, and UniProt IDs

(www.geneontology.org; Non-redundant Reference Protein Database). Annotation of the sequences then followed, which for this application involves the use of an annotation rule used to select GO terms for each sequence from the total pool of GO terms obtained during the mapping step. Several rounds of annotation were performed so that most sequences were subjected to stringent annotation parameters, and more permissive parameters were used only for sequences that were harder to annotate. 6495 sequences were annotated using the applications default parameters (E-Value Hit Filter=1*e*-6, Annotation cut-off threshold=55, GO-Weight=5). An additional 99 genes that failed to be annotated in the first round were then annotated with an E-Value Hit Filter adjusted to 1*e*-3, then 1,246 genes with a cut-off threshold of 45 and Hit Filter 1*e*-6, and then of the remaining unnanotated genes, 68 genes were annotated with an E-Value Hit Filter adjusted to 1*e*-3 and a Cut-Off threshold of 45. Next, annotation number was increased by running the InterProScan search against all EBI databases to retrieve GO terms associated with domain/motif information, and the information was merged with existing annotations for a final total of 8867 annotated genes. Annotation was augmented using the Annex function prior to further analysis. Generic GOSlim mapping terms were also used where indicated (goslim_generic.obo).

Differential gene expression. Differential gene expression analysis between selected pairs of libraries was performed using the DESeq R package that uses a model based on the negative binomial distribution (Anders & Huber 2010). Using the mapping data generated for a pair of libraries as input, the method reported for each gene an estimated

expression fold change value, as well as a p-value for the statistical significance of differential expression. For the purposes of this study, genes were considered differentially-expressed if fold change values were >2 or <0.5, and the p-value was <0.1.

Gene ontology (GO) enrichment analysis. Identification of enriched functional terminology was done using the GOSSIP package (Bluthgen et al 2005) that is incorporated into BLAST2GO. The GOSSIP package utilizes Fisher's exact test and corrects for multiple testing. All enrichment analyses were carried out using one-tailed tests (search for overrepresentation) with a false discovery rate (FDR) $\leq$0.5.

Cluster analysis. Assignment of genes into clusters with similar expression profiles was carried out using the software program Short Time-series Expression Miner (STEM) (Ernst & Bar-Joseph 2006). Using permutation tests and correlation coefficients, the STEM algorithm assigns genes to a predefined set of model profiles, calculates the significance of each profile by comparing the number of assigned genes to the number of genes expected for that profile, and groups similar profiles into final gene clusters (Ernst et al 2005). Only genes showing an absolute fold change greater than 2, and a p-value <0.1 for at least one stage relative to the reference stage (-30 hrs) were used for cluster analysis. Genes with infinite-fold changes were excluded from this analysis. We used a set of 1,250 profiles, and profile significance was corrected for multiple testing (Bonferroni correction with a FDR $\leq$ 0.05). Similar profiles were grouped into clusters

based on a correlation coefficient $\geq$ 0.7. For all other settings we used the default settings specified in the user manual (STEM v1.3.7).

Systems screenings. Identification of genes with potential arousal-related function was carried out by manually screening the descriptions and GO terminologies of the entire set of BLAST2GO annotated, differentially expressed genes. Genes were assigned to the following categories based on their annotations: 1)-Neurotransmitter-gated ion channels and G-protein coupled receptors, 2)-Neurotransmitters, neuropeptides and proteins involved in their synthesis and regulation, 3)-Ion channels and ion channel-regulating proteins, and 4)-Epidermal growth factor and insulin signaling. Identities of all sequences assigned to any of the above-mentioned categories were further scrutinized by searching for orthologs in FlyBase (htt://flybase.org). Sequence orthology was determined using the reciprocal BLAST approach (Fan et al 2010). Each *B. mori* protein sequence was first queried against the FlyBase database using default blastx parameters (Altschul et al 1990), and the highest scoring *D. melanogaster* sequences were then queried against SilkDB. If the *D. melanogaster* sequence reciprocally identified the original *B. mori* sequence as the highest scoring blastx hit, the two sequences were considered orthologous.

Quantitative PCR (qPCR). Total RNA was extracted from pooled brain samples using TRIzol (guanidinium thiocyanate/phenol solution for RNA extraction) (Invitrogen, Carlsbad, CA), and for each sample, the quantity of total RNA extracted was assessed

using a Nanodrop ND-1000 Spectrophotometer. Total RNA (1 ug) was reverse-transcribed into cDNA using the Superscript First Strand Synthesis System for RT-PCR kit (Invitrogen) according to the manufacturer's protocol. To minimize the possibility of genomic DNA contamination, samples were DNase treated using TURBO DNA-*free* (Applied Biosystems/Ambion) prior to reverse-transcription, and no-RT controls were used to check for contamination.

Primers were designed from six known *M. sexta* mRNA sequences reported in the NCBI database. Information about the sequences and primers that were used are reported in Table 3-2. Gradient PCRs followed by electrophoresis on 2% agarose with ethidium bromide gels were first used to check for specificities of primers and optimal annealing temperatures. All PCR reactions were carried out using Accupower PCR PreMix (Bioneer). Sequence identity of each amplicon was verified using Sanger (BigDye) sequencing (Applied Biosystems; Genomics Core at the University of California, Riverside). Serial dilutions of cDNA were then used with qPCR to generate standard curves to evaluate amplification efficiency and to further check the specificity of primers. QPCR was carried out in 25 µl reaction volumes containing 12.5 µl of IQ SYBR Green Supermix (Bio-Rad, USA), 2 µl of cDNA template, primers at the optimized concentration, and water. The Bio-Rad iQ5 Real Time PCR Dectection System (Bio-Rad, USA) was used according to the manufacturer's specifications. For each biological replicate, cDNA (diluted 10-fold) from every developmental time-point sampled was run in triplicate on the same plate. For all reactions, the cycling parameters were 1x 3 min @95°C, 40x (20 sec @95°C, 20 sec @60°C, 20 sec @72°C), 1x 1 min @95°C, 1x 1 min

@55°C, followed by a melt curve from 55 to 95°C at 0.5°C steps (10 sec/step) to verify amplification specificity. All primers were used at a concentration of 200 nM.

For all profiles, *Manduca sexta* ribosomal protein *L32* was used as an internal reference gene. For dopa decarboxylase profiles, non-muscle actin was also used as a reference gene. All control reactions were run in triplicate in parallel (on the same plate) with experimental reactions. Results were analyzed using the iCycler iQ Optical System Software v2.0 (Bio-Rad Laboratories). The threshold was set manually within the linear amplification range for all expression data. The crossing point of an amplification curve with the threshold represents the cycle threshold (Ct). Ct values were exported to Microsoft Excel for further analysis. Relative expression ratios were calculated by the Pfaffl equation (Pfaffl 2001).

Results and Discussion

Illumina sequencing and mapping to the reference proteome. Across the 7 libraries corresponding to the time points sampled, a total of 180,966,360 sequence reads (totaling ~13.4Gb of sequence data) were generated (Table 3-1*)*. Each library generated an average of 25,852,337 +/-2,662,408 (s.d.) reads. According to the methods outlined above, reads were mapped onto the proteome of *B. mori,* which is the most closely related species for which a genome has been sequenced. The reference proteome was composed of the 14,623 protein sequences provided in the most recently up-dated SilkDB (v2.0) consensus non-redundant dataset (Duan et al 2010). Of the sequences that passed our filter, an average of 27.8% of reads from each library were assigned to a unique

protein coding gene. In total, 10,664 *B. mori* genes were mapped by our *M. sexta* Illumina reads (75bp reads) during at least one developmental stage, and this gene set was used for further analysis.

BLAST2GO annotation. All 10,664 mapped *B. mori* proteins were subjected to functional annotation and analysis using BLAST2GO, a bioinformatics application designed for labs with minimal bioinformatics support (Conesa et al 2005). Nucleotide sequences corresponding to the mapped proteins were blastx searched against the nonredundant (nr) NCBI protein database according to the parameters outlined in "Materials and Methods." The blastx algorithm compares a nucleotide sequence in all 6 frames against a protein database (Altschul et al 1990). The application was set to allow for recovery of up to 20 hits per sequence. The similarity distribution indicates that most recovered sequences show sequence similarities above 50% (Figure 3-2). The species distribution of blastx hits shows that the majority of hits are attributable to insect proteomes (Figure 3-3). Although blastx parameters allow for association of multiple hits to each gene, GO terms associated with higher homology hits are weighted more strongly during the final annotation process. The Top-Hit species distribution chart shows that the highest number of top hits were to protein sequences of the red flour beetle *Tribolium castaneum,* the silkworm *B. mori,* the mosquito *Aedes aegypti,* and the honey bee *Apis mellifera*—all insects for which a full genome is available (Figure 3-4). In a recent 454 pyrosequencing study of the *M. sexta* larval midgut, the same application was used to annotate *M. sexta* nucleotide sequences, and a similar distribution of top-hits was

reported by the authors (Pauchet et al 2010). In this study, it might be expected that *B. mori* proteins would form the *only* category of top-hits, considering that blastx was performed using *B. mori* sequences; however, the sequences were run against the NCBI database, and this database does not contain all of the sequences found in SilkDB. With the aid of more bioinformatics support, future analysis could include blastx searches against SilkDB, as well as other resources such as the lepidopteran-specific ButterflyBase. It should be noted however, that much of the SilkDB nr database was also annotated by searching for homologs using the NCBI and InterPro databases (Duan et al 2010). It is possible that use of the BLAST2GO application would result in an annotation set that is not very different, or perhaps even more informative, than that found on SilkDB.

GO terms associated with BLAST hits were retrieved, and sequences were annotated according to procedures outlined in "Materials and Methods". The BLAST2GO application applies an annotation rule that takes into account sequence similarity, evidence codes (the procedure used for GO assignment), and relationships to other GO terms assigned to that sequence. Figure 3-5 shows the evidence code (EC) distribution for all sequences with mapped GO terms. The majority of sequences show GO term mappings that were acquired from electronically annotated databases, but these terms will contribute less to the final annotation of a sequence when there is also a GO term with a stronger EC code, such as one supported by experimental evidence (EXP).

Of the original 10,664 mapped genes, a total of 8,831 genes were annotated successfully (Fig 3-6A). Of the unmapped genes, 9 sequences did not BLAST, 494 sequences were not matched with any sequence, 1,106 sequences were matched to

sequences for which there were no known GO terms, and 224 sequences were successfully mapped, but not annotated. Only the genes successfully annotated were used for further functional analysis. A total of 47,061 GO terms were mapped to the annotated genes at a mean GO level of 5.71 +/-1.88 (Figure 3-6B). Since the number of GO terms mapped to the total genes was large, a generic GO-Slim view was used to visualize the functional diversity attributable to the larval brain transcriptome. GO-Slim annotation (an option incorporated into BLAST2GO) results in a reduced version of gene ontology terms that includes only key ontological terms. GO-Slim annotations were used *only* for this specific analysis of the entire set of mapped and annotated genes. Multilevel pie graphs are provided to illustrate the sequence distribution by GO for the parent categories cellular component (CC), biological process (BP) and molecular function (MF). The highest percentages of CC GO terms indicate that the products of most sequences are located in protein complexes, the nucleoplasm, and the plasma membrane (Figure 3-7). The highest percentages of BP GO terms are associated with the processes of signal transduction, anatomical structural morphogenesis, and cell differentiation (Figure 3-8). The highest percentage of MF GO terms in the MF category are annotated with GO terminologies associated with nucleotide binding, peptidase activity, and receptor activity (Figure 3-9). The MF and BP GO terminology distributions indicated that the 8,831 annotated sequences are representative of a wide range of functions and processes. That processes related to transcription are so dominant within the MF category is not surprising, since brain samples were selected at time-points correlating with the rise and fall of steroid hormones. Brain transcription factor activity will be

explored further in the sections to follow. Also highly represented are MFs and BPs associated with protein, lipid and carbohydrate metabolism, and many of these terminologies were likely to have been assigned to genes important to synthesis and breakdown of tracheal cuticle during the molt. In addition, many GO terminologies are potentially related to processes specific to the nervous system, such as response to external stimulus, response to endogenous activity, behavior, response to stress, signal transduction, neurotransmitter transporter activity, ion channel activity, protein kinase activity and receptor activity. In the sections to follow, our set of annotated genes will serve as a reference set with which we explore stage-specific enrichment of GO terminologies, the functions of sets of differentially expressed genes that change together across developmental time, and specific genes that might contribute to arousal-state modulation during the molt.

Differential expression analysis. The main focus of this study was to investigate possible direct or indirect steroid-induced changes in brain gene transcription that might underlie the changes in behavioral state associated with the transition from feeding to molting. We sampled the brain transcriptome at several time-points during the late 4th instar feeding period (during the predicted rise in ecdysteroids) and during the early onset of the molt-sleep behavior (during the predicted peak and fall of ecdysteroids). The transcriptome also was sampled during the late molt and during the very early 4th instar feeding period. Each individual transcriptome from these stages was compared to the brain transcriptome sampled at 30 hrs prior to HCS. HCS -30 hrs is approximately mid-

way through the 4th inter-molt feeding period, a time that precedes the rise in molting hormones. Due to the current high cost of Illumina sequencing, biological replicates are not available. Differential expression between samples was tested using the "DESeq" package, which allows for an estimate of variance and a testing for differential expression in non-replicated count data (Anders & Huber 2010). In this application, a negative binomial test is used to contrast the two conditions. The estimate of variance is based on the assumption that genes with a similar expression level show similar variance across replicates. In the case of non-replicate data, a presumption is made that *most* genes are *not* differentially expressed across conditions, and the two conditions are treated as replicates for the purpose of calculating variance. In comparisons for which there are many differentially-expressed genes, the estimate of variance is high. In the present case, as the rise and fall of ecdysteroids are thought to influence the expression of a large number of genes, the estimate of variance is likely to err on the side of being too conservative. On the other hand, fold-change values are calculated independently of the estimate of variance. To identify sets of differentially-expressed genes, we first selected only those genes that showed an across-condition fold-change that was >2.0, or <0.5. The variance-dependent, non-adjusted p-values were then used at a permissive level ($p<0.1$) to exclude many fold-change values obtained for genes with very few mapped reads. A cautionary note should be inserted: due to the potentially high false discovery rate, final conclusions should be drawn only following verification using either 1)-biological replication or 2)-quantitative PCR (qPCR). By way of example, we compared a 4th stage (brain) qPCR expression profile of dopa-decarboxylase (*ddc*)—an enzyme

involved in the synthesis of the neurotransmitter, dopamine—to the expression profile obtained from Illumina sequencing. The profiles correlate well, and with both methods, fold-change is significant at 18 hrs following HCS (see *method validation*). In the Illumina sequencing profile, the *ddc* gene expression during the fall of ecdysteroids was slightly over 2-fold with a p-value <0.1, and therefore passed our current standard for the determination of differential expression; however, this gene would not be identified as being differentially expressed when applying the adjusted p-value (adjusted p-value=0.5). As we are interested in genes that might show similar expression level and fold-change values, we chose the use of fold-change and the more permissive p-value for determination of differential expression.

To visualize at each time point the extent of differential expression compared to the inter-molt reference library, $\log_2$fold changes were plotted against the base mean, which is an average measure of the number of reads mapped to that gene adjusted for library size (Figure 3-10). For each stage, data-points represent the expression fold change value for a unique gene, and all genes that passed our test for differential expression are colored in red. 1,844 genes (~17%) were identified as differentially-expressed during at least one developmental stage. In a recent microarray-based study that examined the brain transcriptome of pupating *B. mori*, ~26% of all detected genes were found to be differentially expressed during at least one of the stages, which were sampled across the rise and fall of the pupal ecdysteroid surge (Gan et al 2011). That more genes may be differentially expressed in the brain during pupation and metamorphosis is to be expected. Reorganization of the CNS has already begun by the

time of pupation, whereas the CNS is relatively immune from these structural changes during the larval molts (Copenhaver & Truman 1986). It is also possible that the number of genes found to be differentially expressed using microarray is underestimated. In pupating *B. mori* brains, only 4,550 genes were found to be transcribed during at least one stage, which is less than half of the number of unique transcripts detected here in the brains of molting *M. sexta*. This latter discrepancy could be due to the ability of mRNA-seq to detect novel genes, to the increased number of stages sampled in our study, or to differences in stringency for filtering significant fold-change. In any case, our gene-set adds a large number of transcripts that can be attributed to the brain transcriptome of developing Lepidoptera.

Most of the differential expression could be attributed to the up- or down-regulation of genes that are also expressed at HCS -30 hrs. For genes that were not expressed in the reference sample, but were expressed in test-stages, a $\log_2$fold change value of 10 was assigned arbitrarily. Similarly, genes that were expressed in the reference sample, but not in the test-set were assigned a $\log_2$fold change value of -10. Samples from HCS -18 hrs and HCS -12 hrs are representative of the brain transcriptome during the predicted rise in ecdysteroids. At -18 hrs, 168 genes (~1.6% of all mapped genes) are significantly up-regulated, and 131 genes (~1.2%) are significantly down-regulated when compared to expression levels of mid-intermolt brains. At HCS -12 hrs, 240 genes (~2.3%) show significant up-regulation, and 183 genes (1.7%) are down-regulated compared to inter-molt levels. This progressive increase in overall differential expression observed between HCS -18 and 12 hrs was expected, as levels of molting hormones that

are thought to induce expression changes are predicted to be much more elevated at HCS -12 hrs compared to HCS -18 hrs, when they are just beginning to rise.

At HCS -6 hrs, 314 genes (~2.9%) are significantly up-regulated, and 276 genes (~2.6%) are significantly down-regulated. At this stage of development, the animal's quiescent behavior begins to rise suddenly, and this time-point is also correlated with the predicted peak of ecdysteroids. At the time of HCS, when larvae are displaying fractions of quiescence characteristic of the molt-sleep, and ecdysteroids are predicted to be in decline, 523 genes (~4.9%) are significantly up-regulated, and 314 genes (~2.9%) are significantly down-regulated when compared to inter-molt levels. At ~9-12 hrs prior to ecdysis, when ecdysteroid levels have fallen to low levels (HCS +18 hrs), the animal remains in a molting-quiescent state, but changes in gene expression may also be taking place in preparation for late molting behavior. In the brains of these late-molt larvae, 570 (~5.3%) of the genes are significantly up-regulated, and 128 genes (~1.2%) are significantly down-regulated. For comparison with changes in molting brains, brains were also taken approximately 6-9 hrs *following* ecdysis to the 4th instar (*early* inter-molt) and at this stage, 278 genes (~2.6%) show significant up-regulation and 103 genes (~1.0%) are significantly down regulated compared to the later inter-molt reference stage.

When adult fly whole-head transcriptomes were compared between sleeping and awake animals using microarray, behavioral-state-dependent transcripts represented ~1.4% of all detectable genes (Cirelli et al 2005b). In this case, because fly heads are composed of various tissues, many of the genes may be more appropriately associated with tissues other than the brain, and changes in gene expression for genes that show low

expression in the brain could be obscured by highly expressed transcripts that do not show changes in peripheral tissues. In the cerebral cortex of rats, ~5% of all detected transcripts showed behavioral state-dependent differential expression (Cirelli 2005). In the fly and rat studies, samples were taken at only two-time points several hours prior to natural sleep-wake transitions. In our study, we have the advantage of sampling across behavioral state as well as during the approach and onset of a behavioral-state change. A disadvantage in our study is the obscuring of behavior-related gene expression by transcripts associated with processes related to the purely physiological and structural components of molting. In the future, the recognition of conserved, arousal-related genes will be aided by comparison between genome-wide studies in a variety of organisms. This study should aid in such a process.

Validation of methodology using available *M. sexta* sequences. To our knowledge, this is the first attempt at mapping Illumina reads onto a proteome using the blastx alignment method. In more conventional studies, Illumina nucleotide reads are mapped directly onto a known genome. To test the validity of our alignment method (the alignment of *M. sexta* nucleotide read translations onto the *B. mori* proteome), we compared results from the proteome alignment to those obtained by mapping nucleotides directly onto a set of 647 *M. sexta* genes currently available on the NCBI database. (It should be noted, that some of these sequences may share the same identity; for example, some submissions contain partial, and some complete mRNA sequences, so fewer than 647 unique genes were likely to have been available). Using only fold-change as a filter

for determination of differentially expressed *M. sexta* genes, these genes were selected and then paired to the best-matching *B. mori* protein (SilkDB) using blastx with an Expect value (E) of 10^{-6}. If multiple *M. sexta* sequences were paired to the same *B. mori* protein, E-values were used to select and retain only the gene with the highest sequence similarity. The corresponding *B. mori* gene IDs were then screened for significant differential-expression using the DEseq results discussed in the previous section. Only sequences that showed significant differential-expression using the proteome alignment method were retained, resulting in a final total of 56 paired profiles (Figure 3-11).

As it was desirable to evaluate the BLAST2GO annotation method, a comparison was made between descriptions assigned to each gene in a pair. The sequence descriptions assigned to each of the *B. mori* genes by BLAST2GO were compared to the gene definitions assigned to each gene in the NCBI GenBank database from which the *M. sexta* sequences were retrieved. Descriptions for 43 (~77%) of the 56 pairs were obvious matches (Figure 3-12). For example, the *B. mori* gene BGIBMGA001531 is described by BLAST2GO as a corazonin receptor, and the paired *M. sexta* gene with accession number AY369029.1 is defined also as a corazonin receptor. Here we assume that functional matches can be inferred from description matches. 14 paired descriptions were not obvious matches. In most cases, this was because either the BLAST2GO or the NCBI database assigned a more general gene description. Many genes in this study represent uncharacterized genes for which GO terminologies were assigned by BLAST2GO based on conserved protein domains. For each pair that showed unmatched descriptions, BLAST2GO GO term and protein feature annotations were compared to the protein

features assigned by NCBI. 13 of the 14 pairs were matched based on similarities in biological process and/or molecular function. Only 1 sequence was not matched using either descriptions or putative functional similarities.

In some cases, descriptions are similar, but sequences are identified as different splicing variants. For example, the BLAST2GO description of gene BGIBMGA00716 is described as the nuclear hormone receptor FTZ-F1 alpha, while the matching *M. sexta* gene is defined as FTZ-F1 beta. Investigations using reciprocal BLASTing led us to conclude that these are both FTZ-F1 beta splice variants. Although we consider the descriptions to be closely matched (and these are counted as description-matched), these results indicate that details of the BLAST2GO annotation descriptions should be scrutinized prior to final conclusions as to the identity of the gene, especially where multiple splicing variants are known.

The number of reads that mapped to each gene was compared across protocols. As would be expected, the average number of reads that mapped to each gene was much higher when *M. sexta* reads were mapped to sequences from its own genome (Figure 3-13). For each gene, the average of all base means (across stages) were calculated to obtain an estimate of the number of reads that mapped to each specific gene. For each method, the sum of these values indicates that on average, ~2.6 times more reads are mapped to each individual gene when Illumina reads are mapped to sequences of the same genome (*M. sexta* reads onto *M. sexta* nucleotide sequences), compared to the number of reads that are mapped to each protein ID when the same reads are translated and mapped onto the *B. mori* proteome.

The validity of this method, in terms of its reliability in detecting differential expression, lies not in the similarity of the absolute number of mapped reads, but in the similarity between the relative fold-change across conditions. If the results obtained using the proteome alignment method are comparable to those obtained by mapping nucleotide reads onto a same-species genome, then for each gene, the extent of differential-expression across conditions should closely agree. When $\log_2$fold changes for each gene at each developmental stage are compared across protocols, there is indeed a strong correlation (Figure 3-14A). Calculation of the correlation coefficient necessitated exclusion of infinite fold changes. To include infinite fold changes and to gain an overall estimate of the number of potential false positives that may be present in our study, we calculated false-positive scores for each gene using the following method: 1)-For each gene-pair, the number of stages in which significant fold-changes were detected using the proteome alignment (>2-fold <0.5-fold, $p<0.1$) were summed (S), 2)-then, for a given gene, across-method agreement was scored and the total number of agreements was subtracted from (S), and this value was then divided by (S), so that for gene-pairs with a score of "0", the expression profiles are in perfect agreement, and gene-pairs with a score of "1" have dissimilar expression profiles (false-positive). Since many of the genes show differential-expression across multiple stages, we wanted such an assessment that is based on partial scoring. For example, gene BGIBMGA003895 is significantly up-regulated at 3 stages, but the paired *M. sexta* gene is up-regulated during only two of these stages, so this gene-pair would receive a score of 0.3. This means that if the nucleotide alignment is considered "true", 1/3 of the profile was falsely assigned

significance using the proteome alignment method. Because of the small number of the available *M. sexta* genes, agreement was based on matching significance from the proteome alignment with *fold-change* agreements from the nucleotide alignment. 11 gene pairs (~20%) received the score of "1" (false-positives) and 40 gene pairs (~71%) received a score of "0" (expression profiles were in total agreement) (Figure 3-14B). 5 gene pairs (~9%) received partial scores, ranging from 0.25 to 0.67. False-positive (FP) scores are listed beside each gene pair in Figure 3-11. Of the 11 pairs with scores of "1", three of the pairs show very low (below 10) mapped read averages. Three of the false-positive gene pairs show inverted mapped read ratios, so that more reads were mapped to the matched *B. mori* gene than to the actual *M. sexta* gene. Of these genes, 2 pairs shared similar GO terminologies but did not share the same description, and 1 gene (*chitin synthase*) had GO terminologies and descriptions that did match. It is likely that false-positives identified for gene-pairs with inverted ratios are due to the lack of availability of the appropriate *M. sexta* gene.

The above analyses were designed to asses the validity of our alignment and annotation methods, but they do not validate the Illumina sequencing data itself (they only compare different analyses of the same raw sequencing data). Quantitative PCR (qPCR) was used to validate our sequencing data. Primers were designed for partial amplification of six *M. sexta* genes selected from our paired profiles. Primers were designed for the *M. sexta* enzymes *Chitinase, Dopa-decarboxylase (ddc), Nitric Oxide Synthase,* the nuclear hormone receptor *betaFTZ-F1*, the peptide receptor *Corozonin receptor*, and an uncharacterized *Putative Cuticle Protein* (Table 3-2). Three complete

sets of tissue were used for isolation of mRNA (mRNA was not from the same samples as those used for RNA-seq, and could therefore serve as biological replicates to validate Illumina data). With the exception of *ddc*, qPCR fold-change values are the averages of two biological replicates, and ribosomal protein *RPL32* was used as an internal reference gene. *Ddc* values are the mean of three biological replicates, and non-muscle *actin* was used as an internal reference gene. For comparison, one *ddc* biological replicate was run using *RPL32* as a reference gene. Profiles for all six genes are shown in Figure 3-15. For all profiles, there is strong agreement between data obtained using Illumina sequencing and with qPCR. Where significant down-regulation (blue stars) or up-regulation (red stars) was called in Illumina sequencing data (proteome alignment method), qPCR results almost always show a corresponding down- or up-regulation that is 2-fold or greater. One exception is seen in stage HCS -18 hrs in the profile for the *putative cuticle protein*, but it is likely that the very low expression level of this gene leads to a large amount of variability across biological replicates. Although the profile for *betaFTZ-F1* is in agreement with Illumina sequencing data at the stage where significance was called (HCS +18 hrs), fold-change values are highly variable both across biological replicates and alignment method at other stages of development. At HCS -12 and -6 hrs, the RNA-seq data itself is not consistent (they diverge in different directions), indicating that in this case, the *B. mori* protein is likely being mapped by too many reads; but this is the only case where Illumina data diverges in different directions.

The *ddc* profile demonstrates the importance of the choice of reference gene when using qPCR. When qPCR expression levels are normalized against *RPL3*, profiles are

very similar to those obtained using the reference-independent RNA-seq data. When *ddc* expression levels are normalized using *actin* as a reference gene, expression levels at HCS +18 hrs are overestimated. Our Illumina sequencing data indicates that *RPL3* is relatively stable across all developmental stages, but this is not true for *actin*, which shows a slight down-regulation at HCS +18 hrs. These findings indicate that use of *actin* as a reference gene for mRNA profiling during this developmental period leads to false positives.

Although available *M. sexta* sequences make up only a small sample size for comparison, these data suggest that when sequences are identified as differentially-expressed using translated alignments onto the closely related proteome, expression profiles are in close agreement (maximum ~20% false positives). As the DEseq method will have an inherent false discovery rate due to the number of sequences involved in such high throughput sequencing, it is not known how many of the false identifications are due to alignment methods, and how many are due to random variability. Also, a number of profile disagreements could be due to the limited number of sequence databases used for proteome alignment; future studies that include an expansion of the number of lepidopteran databases might increase the power of this technique. For now, the agreement between paired profiles here is considered sufficient to explore and to generate hypotheses about types of genes that are differentially expressed in brains of molting *M. sexta* larvae. Final conclusions about the expression profile of a given gene should be validated using biological replicates, or by using complimentary methods, such as qPCR.

Enrichment analysis.

We were interested in identifying functional categories that might be enriched in the brain across the selected developmental time points. The BLAST2GO suit incorporates an enrichment analysis function that utilizes the GOSSIP package to identify the overrepresentation of GO terminologies in a given set of genes (Bluthgen et al 2005). The GOSSIP package statistically assesses differences in GO term abundance between a test and a reference gene set. The reference set was composed of 8,831 genes that had been mapped by Illumina reads, and were also successfully annotated using BLAST2GO (Figure 3-6). Each set of differentially-expressed genes was compared to the reference set using Fisher's Exact Test with a false discovery rate of <0.05. We performed this analysis separately on sets of both up- and down-regulated genes of a given stage. Results from enrichment analysis are displayed as bar charts. The GOSSIP program also generates directed acyclic graphs (not shown), which display parent/child relationships between enriched GO terminologies. To simplify interpretation, directed acyclic graphs were used to group enriched GO terminologies according to their relationship to a unifying parent term. Enriched GO terminologies in sets of up-regulated genes at a given stage are representative of processes that are associated with either that stage or an upcoming developmental stage. Enriched terms found in sets of down-regulated genes are presumably associated with processes that are either less important for, or perhaps conflict with, the physiology and/or behavior of a given stage.

At HCS -18 and -12 hrs, larvae are still actively feeding and average quiescence level is declining over time. At these two stages, ecdysteroid levels are predicted to be rising. As brains from these two stages are taken from animals of similar behavioral and physiological state, sets of differentially-expressed genes from these two stages were merged for use in enrichment analysis. At this stage of development, there were no enriched GO terms in the set of significantly down-regulated genes. In contrast, the set of up-regulated genes contained many enriched GO terms under the parent "umbrella" terminologies *biological process* (BP), *molecular function* (MF) and *cellular component* (CC) (Figure 3-16). At HCS -6 hrs, when average quiescence level begins to rise (the time of the putative ecdysteroid peak), and at the time of HCS, when animals display quiescent levels characteristic of the molt-sleep (during the predicted fall of ecdysteroids), enriched GO terminologies are found in both sets of up-regulated and down-regulated genes (Figure 3-16A/B and Figure 3-17A/B, respectively). At HCS +18 hrs, during the late molt (~9-12 hrs prior to ecdysis), and when ecdysteroid levels are thought to have declined, enriched terms are found in the set of up-regulated genes and in the set of down-regulated genes, but enrichment in the set of down-regulated genes was sparse (only one term) (Figure 3-19A/B). There were also many enriched GO terms detected in early inter-molt feeding stage larvae (HCS -48 hrs, Figure 3-20), which indicates that there are differences in brain physiology at different stages of the feeding period.

At each stage, enriched GO categories are dominated by terminologies associated with cuticle synthesis and degradation. Larval brains are infiltrated by cerebral trachea, which split into smaller branches that grow around the brain neuropil (Pereanu et al

2007). Research into mechanisms underlying cuticle formation and shedding during molting periods has focused largely on processes related to body-wall cuticle, but cuticle also lines the insect foregut, hindgut and trachea (Moussian 2010). During each molt, the tracheal system increases in size via differentiation of new branches and secretion of a larger-diameter cuticle. Like cuticle of the body wall, synthesis and shedding of tracheal cuticle is also under the control of molting hormones (Ryerse & Locke 1978). The major constituents of insect cuticle are polysaccharides (chitin), proteins and lipids, and in all enrichment analyses we see an enrichment of GO terminology associated with metabolism of these three structural components (Moussian 2010). Enrichment of the term *extracellular region* under CC reflects the function of many of these structural components and enzymes, which must be secreted by the epidermis prior to their involvement in cuticle synthesis or breakdown.

Other enriched categories include those associated with hormone receptor and transcription factor activity. In the previous chapter, we demonstrated a correlation between changes in quiescent behavior and known changes in levels of molting hormones. That the onset of molt-sleep is correlated with the predicted rise and early fall of ecdysteroids suggests that molting hormones act either directly or indirectly on the nervous system to alter behavior during that period. It is thought that, in addition to their peripheral actions, molting hormones also act on the central nervous system of insects to program the innate ecdysis sequence necessary for shedding of old cuticle at the end of the molt (Zitnan et al 2007). Ecdysteroids are necessary for induction of new gene expression associated with central peptidergic networks that control ecdysis motor

patterns (Kim et al 2006a; Kim et al 2006b; Zitnan et al 2007). Also, exposure of the brain to ecdysteroids during the final larval stage is both necessary and sufficient to induce wandering behavior (Dominick & Truman 1986). During the larval stages of earlier molts (in the presence of JH), the neurons of the CNS are relatively insensitive to ecdysteroid surges in terms of their responding with changes in morphology (Truman et al 1994). Just how ecdysteroids act on the neurons of the CNS to alter behavior during the late larval molt and final larval stage has not been determined. Radio-immunoassay's and antibody staining revealed at least a transient expression of the canonical ecdysteroid receptor in neurons of the proto- and tritocerebrum during the late molting period (following air-filling of the head capsule), but receptor expression in the brain has not been studied at earlier time-points that surround the onset of the molt-sleep (Bidmon et al 1991). It is possible that ecdysteroid-mediated changes in the *periphery* lead indirectly to changes in CNS gene expression. It is also possible that ecdysteroids *do* act directly on neurons of the early molting larval brain and ventral nerve cord through either typical or even atypical ecdysteroid signaling pathways. Several atypical ecdysteroid actions have been identified in tissues of *Drosophila*. Typically, ecdysteroids bind to a heterodimer composed of *ecdysone receptor* (EcR) and ultraspiracle (USP), which are both members of the nuclear receptor family, and binding of the ligand to the receptor complex then alters gene expression (Nakagawa & Henrich 2009). The effects of ligand-binding are of course more complicated, as the receptor-ligand complex can itself be regulated by various cofactors. In any case, there is evidence that ecdysteroids can act through heterodimer receptor complexes composed of USP and nuclear receptors other than EcR,

and also complexes composed of EcR but not USP (Baker et al 2003; Brennan et al 2001). Also, recent studies have shown that ecdysteroids can act on G-protein-coupled receptors to produce rapid non-genomic effects (Srivastava et al 2005). Whether or not the non-genomic effects lead eventually to longer lasting changes in gene expression has not been investigated.

Although this study does not identify the mechanisms of ecdysteroid actions that lead to the changes in gene expression observed for the brains of molting larvae, we have provided a list of all differentially-expressed transcripts that are annotated with descriptions and GO terminologies that identify transcripts as either putative transcription factors, or as putative transcription factor regulators (Figure 3-21). Significantly up-regulated genes are shown in red (Figure 3-21A/B), and down-regulated genes are shown in blue (Figure 3-21B/C). In this list, 39 transcripts are shown as significantly up-regulated during the molting period, 8 as up-regulated only during the early inter-molt period, 4 as both up- and down-regulated during the molting period, 24 as down-regulated during the molting period, and 6 as down-regulated only during the early inter-molt period. Reciprocal BLASTs using SilkDB and FlyBase confirm the identities of many of these transcripts, and several of the transcript identities also are confirmed through sequence similarities to available *M. sexta* sequences. The expression profiles of these genes are provided, and should prove useful in future studies that investigate hormonal actions on the larval CNS. We will discuss only a few genes of interest.

Several genes are recognizable for their roles in the regulation of the endogenous circadian clock (putative clock genes *vrille*, *clockwork orange*, *clock, cryptochrome*), so

although the previous chapter demonstrated a lack of circadian rhythm in the expression of the core clock gene *period*, the differential expression of other clock genes does suggest a possible role for the central clock in the regulation of developmental events.

Also of interest is the differential expression of cAMP response-element binding protein (CREB). In *Drosophila*, CREB-responsive gene expression is correlated with the rest-activity cycle, such that both expression and quiescent behavior peak at the same time during the 24 hour cycle (Belvin et al 1999). In flies, CREB-related gene expression during rest was shown to play a restorative role that enabled maintenance of subsequent waking behavior, and blocking CREB-activity increased rest-rebound (Hendricks et al 2001). Here we see that in the brain of *M. sexta*, putative *creb* up-regulation is correlated with onset and early stages of the molt-sleep. The role of this transcription factor in the insect brain at this time during development is not known. CREB is associated with neuronal plasticity, and in adult flies, ecdysteroids affect consolidation of courtship memories through the reinforcement of CREB activity (Ishimoto et al 2009). CREB-mediated gene expression in the nervous system is also associated with many other possible downstream effects, such as synthesis of growth factors, enzymes, and neuropeptides.

Several "classic" ecdysone-induced transcription factors are also listed in Figure 3-21. The actions of ecdysteroids on giant polytene chromosomes of salivary glands of insects provided the first evidence that steroid hormones act directly on the genome to alter gene transcription (Clever 1964; Clever & Karlson 1960). Based on subsequent observations of the *Drosophila* salivary glands, Ashburner and colleagues proposed a

model, whereby ecdysone acted on the chromosomes to induce early gene transcription (originally observed as specifically located chromosomal "puffs"), the protein products of which would then influence activation of late genes, as well as the suppression of early gene transcription (Ashburner 1973; 1974). Many early and late genes have been identified, and their expression profiles have been examined in various tissues during larval molting, pupation and metamorphosis; and although there are similarities across these conditions, the identities and exact timing of expression have proven to be both tissue- and stage-specific. In *M. sexta*, the ecdysone-induced transcriptional cascade in epidermis of the larval body wall during the molt to the 5^{th} instar has been studied for over two decades using techniques such as dot blot and northern hybridization. Many early and late genes described for the *M. sexta* epidermal cascade, as well as other genes identified in the Ashburner cascade of the salivary gland are here found to be differentially-expressed in the brains of molting larvae. This section compares and contrasts the cascade found here in the *M. sexta* brain to that which is known to occur in the epidermis during the same developmental stage (molt to the 5^{th} instar). We identified 10 differentially-expressed hormone receptors/transcription factors that have been previously associated with the canonical ecdsyteroid transcriptional cascade in flies, moths and other insects. The $\log_2$fold expression changes of these genes are shown in relation to larval quiescent behavior (Figure 3-22).

Gene E75 codes for several isoforms of a product that is a member of the nuclear receptor family. Our profiles show differential expression of E75A and E75B. The identity of E75B was confirmed in FlyBase, and with the available *M. sexta* sequence in

the NCBI database. The gene identified as E75A was originally annotated as 78C, but the profile of this gene had been previously paired with that of the *M. sexta* E75A gene (Figure 3-11). As there is no E75A sequence available in the SilkDB, we assume that sequences were matched to the E78C gene by default, and have therefore assigned the identity E75A to this gene; therefore, caution should be used prior to making any final conclusions about the expression profile of this gene. In the epidermis, expression of E75A is induced by the rise of ecdysteroids, and levels begin to decline by the time of the ecdysteroid peak (Zhou et al 1998). Here we see a similar profile of E75A expression in brains of molting larvae. Epidermal E75B mRNA levels reportedly peak a short time after E75A, during the decline of ecdysteroids (Zhou et al 1998). Here we do not see delayed expression of E75B, which mirrors that of E75A; nevertheless, it should be noted that the sampling of more time-points might reveal differences in the timing of peak expression levels. In agreement with levels in the epidermis, the mRNA of both receptors declines to low levels by the late molt (HCS +18).

HR3 is another member of the nuclear receptor family. In the epidermis, levels of MHR3 rise with rising ecdysteroid titre, (but this rise is delayed until suppressive effects of E75A decline), peak at peak ecdsyteroid levels, and then declin to low levels by the late molt (Langelan et al 2000; Palli et al 1992). Our profiles show differential-expression of two HR3 isoforms. In the brain, we see that HR3 mRNA rises without delay with the predicted rise of ecdysteroids, peaks at HCS -6 hrs, and declines to lower levels by HCS +18 hrs. A similar profile is observed for HR4. In the epidermis, appearance of MHR4 is delayed relative to the peak of MHR3, and its expression is

thought to be temporarily suppressed by ecdsyteroid-induced inhibitory proteins (Hiruma & Riddiford 2001). This does not seem to be the case in the brains of molting larvae, as levels rise with the predicted rise in ecdysteroid titres, and peak prior to the predicted steroid decline.

In *M. sexta*, mRNA levels of transcription factor E74 isoform A (E74A) appear in the epidermis at high levels following the decline of ecdysteroids at the end of the molt. Here, we also see significant up-regulation of E74A toward the end of the molt (at HCS +18 hrs). In addition, E74A mRNA levels are significantly down-regulated during the rise and early part of the molt, suggesting that early gene expression acts to suppress expression of this transcription factor.

The expression profile of another nuclear receptor, βFTZ-F1, agrees very closely with that found in the epidermis. In the epidermis, up-regulation of βFTZ-F1 occurs toward late in the molt following the decline of ecdysteroids (Hiruma & Riddiford 2001). It has been suggested that βFTZ-F1, MHR4, and E75B participate in the timing of *dopa decarboxylase (ddc)* expression in the epidermis during the late molting periods (Hiruma & Riddiford 2009). In the epidermal cascade, βFTZ-F1 is thought to be an activator of *ddc* because its expression precedes it, while the disappearance of MHR4 and 75B is thought to release *ddc* expression from inhibition (Hiruma & Riddiford 2001). In our brain profiles, *ddc* mRNA levels become significantly elevated at the time of HCS, prior to the up-regulation of βFTZ-F1. Significant up-regulation of HR4 persists in brains at the time of HCS and at HCS +18 hrs, so although levels of this receptor do begin to decline following the ecdysteroid peak, there is no clear indication that this factor is

involved in the timing of DDC expression. As levels of 75B decline following the predicted ecdysteroid peak and fall to low levels by HCS +18 hrs, it is possible that this factor may play an inhibitory role similar to that found in the epidermis.

Two other transcripts associated with the ecdysteroid-induced transcription cascade that have not been profiled in the epidermis of *M. sexta* are here identified as differentially-expressed in brains of molting larvae. HR39 and HR38 are members of the nuclear receptor family (Nakagawa & Henrich 2009). HR39, along with βFTZ-F1, is a member of the NR5 sub-family of nuclear receptors (Nakagawa & Henrich 2009). In *Drosophila* brains, HR39 and βFTZ-F1 act oppositely on common target genes to regulate neuronal remodeling during metamorphosis, and their expression is inversely related with HR39 expression preceding that of βFTZ-F1 (Boulanger et al 2011). This data provides evidence that the putative *M. sexta* HR39 orthologue is also expressed in the brains of molting larvae, and that levels of mRNA are also elevated (transiently at the time of the predicted ecdysteroid peak) prior to the appearance of βFTZ-F1.

In contrast to the other above-mentioned differentially-expressed nuclear receptors, the putative *M. sexta* HR38 homologue is not up-regulated at any time during the molting period, but HR38 does show a significant down-regulation during the late molting period, (at HCS +18 hrs), suggesting a possible suppression of this factor by products of late gene expression. HR38 can heterodimerize with USP, and there is evidence to suggest that DHR3/USP responds to ecdysteroids, raising the possibility of a second, EcR-independent ecdysteroid signaling pathway (Baker et al 2003; Sutherland et al 1995). In contrast to EcR, USP is expressed ubiquitously in all tissues including those

of the CNS, during all larval stages (Asahina et al 1997). Although there is as yet no evidence of direct action of ecdsyteroids on CNS neurons during the *early* larval molt, the presence of EcR's (which are present, but not differentially expressed) expression in the brain, and of transcripts that code for HR38 and DopEcR (*see list of differentially expressed GPCRs*) raises the possibility of direct interactions through either typical or atypical ecdysteroid signaling pathways.

Cluster analysis.

Although enrichment analysis provides information as to which genes may be important at a given stage of development, we were also interested in identifying groups of genes that are changing together (with a similar pattern) across developmental time, as this could provide information about the regulation of biological processes in relation to behavioral and endocrinology events. We used the software Short Time-series Expression Miner (STEM) to cluster groups of genes with similar expression profiles (see "Materials and Methods"). The STEM algorithm is specifically designed for analysis of short time-series expression data (Ernst & Bar-Joseph 2006). Genes were assigned to a set of 1,250 predetermined model expression profiles (Figure 3-23). The significance of each profile is determined by comparing the number of expected matches (by random chance) to the number of genes actually assigned. A total of 34 significant profiles were identified using the parameters specified in "Materials and Methods," and highly-correlated profiles were grouped to form a total of 11 clusters (Figure 3-24). Figure 3-25 shows the expression profiles of all genes in these 11 clusters, along with the mean

expression profile for each cluster. Gene sets for each of the 11 clusters were tested for enrichment of GO terminologies using the GOSSIP enrichment analysis platform as outlined above. Enriched GO terminologies were found for Cluster0 (C0), C2, C3 and C4. Although only some of these enriched processes will be discussed, the full list of GO terminologies is provided in Table 3-3. In addition, a list of heavily-annotated GO terminologies (as identified by BLAST2GO node scores) is listed for all clusters, even for those where enrichment analysis failed to produce significant results (Table 3-4). In this study, we will only address clusters with enriched GO terminologies.

Cluster 0 (C0)

(Figure 3-25 and Table 3-3A). 95 genes were assigned to C0, and this cluster contains genes with transcript levels that are down-regulated throughout both the late inter-molt feeding period (during the predicted rise of molting hormone) and during the early molt-sleep period (the predicted peak and fall of ecdysteroids). Transcript levels decrease most dramatically following the predicted peak of ecdysteroids, and fold-change is maximal at the time of HCS. During the late molt, transcript levels approach intermolt values. There is little difference between control and early intermolt (-48 hrs) values. These transcripts are therefore associated with processes that are likely important to the intermolt and late molting stages, and but not during the early stages of the molt-sleep period, during which time levels decline. GO terms enriched in C0 include processes related to monooxygenase activity. A search through sequences assigned to these processes revealed the presence of four genes that encode cytochrome P450 (CYP)

enzymes. As a result of gene duplication followed by sequence divergence, CYP genes make up one of the largest families of genes in all plants and animals. In *B. mori*, 86 putative CYP genes have been identified through comparative genomic analyses (Li et al 2005). Although in insects, CYP genes are most well-known for their roles in the metabolism and detoxification of plant chemicals and insecticides, cuticle synthesis and hormone metabolism are also included among possible CYP functions. CYP genes are inducible or suppressible by a variety of stimuli, including hormones, infection, oxidative stress and xenobiotics. Of the five CYP genes found in C0, four are most similar to the CYP9A, and one to the CYP6AE CYP sub-families. The mRNA of a number of CYP6 family members is known to be induced by exposure to xenobiotics, and CYP9 family members cloned from the midgut of *M. sexta* also were shown to be differentially inducible following addition of a number of plant chemicals to artificial larval diet (Stevens et al 2000). In *B. mori*, (as in other species), CYP genes are arranged in clusters (Ai et al 2010). In a recent study, four *B. mori* genes belonging to the CYP9A subfamily (which as yet have only been found in lepidopteran insects) were characterized, and it was determined that three of the CYP genes were arranged in tandem on chromosome 17. The 4th CYP gene was located downstream on the same chromosome, but separated from the others by multiple alcohol-dehydrogenase-like genes (Ai et al 2010). In C0, we also find two sequences described by BLAST2GO as alcohol-dehydrogenase, which suggests a co-regulation of these CYP9A genes and some alcohol-dehydrogenase genes in the brain during larval development. In *B. mori*, CYP9A genes were shown to be expressed selectively in the epidermis, gut, fat body and brains of inter-

molt feeding larvae, where defense and detoxification roles have been proposed; however, the functional roles of these enzymes in nervous system tissues have not been investigated (Ai et al 2010).

This is the first developmental expression profiling of CYP9A genes. Our data suggests the possibility of an endogenous regulation of CYP9A gene expression in nervous tissue of developing larvae. It is tempting to speculate that these genes are up-regulated in response to larval diet and then transcripts decline to low levels following the inhibition of feeding at the onset of the molt-sleep; but transcript levels begin to decline prior to HCS, and levels do return to intermolt values prior to ecdysis, which suggests that in the brain, CYP9A genes are not induced by components present in the larval diet. Other CYP genes are known to be regulated by ecdysteroid-induced transcriptional cascades. Future studies are needed to clarify the identities of possible regulatory factors, as well as the actual function of CYP9A genes in the nervous system.

Also enriched in C0 are seven sequences annotated by BLAST2GO as udp-glucosyltransferases (UGT). UGT's are a superfamily of enzymes that, like CYPs, can mediate detoxification and elimination of many endogenous and exogenous compounds (Feyereisen 1995). Some UGTs have also been implicated in the catabolism of insect molting hormones (O'Reilly & Miller 1989). The expression profiles of these enzymes are consistent with a possible role in ecdysteroid catabolism; however, annotations on SilkDB indicate that most of these sequences identified in this cluster are involved in the inactivation of phenolic compounds.

Also enriched in C0 are four genes annotated by BLAST2GO as juvenile hormone (JH) epoxide hydrolases. Levels of JH are regulated by rates of biosynthesis and degradation. Active forms of JH are catabolized by either JH esterase, which converts JH into JH acid, or by JH epoxide hydrolase, which converts JH (irreversibly) to JH diol (Casas et al 1991). JH esterase is secreted into the hemolymph, whereas JH epoxide hydrolase is not secreted, and expression of these enzymes seems to be regulated differently in various tissues and organs (Seino et al 2010). In *M. sexta*, hemolymph JH levels are high during initiation of endocrine events that lead to the molt to the 5^{th} instar, after which hemolymph JH levels begin to decline (Fain & Riddiford 1975). Although hemolymph levels during the molt-sleep are relatively low compared to those measured during the inter-molt period, JH activity in different tissues might vary depending upon levels of JH catabolic activity. Down-regulation of JH epoxide hydroxylases observed here indicates that JH activity in the brain might remain high during much of the molt-sleep period, (at least during the early stages of the molt). Although JH is known to influence ecdysteroid signaling, the mode of JH action has not been fully worked out. There is some evidence to suggest that JH might influence ecdysteroid-induced gene expression by binding to ultraspiracle (USP), but the relationship between JH and USP *in vivo* has not been resolved (Jones & Sharp 1997). In any case, the potential role of JH in the regulation of arousal-related gene expression during the molting period should not be disregarded.

Cluster 2 (C2)

(Figure 3-25 and Table 3-3B). 90 genes were assigned to C2. For this cluster, gene expression rises slowly, and only slightly, during the late intermolt and early molting periods. At HCS +18 hours, these genes show a strong up-regulation, indicating that products of these genes are important for the late molt. Levels at -48 hrs are not different from those of the inter-molt reference time point. 72 of the 90 genes were annotated with BLAST2GO, and these were used for enrichment analysis. Enriched GO categories all seem to be associated with catabolism of carbohydrates and proteins, as well as transport of protein catabolic products, which we presume are necessary for the breakdown and recycling of 4^{th} instar tracheal cuticle during the late molting period. 8 of the 11 enriched categories are related to carbohydrate metabolic processes, particularly those associated with the breakdown of chitin.

Cluster 3

(Figure 3-25 and Table 3-3C). Transcript levels for genes clustered in C3 also rise during the late intermolt and just prior to HCS (during the predicted rise and peak of ecdysteroids), but in contrast to genes in C2, expression peaks at the time of HCS, and then drops to inter-molt levels by the late molting period. Levels at -48 hrs are similar to intermolt reference levels. 82 genes were clustered in C3, and 67 of these were annotated and used for subsequent enrichment analysis. Among the enriched GO terminologies in C3 are processes related to protein catabolism, and within this category there are a number of genes annotated by BLAST2GO as serine proteases. Degradation of the old

cuticle is accomplished by enzymes secreted into the molting fluid. A series of studies that examined enzymatic activity in the pre-adult stages of *M. sexta* revealed that the activity of proteases on the body-wall cuticle preceded, and was a prerequisite for the activity of enzymes that break down chitin components (Samuels & Reynolds 1993b). Also, injections of molting hormone delayed the activity of these proteases, indicating that the fall of ecdysteroids was necessary for their activation (Samuels & Reynolds 1993a). Our data shows a temporal relationship between the expression of specific protease and chitinase mRNA. Proteases clustered in C3 seem to be positively-regulated during the rise and early fall of ecdysteroids (when levels peak), whereas chitinases clustered in C2 are not up-regulated until after the fall of ecdysteroids.

Cluster C3 is also enriched in GO terminologies related to cell division, as well as the negative regulation of autophagy. Up-regulation of genes associated with cell division during the predicted rise in ecdysteroids, as well as their peak during the time of HCS, is expected, as epidermal cells of the trachea (similar to the epidermal cells of the body wall) undergo a round of cell division around the time of apolysis, so as to increase the diameter of the trachea of the subsequent instar (Ryerse & Locke 1978). Both cell division and cell death are known to be regulated by molting hormones. During metamorphosis in *M. sexta*, autophagy plays an important role in remodeling of the CNS (Kinch et al 2003). During larval molts, this remodeling does not occur, and here we see a negative regulation of cell death processes, which is presumably driven by molting hormones.

The most significantly enriched GO terminologies belong to functional categories connected to the targeting of secretory proteins. Most of the genes identified in these categories express components of the Sec61 protein translocation complex, which is a protein translocator that shuttles polypeptides into the endoplasmic reticulum. This complex is important for packaging and targeting of proteins destined for secretion, such as enzymes and structural proteins involved in cuticle synthesis and degradation, or for packaging of peptide neurotransmitters. A microarray analysis of gene expression in wing disks of *B. mori* during pupal formation also showed a similar expression profile of Sec61 genes, so this regulation seems to be conserved for different tissues and developmental stages (Ote et al 2004).

Cluster 4

(Figure 3-25 and Table 3-3D). 47 genes were clustered in C4, and the 37 annotated genes from this cluster were used for enrichment analysis. C4 gene expression is down-regulated during the predicted rise in ecdysteroids, and then rises following the predicted peak of ecdysteroids, with maximal levels occurring at the late molting stage (HCS +18 hrs). Enriched GO terminologies were dominated by cGMP metabolic processes. 3 genes that code for soluble guanylate cylases (GCs) were identified as belonging to these enriched categories. GCs exist in either soluble or membrane-bound forms. Membrane-bound forms are known to bind various neuropeptides, and soluble forms are best known for their binding of the gaseous neurotransmitter nitric oxide. BLAST results indicate that all three GCs share highest sequence homology with soluble

GCs from other insects. It is likely that at least one of these GCs (BGIBMGA010713) was mapped by fragments of the *M. sexta* MsGC-ß3 subunit, which forms a novel homodimer that, unlike most soluble GCs, is only weakly activated by NO (Nighorn et al 1999). The physiological role of this particular subunit has yet to be characterized, but the profile of the cluster to which these genes belongs suggests that it plays a role in signaling toward the end of the molt.

Arousal-related genes

Although enrichment and cluster analysis have here provided information about many groups of functionally related genes, this information has not provided much information about arousal-related systems that might be important for the induction and maintenance of the molt-sleep. It is possible that changes in arousal-state that occur during the transition from feeding to molting are not dependant upon changes in brain gene expression, or that arousal-related changes in brain chemistry are regulated at a level downstream of transcription. It is also possible that many changes in arousal-related transcription are not detected by enrichment analysis. Since the main focus of this study is to generate hypotheses as to what systems might be involved in the modulation of arousal-state during development of holometabolous larvae, we used a targeted gene approach to search for differentially-expressed, putative arousal-related genes. The BLAST2GO list of annotated, differentially-expressed genes was used to screen for genes with descriptions and GO terminologies associated with G-protein-coupled receptors and neurotransmitter-gated ion channels, neurotransmitter and neurosecretory systems, ion

channels and ion channel regulating proteins, and epidermal growth factor (EGF) and insulin signaling.

G-protein-coupled receptors (GPCRs) and neurotransmitter-gated ion channels. When annotations were screened for differentially-expressed GPCRs and neurotransmitter-gated ion channels, a total of 27 putative receptors were identified (Figure 3-26AB). Expression profiles and BLAST2GO descriptions of the relevant *B. mori* genes are provided. In addition, further confirmation of receptor identity was obtained (when possible) using reciprocal BLASTs between SilkDB and FlyBase.

Down-regulated GPCRs and NT-gated ion channels

16 putative receptors were identified as being significantly down-regulated during at least one stage (Figure 3-26B), and 9 of these receptors were significantly down-regulated during the rise and/or peak of ecdysteroids, suggesting a possible influence over the onset of molting-quiescence. The greatest fold-change is attributable to the putative ortholog of the *B. mori* gene BGIBMGA012730, which codes for a protein that shows highest sequence similarity to Hypocretin (a.k.a., Orexin) receptors. Significant down-regulation of this receptor can be observed throughout the early rise of ecdysteroids, at the time of HCS, and during the late molt; but expression levels are not significantly different in brains of early inter-molt larvae. In mammals, the Hypocretin/Orexin system is known to stimulate food intake and to promote energy expenditure, and animals have difficulty maintaining wakefulness in the absence of either receptor or ligand (Chemelli

et al 1999; de Lecea et al 1998; Sakurai et al 1998). No homologue for the Hypocretin/Orexin peptide has been identified in insects. Receptors with high sequence similarity to mammalian Hypocretin/Orexin GPCRs have been identified in several insect species, but none has been functionally characterized, nor have any been localized to specific cell-types within the central nervous system. That levels of this receptor are down-regulated just prior to and for the duration of decreased food intake and activity, and that levels are restored at a time when feeding and activity is resumed, makes this receptor an excellent candidate for future research into mechanisms underlying modulation of larval arousal states.

Several other genes that code for proteins with similarity to receptors implicated in modulation of feeding behavior in insects and mammals were down-regulated just prior to and at the onset of molting quiescence. Gene BGIBMGA002442 is significantly down-regulated by -6 hrs, and BGIBMGA008802 and BGIBMGA009039 are significantly down-regulated at -12 hrs. BGIBMGA008802 and BGIBMGA009039 are described by BLAST2GO as genes that code for putative Bombesin-like receptors. The role of Bombesin-like peptides in insects is not known, but in mammals, Bombesin signaling acts as a source of negative feedback that halts feeding behavior (Yamada et al 2000). A very recent article has identified orthologs of these two *Drosophila* genes as being receptors for the neuropeptide CCHamide (Hansen et al 2011). CCHamide itself was only identified a few years ago, and *in-situ* hybridization revealed that in *B. mori*, the peptide is expressed in the larval brain and ventral nerve cord, as well as the gut (Roller et al 2008a). The functional role of CCHamide signaling in the brain and periphery is

unknown, but down-regulation of this receptor shown here in the brain during the molting period suggests that it is more likely to have functions that facilitate feeding-stage behaviors. BLAST2GO annotations of gene BGIBMGA002442 indicate that this gene codes for a Neuropeptide Y-like receptor. Neuropeptide F (NPF) is the insect version of mammalian Neuropeptide Y. NPF is expressed in brain, ventral nerve cord and peripheral tissue of *Drosophila* and other insects during larval feeding stages, when NPF signaling is known to promote foraging behavior (Wu et al 2003; Wu et al 2005; Xu et al 2010). In *Bombyx*, *npf* transcripts have been detected in the larval CNS, and 24-32 small NPF neurons were detected specifically in the larval brain (Roller et al 2008b). In the corn earworm, *Helicoverpa zea*, changes in levels of NPF in the CNS, hemolymph, and gut tissue indicate a correlation with changes in feeding behavior during development (Huang et al 2010). Here, although reads were mapped to the NPF peptide sequence, levels of this peptide were not found to be differentially-expressed in the brain. Nevertheless, a role for this peptide in feeding regulation in *Manduca* is suggested, its receptor is down-regulated in the brain at a time when a decrease foraging drive would be adaptive.

Other GPCRs that are down-regulated in the brain during the molting period include a putative prostaglandin receptor (BGIBMGA010037), 2 putative adenosine receptors (BGIBMGA006593 and BGIBMGA006596), and the Corazonin receptor (BGIBMGA001531). Putative adenosine receptors are down-regulated at -12 and -6 hrs, as well as at the time of HCS. In the early stages of sleep research in *Drosophila*, the effects of caffeine on fly sleep-like behavior led to the notion of a conserved role for

adenosine in the modulation of arousal state in both insects and mammals (Hendricks et al 2000; Shaw et al 2000). It is now known that caffeine-induced arousal is mediated through *Drosophila* D1 dopamine receptors (Andretic et al 2008). Thus, the functional role of this putative adenosine signaling in insects has not yet been determined.

A putative prostaglandin EP4 receptor is here reported to be down-regulated at -12 and -6 hrs. Prostaglandins mediate immune response in insects, but little is known about their receptors, or their possible roles in the modification of insect behavior (Stanley 2006; Stanley et al 2009). In rodents and primates, prostaglandins exert a wide variety of effects on both physiology and behavior, but in terms of their role in arousal-modulation, prostaglandins are most well known as sleep-promoting agents (Hayaishi & Urade 2002). The mammalian sleep-promoting effects of prostaglandins, however, are location and receptor subtype-dependent; actions on the EP4 receptor subtype in the area of the posterior hypothalamus promotes wakefulness through activation of the histaminergic system (Huang et al 2003).

Although the Corazonin receptor is not down-regulated until the time of HCS, the brain expression profile is worth mentioning. In *M. sexta,* Corazonin is released into the hemolymph towards the termination of the molting period, at which time it has been shown to act on receptors expressed in the epitracheal glands to facilitate initiation of pre-ecdysis behavior (Kim et al 2004). Here, results indicate that receptor levels are significantly down-regulated at the time of HCS, suggesting that Corazonin signaling in the brain plays a more important role during the intermolt period.

Two receptors associated with glutamateric signaling were down-regulated during at least 1 stage. BGIBMGA004625 is a putative metabotropic glutamate receptor, and BGIBMGA009470 is a putative glutamate ionotropic receptor (kainate 3 receptor). In the brain, glutamatergic transmission is largely associated with arousal. In mircroarray studies in both rats and flies, levels of brain mRNA expressed by genes related to glutamatergic signaling are higher during wake compared to sleep states (Cirelli 2009; Cirelli & Bushey 2008; Cirelli et al 2004; Cirelli et al 2005b). Decreased levels of putative kainite receptor mRNA also suggest a possible conservation of function across the developmental stages; however, a putative glutamate kainate 2 receptor is also included in the list of up-regulated genes (BGIBMGA011527).

Up-regulated GPCRs and NT-gated ion channels

11 putative receptors are significantly up-regulated during at least one stage (Figure 3-26A). It should be noted that the previously-described list of down-regulated receptors provides clues as to what types of signaling might be important to the inter-molt period. The down-regulation of the expression of those receptors suggests that they function in behavioral circuits that might conflict with molting physiology and behavior, such as those involved in the promotion of foraging behavior. In other words, genes down-regulated in the brain just prior to and during the molt are more likely to be arousal-promoting. On the other hand, the list of up-regulated genes might provide insight into what systems, if any, are involved in the induction and maintenance of molting quiescent behavior.

Factors that promote sleep-like states are termed *somnogens*. The neurotransmitter γ-aminobutyric acid (GABA) is a major sleep-promoting agent in both mammals and flies, where GABA transmission acts to shut down wake-promoting circuitry in the brain (Agosto et al 2008; Chung et al 2009; Parisky et al 2008). Gene BGIBMGA007240 is significantly up-regulated both during the rise of ecdysteroids and throughout the duration of the molt-sleep period, returning to intermolt reference values only following ecdysis. All BLAST hits show sequence similarity to NT-gated ion channel subunits, and although this gene has not been functionally characterized, electronic annotations of the reciprocally-BLASTed *Drosophila* ortholog indicate that the protein may be either a glycine-gated or a GABA-gated ion channel, suggesting a role for GABA transmission in the onset and maintenance of molting quiescence.

Several putative GPCRs are listed as significantly up-regulated during at least one stage, 3 have un-ambiguous annotations, and only 2 of these are differentially-expressed during the molting period. BGIBMGA011935 encodes a putative Tachykinin-like receptor. In *Drosophila,* Tachykinin receptors are expressed in the brain and ventral nerve cord throughout embryonic and post-embryonic development, and in the adult stages where they are thought to be involved in olfactory processing and locomotor activity (Van Loy et al 2010; Winther et al 2006). The other GPCR is annotated as a putative dopamine invertebrate receptor (BGIBMGA008273). GO annotations mapped to this sequence indicate a coupling to Gi/Go signaling, so this is likely to be a dopamine 2-like (D2-like) receptor. One D2-like receptor has been identified and functionally characterized in *Drosophila*, and BLAST searches using this sequence (FlyBase ID:

CG33517) in the SilkDB retrieve best hits to sequences BGIBMGA008272 and BGIBMGA008273; for both of these sequences, CG33517 is also the best BLAST hit in the *Drosophila* database. Sequence BGIBMGA008272 is a closer match, which is the reason that the reciprocal BLAST column is negative for BGIBMGA008273.

In a previous investigation into a possible dopaminergic influence over molting arousal state (see appendix A), we used sequence BGIBMGA008272 to partially clone a putative *Manduca sexta* D2-like receptor. Degenerate primers were designed from regions of high sequence homology between *Drosophila melanogaster*, *Apis mellifera*, *Tribolium castaneum*, and *Bombyx mori* sequences, and the resulting 1012 bp partial clone was used to profile the putative D2-like receptor expression across the 4th larval stage (See Appendix A). QPCR expression profiles did not reveal any significant fold-changes across the 4th larval stage, and although Illumina sequences were mapped to BGIBMGA008272, there were also no significance changes revealed using the next-generation sequencing technique. The Illumina expression profile of BGIBMGA008273 does, however, indicate that a putative D2-like receptor (the paralogue to BGIBMGA008272) is differentially-expressed during the molting period. Antibody staining against dopamine and an enzyme necessary for its synthesis—Tyrosine hydroxylase—demonstrate robust staining in interneurons of the brains of late 4th instar *M. sexta* (Mesce 2002).

In adult insects, dopamine is a potent modulator of arousal, and in the fly brain, the type of arousal that is modulated by dopamine is receptor-subtype and circuit dependent (Kume et al 2005; Lebestky et al 2009). In larval stages, D2-like receptor

expression has been observed in neuropeptide-producing cell bodies, projections of the ventral nerve cord, and projections in the larval brain, and it has been hypothesized that these receptors may play a role in the fine-tuning of neurosecretory function (Draper et al 2007). That this putative D2-like receptor is up-regulated during the early stages of the molt when central release of neuropeptides is largely inhibited, and then later down-regulated prior to the onset of ecdysial behaviors known to be orchestrated by ensembles of central peptidergic networks also suggests a possible role for this receptor in the fine tuning of molting behaviors. Other aspects of dopaminergic transmission also seem to be regulated across the molting period, and this will be discussed in the section to follow.

Neurotransmitter and neuropeptide systems. In this section, we report differentially-expressed genes associated with neurotransmitter and neuropeptide systems (Figure 3-27AB). A screen of BLAST2GO descriptions and GO terminologies identified a total of 14 genes in this category. 3 of the genes code for the neuropeptides, Bursicon, Allatotropin and the insulin-like peptide Bombyxin. Bombyxin (ID # BGIBMGA011926) will be discussed in a later section, in conjunction with profiles of other transcripts related to insulin and epidermal growth factor. Allatotropin (ID # BGIBMGA011850) was excluded from our discussion (and figure), as comparison with the nucleotide alignment on the existing *M. sexta* gene yields conflicting results (Figure 3-11). All other genes were identified as coding for products involved in regulation of non-peptide neurotransmitter systems.

Bursicon

Bursicon is a neuropeptide that is released both centrally and peripherally into the hemolymph during the final steps of the peptide signaling cascade that regulates ecdysis behavior in insects. Bursicon regulates cuticular tanning and melanization at the end of molting, as well as wing expansion during adult emergence. In the emerging fly, Bursicon acts centrally to activate motor programs that underlie wing expansion (Peabody et al 2008). Other possible behavioral roles for the central release of Bursicon have yet to be investigated. In this study, we observe that transcripts of gene BGIBMGA011086 are up-regulated in the brain during the entire molting process, as well as during the early inter-molt stage that follows ecdysis. This gene was annotated as *pburs* by BLAST2GO—one of the two possible proteins that forms the mature hormone, which is usually a heterodimer composed of *pburs* and *burs* (Luo et al 2005). Bursicon has been cloned in *M. sexta* (Dai at al 2008), and the nucleotide expression profile of this gene also verifies an up-regulation of *pburs* in the brain of *M. sexta* during the molting period (Figure 3-11). In *M. sexta*, Bursicon-positive cells occur in abdominal, thoracic and subesophageal ganglia, as well as cells in the corpora cardiaca of pharate larvae, pupal and adult moths (Dai et al 2008). As cells in the brain were not detected in any of these pharate stages, it was surprising that Illumina reads mapped to this gene. In *D. melanogaster*, very weak immunostaining was detected in a pair of neurons in the brain of pharate pupae (pharate larvae were not tested) (Peabody et al 2008). Our data indicates that the number of reads that mapped to this gene was very low, so it is possible that expression levels were too low for detection in the brains of *M sexta* using anti-body

staining and/or *in situ* hybridization. This further demonstrates that the highly-sensitive Illumina sequencing technique could prove useful for detection of genes with very low expression levels.

Nitric oxide signaling

At -6 hrs and at the time of HCS, there is a significant down-regulation of transcript from gene BGIBMGA002938, which was identified by the BLAST2GO annotation procedure as coding for the enzyme nitric oxide synthase (NOS). In nerve cells, NOS generates the gaseous neurotransmitter, nitric oxide (NO). Since NOS has been cloned and characterized in *M. sexta* (Nighorn et al 1998), the reciprocal BLAST approach with the NCBI database was also used to confirm identity of the transcript. In insects, as in vertebrates, NO is implicated as a modulator of a wide range of processes, including development, learning and memory, sensory processing, locomotion, olfaction and vision (Bicker 2001). *M. sexta* has served as one of the many insect models used to characterize NO transmission. During metamorphosis, NO acts oppositely to ecdysteroids in its role as a suppressor of the proliferation of neural precursors in the optic lobe (Champlin & Truman 2000). GO enrichment analysis of up-regulated genes show the enrichment of GO terms associated with M-phase and cytokinesis at the same time that the NOS gene is down-regulated (Figure 3-18A). In terms of the neuronal structure of the CNS, morphological changes are thought to be largely absent during larval-larva molts; so facilitation of proliferation by NO down-regulation is more likely to be associated with the cells of the tracheal epithelium.

In *M. sexta*, NO signaling can be influenced by input from cholinergic sensory afferents. Release of acetylcholine from primary sensory afferents is thought to increase production of NO in central neurons, which in turn acts on NO-sensitive interneurons and motor neurons to increase excitability and rates of spontaneous activity (Qazi & Trimmer 1999; Zayas et al 2002). Down-regulation of NO synthesis just prior to and at the onset of the molting quiescence is consistent with a role for NO as a neuromodulator during the active inter-molt feeding stage. NO-signaling also has been associated with neurosecretion in insects. In the locust, NOS is co-localized with octopamine and RFamide-like peptides in neurosecretory cells that project to the heart, and release of NO from these neurosecretory cells acts as a cardio-accelerator (Bullerjahn et al 2006). In *M. sexta,* NOS also is present in neurosecretory cells of the brain and ventral nerve cord; in the brain, NO producing cells include neurosecretory cells that project to the corpora allata/corpora cardiaca complex, but a role for brain NO in the regulation of neurosecretion has yet to be explored (Zayas et al 2000).

Dopaminergic signaling and metabolism

In both insects and mammals, monoamine and amino acid neurotransmitters have long been known to play a role in the modulation and regulation of arousal state. In the fly, the neurotransmitters dopamine (DA), serotonin, octopamine, tyramine and GABA have been shown to affect sleep-wake and other forms of arousal (Crocker & Sehgal 2010). In addition to our screen for generic terms such as "neurotransmitter," we searched the annotated set of differentially-expressed genes for proteins involved in

synthesis, packaging, release, re-uptake and catabolism of these neurotransmitters. Of the above-mentioned neurotransmitter candidates, our results show differential-expression of genes related to pathways that regulate levels of DA and DA metabolites.

In larval *M. sexta*, dopaminergic neurons are located throughout the brain and ventral nerve cord (Mesce 2002; Mesce et al 2001). During late larval and pupal stages, there is a large increase in the numbers of DA-synthesizing neurons, and although it has not been directly tested, metamorphosis of the dopaminergic system is thought to be controlled by ecdysteroids (Mesce et al 2001). DA-containing neurons in the larval brain are present, but have not been well characterized. Considering that DA acts in the brain of adult insects to modulate multiple forms of arousal, it is tempting to speculate that the rise and fall of ecdysteroids programs a shift in arousal threshold at least partially through regulation of dopaminergic signaling, especially when so many of the genes involved in DA synthesis and degradations are here shown to exhibit changes in their expression levels across the early and late molting period. The dopamine synthesis pathway, however, is also a key pathway in processes related to cuticle formation and tracheal morphogenesis, so it is not known if these pathways are being regulated in the epidermal lining of the trachea, the dopaminergic neurons, or both (Andersen 2010; Hiruma & Riddiford 2009; Hsouna et al 2007). In order to clarify the role of DA in the brain during the larval stages, future research will need to identify specific brain locations in which this regulation is occurring, as well as downstream targets of DA-signaling. In this study, we can only report identities and expression profiles of the differentially-expressed DA synthesis pathway-related genes. Many of these genes are involved in metabolic

pathways of compounds other than DA, but here we focus solely on their role in DA metabolic pathways.

Synthesis of DA begins with conversion of tyrosine into dihydroxyphenylalanine (DOPA). DOPA is then converted into DA, which is packaged into synaptic vesicles for release at synaptic terminals in neurons. Alternatively, during the process of cuticle formation, DA in the epidermal cells can also be used as a precursor for melanin formation and/or for synthesis of one of two ortho-diphenol sclerotization precursors, N-acetyldopamine (NADA) and N-beta-alanyldopamine (NBAD). The relative contribution of these pathways (locally) dictates the type of cuticle formed during each molt (True 2003). Our expression profiles show that in the brains of molting larvae, there is regulation at every level of the above-described pathways (Figure 3-28). During the predicted rise of ecdysteroids and throughout the entire sampled molt-sleep period, expression of gene BGIBMGA002077 is up-regulated. BLAST2GO assigned to this gene the description *tan*, the identity of this gene was confirmed by reciprocal BLASTs. Biochemical and genetic evidence suggests that *tan* (also known as NBAD hydrolase) encodes a product that converts NBAD into DA, suggesting that during the molt to the 5th larval stage, the pathway leading to NBAD synthesis is largely inhibited (at least up to ~9-12 hrs prior to ecdysis) (Wright 1987). During the predicted peak and fall of ecdysteroids, gene BGIBMGA008538 is down-regulated. This gene has been identified as Dopamine N-acetyltransferase, the enzyme that converts DA into NADA. This pathway then, might also be inhibited during the early molting period, but since levels are not down-regulated at 18 hrs following HCS, it is likely that formation of NADA is

released from inhibition late in the molt. In *M. sexta*, levels of NADA dominate and NBAD is low in both the cuticle and hemolymph during the molt to the 5th and final larval stage, a time when NADA is thought to be the major precursor used for the formation of the larval cuticle (Hopkins et al 1984). It is then likely that the regulation of *dopamine N-acetyltransferase* and *tan* are related to tracheal cuticle formation; however, catabolism by Dopamine N-acetyltransferase is also thought to be the main route for DA neurotransmitter degradation in insects, and regulation of this enzyme might also influence, or perhaps be influenced by, neuronal dopaminergic transmission (Sloley 2004).

During the time of the predicted rise, peak, and early fall of ecdysteroids, (developmental time-points that precede and correlate with changes in quiescent behavior), it seems that through the regulation of gene expression, pathways leading to formation of sclerotization precursors are inhibited. Diversion of DA away from the NBAD and NADA synthesis pathways might lead to a build up of DA in the epithelial and nerve cells of the brain. Down-regulation of gene BGIBMGA001149, identified as the melanin-promoting gene *yellow*, suggests that available DA is not being shunted into melanin synthesis pathways (Wittkopp et al 2002). As mentioned previously, during the predicted fall of ecdysteroids and prior to ecdysis (stages HCS, and HCS +18 hrs), expression of the *dopa-decarboxylase* (*ddc*) genes BGIBMGA002958 and BGIBMGA003199, the products of which convert DOPA into DA, are both significantly up-regulated. Just prior to and during up-regulation of *ddc*, there are also changes in the expression level of genes that encode products that regulate Tyrosine hydroxylase, the

enzyme that converts tyramine to DOPA, and the rate limiting step of the DA synthesis pathway. For example, at -6 hrs and at HCS, gene BGIBMGA008538 is significantly down-regulated. This gene is identified as a GTP cyclohydrolase (*punch*, in *Drosophila*), the rate-limiting enzyme in synthesis of the regulatory cofactor tetrahydrobiopterin, which is required for Tyrosine hydroxylase activity (Krishnakumar et al 2000). At HCS, gene BGIBMGA002971 is significantly up-regulated; this gene is identified as coding for a zinc ion transporter named *catecholamines up* (*catsup)* in *Drosophila*, which is known to be a negative regulator of Tyrosine hydroxylase activity (Stathakis et al 1999). So although *ddc* genes are up-regulated at HCS and HCS +18 hrs, these changes in expression of the *punch* and *catsup* may lead to an overall reduction in DA levels, at least during the early molt.

Two uncharacterized genes (BGIBMGA010779 and BGIBMGA013957) were assigned GO terms related to catecholamine metabolism. Neither of these genes was assigned a clear definition by BLAST2GO, and reciprocal BLASTing within FlyBase did not clarify the identity of these genes or their protein products. It should be noted however, that these genes show higher levels of up-regulation than any of the others in Figure 3-27, suggesting they may play an important role in the tight regulation of catecholamine metabolism that we see here. Lastly, gene BGIBMGA002922 has been associated with regulation of biogenic amine levels in insects. This gene, which encodes an ABC transporter and its binding partner, is identified as the *Drosophila white* gene, which is well known for its use as a reporter gene in the construction of transgenic lines. In addition to mediating reduced eye pigmentation, mutants of the *white* gene also display

behavioral changes that are thought to be due to lowered levels of several neurotransmitters, including DA (Anaka et al 2008; Borycz et al 2008).

In its role as a neurotransmitter in the fly brain, DA is thought to participate in the modulation of some aspect of every fly behavior studied (Van Swinderen & Andretic 2011). There is a linear effect of DA levels on sleep-wake arousal states, with increasing levels leading to heightened activity and decreased amounts of sleep-time. Also in the fly, DA can modulate specific forms of arousal, such as those underlying selective attention and courting behaviors, the direction of which is dependant upon receptor sub-type and anatomical specificity.

DA can influence activity levels and arousal states in many other insects as well. At present, it is not known if DA exerts an influence over activity levels and arousal states in larval *M. sexta*. In certain lepidopteron larvae destined for pupal diapause, DA is elevated in the brain, hemolymph and integument, and injections of DA can induce diapause in non-destined larvae (Noguchi & Hayakawa 1997). How DA acts to induce this diapause, which is a state characterized by a prolonged quiescent state, is not known. Although the regulation of DA metabolic pathways in the molting larval brain of *M. sexta* is likely associated with tracheal cuticle formation, such regulation could also occur in dopaminergic neurons of the CNS to regulate arousal state during the molt. That a putative D2-like receptor shows differential expression during the molting period suggests that brain DA-signaling may be regulated during the molting period.

Hormonal mechanisms leading to regulation of *ddc* in the epidermis of *M. sexta* during the molt to the 5th instar have been extensively studied, and here we show that in

the larval brain, *ddc* is also up-regulated during the molting period both during and following the decline of ecdysteroids. We also report differential-expression of a number of genes related to the same metabolic pathway, which are also likely to be hormonally regulated. Although *M. sexta* has served as a useful model system for study of molting physiology using techniques such as electrophysiology, immunohistochemistry and *in situ* hybridizations, lack of an available genome has made it difficult to link the rich body of knowledge regarding its physiology with the underlying genetic regulation. In over fifteen years of research into the hormonal regulation of cuticular mealnization in *M. sexta*, expression profiles for only a handful of hormone receptors, transcription factors, and target genes have been produced for this model system. Here, we demonstrate that the use of Illumina sequencing, coupled with the availability of a genome from a closely related species could greatly facilitate discovery of the identities, and elucidate the expression profiles of genes that act together to regulate a physiological process such as cuticular sclerotization and melanization.

Ion channels and ion channel regulators. BLAST2GO annotations were searched for descriptions and GO terminologies that identified differentially-expressed genes as coding for ion channels or ion channel-regulating molecules. In this category, 14 differentially-expressed genes were identified (Figure 3-29AB).

Potassium channels

In *Drosophila*, forward genetic screens have identified K^+ channel activity as being important for sleep-regulation. Flies mutant for the *shaker* gene, (which codes for a pore-forming alpha subunit of a voltage-gated K^+ channel), display a short-sleeping phenotype (Cirelli et al 2005a). The Shaker K^+ channel facilitates the rapid repolarization of the neuronal membrane following action potentials and neurotransmitter release, and this channel is expressed in terminals of the neuromuscular junction and is also highly enriched in the terminals and processes of fly brains (Schwarz et al 1988). Voltage-gated K^+ channels are expressed with accessory beta subunits that can modify their activity. In a later study, it was found that mutations for *hyperkinetic*, a gene that encodes a beta subunit that modifies Shaker K^+ current to increase conductance, also results in a short-sleep phenotype (Bushey et al 2007). Central effects of K^+ channel and accessory units on sleep-phenotypes can be dissociated from phenotypes that result from modification of currents at the neuromuscular junction.

In annotation screenings, we identified several putative K^+ channel or K^+ channel-modifying genes that show differential-expression during at least one developmental stage. Only one of these genes is up-regulated during the molt-sleep. Gene BGIBMGA002286 is identified by BLAST2GO as coding for a potassium channel. Although uncharacterized, the *Drosophila* ortholog (CG34396) is annotated with GO terminologies that identify the protein product as being an open-rectifier K+ leak channel. This type of channel can contribute to resting membrane potentials of neurons and/or glia. Differential-expression analysis of this gene shows a rising trend starting at -6 hrs, and

expression is significantly elevated at HCS, +18 hrs and also during the early inter-molt period when expression levels appear to be in decline. No other K^+ channel or modulatory subunit is up-regulated at any stage of the molt, but gene BGIBMGA009560 is significantly up-regulated during the early inter-molt period, and although the identity of this gene was not verified using reciprocal blasts, BLAST2GO annotation suggests that this gene encodes a K^+ channel-interacting protein.

Surprisingly, more K^+-associated genes are shown to be down-regulated during the molting period. Levels of a putative voltage-gated K^+ channel (BGIBMGA013356) are down-regulated just prior to and during the time of HCS. A putative inwardly-rectifying K^+ channel (BGIBMGA007070) and a putative open rectifier K^+ channel (BGIBMGA008375) are down-regulated at HCS +18 hrs, and at HCS, respectively, and descriptions match those assigned to *Drosophila* orthologs. The actual influence of increased or decreased K^+ current on arousal state is likely to be circuit-specific. For example, increased membrane excitability due to lowered K^+ leak channel function targeted to GABAergic neurons is likely to have a different effect on behavioral state compared to the same changes taking place in cholinergic systems, for example. Future studies should aim at co-localization of these specific channels with neurotransmitters and enzymes involved in the synthesis of neurotransmitters.

The profile of one last K^+ current-associated gene remains to be mentioned, and this is the only gene that could (through reciprocal BLAST) be directly linked to Shaker channel activity. Gene BGIBMGA001376 is described by BLAST2GO as *quiver*, which is an allele of the gene (as identified in *Drosophila*) *sleepless*. The *sleepless* gene codes

for a brain-enriched glycosylphosphatidylinositol-anchored protein that can regulate the expression and localization, and enhance the activity of the Shaker channel (Koh et al 2008; Wu et al 2010). Interestingly, flies with moderate reduction of Sleepless levels do not show considerably altered levels of baseline sleep, but do show a lack of rebound-sleep following sleep-deprivation, suggesting impairment in the elusive mechanisms underlying the homeostatic regulation of quiescent behavior (Koh et al 2008). Here we show that a *sleepless* orthologue is significantly down-regulated around the time of molt-sleep onset. In the previous chapter, results from quiescence-deprivation experiments suggest that quiescence-rebound is robust during the mid-intermolt feeding period, but is non-existent during the mid-molting period. This data suggests the possibility that the regulation of ion-channel function via ion channel accessory proteins may contribute to this change in the homeostatic regulation of *M. sexta* larval quiescent behavior.

Calcium channels

Forward genetic screens have not revealed involvement of calcium channels in the regulation of fly sleep and arousal states, but reverse genetics approaches have shown the importance of these channels in mammalian arousal state (Crocker & Sehgal 2010). Here, we show differential-expression of two putative proteins with voltage-gated calcium channel activity, as well as a putative alpha(2)-delta accessory subunit. Voltage-gated calcium channels are composed of a pore-forming alpha(1) subunit, the function of which can be modified by alpha(2)-delta, beta and gamma accessory subunits. Genes BGIBMGA007008 and BGIBMGA013345 code for two uncharacterized proteins that are

described by BLAST2GO as having calcium channel activity. Since expression levels of these genes do not change significantly at -12, -6 or HCS, it is unlikely that they play a role in induction of the molt-sleep; but there may be a possible involvement of these channels in the regulation of late-molting and/or early intermolt behavior.

Gene BGIBMGA003640 is described by BLAST2GO as coding for an L-type calcium channel, but reciprocal BLASTing indicates that this gene is more likely to be the *B. mori* orthologue to the alpha(2)-delta accessory subunit *straightjacket* in *Drosophila*. Alpha(2)-delta accessory subunits are known to influence alpha(1) channel conductance and kinetics. In *Drosophila*, Straightjacket enhances pre-synaptic calcium-dependant neurotransmitter release, and facilitates localization of calcium channels to the pre-synaptic membrane (Ly et al 2008). Fly larvae mutant for *straightjacket* show severely impaired neuromuscular transmission (Ly et al 2008). Centrally, this accessory subunit is expressed in GABA inhibitory interneurons, where it is also localized to synaptic terminals (Ly et al 2008). Our data indicates that this putative alpha(2)-delta subunit is up-regulated in *M. sexta* brains at -6 hrs and at the time of HCS. If this subunit is also localized to GABAergic inter-neurons, this could lead to an enhancement of inhibitory interneuron transmission during the molt-sleep period.

Transient receptor potential (TRP) channels

TRP channels are expressed in central and peripheral nervous systems of vertebrates and invertebrates and are highly-conserved non-selective cation channels that respond to a variety of stimuli, including (but not limited to) taste, mechanical stress,

vibration, temperature changes, and alterations in osmolarity and of course photo stimulation. A role for TRP channels in the modulation of sleep-wake type arousal states in insects has not yet been found. In mammals, TRP channels can influence arousal state through the depolarization of specific arousal-related circuitries. For example, TRP currents drive spontaneous activity in arousal-promoting Hypocretin/Orexin neurons during the waking state (Cvetkovic-Lopes et al 2010). The effects of central TRP channel expression are circuit-dependent. Whereas TRP channel expression in Hypocretin/Orexin neurons leads to tonic excitation of target arousal-promoting centers, TRP channel expression in GABAergic projection neurons of the substantia nigra lead to tonic inhibition of target cells (Zhou et al 2008).

Our data show differential expression of 3 putative TRP channel genes—genes BGIBMGA001166, BGIBMGA002131, and BGIBMGA014186. Two of these genes are differentially-expressed during the molting period. Gene BGIBMGA001166 is significantly up-regulated at the time of HCS, and is described by BLAST2GO as the ortholog of the *Drosophila* TRP channel gene *painless*. Painless is well known for its role in sensing noxious temperature and noxious mechanical stress in both larvae and adults (Tracey et al 2003). In the fly CNS, *painless* in also expressed in GABAergic and cholinergic neurons, where it is thought to play a role in regulation of female sexual receptivity (Sakai et al 2009). Also at the time of HCS, gene BGIBMGA014186 is down-regulated. This gene was identified by BLAST2GO as an ortholog of the *Drosophila* TRP channel gene *pyrexia* (but the identity of this gene could not be verified using reciprocal blast). In adult flies, Pyrexia is known as a high temperature-sensitive

channel that is distributed ubiquitously throughout the neurites of CNS neurons in which it is expressed, and it has been shown to play a role in protection from thermal stress (Lee et al 2005). A role for TRP channels in molting behavior and physiology awaits further investigation.

Cyclic-nucleotide-gated channels

Lastly we mention the up-regulation of gene BGIBMGA000577. This gene (as well as the *Drosophila* ortholog), is described as a cyclic-nucleotide-gated cation channel. GO annotation assigned to this gene the biological process *cGMP-mediated signaling.* Up-regulation of this gene is correlated with peak expression levels of *cluster 4* genes, which were previously shown to be enriched in cGMP-related processes. The up-regulation of this gene only at +18 hrs suggests that this channel might play a role in late molting processes, such as ecdysis behavior. In the CNS of *M. sexta* and in other insects, ecdysis is preceded by an elevation of cGMP in a small network of peptidergic cells in the ventral nerve cord, which release peptides necessary for a stereotyped sequence of events that lead to the shedding of the cuticle (Ewer & Truman 1997). cGMP is thought to increase excitability of these cells through activation of a cGMP-gated cation channel, the identity of which remains unknown (Gammie & Truman 1997). The role of cGMP-signaling during the late molt has focused largely on networks of the ventral nerve cord, but the up-regulation of this gene here suggests that cGMP-signaling in the brain might also play a role in late-molt physiology or behavior.

Epidermal growth factor (EGF) and insulin signaling. BLAST2GO annotations were screened for differentially expressed genes annotated with descriptions and GO terminologies associating them with EGF or insulin signaling, and nine genes were identified (Figure 3-30AB).

Epidermal growth factor signaling

EGF signaling is sleep-promoting in both flies and mammals. In *Drosophila,* there is one identified EGF receptor (EGFR), and four known receptor ligands. Ligand activation requires processing by a transmembrane cargo receptor and an integral membrane serine protease, and this is followed by secretion of ligands and activation of EGFR (Shilo 2003; 2005). EGFR is a receptor tyrosine kinase that can activate the RAS/RAF/MEK/MAPK pathway, which can result in the modification of protein function (including ion channel function), and possibly gene transcription (Schrader et al 2006; Shilo 2005).

In adult *Drosophila,* gain-of-function mutations in the EGFR pathway lead to excessive sleep, whereas loss-of-function mutations result in sleep loss. These sleep-related effects have been localized to EGF-expressing cells of the pars intercerebralis that project to the tritocerebrum (Foltenyi et al 2007). Interestingly, in adult and larval *C. elegans*, EGF pathway gain-of-function mutants show a *reversible* state of decreased feeding and locomotion that is dependent upon synaptic transmission, and EGF-pathway loss-of-function mutations result in increased locomotion and feeding behaviors during

the molting period when animals would normally display a sleep-like behavior (Van Buskirk & Sternberg 2007).

In a screen of our annotations for differentially-expressed genes related to EGF signaling, we identified 2 genes potentially related to the processing of ligand, and 2 genes related to receptor activity. Gene BGIBMGA010766 was identified as an ortholog of *star*, which encodes a protein that facilitates translocation of EGFR ligands from the ER to the golgi apparatus, and gene BGIBMGA002855 was identified as an ortholog to a *rhomboid* gene, which encodes one of a family of intramembrane proteases necessary for the cleavage of the ligand into its active form. The EGF pathway is thought to be spatially and temporally regulated largely through the regulation of ligand processing by Star and Rhomboid (Shilo 2003; 2005). It seems that Rhomboid, but not Star, is the rate limiting step in the process, and Rhomboid expression is dynamic and precedes the activation of EGF pathways (Shilo 2005). The Rhomboid protein here was identified as Rhomboid-6 using reciprocal BLAST in FlyBase. In the fly, 7 members of the Rhomboid family have been identified. Although Rhomboid-6 has not been shown yet to cleave EGF ligands, 4 of the members that were studied do show this activity, so it is possible that Rhomboid-6 also has a similar function (Urban et al 2002). Most cases of EGFR signaling can be described as "bursting," which involves temporary elevations of the expression of *rhomboid* in individual cells/cell types that then leads to activation of the ligand (Shilo 2005). Our data shows that Rhomboid expression is detectable at -12 hrs, is significantly elevated at HCS, and is undetectable at any other time-point. In contrast, *star* is significantly down-regulated across most of the stages, including the

early inter-molt stage. The down-regulation of *star* would not affect ligand that has already translocated to the Golgi, so it is possible that the surge of *rhomboid* expression at the time of HCS could have a profound effect on EGFR signaling. Also up-regulated at -6 hrs and at the time of HCS are genes BGIBMGA004550 and BGIBMGA004551, which are both identified as ecoding putative epidermal growth factor receptor kinase substrate 8, which among other functions, has been shown in mammals to enhance EGFR signaling (Xu et al 2009).

Insulin and insulin-like growth factor signaling

A recent study has identified brain circuitry in adult flies that underlies the wake-promoting effects of octopamine (Crocker et al 2010). The target cells were identified as insulin-secreting neurons of the pars intercerebralis that express octopamine receptors, the activation of which leads to a reduction in an outward potassium current (Crocker et al 2010). The role of insulin and insulin-like growth factor signaling in the modulation of sleep-wake arousal during larval stages has not yet been investigated, but it is known that insulin signaling plays an important role in the control of postembryonic growth rate. Insulin signaling both stimulates and is inhibited by ecdysone production, and interactions between these two hormonal systems determine the animal's final body size (Clemmons et al 2010; Orme & Leevers 2005).

In *Drosophila*, there are 7 insulin-like peptides that activate receptor tyrosine kinase cascades that can lead to altered sugar metabolism, growth and proliferation (Clemmons et al 2010). In the larval nervous system, these peptides are expressed in

medial neurosecretory cells that project to the lateral protocerebrum, suboesophageal ganglion, ring gland and secretion sites on the heart (Clemmons et al 2010). During larval development, elevated ecdysteroid levels antagonize insulin signaling by way of their actions on the fat body, leading to an ecdysteroid-dependent inhibition in growth (Colombani et al 2005). Could the interplay between ecdysone and insulin signaling also lead to a concomitant modulation of sleep-wake-type arousal during the molting period? We screened our set of annotated, differentially-expressed genes for descriptions and GO terminology related to insulin and insulin-like growth factor signaling, and identified 3 up-regulated genes and 1 down-regulated gene.

Only 1 gene encoding an insulin-like peptide was found to be differentially-expressed during the molting period. Gene BGIBMGA011926 was identified as the *bombyxin* precursor, and this gene is significantly up-regulated at the time of HCS. The *B. mori* genome codes for over 30 Bombyxin-like peptides, but the functions of all individual peptides are not yet characterized. Interestingly, in one study- in contrast to mammalian insulin- injections of bombyxin led to promotion of the consumption of glycogen stores (Satake et al 1997). Expression, synthesis and release of a peptide that might trigger use of food reserves during a time of prolonged starvation would be beneficial to the molting larvae. Up-regulation of gene BGIBMGA007045 and down-regulation of BGIBMGA011826 at the time of head capsule slippage suggests that different pathways downstream of insulin-receptor signaling might be favored during the molting period. Both are described as encoding proteins involved in the insulin receptor tyrosine kinase cascade.

Gene BGIBMGA008174 is described as encoding an insulin-related peptide-binding protein, and reciprocal BLAST using FlyBase confirms that this gene is an ortholog of the *Drosophila ecdysone-inducible gene L2* (a.k.a., *Imp-L2*). This gene shows significant up-regulation at -12 hrs, -6 hrs, time of HCS, and +18 hours, suggesting that up-regulation is specific and important to the molting period. In mammals, IGF- binding proteins act as regulators of IGF activity. In *Drosophila*, Imp-L2 is a negative regulator of IGF-signaling (Alic & Partridge 2008). It makes sense that inhibition of growth-promoting pathways occurs during the ~30 hr molt-sleep period. Whether insulin signaling also plays a role in the modulation of larval arousal state, or if the negative regulation of this system is required for the maintenance of molting quiescence awaits further investigation.

Differentially expressed genes in the brains of larval-stage *M. sexta* and pupal-stage *B. mori* — a comparison.

Recently, the brain transcriptome of pupal-stage *B. mori* was examined using a microarray-based approach (Gan et al 2011). In this study, the transcriptome was examined at stages V7, P1, P3, and P5, which allowed for the identification of transcripts present during the rise and fall of the pupal ecdysteroid surge. Using hierarchical clustering methods, the authors identified 1,175 genes that were variably expressed (with fold-cutoff values at >4 or <0.25) during at least one of the sampled developmental stages (Gan et al 2011). We were interested in comparing this set of differentially-expressed genes to our own set, as overlap would provide insight into conservation of function.

Microarray probe ID's that corresponded to the 1,175 variably-expressed genes in the above-mentioned study were matched to SilkDB gene IDs, and our set of significantly differentially-expressed genes were screened for the presence of these genes. A total of 231 genes are common to the two sets of differentially-expressed genes. Within this set of genes, 161 genes had been annotated by BLAST2GO. We used this set to test for enriched GO terminologies. 10 enriched GO terms were identified (Figure 3-31). As with the enrichment analyses that were performed in previous sections, enriched GO terms were dominated by BP, MF and CC terminologies associated with cuticle-related metabolic processes. For example, 25 sequences alone were annotated with the description "cuticle protein". This list of overlapping genes should prove useful for future investigations into the processes of tracheal cuticle synthesis and degradation.

We screened the set of overlapping genes for descriptions and GO terminologies associated with arousal-related systems (as described in previous sections), and found genes that encode the neuropeptide Allatotropin (BGIBMGA011850), an insulin-related peptide binding protein (BGIBMGA008174), and the enzyme Aromatic Amino Acid Decarboxylase (*ddc gene*) (BGIBMGA002958). That there were so few overlapping genes that could be assigned to our arousal-related categories is likely due to the high fold-change cutoff used in the *B. mori* study; many of our arousal-related genes showed fold-changes below the cut-off used in their study. Also, many arousal-related genes, such as neuropeptide receptors and enzymes involved in the synthesis of neurotransmitters, are expressed only in a few cells, and so these transcripts in brain tissue may be present at relatively low levels (compared to cuticular proteins, for

example). The possible superiority of Illumina sequencing over microarray in terms of sensitivity may have led to the identification of more of these arousal-related genes. Future across-species and across-development studies that target low-expressed genes should benefit greatly from this new technology.

Summary and Conclusion

This is the first profile of the *M. sexta* brain transcriptome. Illumina sequencing (RNA-seq) was used to sequence mRNA in the brains of inter-molt and molting larvae. To identify those sequences, a novel mapping method was employed that involved the alignment of translated reads onto the proteome of *B. mori*—the most closely related species for which a genome has been sequenced. Method comparisons using available *M. sexta* sequences showed a strong correlation between fold-change and annotations. This method should prove useful to other investigators who are researching organisms for which no genome has been sequenced, but who would like to take advantage of the new high-throughput sequencing technology.

Across the 7 sampled 4th instar developmental time points, a total of 10,664 *B. mori* protein-coding genes were mapped by at least one *M. sexta* read. As brains were taken from stages that spanned the intermolt and molting period, this set of genes is fairly representative of the brain transcriptome of developing *M. sexta* larvae. When compared to levels of transcription occurring during the mid-intermolt feeding stage, 1,844 genes (~17%) were identified as differentially-expressed during at least one developmental stage. Enrichment analysis of the sets of both up- and down-regulated genes at each

stage indicate that terms associated with cuticle synthesis and degradation predominate at all stages. Also, during time-points correlated with the ecdysteroid surge, terms associated with transcription regulation are highly enriched. When across-development patterns of expression were analyzed, genes were grouped into 11 unique clusters, and 4 of these clusters showed enrichment of GO terminologies. Clusters were enriched in functions related to detoxification and JH metabolism (C0), carbohydrate and protein metabolism (C2), targeting of secretory proteins, protein catabolism and cell division (C3), and cGMP metabolic process (C4).

For identification of arousal-related systems underlying the induction and maintenance of the molt-sleep, enrichment and cluster analyses were not informative. We then manually searched the set of annotated, differentially-expressed genes for descriptions and GO terminologies associated with G-protein-coupled and neurotransmitter-gated ion channels, neurotransmitters and neuropeptides, ion channels and ion channel regulators, and epidermal growth factors and insulin signaling. Sets of up- and down-regulated genes were identified for each of the putative arousal-related categories. 27 putative receptors were identified. Several down-regulated receptors were identified as orthologs to receptors associated with modulation of feeding behavior in both insects and mammals. Among down- and up-regulated receptors, we identified several uncharacterized receptors, including a putative neurotransmitter-gated channel that is highly up-regulated in molting, but not feeding-stage larvae. 14 genes coding for proteins associated with neurotransmitter and neuropeptide systems were identified, and most of these coded for products involved in the DA metabolic pathway. 14 genes were

identified as coding for subunits of ion channels or ion channel regulating proteins. Many were related to K^+ channel functions, but we also identified genes that code for TRP and calcium channels. 9 genes coding for EGF- and insulin-related products were differentially-expressed during the molting period. Since EGF-signaling is a potent sleep-promoting agent in molting *C. elegans* larvae, it was particularly interesting to see the up-regulation of a rhomboid protein around the time of the early molt-sleep, as this might imply conservation of larval sleep-promoting function for this system across phyla (Van Buskirk & Sternberg 2007).

In conclusion, there were many putative arousal-related genes shown to be differentially-expressed in the brain just prior to and during the molt-sleep period of *M. sexta*. Some of these genes code for products that are already well known for their roles as modulators of arousal-state in adult insects, and their presence and differential-expression in the brains of larvae suggests a conservation of these functions across developmental stages. Also, we have provided gene IDs and expression profiles of many currently uncharacterized, putative arousal-related genes. This entire list of genes, along with information as to the timing of expression in relation to behavioral changes and hormone profiles, should aid investigations into both neural and neuroendocrine mechanisms underlying modulation of arousal state in insects.

References

Agosto J, Choi JC, Parisky KM, Stilwell G, Rosbash M, Griffith LC. 2008. Modulation of GABAA receptor desensitization uncouples sleep onset and maintenance in Drosophila. *Nat Neurosci* 11:354-9

Ai J, Yu Q, Cheng T, Dai F, Zhang X, et al. 2010. Characterization of multiple CYP9A genes in the silkworm, Bombyx mori. *Mol Biol Rep* 37:1657-64

Alic N, Partridge L. 2008. Stage debut for the elusive Drosophila insulin-like growth factor binding protein. *J Biol* 7:18

Altschul SF, Gish W, Miller W, Myers EW, Lipman DJ. 1990. Basic local alignment search tool. *J Mol Biol* 215:403-10

Anaka M, MacDonald CD, Barkova E, Simon K, Rostom R, et al. 2008. The white gene of Drosophila melanogaster encodes a protein with a role in courtship behavior. *J Neurogenet* 22:243-76

Anders S, Huber W. 2010. Differential expression analysis for sequence count data. *Genome Biol* 11:R106

Andersen SO. 2010. Insect cuticular sclerotization: a review. *Insect Biochem Mol Biol* 40:166-78

Andretic R, Kim YC, Jones FS, Han KA, Greenspan RJ. 2008. Drosophila D1 dopamine receptor mediates caffeine-induced arousal. *Proc Natl Acad Sci U S A* 105:20392-7

Asahina M, Jindra M, Riddiford LM. 1997. Developmental expression of Ultraspiracle proteins in the epidermis of the tobacco hornworm, Manduca sexta, during larval life and the onset of metamorphosis. *Dev Genes Evol* 207:381-8

Ashburner M. 1973. Sequential gene activation by ecdysone in polytene chromosomes of Drosophila melanogaster. I. Dependence upon ecdysone concentration. *Dev Biol* 35:47-61

Ashburner M. 1974. Sequential gene activation by ecdysone in polytene chromosomes of Drosophila melanogaster. II. The effects of inhibitors of protein synthesis. *Dev Biol* 39:141-57

Baker KD, Shewchuk LM, Kozlova T, Makishima M, Hassell A, et al. 2003. The Drosophila orphan nuclear receptor DHR38 mediates an atypical ecdysteroid signaling pathway. *Cell* 113:731-42

Bell RA, Joachim FG. 1976. Techniques for Rearing Laboratory Colonies of Tobacco Hornworms and Pink Bollworms Lepidoptera-Sphingidae-Gelechiidae. *Ann Entomol Soc Am* 69:365-73

Belvin MP, Zhou H, Yin JC. 1999. The Drosophila dCREB2 gene affects the circadian clock. *Neuron* 22:777-87

Bicker G. 2001. Sources and targets of nitric oxide signalling in insect nervous systems. *Cell Tissue Res* 303:137-46

Bidmon HJ, Granger NA, Cherbas P, Maroy P, Stumpf WE. 1991. Ecdysteroid receptors in the central nervous system of Manduca sexta: their changes in distribution and quantity during larval-pupal development. *J Comp Neurol* 310:337-55

Bluthgen N, Brand K, Cajavec B, Swat M, Herzel H, Beule D. 2005. Biological profiling of gene groups utilizing Gene Ontology. *Genome Inform* 16:106-15

Borycz J, Borycz JA, Kubow A, Lloyd V, Meinertzhagen IA. 2008. Drosophila ABC transporter mutants white, brown and scarlet have altered contents and distribution of biogenic amines in the brain. *J Exp Biol* 211:3454-66

Boulanger A, Clouet-Redt C, Farge M, Flandre A, Guignard T, et al. 2011. ftz-f1 and Hr39 opposing roles on EcR expression during Drosophila mushroom body neuron remodeling. *Nat Neurosci* 14:37-44

Brennan CA, Li TR, Bender M, Hsiung F, Moses K. 2001. Broad-complex, but not ecdysone receptor, is required for progression of the morphogenetic furrow in the Drosophila eye. *Development* 128:1-11

Bullerjahn A, Mentel T, Pfluger HJ, Stevenson PA. 2006. Nitric oxide: a co-modulator of efferent peptidergic neurosecretory cells including a unique octopaminergic neurone innervating locust heart. *Cell Tissue Res* 325:345-60

Bushey D, Huber R, Tononi G, Cirelli C. 2007. Drosophila Hyperkinetic mutants have reduced sleep and impaired memory. *J Neurosci* 27:5384-93

Casas J, Harshman LG, Hammock BD. 1991. Epoxide Hydrolase Activity on Juvenile Hormone in Manduca-Sexta. *Insect Biochem* 21:17-26

Champlin DT, Truman JW. 2000. Ecdysteroid coordinates optic lobe neurogenesis via a nitric oxide signaling pathway. *Development* 127:3543-51

Chemelli RM, Willie JT, Sinton CM, Elmquist JK, Scammell T, et al. 1999. Narcolepsy in orexin knockout mice: Molecular genetics of sleep regulation. *Cell* 98:437-51

Chung BY, Kilman VL, Keath JR, Pitman JL, Allada R. 2009. The GABA(A) receptor RDL acts in peptidergic PDF neurons to promote sleep in Drosophila. *Curr Biol* 19:386-90

Cirelli C. 2005. A molecular window on sleep: changes in gene expression between sleep and wakefulness. *Neuroscientist* 11:63-74

Cirelli C. 2009. The genetic and molecular regulation of sleep: from fruit flies to humans. *Nat Rev Neurosci* 10:549-60

Cirelli C, Bushey D. 2008. Sleep and wakefulness in Drosophila melanogaster. *Ann N Y Acad Sci* 1129:323-9

Cirelli C, Bushey D, Hill S, Huber R, Kreber R, et al. 2005a. Reduced sleep in Drosophila Shaker mutants. *Nature* 434:1087-92

Cirelli C, Gutierrez CM, Tononi G. 2004. Extensive and divergent effects of sleep and wakefulness on brain gene expression. *Neuron* 41:35-43

Cirelli C, LaVaute TM, Tononi G. 2005b. Sleep and wakefulness modulate gene expression in Drosophila. *J Neurochem* 94:1411-9

Clemmons D, Robinson I, Christen Y. 2010. IGFs: Local Repair and Survival Factors Throughout Life Span.

Clever U. 1964. Actinomycin and Puromycin: Effects on Sequential Gene Activation by Ecdysone. *Science* 146:794-5

Clever U, Karlson P. 1960. Induction of puff alterations in the salivary gland chromosomes of Chironomus tentans by Ecdysorie. *Exptl Cell Res* 20:623-6

Colombani J, Bianchini L, Layalle S, Pondeville E, Dauphin-Villemant C, et al. 2005. Antagonistic actions of ecdysone and insulins determine final size in Drosophila. *Science* 310:667-70

Conesa A, Gotz S, Garcia-Gomez JM, Terol J, Talon M, Robles M. 2005. Blast2GO: a universal tool for annotation, visualization and analysis in functional genomics research. *Bioinformatics* 21:3674-6

Copenhaver PF, Truman JW. 1986. Metamorphosis of the cerebral neuroendocrine system in the moth Manduca sexta. *J Comp Neurol* 249:186-204

Crocker A, Sehgal A. 2010. Genetic analysis of sleep. *Gene Dev* 24:1220-35

Crocker A, Shahidullah M, Levitan IB, Sehgal A. 2010. Identification of a neural circuit that underlies the effects of octopamine on sleep:wake behavior. *Neuron* 65:670-81

Cvetkovic-Lopes V, Eggermann E, Uschakov A, Grivel J, Bayer L, et al. 2010. Rat hypocretin/orexin neurons are maintained in a depolarized state by TRPC channels. *PLoS One* 5:e15673

Dai L, Dewey EM, Zitnan D, Luo CW, Honegger HW, Adams ME. 2008. Identification, developmental expression, and functions of bursicon in the tobacco hawkmoth, Manduca sexta. *J Comp Neurol* 506:759-74

de Lecea L, Kilduff TS, Peyron C, Gao XB, Foye PE, et al. 1998. The hypocretins: Hypothalamus-specific peptides with neuroexcitatory activity. *Proceedings of the National Academy of Sciences of the United States of America* 95:322-7

Dominick OS, Truman JW. 1986. The physiology of wandering behaviour in Manduca sexta. IV. Hormonal induction of wandering behaviour from the isolated nervous system. *J Exp Biol* 121:133-51

Draper I, Kurshan PT, McBride E, Jackson FR, Kopin AS. 2007. Locomotor activity is regulated by D2-like receptors in Drosophila: an anatomic and functional analysis. *Dev Neurobiol* 67:378-93

Duan J, Li R, Cheng D, Fan W, Zha X, et al. 2010. SilkDB v2.0: a platform for silkworm (Bombyx mori) genome biology. *Nucleic Acids Res* 38:D453-6

Ernst J, Bar-Joseph Z. 2006. STEM: a tool for the analysis of short time series gene expression data. *BMC Bioinformatics* 7:191

Ernst J, Nau GJ, Bar-Joseph Z. 2005. Clustering short time series gene expression data. *Bioinformatics* 21 Suppl 1:i159-68

Ewer J. 2005. How the ecdysozoan changed its coat. *Plos Biol* 3:1696-9

Ewer J, Truman JW. 1997. Invariant association of ecdysis with increases in cyclic 3',5'-guanosine monophosphate immunoreactivity in a small network of peptidergic neurons in the hornworm, Manduca sexta. *J Comp Physiol A* 181:319-30

Fain MJ, Riddiford LM. 1975. Juvenile hormone titers in the hemolymph during late larval development of the tobacco hornworm, Manduca sexta (L.). *Biol Bull* 149:506-21

Fan Y, Sun P, Wang Y, He XB, Deng XY, et al. 2010. The G protein-coupled receptors in the silkworm, Bombyx mori. *Insect Biochemistry and Molecular Biology* 40:581-91

Feyereisen R. 1995. Molecular biology of insecticide resistance. *Toxicol Lett* 82-83:83-90

Foltenyi K, Greenspan RJ, Newport JW. 2007. Activation of EGFR and ERK by rhomboid signaling regulates the consolidation and maintenance of sleep in Drosophila. *Nat Neurosci* 10:1160-7

Gammie SC, Truman JW. 1997. An endogenous elevation of cGMP increases the excitability of identified insect neurosecretory cells. *J Comp Physiol A* 180:329-37

Gan L, Liu X, Xiang Z, He N. 2011. Microarray-based gene expression profiles of silkworm brains. *BMC Neurosci* 12:8

Gotz S, Garcia-Gomez JM, Terol J, Williams TD, Nagaraj SH, et al. 2008. High-throughput functional annotation and data mining with the Blast2GO suite. *Nucleic Acids Res* 36:3420-35

Hansen KK, Hauser F, Williamson M, Weber SB, Grimmelikhuijzen CJ. 2011. The Drosophila genes CG14593 and CG30106 code for G-protein-coupled receptors specifically activated by the neuropeptides CCHamide-1 and CCHamide-2. *Biochem Biophys Res Commun* 404:184-9

Hayaishi O, Urade Y. 2002. Prostaglandin D2 in sleep-wake regulation: recent progress and perspectives. *Neuroscientist* 8:12-5

Hendricks JC, Finn SM, Panckeri KA, Chavkin J, Williams JA, et al. 2000. Rest in Drosophila is a sleep-like state. *Neuron* 25:129-38

Hendricks JC, Williams JA, Panckeri K, Kirk D, Tello M, et al. 2001. A non-circadian role for cAMP signaling and CREB activity in Drosophila rest homeostasis. *Nat Neurosci* 4:1108-15

Hiruma K, Riddiford LM. 2001. Regulation of transcription factors MHR4 and betaFTZ-F1 by 20-hydroxyecdysone during a larval molt in the tobacco hornworm, Manduca sexta. *Dev Biol* 232:265-74

Hiruma K, Riddiford LM. 2009. The molecular mechanisms of cuticular melanization: the ecdysone cascade leading to dopa decarboxylase expression in Manduca sexta. *Insect Biochem Mol Biol* 39:245-53

Hopkins TL, Morgan TD, Kramer KJ. 1984. Catecholamines in Hemolymph and Cuticle during Larval, Pupal and Adult Development of Manduca-Sexta (L). *Insect Biochem* 14:533-40

Hsouna A, Lawal HO, Izevbaye I, Hsu T, O'Donnell JM. 2007. Drosophila dopamine synthesis pathway genes regulate tracheal morphogenesis. *Dev Biol* 308:30-43

Huang Y, Crim JW, Nuss AB, Brown MR. 2010. Neuropeptide F and the corn earworm, Helicoverpa zea: A midgut peptide revisited. *Peptides*

Huang ZL, Sato Y, Mochizuki T, Okada T, Qu WM, et al. 2003. Prostaglandin E2 activates the histaminergic system via the EP4 receptor to induce wakefulness in rats. *J Neurosci* 23:5975-83

Ishimoto H, Kitamoto T. 2010. The steroid molting hormone Ecdysone regulates sleep in adult Drosophila melanogaster. *Genetics* 185:269-81

Ishimoto H, Sakai T, Kitamoto T. 2009. Ecdysone signaling regulates the formation of long-term courtship memory in adult Drosophila melanogaster. *Proc Natl Acad Sci U S A* 106:6381-6

Jones G, Sharp PA. 1997. Ultraspiracle: an invertebrate nuclear receptor for juvenile hormones. *Proc Natl Acad Sci U S A* 94:13499-503

Kim YJ, Spalovska-Valachova I, Cho KH, Zitnanova I, Park Y, et al. 2004. Corazonin receptor signaling in ecdysis initiation. *Proc Natl Acad Sci U S A* 101:6704-9

Kim YJ, Zitnan D, Cho KH, Schooley DA, Mizoguchi A, Adams ME. 2006a. Central peptidergic ensembles associated with organization of an innate behavior. *Proc Natl Acad Sci U S A* 103:14211-6

Kim YJ, Zitnan D, Galizia CG, Cho KH, Adams ME. 2006b. A command chemical triggers an innate behavior by sequential activation of multiple peptidergic ensembles. *Curr Biol* 16:1395-407

Kinch G, Hoffman KL, Rodrigues EM, Zee MC, Weeks JC. 2003. Steroid-triggered programmed cell death of a motoneuron is autophagic and involves structural changes in mitochondria. *J Comp Neurol* 457:384-403

Koh K, Joiner WJ, Wu MN, Yue Z, Smith CJ, Sehgal A. 2008. Identification of SLEEPLESS, a sleep-promoting factor. *Science* 321:372-6

Krishnakumar S, Burton D, Rasco J, Chen X, O'Donnell J. 2000. Functional interactions between GTP cyclohydrolase I and tyrosine hydroxylase in Drosophila. *J Neurogenet* 14:1-23

Kume K, Kume S, Park SK, Hirsh J, Jackson FR. 2005. Dopamine is a regulator of arousal in the fruit fly. *J Neurosci* 25:7377-84

Langelan RE, Fisher JE, Hiruma K, Palli SR, Riddiford LM. 2000. Patterns of MHR3 expression in the epidermis during a larval molt of the tobacco hornworm Manduca sexta. *Dev Biol* 227:481-94

Lebestky T, Chang JS, Dankert H, Zelnik L, Kim YC, et al. 2009. Two different forms of arousal in Drosophila are oppositely regulated by the dopamine D1 receptor ortholog DopR via distinct neural circuits. *Neuron* 64:522-36

Lee Y, Lee J, Bang S, Hyun S, Kang J, et al. 2005. Pyrexia is a new thermal transient receptor potential channel endowing tolerance to high temperatures in Drosophila melanogaster. *Nat Genet* 37:305-10

Li B, Xia Q, Lu C, Zhou Z, Xiang Z. 2005. Analysis of cytochrome P450 genes in silkworm genome (Bombyx mori). *Sci China C Life Sci* 48:414-8

Luo CW, Dewey EM, Sudo S, Ewer J, Hsu SY, et al. 2005. Bursicon, the insect cuticle-hardening hormone, is a heterodimeric cystine knot protein that activates G protein-coupled receptor LGR2. *Proc Natl Acad Sci U S A* 102:2820-5

Ly CV, Yao CK, Verstreken P, Ohyama T, Bellen HJ. 2008. straightjacket is required for the synaptic stabilization of cacophony, a voltage-gated calcium channel alpha1 subunit. *J Cell Biol* 181:157-70

Mesce KA. 2002. Metamodulation of the biogenic amines: second-order modulation by steroid hormones and amine cocktails. *Brain Behav Evol* 60:339-49

Mesce KA, DeLorme AW, Brelje TC, Klukas KA. 2001. Dopamine-synthesizing neurons include the putative H-cell homologue in the moth Manduca sexta. *J Comp Neurol* 430:501-17

Moussian B. 2010. Recent advances in understanding mechanisms of insect cuticle differentiation. *Insect Biochem Mol Biol* 40:363-75

Nakagawa Y, Henrich VC. 2009. Arthropod nuclear receptors and their role in molting. *FEBS J* 276:6128-57

Nighorn A, Byrnes KA, Morton DB. 1999. Identification and characterization of a novel beta subunit of soluble guanylyl cyclase that is active in the absence of a second subunit and is relatively insensitive to nitric oxide. *J Biol Chem* 274:2525-31

Nighorn A, Gibson NJ, Rivers DM, Hildebrand JG, Morton DB. 1998. The nitric oxide-cGMP pathway may mediate communication between sensory afferents and projection neurons in the antennal lobe of Manduca sexta. *J Neurosci* 18:7244-55

Nijhout HF. 1994. *Insect hormones*. Princeton, N.J.: Princeton University Press. xi, 267 p. pp.

Noguchi H, Hayakawa Y. 1997. Role of dopamine at the onset of pupal diapause in the cabbage armyworm Mamestra brassicae. *FEBS Lett* 413:157-61

Noguchi H, Hayakawa Y. 2001. Dopamine is a key factor for the induction of egg diapause of the silkworm, Bombyx mori. *Eur J Biochem* 268:774-80

O'Reilly DR, Miller LK. 1989. A baculovirus blocks insect molting by producing ecdysteroid UDP-glucosyl transferase. *Science* 245:1110-2

Orme MH, Leevers SJ. 2005. Flies on steroids: the interplay between ecdysone and insulin signaling. *Cell Metab* 2:277-8

Ote M, Mita K, Kawasaki H, Seki M, Nohata J, et al. 2004. Microarray analysis of gene expression profiles in wing discs of Bombyx mori during pupal ecdysis. *Insect Biochem Mol Biol* 34:775-84

Palli SR, Hiruma K, Riddiford LM. 1992. An ecdysteroid-inducible Manduca gene similar to the Drosophila DHR3 gene, a member of the steroid hormone receptor superfamily. *Dev Biol* 150:306-18

Parisky KM, Agosto J, Pulver SR, Shang Y, Kuklin E, et al. 2008. PDF cells are a GABA-responsive wake-promoting component of the Drosophila sleep circuit. *Neuron* 60:672-82

Pauchet Y, Wilkinson P, Vogel H, Nelson DR, Reynolds SE, et al. 2010. Pyrosequencing the Manduca sexta larval midgut transcriptome: messages for digestion, detoxification and defence. *Insect Mol Biol* 19:61-75

Peabody NC, Diao F, Luan H, Wang H, Dewey EM, et al. 2008. Bursicon functions within the Drosophila CNS to modulate wing expansion behavior, hormone secretion, and cell death. *J Neurosci* 28:14379-91

Pereanu W, Spindler S, Cruz L, Hartenstein V. 2007. Tracheal development in the Drosophila brain is constrained by glial cells. *Dev Biol* 302:169-80

Pfaff DW, Phillips IM, Rubin RT. 2004. *Principles of hormone behavior relations*. Amsterdam ; Boston, MA: Elsevier Academic Press. xviii, 335 p. pp.

Pfaffl MW. 2001. A new mathematical model for relative quantification in real-time RT-PCR. *Nucleic Acids Res* 29:-

Qazi S, Trimmer BA. 1999. The role of nitric oxide in motoneuron spike activity and muscarinic-evoked changes in cGMP in the CNS of larval Manduca sexta. *J Comp Physiol A* 185:539-50

Roller L, Yamanaka N, Watanabe K, Daubnerova I, Zitnan D, et al. 2008a. The unique evolution of neuropeptide genes in the silkworm Bombyx mori. *Insect Biochem Mol Biol* 38:1147-57

Roller L, Yamanaka N, Watanabe K, Daubnerova I, Zitnan D, et al. 2008b. The unique evolution of neuropeptide genes in the silkworm Bombyx mori. *Insect Biochemistry and Molecular Biology* 38:1147-57

Ryerse JS, Locke M. 1978. Ecdysterone Mediated Cuticle Deposition and the Control of Growth in Insect Tracheae. *Journal of Insect Physiology* 24:541-50

Sakai T, Kasuya J, Kitamoto T, Aigaki T. 2009. The Drosophila TRPA channel, Painless, regulates sexual receptivity in virgin females. *Genes Brain Behav* 8:546-57

Sakurai T, Amemiya A, Ishii M, Matsuzaki I, Chemelli RM, et al. 1998. Orexins and orexin receptors: A family of hypothalamic neuropeptides and G protein-coupled receptors that regulate feeding behavior. *Cell* 92:573-85

Samuels RI, Reynolds SE. 1993a. Molting Fluid Enzymes of the Tobacco Hornworm, Manduca-Sexta - Inhibitory Effect of 20-Hydroxyecdysone on the Activity of the Cuticle Degrading Enzyme Mfp-1. *Journal of Insect Physiology* 39:633-7

Samuels RI, Reynolds SE. 1993b. Molting Fluid Enzymes of the Tobacco Hornworm, Manduca-Sexta - Timing of Proteolytic and Chitinolytic Activity in Relation to Pre-Ecdysial Development. *Arch Insect Biochem* 24:33-44

Satake S, Masumura M, Ishizaki H, Nagata K, Kataoka H, et al. 1997. Bombyxin, an insulin-related peptide of insects, reduces the major storage carbohydrates in the silkworm Bombyx mori. *Comp Biochem Physiol B Biochem Mol Biol* 118:349-57

Schrader LA, Birnbaum SG, Nadin BM, Ren Y, Bui D, et al. 2006. ERK/MAPK regulates the Kv4.2 potassium channel by direct phosphorylation of the pore-forming subunit. *Am J Physiol Cell Physiol* 290:C852-61

Schwarz TL, Tempel BL, Papazian DM, Jan YN, Jan LY. 1988. Multiple potassium-channel components are produced by alternative splicing at the Shaker locus in Drosophila. *Nature* 331:137-42

Seino A, Ogura T, Tsubota T, Shimomura M, Nakakura T, et al. 2010. Characterization of Juvenile Hormone Epoxide Hydrolase and Related Genes in the Larval Development of the Silkworm Bombyx mori. *Bioscience Biotechnology and Biochemistry* 74:1421-9

Shaw PJ, Cirelli C, Greenspan RJ, Tononi G. 2000. Correlates of sleep and waking in Drosophila melanogaster. *Science* 287:1834-7

Shilo BZ. 2003. Signaling by the Drosophila epidermal growth factor receptor pathway during development. *Exp Cell Res* 284:140-9

Shilo BZ. 2005. Regulating the dynamics of EGF receptor signaling in space and time. *Development* 132:4017-27

Sloley BD. 2004. Metabolism of monoamines in invertebrates: the relative importance of monoamine oxidase in different phyla. *Neurotoxicology* 25:175-83

Srivastava DP, Yu EJ, Kennedy K, Chatwin H, Reale V, et al. 2005. Rapid, nongenomic responses to ecdysteroids and catecholamines mediated by a novel Drosophila G-protein-coupled receptor. *J Neurosci* 25:6145-55

Stanley D. 2006. Prostaglandins and other eicosanoids in insects: Biological significance. *Annual Review of Entomology* 51:25-44

Stanley D, Miller J, Tunaz H. 2009. Eicosanoid Actions in Insect Immunity. *Journal of Innate Immunity* 1:282-90

Stathakis DG, Burton DY, McIvor WE, Krishnakumar S, Wright TR, O'Donnell JM. 1999. The catecholamines up (Catsup) protein of Drosophila melanogaster functions as a negative regulator of tyrosine hydroxylase activity. *Genetics* 153:361-82

Stevens JL, Snyder MJ, Koener JF, Feyereisen R. 2000. Inducible P450s of the CYP9 family from larval Manduca sexta midgut. *Insect Biochem Mol Biol* 30:559-68

Sutherland JD, Kozlova T, Tzertzinis G, Kafatos FC. 1995. Drosophila hormone receptor 38: a second partner for Drosophila USP suggests an unexpected role for nuclear receptors of the nerve growth factor-induced protein B type. *Proc Natl Acad Sci U S A* 92:7966-70

Tracey WD, Jr., Wilson RI, Laurent G, Benzer S. 2003. painless, a Drosophila gene essential for nociception. *Cell* 113:261-73

Trapnell C, Pachter L, Salzberg SL. 2009. TopHat: discovering splice junctions with RNA-Seq. *Bioinformatics* 25:1105-11

True JR. 2003. Insect melanism: The molecules matter. *Trends in Ecology & Evolution* 18:640-7

Truman JW, Talbot WS, Fahrbach SE, Hogness DS. 1994. Ecdysone receptor expression in the CNS correlates with stage-specific responses to ecdysteroids during Drosophila and Manduca development. *Development* 120:219-34

Urban S, Lee JR, Freeman M. 2002. A family of Rhomboid intramembrane proteases activates all Drosophila membrane-tethered EGF ligands. *EMBO J* 21:4277-86

Van Buskirk C, Sternberg PW. 2007. Epidermal growth factor signaling induces behavioral quiescence in Caenorhabditis elegans. *Nat Neurosci* 10:1300-7

Van Loy T, Vandersmissen HP, Poels J, Van Hiel MB, Verlinden H, Vanden Broeck J. 2010. Tachykinin-related peptides and their receptors in invertebrates: a current view. *Peptides* 31:520-4

Van Swinderen B, Andretic R. 2011. Dopamine in Drosophila: setting arousal thresholds in a miniature brain. *Proc Biol Sci*

Wang Z, Gerstein M, Snyder M. 2009. RNA-Seq: a revolutionary tool for transcriptomics. *Nat Rev Genet* 10:57-63

Winther AM, Acebes A, Ferrus A. 2006. Tachykinin-related peptides modulate odor perception and locomotor activity in Drosophila. *Mol Cell Neurosci* 31:399-406

Wittkopp PJ, True JR, Carroll SB. 2002. Reciprocal functions of the Drosophila yellow and ebony proteins in the development and evolution of pigment patterns. *Development* 129:1849-58

Wright TR. 1987. The genetics of biogenic amine metabolism, sclerotization, and melanization in Drosophila melanogaster. *Adv Genet* 24:127-222

Wu MN, Joiner WJ, Dean T, Yue Z, Smith CJ, et al. 2010. SLEEPLESS, a Ly-6/neurotoxin family member, regulates the levels, localization and activity of Shaker. *Nat Neurosci* 13:69-75

Wu Q, Wen T, Lee G, Park JH, Cai HN, Shen P. 2003. Developmental control of foraging and social behavior by the Drosophila neuropeptide Y-like system. *Neuron* 39:147-61

Wu Q, Zhao Z, Shen P. 2005. Regulation of aversion to noxious food by Drosophila neuropeptide Y- and insulin-like systems. *Nature Neuroscience* 8:1350-5

Xu J, Li M, Shen P. 2010. A G-Protein-Coupled Neuropeptide Y-Like Receptor Suppresses Behavioral and Sensory Response to Multiple Stressful Stimuli in Drosophila. *J Neurosci* 30:2504-12

Xu M, Shorts-Cary L, Knox AJ, Kleinsmidt-DeMasters B, Lillehei K, Wierman ME. 2009. Epidermal growth factor receptor pathway substrate 8 is overexpressed in human pituitary tumors: role in proliferation and survival. *Endocrinology* 150:2064-71

Yamada K, Wada E, Wada K. 2000. Bombesin-like peptides: studies on food intake and social behaviour with receptor knock-out mice. *Ann Med* 32:519-29

Zayas RM, Qazi S, Morton DB, Trimmer BA. 2000. Neurons involved in nitric oxide-mediated cGMP signaling in the tobacco hornworm, Manduca sexta. *J Comp Neurol* 419:422-38

Zayas RM, Qazi S, Morton DB, Trimmer BA. 2002. Nicotinic-acetylcholine receptors are functionally coupled to the nitric oxide/cGMP-pathway in insect neurons. *J Neurochem* 83:421-31

Zhou B, Hiruma K, Jindra M, Shinoda T, Segraves WA, et al. 1998. Regulation of the transcription factor E75 by 20-hydroxyecdysone and juvenile hormone in the epidermis of the tobacco hornworm, Manduca sexta, during larval molting and metamorphosis. *Dev Biol* 193:127-38

Zhou FW, Matta SG, Zhou FM. 2008. Constitutively active TRPC3 channels regulate basal ganglia output neurons. *J Neurosci* 28:473-82

Zitnan D, Kim YJ, Zitnanova I, Roller L, Adams ME. 2007. Complex steroid-peptide-receptor cascade controls insect ecdysis. *Gen Comp Endocrinol* 153:88-96

Zitnan D, Ross LS, Zitnanova I, Hermesman JL, Gill SS, Adams ME. 1999. Steroid induction of a peptide hormone gene leads to orchestration of a defined behavioral sequence. *Neuron* 23:523-35

Table 3-1. Illumina RNA-Seq libraries. Libraries were prepared from brains taken from 7 developmental stages of *M. sexta*. Shown is the size of each library in terms of bases sequenced, the total number of sequences (reads) in each library, and the number of reads from each library that mapped to a *B. mori* protein coding gene (SilkDB).

Table 3-1

Library (staged relative to HCS)	Size in gigabases (GB)	#Sequences /library	#Sequences mapped to B. mori	% mapped
HCS -48hrs	1.8GB	24452940	5767810	23.6
HCS -30hrs (reference)	1.9GB	25532383	8965709	35.1
HCS -18hrs	1.8GB	24398816	5888205	24.1
HCS -12hrs	1.9GB	25498543	7072724	27.7
HCS -6hrs	2.3GB	31050934	9074936	29.2
HCS (time of)	2.0GB	27230965	7834554	28.8
HCS +18hrs	1.7GB	22801779	5899376	25.9

Table 3-2. Quantitaive PCR (qPCR) gene list. Primers were designed from available *M. sexta* mRNA sequences obtained from the NBCI database. Shown are the gene names and NBCI accession numbers, primer sets and sizes (base pairs, bp) of the resulting amplicons. Also shown are the protein IDs of the best-matched (using blastx) *B. mori* proteins (SilkDB). QPCR and corresponding Illumina RNA-seq profiles are shown in Figure 3-15.

Table 3-2

	ID M. sexta (NCBI)	ID B. mori (silkDB)	Forward Primer (5'-3')	Reverse Primer (5'-3')	Amplicon (bp)
Ribosomal Protein L32	GU084281.1	N/A	ACTGGCGTAAACCGAGAG-GTAT	GCATCATAAGGATCTCCA-GTTCG	171
Actin (Non-Muscle)	AJ519536.1	N/A	GTATGGAAGCCAACGGTA-TTCACG	TGTCGAAGGAGCAAGAGCT-GTG	170
Chitinase	U02270.1	BGIBMGA010240	TCAGACAACTCACGGGAGCA	CGGGACCACTTCCACAGAGT	135
Dopa Decarboxylase	U03909.1	BGIBMGA003199	TCCTTGGTGCCAAATCTC-GTATG	TAAGTCCATTGCGAATGTC-CTCGT	237
Nitric Oxide Synthase	AF062749.1	BGIBMGA002938	CTGTAGAGGAACAGTTGGT-TGCGTTG	ACTCCCAATGTTAAGAAC-AGATGGCAC	183
betaFTZ-F1	AF288089.1	BGIBMGA000716	CGTGCCTCCTACAATAGTGCTT	AATCCCTAGCGGTTACTGACC	123
Corazonin Receptor	AY369029.1	BGIBMGA001531	ACGGAGGCAACAATACCACAT	GCTCGTCTATACATTTCTCTA-TTGGC	138
Putative Cuticle Protein	AF117584.1	BGIBMGA011729	TATGCGTCGCTCGTGTACTCT	CCAAGTTTACGTCCAGGGTG	136

Figure 3-2. Sequence similarity distribution. Similarity distribution of the top blastx hits obtained when 10,664 *B. mori* sequences mapped by Illumina reads during at least 1 developmental stage were searched against the non-redundant (nr) NCBI protein database.

Figure 3-2

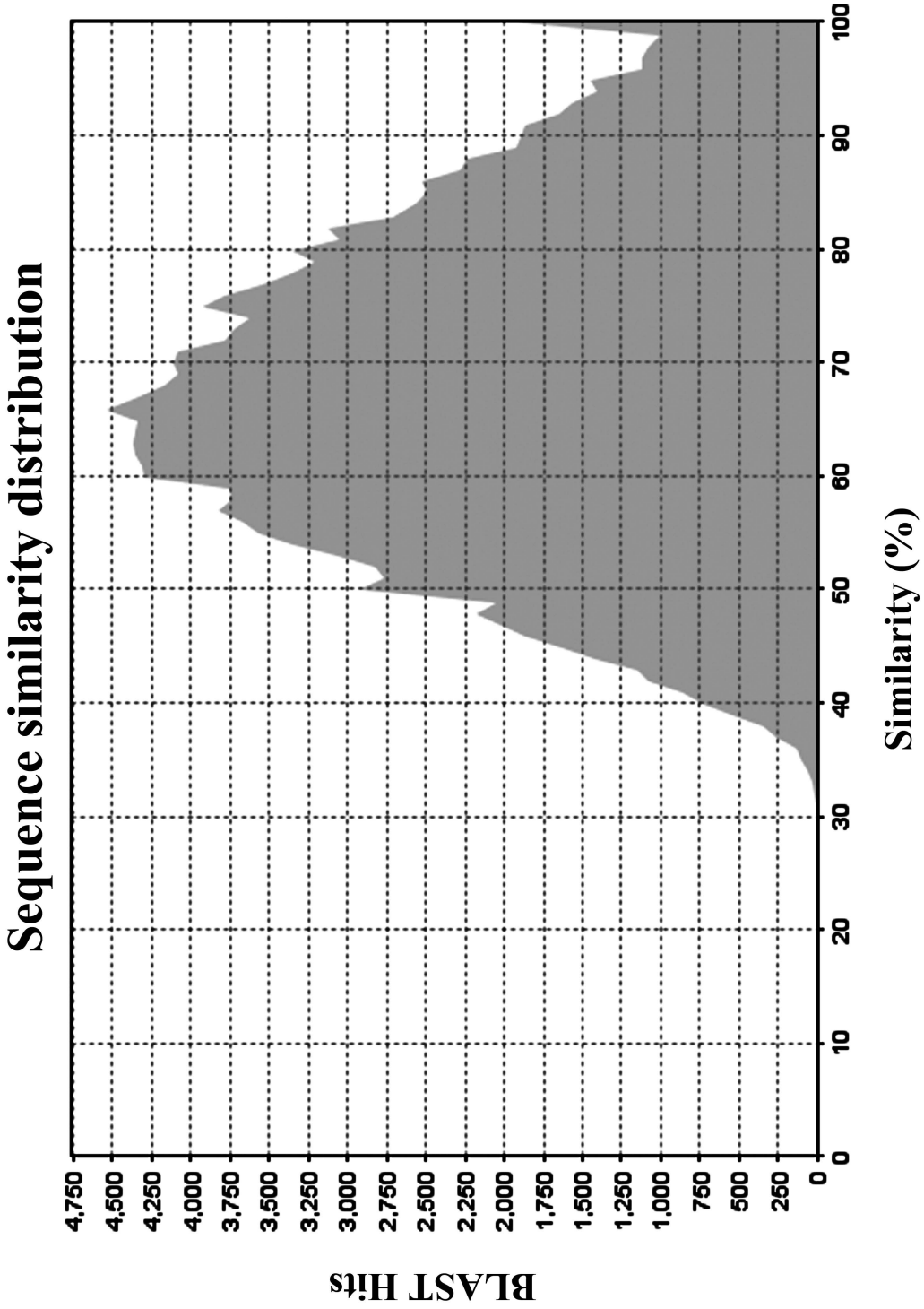
Sequence similarity distribution
BLAST Hits
Similarity (%)
4,750
4,500
4,250
4,000
3,750
3,500
3,250
3,000
2,750
2,500
2,250
2,000
1,750
1,500
1,250
1,000
750
500
250
0
0
10
20
30
40
50
60
70
80
90
100

Figure 3-3. Species distribution. Species distribution of the all blastx hits obtained when 10,664 *B. mori* sequences mapped by Illumina reads during at least 1 developmental stage were searched against the nr NCBI database.

Figure 3-3

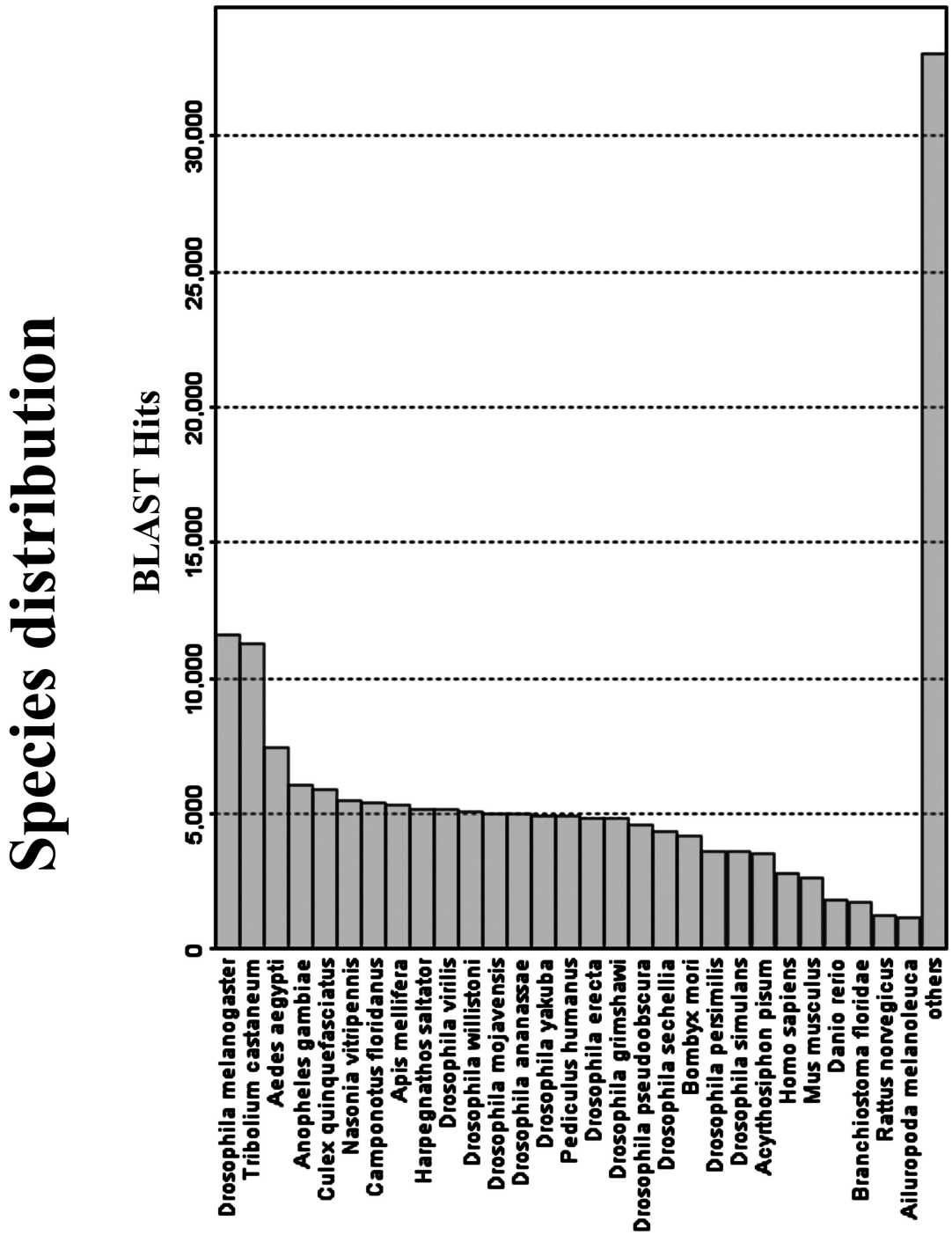
Species distribution
BLAST Hits
0
5,000
10,000
15,000
20,000
25,000
30,000
Drosophila melanogaster
Tribolium castaneum
Aedes aegypti
Anopheles gambiae
Culex quinquefasciatus
Nasonia vitripennis
Camponotus floridanus
Apis mellifera
Harpegnathos saltator
Drosophila virilis
Drosophila willistoni
Drosophila mojavensis
Drosophila ananassae
Drosophila yakuba
Pediculus humanus
Drosophila erecta
Drosophila grimshawi
Drosophila pseudoobscura
Drosophila sechellia
Bombyx mori
Drosophila persimilis
Drosophila simulans
Acyrthosiphon pisum
Homo sapiens
Mus musculus
Danio rerio
Branchiostoma floridae
Rattus norvegicus
Ailuropoda melanoleuca
others

Figure 3-4. Top blastx hit species distribution. Top species distribution of the top blastx hits obtained when the 10,664 *B. mori* sequences mapped by Illumina reads during at least 1 developmental stage were searched against the nr NCBI database.

Figure 3-4

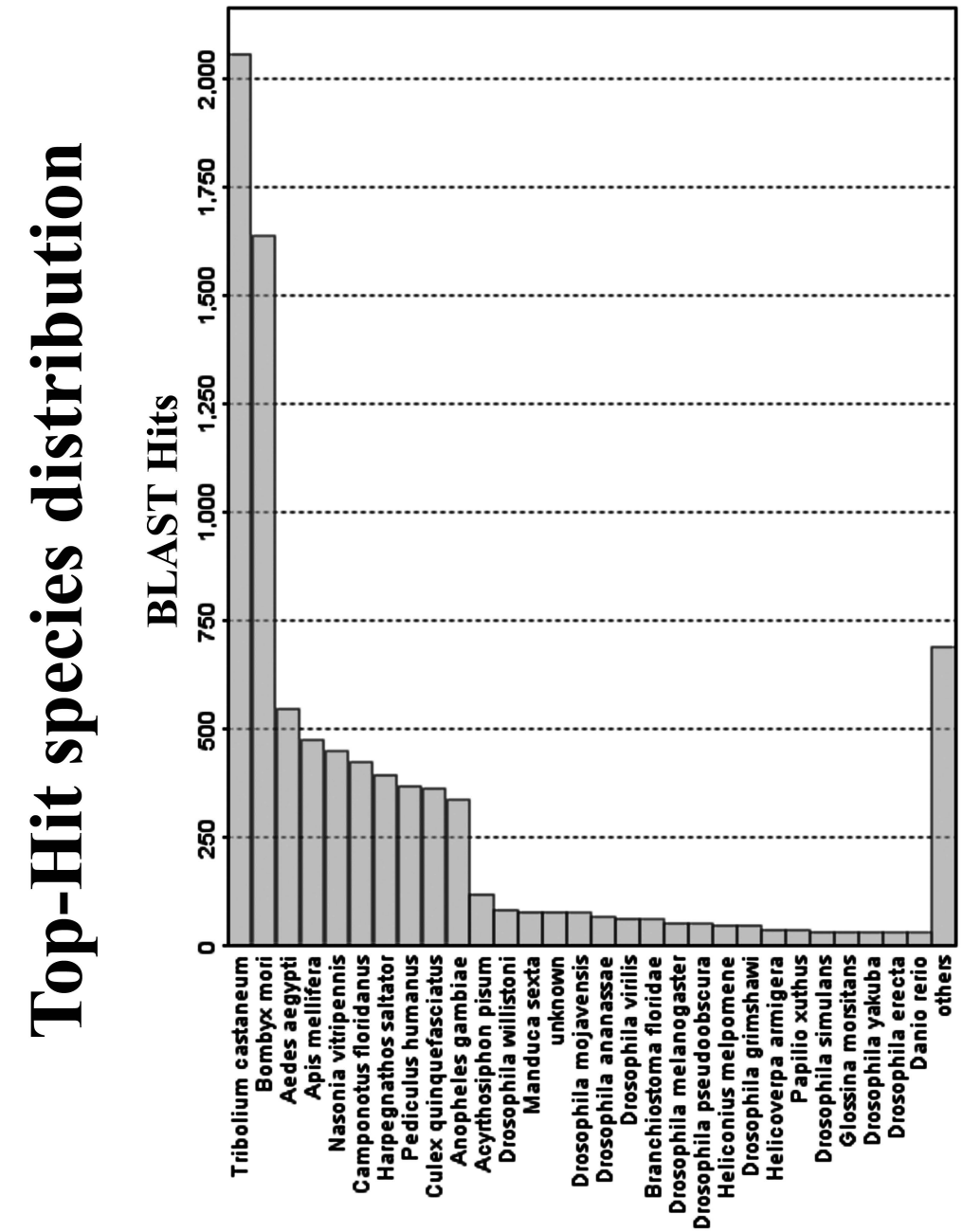
Top-Hit species distribution
BLAST Hits
0
250
500
750
1,000
1,250
1,500
1,750
2,000
Tribolium castaneum
Bombyx mori
Aedes aegypti
Apis mellifera
Nasonia vitripennis
Camponotus floridanus
Harpegnathos saltator
Pediculus humanus
Culex quinquefasciatus
Anopheles gambiae
Acyrthosiphon pisum
Drosophila willistoni
Manduca sexta
unknown
Drosophila mojavensis
Drosophila ananassae
Drosophila virilis
Branchiostoma floridae
Drosophila melanogaster
Drosophila pseudoobscura
Heliconius melpomene
Drosophila grimshawi
Helicoverpa armigera
Papilio xuthus
Drosophila simulans
Glossina morsitans
Drosophila yakuba
Drosophila erecta
Danio rerio
others

Figure 3-5. Evidence code (EC) distribution. EC distribution for the terminologies assigned to the 10,664 sequences mapped by Illumina reads. ECs represent the method of annotation used to assign GO terminologies to the sequences retrieved during the Blast2GO procedure. The “guide to GO evidence codes” can be found at (http://www.geneontology.org).

Figure 3-5

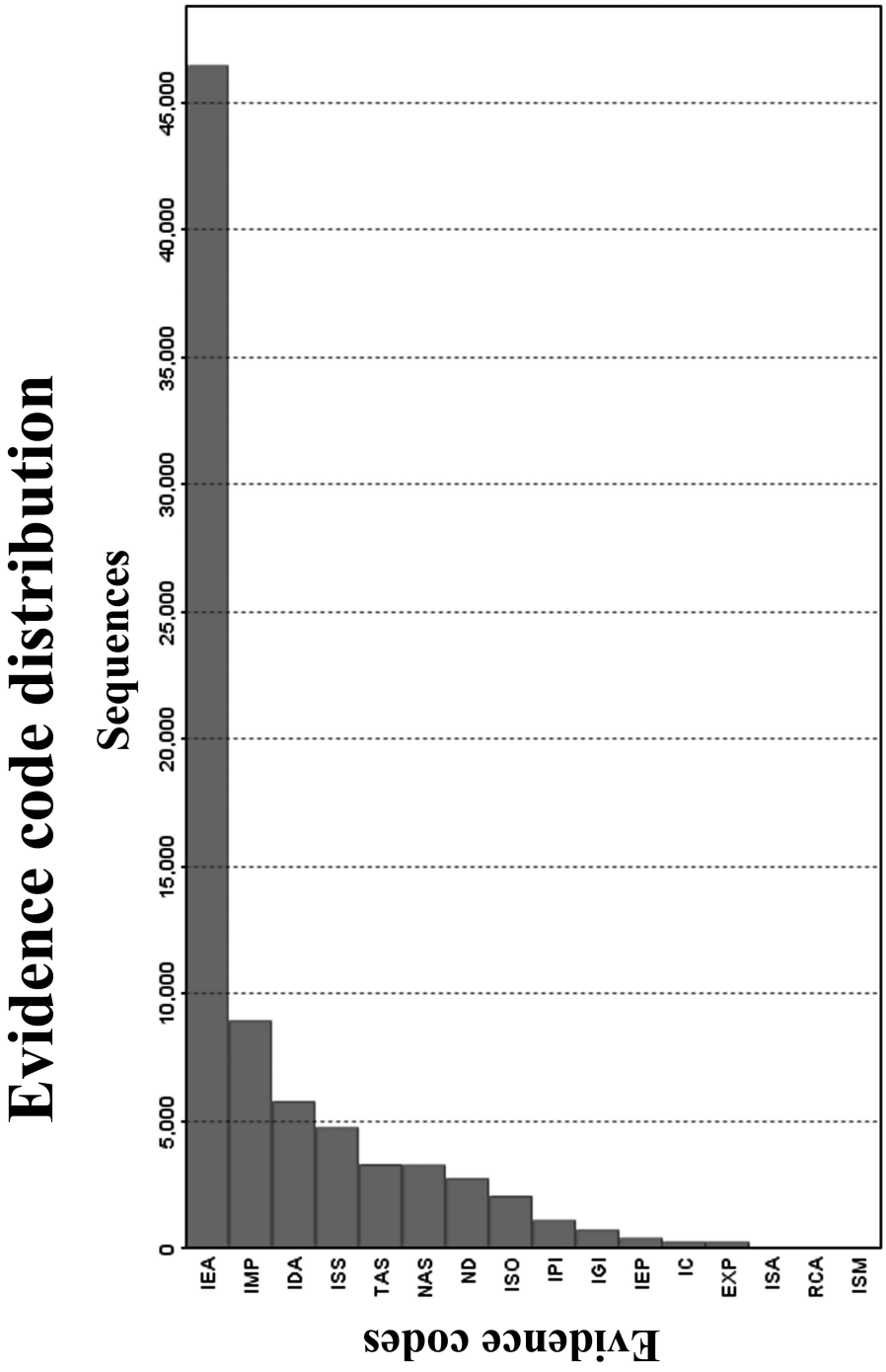
Evidence code distribution
Sequences
0
5,000
10,000
15,000
20,000
25,000
30,000
35,000
40,000
45,000
IEA
IMP
IDA
ISS
TAS
NAS
ND
ISO
IPI
IGI
IEP
IC
EXP
ISA
RCA
ISM
Evidence codes

Figure 3-6. Gene annotations. **(A)** Blast2GO annotation process results for 10,664 genes mapped by Illumina reads. A total of 8,831 genes were successfully annotated using the parameters specified in Materials and Methods. **(B)** GO level distribution of GO terms assigned to all successfully annotated genes. P=biological process, F=molecular function, C=cellular component.

Figure 3-6

A

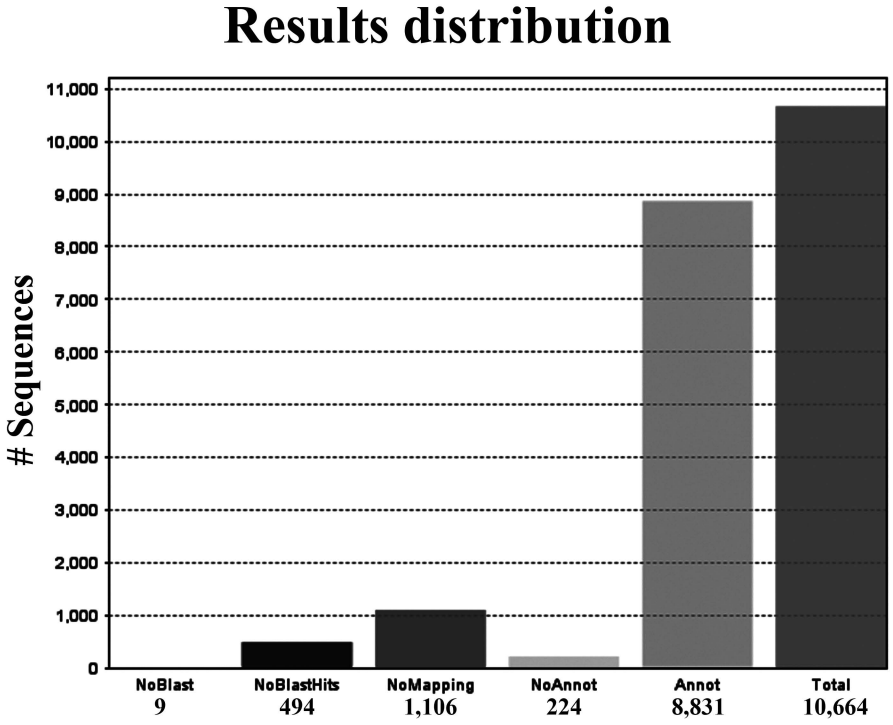
Results distribution
Sequences
11,000
10,000
9,000
8,000
7,000
6,000
5,000
4,000
3,000
2,000
1,000
0
NoBlast 9
NoBlastHits 494
NoMapping 1,106
NoAnnot 224
Annot 8,831
Total 10,664

B

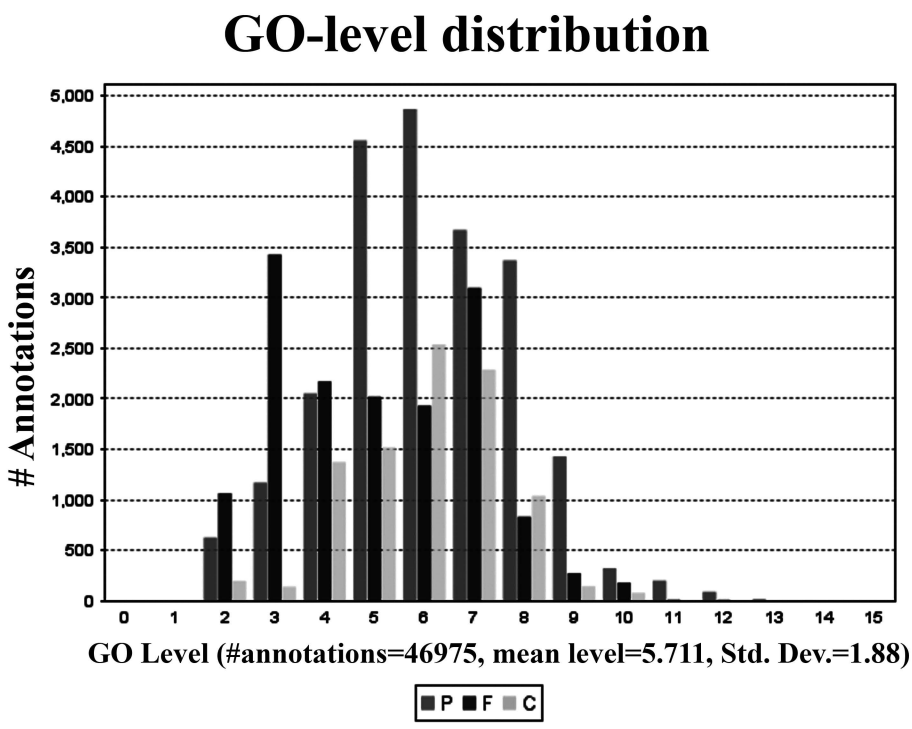
GO-level distribution
Annotations
5,000
4,500
4,000
3,500
3,000
2,500
2,000
1,500
1,000
500
0
0 1 2 3 4 5 6 7 8 9 10 11 12 13 14 15
GO Level (#annotations=46975, mean level=5.711, Std. Dev.=1.88)
P F C

Figure 3-7. Sequence distribution of annotated genes: cellular component. Sequence distribution by GO terminologies annotated under the parent term cellular component (CC). GO terminologies are represented as a multi-level-pie graph with only the lowest term per branch of the directed acyclic graph (DAG) shown. Combined graphs were constructed using Blast2GO default parameters. (Filtered by sequence: cutoff=20.0).

Figure 3-7

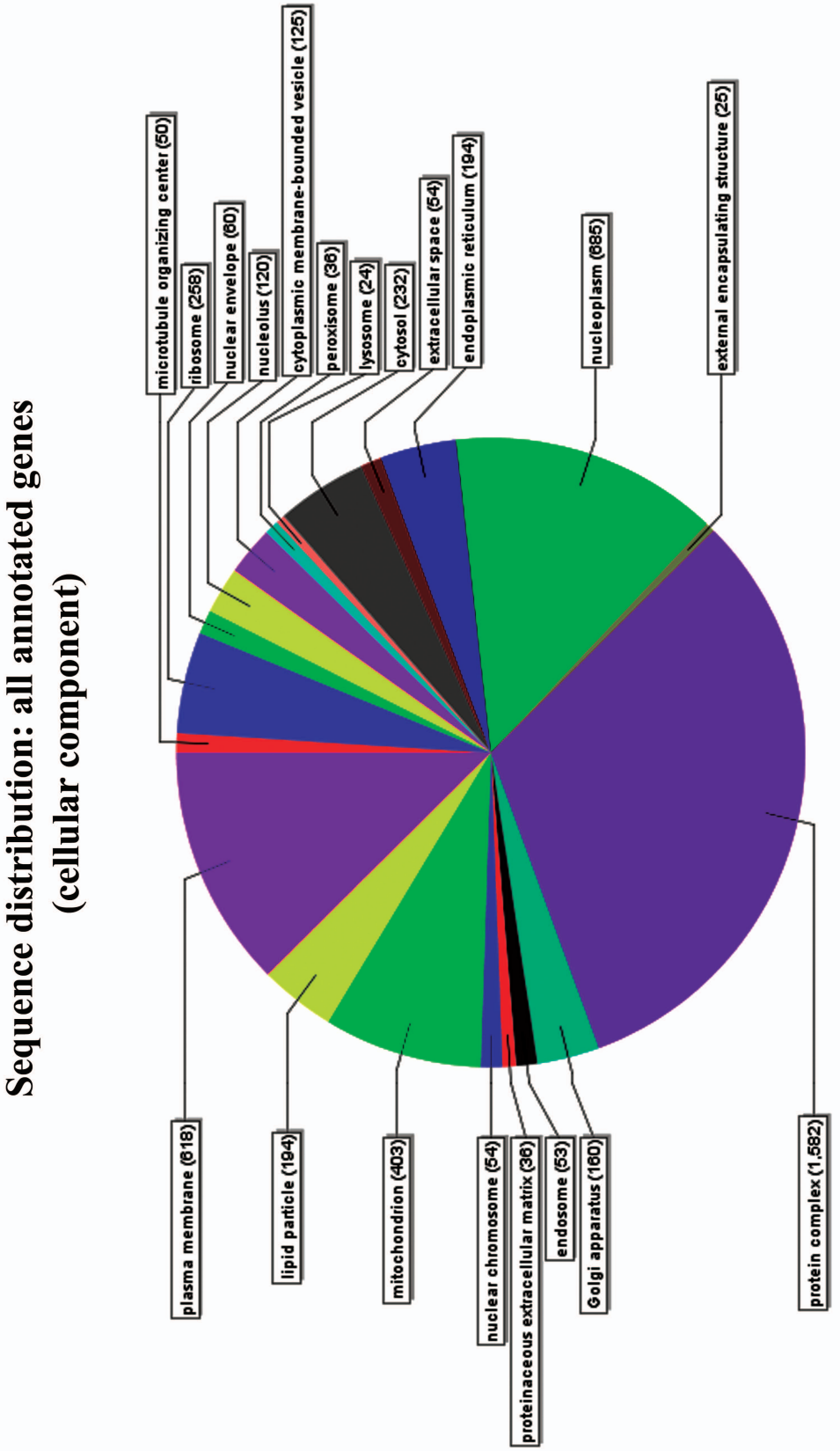
Sequence distribution: all annotated genes
(cellular component)
microtubule organizing center (50)
ribosome (258)
nuclear envelope (60)
nucleolus (120)
cytoplasmic membrane-bounded vesicle (125)
peroxisome (36)
lysosome (24)
cytosol (232)
extracellular space (54)
endoplasmic reticulum (194)
nucleoplasm (685)
external encapsulating structure (25)
plasma membrane (618)
lipid particle (194)
mitochondrion (403)
nuclear chromosome (54)
proteinaceous extracellular matrix (36)
endosome (53)
Golgi apparatus (160)
protein complex (1,582)

Figure 3-8. Sequence distribution of annotated genes: biological processes. Sequence distribution by GO terminologies annotated under the parent term biological process (BP). GO terminologies are represented as a multi-level-pie graph with only the lowest term per branch of the directed acyclic graph (DAG) shown. Combined graphs were constructed using Blast2GO default parameters. (Filtered by sequence: cutoff=20.0).

Figure 3-8

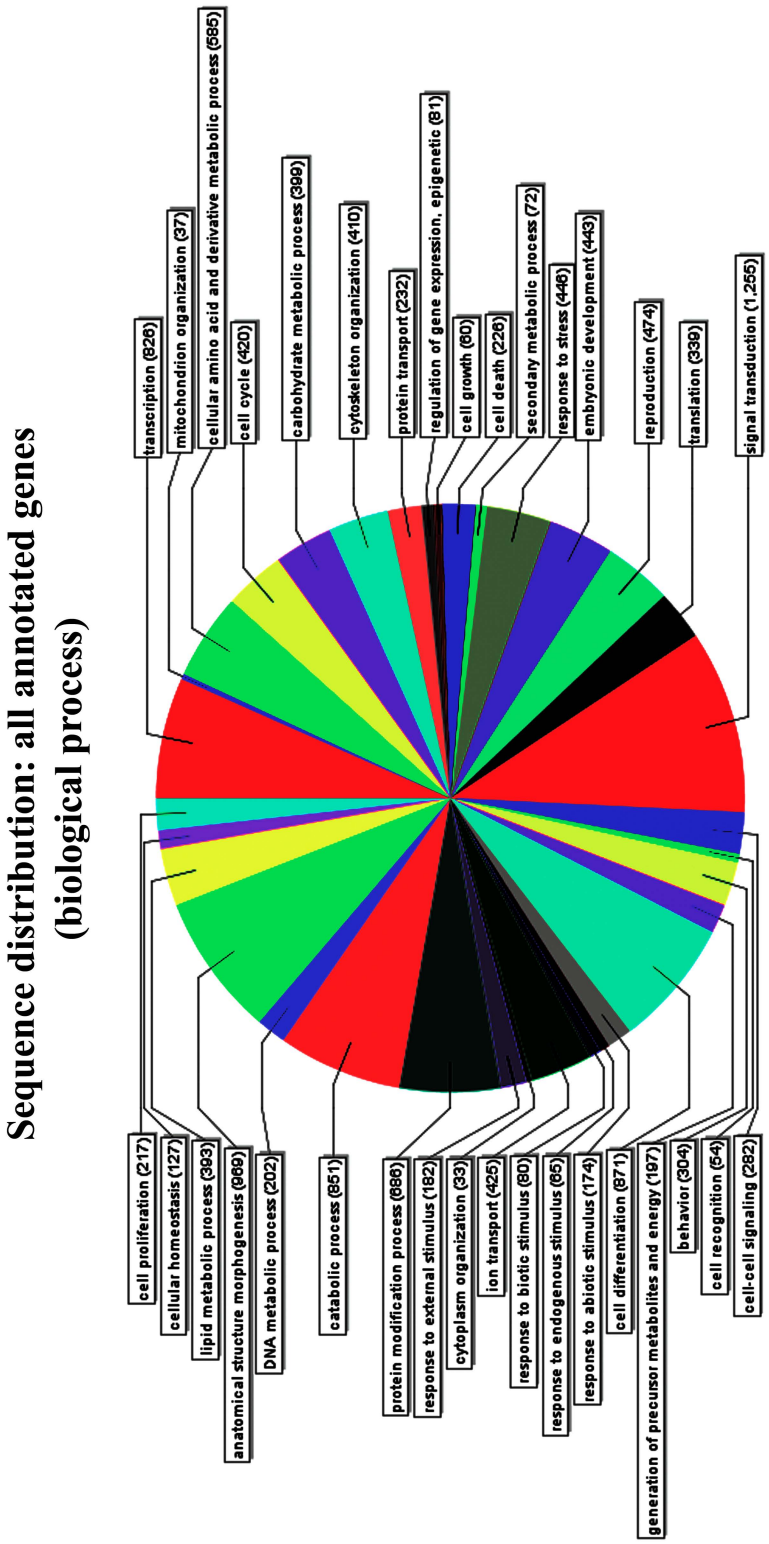
Sequence distribution: all annotated genes
(biological process)
transcription (926)
mitochondrion organization (37)
cellular amino acid and derivative metabolic process (585)
cell cycle (420)
carbohydrate metabolic process (399)
cytoskeleton organization (410)
protein transport (232)
regulation of gene expression, epigenetic (81)
cell growth (60)
cell death (226)
secondary metabolic process (72)
response to stress (446)
embryonic development (443)
reproduction (474)
translation (339)
signal transduction (1,255)
cell proliferation (217)
cellular homeostasis (127)
lipid metabolic process (393)
anatomical structure morphogenesis (969)
DNA metabolic process (202)
catabolic process (851)
protein modification process (986)
response to external stimulus (182)
cytoplasm organization (33)
ion transport (425)
response to biotic stimulus (80)
response to endogenous stimulus (85)
response to abiotic stimulus (174)
cell differentiation (871)
generation of precursor metabolites and energy (197)
behavior (304)
cell recognition (54)
cell-cell signaling (282)

Figure 3-9. Sequence distribution of annotated genes: molecular function. Sequence distribution by GO terminologies annotated under the parent term molecular function (MF). GO terminologies are represented as a multi-level-pie graph with only the lowest term per branch of the directed acyclic graph (DAG) shown. Combined graphs were constructed using Blast2GO default parameters. (Filtered by sequence: cutoff=20.0).

Figure 3-9

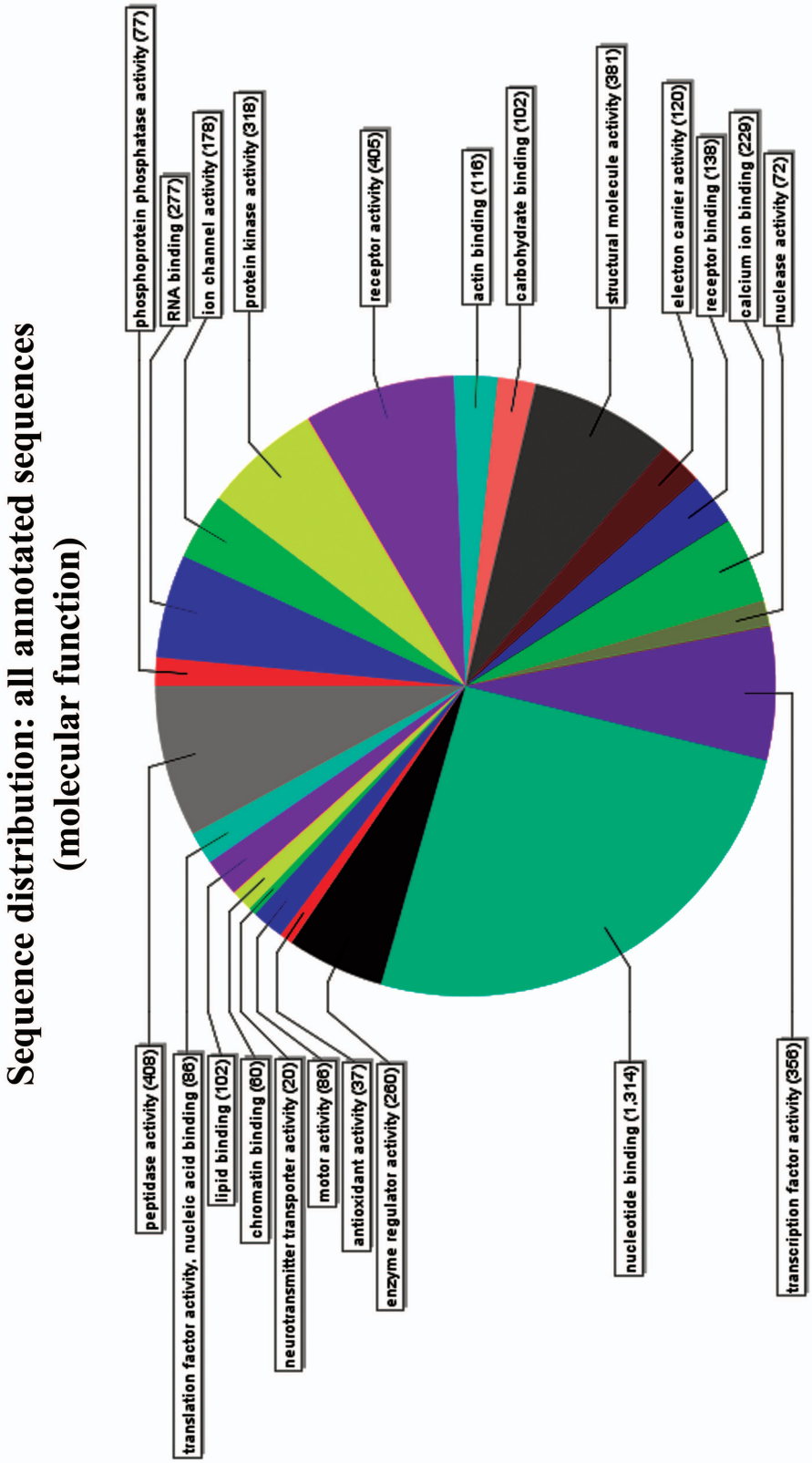
Sequence distribution: all annotated sequences
(molecular function)
phosphoprotein phosphatase activity (77)
RNA binding (277)
ion channel activity (178)
protein kinase activity (318)
receptor activity (405)
actin binding (116)
carbohydrate binding (102)
structural molecule activity (381)
electron carrier activity (120)
receptor binding (138)
calcium ion binding (229)
nuclease activity (72)
peptidase activity (408)
translation factor activity, nucleic acid binding (86)
lipid binding (102)
chromatin binding (60)
neurotransmitter transporter activity (20)
motor activity (86)
antioxidant activity (37)
enzyme regulator activity (280)
nucleotide binding (1,314)
transcription factor activity (356)

Figure 3-10. Stage-specific differential-expression relative to the inter-molt reference stage (reference=HCS -30 hrs). For each unique gene, the $\log_2$fold change is plotted against the base mean, which is an estimate of a genes expression level (averaged across the two developmental stages used for comparison) (Anders & Huber 2010). All genes with fold changes >2 (up-regulated) or <0.5 (down-regulated) with p-values <0.1 were considered significant and are colored in red. The following percentage of genes (out of the total 10,664 mapped genes) were significantly up- or down-regulated at each stage: HCS -18 hrs (1.6% up; 1.2% down), HCS -12 hrs (2.3% up; 1.7% down), HCS -6 hrs (2.9% up; 2.6% down), HCS (4.9% up; 2.9% down), HCS +18 hrs (5.3% up; 1.2% down), HCS -48 hrs (2.6% up; 1% down).

Figure 3-10

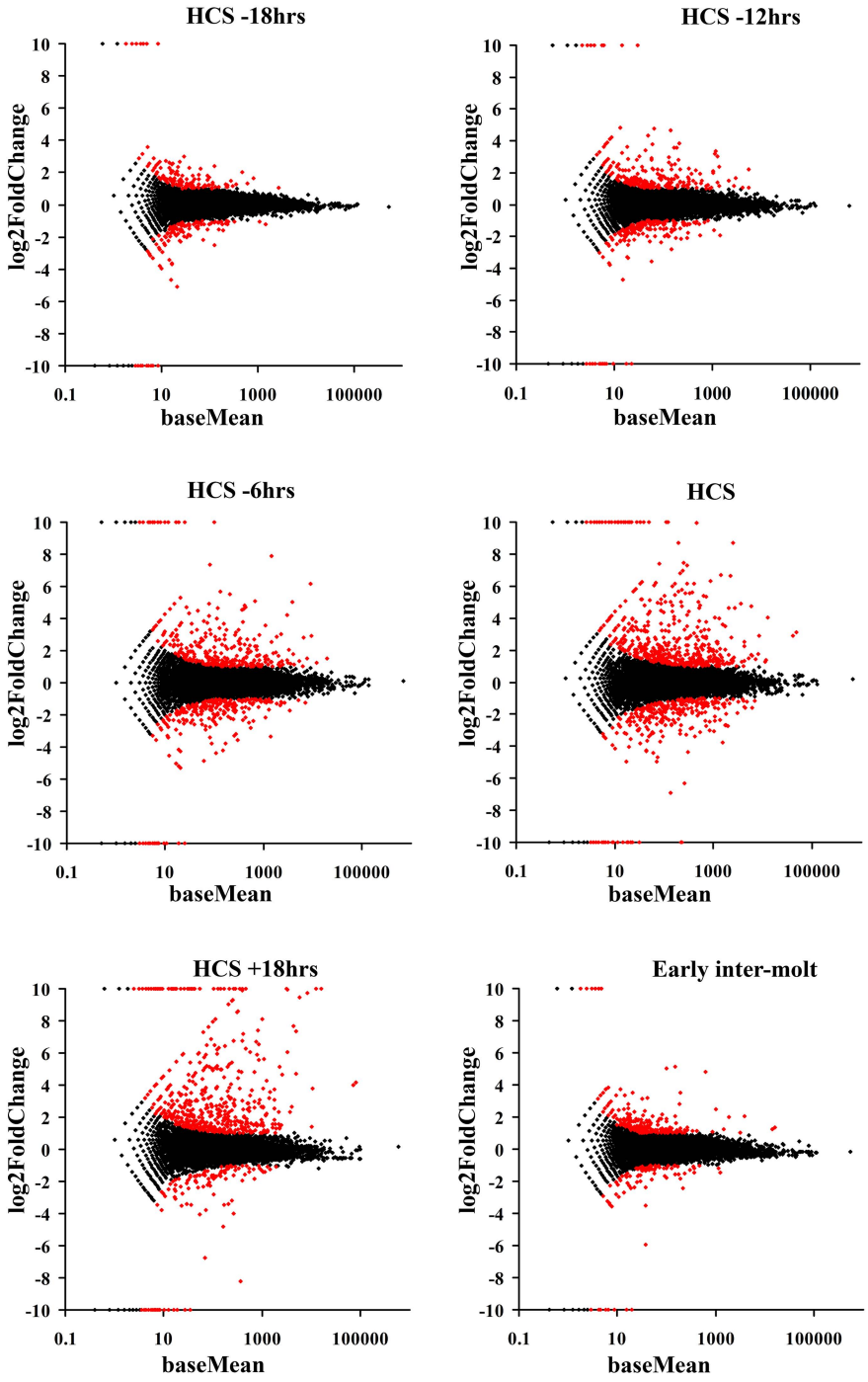
HCS -18hrs
HCS -12hrs
HCS -6hrs
HCS
HCS +18hrs
Early inter-molt
log2FoldChange
baseMean
10
8
6
4
2
0
-2
-4
-6
-8
-10
0.1
10
1000
100000

Figure 3-11. Nucleotide and proteome alignment methods- a comparison. Shown are the 56 paired expression profiles resulting from the nucleotide and proteome alignment methods. The gene ID's and descriptions correspond to SilkDB (for *B. mori*) and NCBI (for *M. sexta*) databases. All genes were matched using blastx filtered with an Expect value (E) of 10^{-6}. For each gene, the average number of mapped reads across all developmental stages is shown. Expression profiles are illustrated using the $\log_2$fold change, and significant fold changes (fc) are color-coded so that fc >2 ($p<0.1$) is colored dark red, and fc <0.5 ($p<0.1$) is dark blue. When fold changes that are not accompanied by p-values <0.1 are colored orange (>2) and light blue (<0.5). Stages are ordered according to developmental time (hrs relative to HCS) except for stage HCS -48 hrs, which is shown last for comparison (early inter-molt feeding period). % false positives (FP) were calculated for each *B. mori* gene by comparing the number of times a significant fc was detected across development to the number of fc agreements in the *M. sexta* profile. (A score of 0.00=maximum agreement, and a score of 1.00=maximum score for disagreement between the two profiles).

Figure 3-11

Gene ID	Annotated gene descritptions	E-value	Ave. #reads	(-18)	(-12)	(-6)	HCS	(+18)	(-48)	FP
BGIBMGA000529	neutral endopeptidase		769.6	-0.2	0.3	1.0	1.2	3.1	0.8	0.00
AF413063.1	Manduca sexta zinc metalloprotease	0	1505.0	-0.1	0.3	1.1	1.4	3.2	0.9	
BGIBMGA000648	imaginal disc growth factor		1795.6	-0.2	-0.5	-0.9	-1.4	-1.2	-0.6	0.00
GQ843826.1	hemocyte aggregation inhibitor protein	0	3788.9	-0.3	-0.6	-1.0	-1.4	-1.3	-0.7	
BGIBMGA000716	nuclear hormone receptor (ftz-f1 alpha)		409.0	-0.8	-0.5	0.5	0.2	2.6	0.5	0.00
AF288089.1	nuclear hormone receptor betaFTZ-F1	0	478.5	-0.9	-1.0	-1.4	-0.2	2.8	0.4	
BGIBMGA000772	juvenile hormone esterase		16.0	-1.2	-Inf	-Inf	-3.2	-0.6	1.8	0.00
AF327882.2	juvenile hormone esterase	0	805.1	-1.7	-3.6	-5.1	-2.0	-0.8	2.0	
BGIBMGA000868	cytochrome p450		48.1	-0.2	-0.3	-0.6	-3.3	-1.4	-0.4	0.00
L38668.1	cytochrome P450	7.00E-27	305.9	0.3	0.0	-0.5	-2.4	-0.7	-0.3	
BGIBMGA001039	tetraspanin		39.9	0.1	0.4	1.1	1.4	1.7	-0.9	1.00
AF274021.1	tetraspanin	1.00E-22	4861.4	0.0	-0.1	-0.1	0.0	0.3	-0.1	
BGIBMGA001162	cytochrome p450		107.3	-1.0	-2.5	-3.4	-4.2	6.1	1.0	0.00
GU731532.1	cytochrome P450	0	170.4	-0.6	-1.7	-2.5	-4.5	6.4	1.1	
BGIBMGA001472	bumetanide-sensitive na-k-cl cotransport		121.3	-1.2	-0.7	-0.9	-1.8	-1.1	-0.3	0.50
U17344.1	bumetanide sensitive NaK2Cl cotransporter	0	212.1	-1.0	-0.8	-0.7	-2.2	-1.6	-0.3	
BGIBMGA001531	corazonin receptor		146.8	0.5	0.0	0.3	-2.4	-0.4	0.2	0.00
AY369029.1	corazonin receptor	8.00E-161	500.0	0.3	0.1	0.0	-2.4	-0.3	0.2	
BGIBMGA002397	protein spaetzle		0.3	Inf	NA	NA	NA	NA	NA	1.00
GQ249944.1	Spz1A	2.00E-56	24.4	0.8	0.1	0.1	-1.3	-0.2	0.6	
BGIBMGA002906	acyl- -binding protein		515.3	0.1	0.2	0.7	1.1	-0.2	-0.6	0.00
S65642.1	diazepam binding inhibitor	8.00E-36	1308.4	0.0	0.3	0.7	1.2	-0.4	-0.5	
BGIBMGA002920	tetraspanin		1.1	Inf	Inf	Inf	NA	Inf	Inf	1.00
AF274022.1	tetraspanin	9.00E-91	8.2	0.3	0.1	0.4	-0.5	1.1	0.4	
BGIBMGA002938	nitric oxide synthase		591.3	-0.4	-0.7	-1.0	-1.8	0.1	0.5	0.00
AF062749.1	nitric oxide synthase (NOS)	0	835.1	-0.3	-0.9	-1.2	-3.2	0.2	0.7	
BGIBMGA002960	chitin synthase		144.2	0.9	1.2	1.6	2.2	2.1	1.0	1.00
AY821560.1	chitin synthase	0	49.3	0.4	-0.5	0.2	0.3	0.4	0.0	
BGIBMGA002963	chitin synthase		943.8	0.6	1.2	1.7	2.1	2.1	0.8	0.00
AY062175.2|	chitin synthase	0	1156.9	0.5	1.1	1.5	2.0	2.0	0.7	
BGIBMGA003199	dopa decarboxylase protein		1217.7	-0.2	-0.3	-0.2	1.1	1.4	0.6	0.00
|U03909.1	dopa decarboxylase	0	2220.4	0.0	-0.2	0.0	1.4	1.4	0.8	
BGIBMGA003895	ecdysone-induced protein 78c		195.6	0.5	1.4	2.4	1.3	0.0	-0.2	0.33
U73683.1	E75A	1.00E-28	306.9	1.0	2.0	2.0	0.7	-2.0	-1.2	
BGIBMGA004066	chemosensory protein		4.6	-0.7	0.8	-1.2	-Inf	-Inf	-Inf	0.00
AJ973454.1	hypothetical protein (ORF5)	3.00E-51	20.8	-1.6	-0.1	-1.0	-3.3	-Inf	-4.7	
BGIBMGA005129	isoform g		341.2	0.5	0.9	1.1	1.6	0.1	-0.2	0.00
AF078161.1	lacunin	0	3590.3	0.4	1.0	1.3	1.6	0.3	-0.1	
BGIBMGA005173	proclotting enzyme		1.0	Inf	Inf	Inf	Inf	NA	NA	0.00
AY672784.1	hemolymph proteinase	3.00E-121	4.9	1.3	1.4	0.7	0.5	-1.4	0.8	
BGIBMGA005277	cuticle protein		19.0	-1.8	-1.2	-1.9	-1.9	-2.5	1.4	0.25
M18546.1	larval cuticle protein	2.00E-21	81.5	-1.3	-2.3	-5.4	-5.5	-6.7	-1.3	
BGIBMGA005899	hexosaminidase isoform a		823.0	-0.1	0.1	0.0	1.1	0.7	-0.2	0.00
AY368703.1	N-acetylglucosaminidase	0	1603.8	0.1	0.1	0.3	1.2	0.8	-0.1	
BGIBMGA006225	golgin subfamily a member 2		47.6	1.1	0.7	0.8	0.5	0.7	1.2	1.00
AF244891.1	golgin-80	7.00E-114	714.6	0.7	0.7	1.0	0.8	0.7	0.8	
BGIBMGA006423	trypsin		66.9	-0.7	-3.6	-4.9	-1.9	-1.6	-1.1	0.00
AF087005.1	scolexin B	2.00E-107	153.1	-0.9	-2.5	-4.2	-1.8	-1.9	-1.3	
BGIBMGA006745	laccase-like multicopper oxidase 1		38.0	-0.2	-0.4	-0.7	-0.3	1.4	0.9	0.00
AY135186.1	Manduca sexta laccase 2	0	56.6	-0.3	-0.4	-0.9	-0.5	1.2	0.8	

Figure 3-11 (Cont'd)

BGIBMGA008584	rh-like protein		276.3	-0.4	-0.7	-1.0	0.1	1.6	0.4	0.00
DQ864985.1	Rh-like protein	5.00E-155	756.4	-0.5	-0.8	-1.1	0.1	1.5	0.2	
BGIBMGA008668	serine protease		11.8	-1.5	-Inf	-0.4	-4.2	-Inf	-1.3	0.00
AY672792.1	hemolymph proteinase 17	9.00E-161	60.3	-1.0	-1.5	-1.4	-2.3	-3.4	-0.8	
BGIBMGA008709	chitinase		406.9	-0.3	-0.2	-0.8	0.0	-3.5	2.5	0.00
DQ288140.1	chitinase-h (Chi-h)	0	550.9	-0.3	-0.3	-0.9	0.1	-3.9	2.4	
BGIBMGA009551	serine protease		186.5	-0.1	-0.2	-0.9	-1.3	-1.5	-0.5	0.00
AF518768.1	serine proteinase-like protein 2	4.00E-156	932.1	-0.1	-0.3	-0.8	-1.3	-1.4	-0.3	
BGIBMGA009610	serine protease		22.8	-0.1	-1.1	-0.4	-2.3	-1.9	-1.1	0.00
AY672797.1	hemolymph proteinase 21	3.00E-115	206.7	-0.6	-0.8	-0.7	-2.2	-1.2	-0.8	
BGIBMGA009688	hormone receptor 3		2455.6	0.6	3.2	6.2	4.9	1.5	-0.2	0.00
X74566.1	M.sexta MHR3	1.00E-138	6274.3	1.4	4.2	7.5	6.2	2.3	0.2	
BGIBMGA009775	cuticle protein		0.9	NA	NA	NA	Inf	Inf	Inf	0.00
AY585211.1	pupal cuticle protein	1.00E-21	22.0	-Inf	-3.3	-5.3	-5.0	-4.6	1.1	
BGIBMGA010093	glutathione s-transferase		289.7	-0.6	-1.3	-1.7	-1.9	0.3	0.2	0.00
L32091.1	glutathione S-transferase	7.00E-79	808.0	-0.6	-1.3	-1.9	-1.8	0.3	0.2	
BGIBMGA010239	ecdysone 20-hydroxylase		25.1	-0.8	-1.5	-0.9	-1.1	-0.7	-1.1	0.00
DQ372988.1	cytochrome P450 CYP314A1	2.00E-79	315.5	0.1	0.0	-0.3	-0.6	-0.3	0.4	
BGIBMGA010240	chitinase		1408.3	1.0	3.0	4.2	3.5	3.7	0.7	0.00
U02270.1	chitinase	0	2397.3	0.9	3.0	4.2	3.5	3.6	0.6	
BGIBMGA010546	serine protease		39.8	0.5	-0.1	-0.7	-2.7	-3.5	0.4	0.00
AM293327.1	prophenoloxidase activating protease I	9.00E-151	80.6	-1.0	-0.8	-1.7	-2.9	-4.0	0.0	
BGIBMGA010713	soluble guanylyl cyclase beta-3		167.8	-0.3	-0.7	-0.4	-0.6	1.5	0.1	0.00
AF064514.1	soluble guanylyl cyclase beta-3	0	160.0	-0.1	-0.8	-0.2	-0.7	2.3	0.4	
BGIBMGA010985	ecdysteroid regulated protein		157.8	-Inf	-Inf	-Inf	-Inf	11.2	-Inf	0.00
L24916.1	ecdysteroid regulated protein (esr20)	2.00E-46	477.6	0.5	-Inf	-Inf	2.5	12.8	1.4	
BGIBMGA011086	partner of burs		1.6	Inf	Inf	Inf	Inf	Inf	Inf	0.00
DQ291147.1	Manduca sexta bursicon (pburs)	1.00E-59	2.6	2.1	3.1	-0.1	1.8	2.2	3.0	
BGIBMGA011399	cg31997 cg31997-pa		183.8	0.5	0.6	0.5	0.1	5.5	0.4	0.00
AF117598.1	clone pMsmaD211 unknown	2.00E-44	436.1	0.9	0.7	0.5	0.5	5.5	0.5	
BGIBMGA011424	transferrin		4028.6	-0.5	-0.7	-0.9	-1.1	-1.1	-0.1	0.00
M62802.1	transferrin gene	0	6060.8	-0.6	-0.8	-1.0	-1.1	-1.1	-0.2	
BGIBMGA011468	juvenile hormone epoxide hydrolase		90.3	-0.3	0.2	-0.9	-1.3	-1.1	0.5	0.00
U46682.1	juvenile hormone epoxide hydrolase	0	62.9	0.7	0.9	-0.2	-1.4	-1.1	0.8	
BGIBMGA011729	putative cuticle protein		46.1	-5.1	-Inf	-Inf	-Inf	2.5	0.6	0.00
AF117584.1	putative cuticle protein	3.00E-32	93.2	-5.7	-Inf	-Inf	-Inf	3.3	0.6	
BGIBMGA011850	allatotropin		75.2	-0.2	-0.8	-1.1	-0.9	-0.6	-0.7	1.00
U62102.1	allatotropin	1.00E-42	645.0	0.5	0.2	0.2	0.0	-0.2	0.6	
	apolipophorin-iii		97.7	-0.5	-1.6	-2.4	-3.7	-3.8	-0.8	0.25
M17286.1	M.sexta apolipophorin-III	2.00E-62	1914.8	-0.3	-0.9	-1.8	-2.9	-3.7	-0.3	
BGIBMGA013812	female neotenic-specific protein 1		167.2	-0.7	-1.2	-1.9	-1.9	-1.6	0.0	1.00
AF060795.1	juvenile hormone esterase-related protein	4.00E-64	102.3	-0.5	-0.7	-0.7	-0.9	-0.7	0.9	
BGIBMGA013975	lupus la		22.6	-1.8	-2.3	-1.4	-1.4	1.3	-0.5	0.00
AF443827.1	acheron	0	47.2	-1.3	-1.8	-1.7	-1.4	1.1	-0.4	
BGIBMGA014057	long-chain fatty acid transport		5699.9	-0.2	-0.3	-0.7	-1.2	0.0	-0.1	0.00
GQ245679.1	FATP	0	17015.8	-0.2	-0.3	-0.7	-1.2	0.0	-0.2	
BGIBMGA014241	death-associated lim only protein dalp		627.4	-0.2	-0.7	-1.4	-0.7	-0.3	-0.3	1.00
AF172845.1	death-associated LIM only protein DALP	7.00E-94	1795.6	0.1	-0.3	-0.9	-0.2	0.1	0.4	
BGIBMGA014370	protein toll		8.6	1.0	1.0	0	2.1	1.4	0.8	1.00
EF442782.1	toll receptor (Toll)	8.00E-88	71.9	0.1	0.3	0.4	-0.1	0.3	0.3	
BGIBMGA014404	serine protease		114.0	-0.2	-1.0	-1.3	-1.8	-2.1	-0.1	0.00
GQ222378.1	serine proteinase-like protein 1b	1.00E-153	244.9	-0.4	-1.2	-1.4	-2.1	-2.3	0.0	

Figure 3-12. Comparison of BLAST2GO and NCBI annotations. For each of the 56 paired profiles, BLAST2GO and NCBI annotations were compared. 43 (~77%) of the 56 paired profiles showed matching definitions, and a total of 55 (~98%) of the profiles showed matching functional annotations (similarities based on GO term assignments). Only 1 (~2%) of the paired profiles was unmatched based on annotation.

Figure 3-12

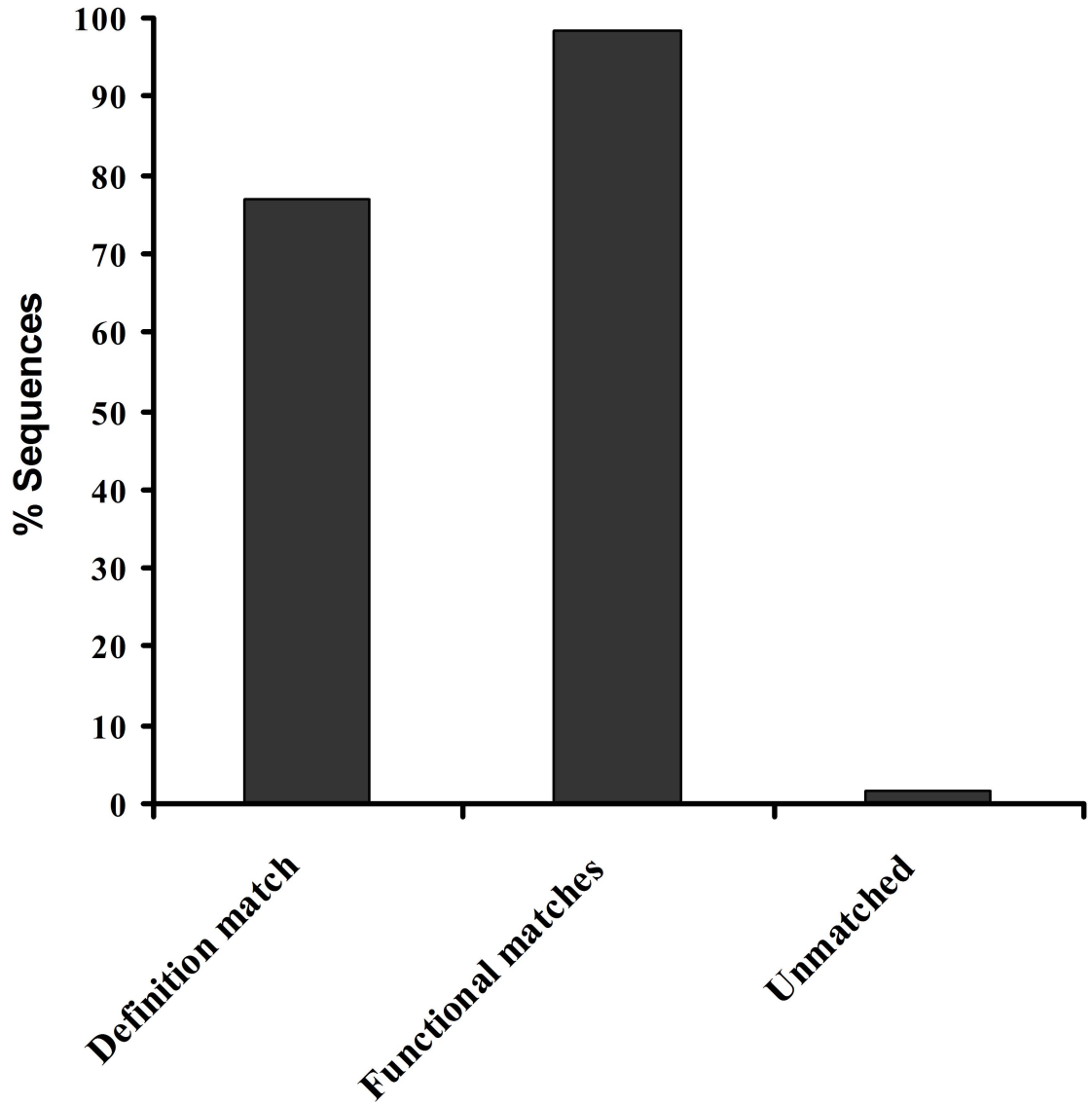
100
90
80
70
60
50
40
30
20
10
0
% Sequences
Definition match
Functional matches
Unmatched

Figure 3-13. Comparison across alignment methods of the # mapped reads. The average number of reads that mapped to each of the 56 paired genes was compared across alignment methods. When *M. sexta* Illumina reads are mapped to the *B. mori* proteome, an average of 488 reads are associated to each protein coding gene/stage. When Illumina reads are mapped onto the available *M. sexta* genes, an average of 1255 reads are mapped to each individual gene/stage (~2.6 times more reads).

Figure 3-13

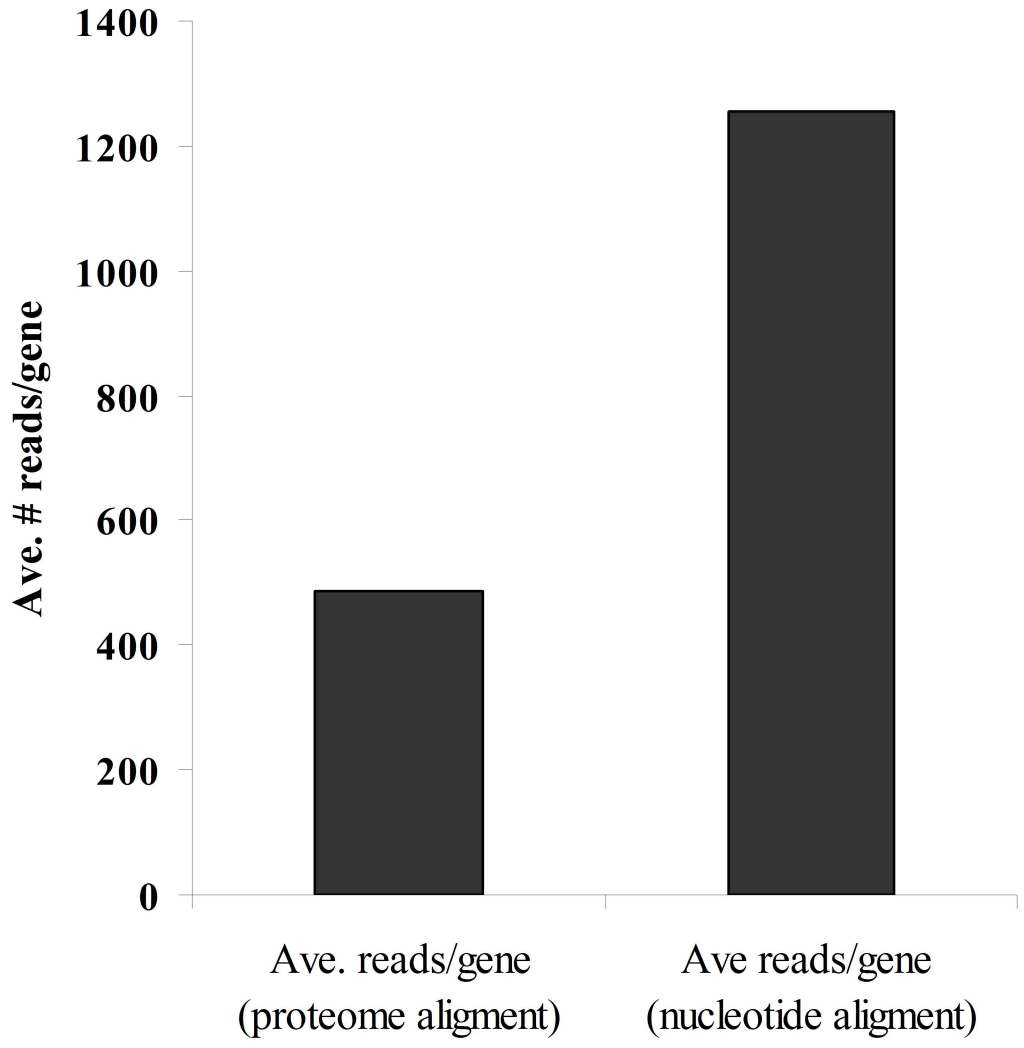
1400
1200
1000
800
600
400
200
0
Ave. # reads/gene
Ave. reads/gene (proteome aligment)
Ave reads/gene (nucleotide aligment)

Figure 3-14. A comparison of fold-change across methodologies and false-positive analysis. **(A)** For all 56 gene-pair profiles obtained using the proteome (p) and nucleotide (n) alignment methods, $\log_2$fold changes for each stage/gene were plotted. Expression profiles show a strong correlation across methodologies (Pearson's correlation coefficient=0.92, p=1.4(E)-119). Stages at which infinite-fold changes were detected were omitted. **(B)** Gene pairs (% out of the 56 gene pairs) are plotted according to their false-positive scores. False-positive scores were calculated for each gene as described in the text. A score of "0" indicates that across-method expression profiles showed maximal agreement, and a score of "1" indicates that all significant fold changes detected for that gene using the (p) method were false positives when the (n) method is considered to be "true".

Figure 3-14

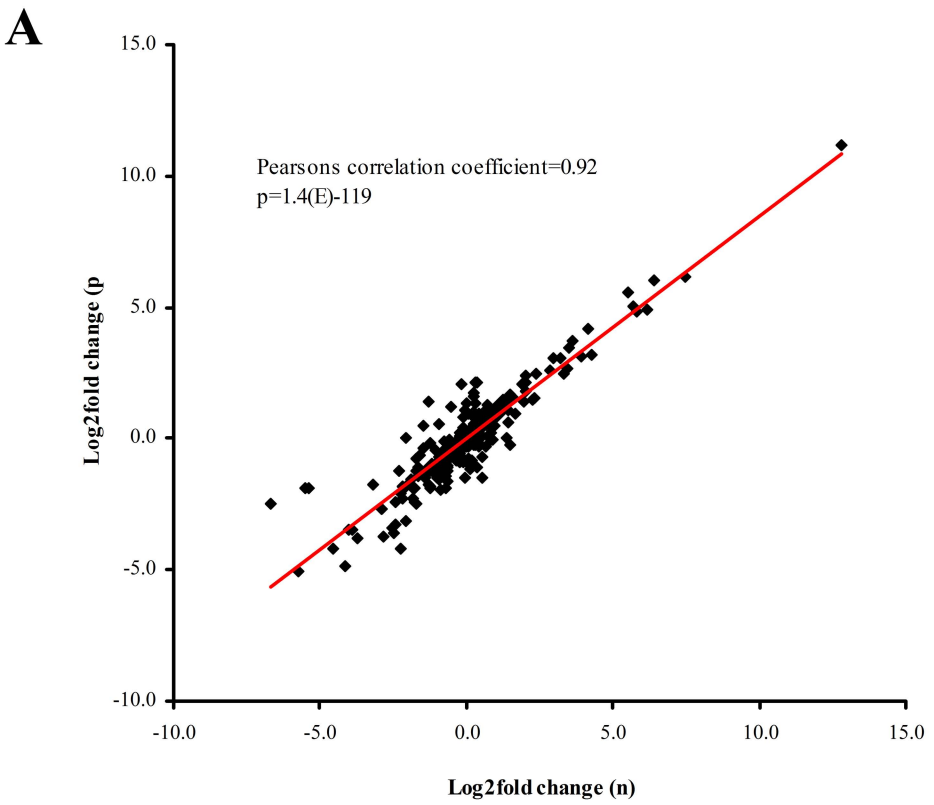
A
Pearsons correlation coefficient=0.92
p=1.4(E)-119
Log2fold change (p
Log2fold change (n)
15.0
10.0
5.0
0.0
-5.0
-10.0
-10.0
-5.0
0.0
5.0
10.0
15.0

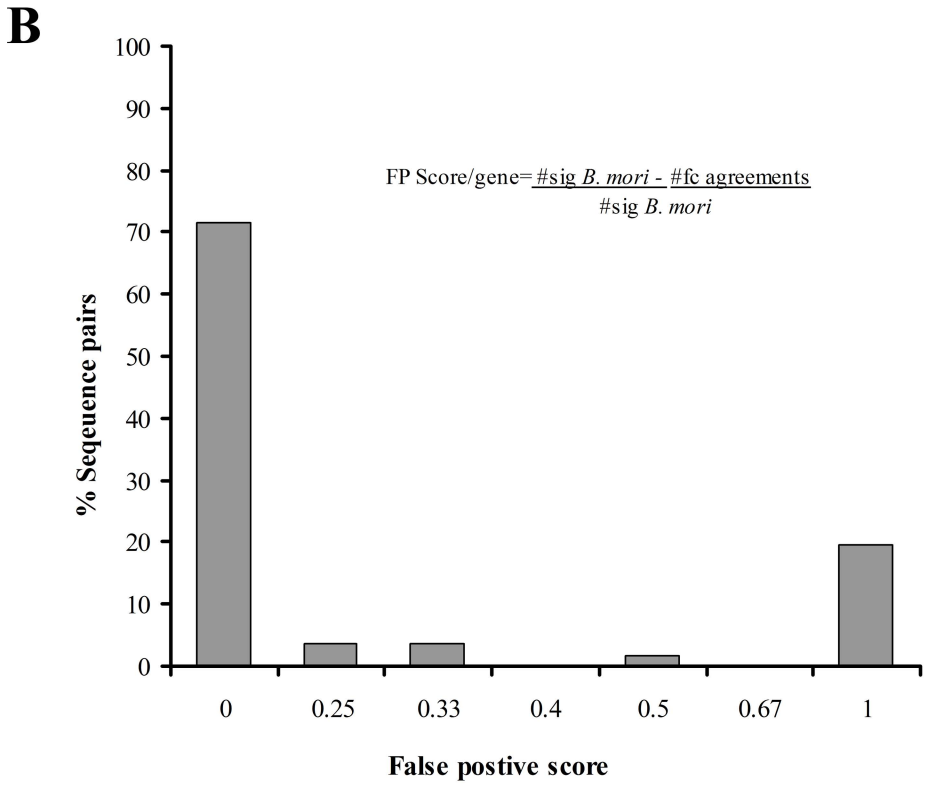
B
FP Score/gene= #sig B. mori - #fc agreements
#sig B. mori
% Sequence pairs
False postive score
100
90
80
70
60
50
40
30
20
10
0
0
0.25
0.33
0.4
0.5
0.67
1

Figure 3-15. Validation of Illumina RNA-seq data using quantitavive PCR (qPCR). (A-F): Primers were designed using *M. sexta* mRNA sequences available on NCBI (see Table 3-2). Shown are the $\log_2$fold expression profiles for six genes at six developmental ages staged relative to the time of head capsule slippage (hour relative to HCS). All fold-change values are relative to levels detected at HCS -30 hrs (reference stage, not shown). Each graph shows 1-Illumina sequencing results using the "proteome alignment method" (white circles), 2-Illumina sequencing results using the "nucleotide alignment method" (grey squares), and 3-qPCR results (black triangles). Tissue was collected separately for use with qPCR, therefore qPCR results act as biological replicates for the validation of Illumina sequencing data. Provided are the gene names, as well as the base means estimated for the nucleotide (first bracket) and proteome (second bracket) alignment methods. On the time-scale is shown the stages where significant up-regulation (red stars) and down-regulation (blue stars) were called for that gene using Illumina sequencing data (proteome alignment method). In **F,** fold-change Illumina fold-change values are infinite at -12 hrs, -6 hrs and at HCS. **(A, C-F)** With the exception of the *dopa decarboxylase* profile, each qPCR fold-change value is the average of two biological replicates. Each biological replicate was run on an independent plate, and on each plate, individual reactions were run in triplicate. Ribosomal protein L32 was used as an internal reference gene. **(B)** For dopa decarboxylase, fold-change values are the averages of three biological replicates normalized to cytoplasmic actin (black circles), and one biological replicate normalized to RPL32 (black triangles).

Figure 3-15

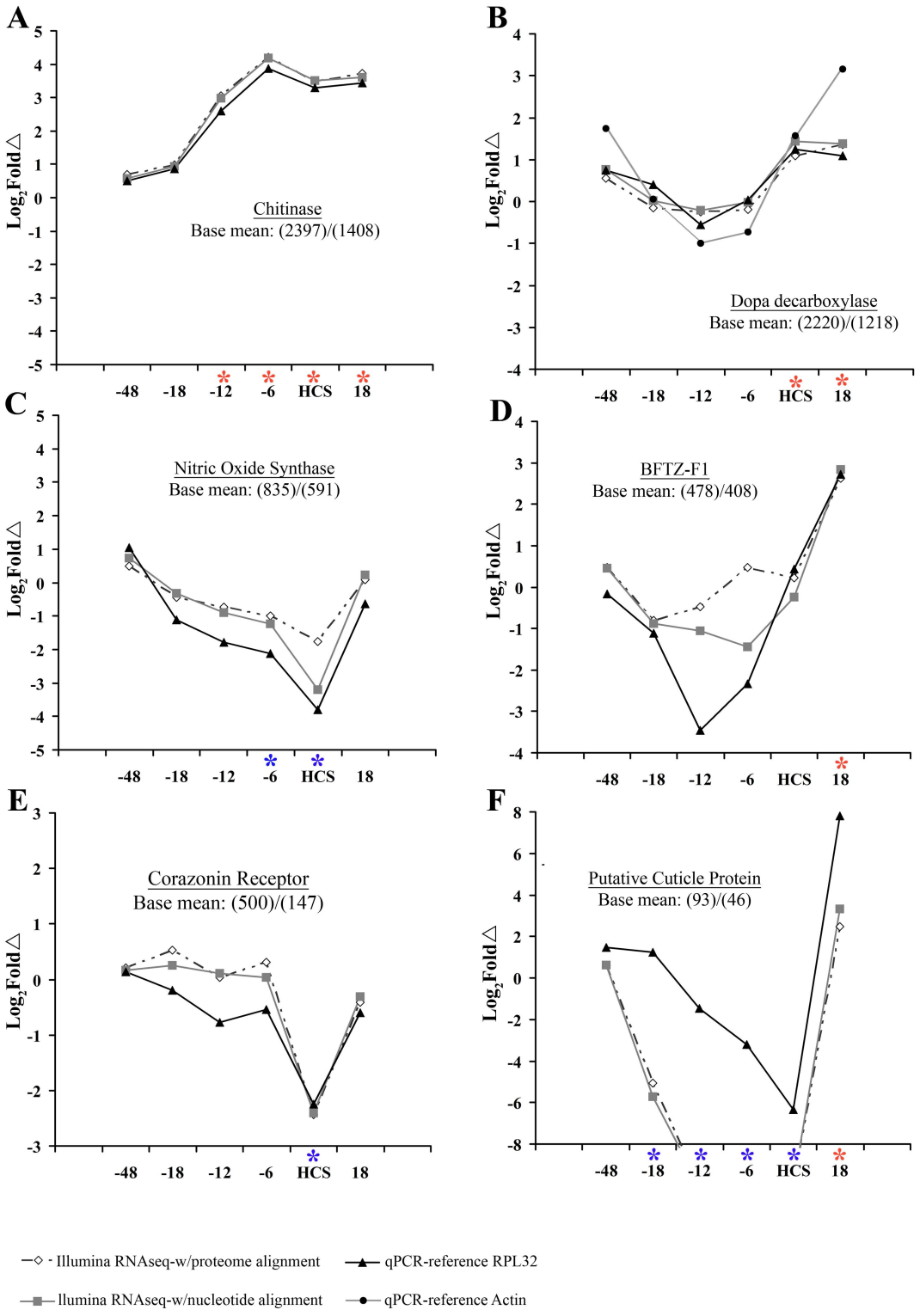
A
Chitinase
Base mean: (2397)/(1408)
B
Dopa decarboxylase
Base mean: (2220)/(1218)
C
Nitric Oxide Synthase
Base mean: (835)/(591)
D
BFTZ-F1
Base mean: (478)/408)
E
Corazonin Receptor
Base mean: (500)/(147)
F
Putative Cuticle Protein
Base mean: (93)/(46)
Log2Fold△
-48 -18 -12 -6 HCS 18
Illumina RNAseq-w/proteome alignment
Illumina RNAseq-w/nucleotide alignment
qPCR-reference RPL32
qPCR-reference Actin

Figure 3-16. Enriched GO terms at HCS -18 and -12 hrs. Sets of significantly up- and down-regulated genes detected for the stages HCS -18 hrs and -12 hrs were tested for the enrichment of GO terminologies. (Fisher's Exact Test corrected for multiple testing, $p<0.05$). Enriched terms were detected only in the set of up-regulated genes. Of the 335 genes up-regulated the stages HCS -18 and -12hrs, 239 had been annotated by Blast2go. The reference set was composed of the entire set of 8,831 genes that were annotated in this study. Shown are the significant GO terminologies arranged by the GO categories biological process (BP), molecular function (MF) and cellular component (CC). Directed acyclic graphs were used to display more general unifying terms in each category. The percentage of sequences in each enriched GO category are shown for test (blue) and reference (black) sets.

Figure 3-16

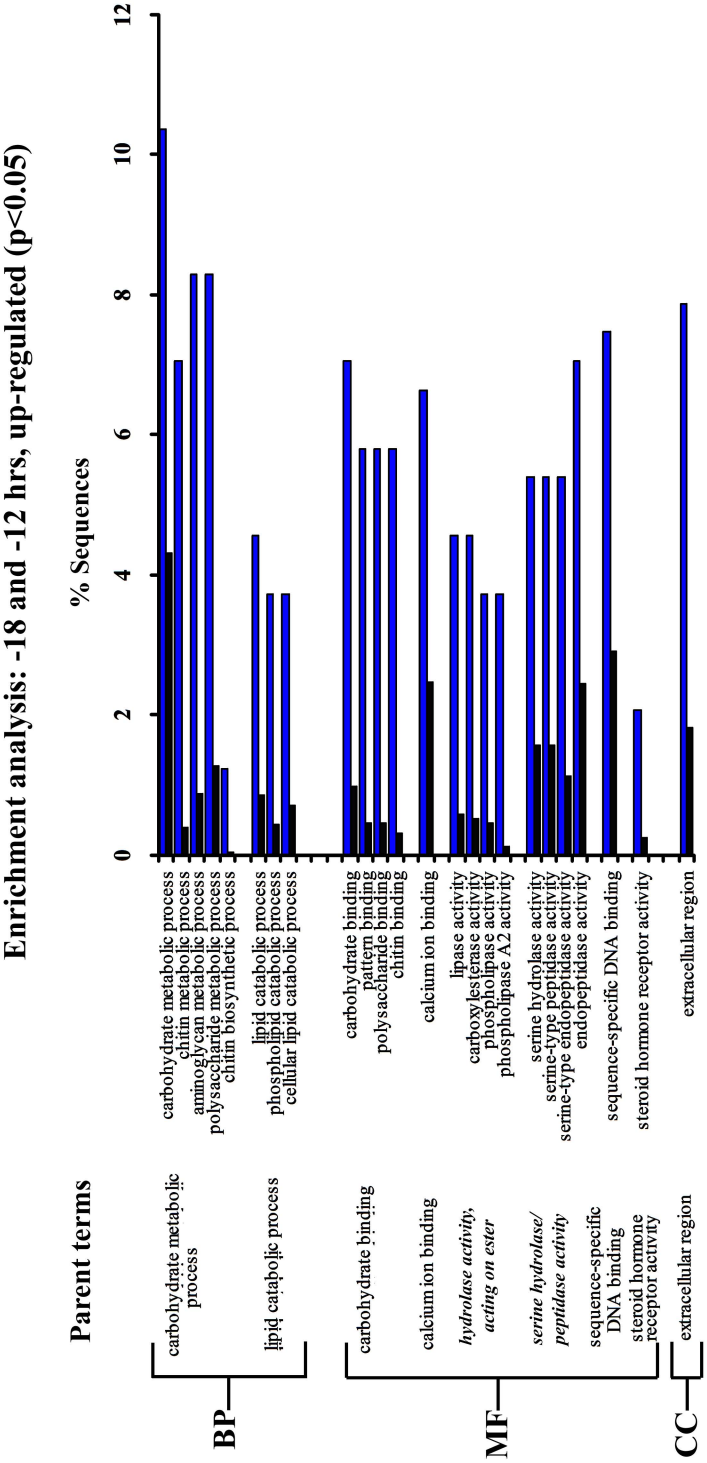
Enrichment analysis: -18 and -12 hrs, up-regulated (p<0.05)
% Sequences
0
2
4
6
8
10
12
carbohydrate metabolic process
chitin metabolic process
aminoglycan metabolic process
polysaccharide metabolic process
chitin biosynthetic process
lipid catabolic process
phospholipid catabolic process
cellular lipid catabolic process
carbohydrate binding
pattern binding
polysaccharide binding
chitin binding
calcium ion binding
lipase activity
carboxylesterase activity
phospholipase activity
phospholipase A2 activity
serine hydrolase activity
serine-type peptidase activity
serine-type endopeptidase activity
endopeptidase activity
sequence-specific DNA binding
steroid hormone receptor activity
extracellular region
Parent terms
BP
carbohydrate metabolic process
lipid catabolic process
MF
carbohydrate binding
calcium ion binding
hydrolase activity, acting on ester
serine hydrolase/ peptidase activity
sequence-specific DNA binding
steroid hormone receptor activity
CC
extracellular region

Figure 3-17. Enriched GO terms at HCS -6 hrs. Sets of significantly up- and down-regulated genes detected for the stage HCS -6hrs were tested for the enrichment of GO terminologies. (Fisher's Exact Test corrected for multiple testing, $p<0.05$). Enriched terms were detected only in both the set of up-regulated **(A)** and the set of down-regulated **(B)** genes. The set of up-regulated and down-regulated genes contained 251 and 218 Blast2go annotated genes, respectively. The reference set was composed of the entire set of 8,831 genes that were annotated in this study. Shown are the significant GO terminologies arranged by the GO categories biological process (BP), molecular function (MF) and cellular component (CC). Directed acyclic graphs were used to display more general unifying terms in each category. The percentage of sequences in each enriched GO category are shown for test (blue) and reference (black) sets.

Figure 3-17

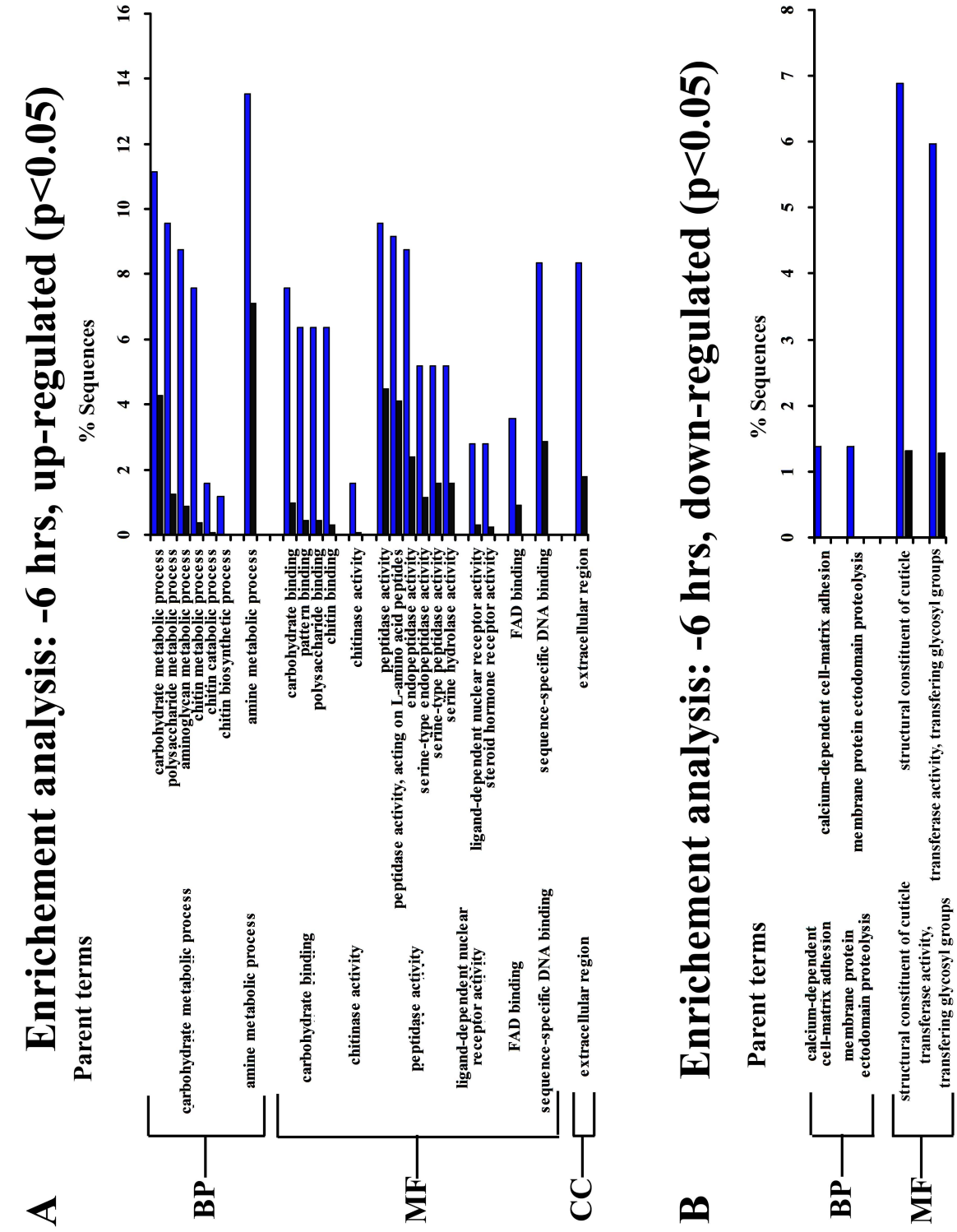
A
Enrichement analysis: -6 hrs, up-regulated (p<0.05)
Parent terms
% Sequences
0
2
4
6
8
10
12
14
16
BP
carbohydrate metabolic process
amine metabolic process
MF
carbohydrate binding
chitinase activity
peptidase activity
ligand-dependent nuclear receptor activity
FAD binding
sequence-specific DNA binding
CC
extracellular region
carbohydrate metabolic process
polysaccharide metabolic process
aminoglycan metabolic process
chitin metabolic process
chitin catabolic process
chitin biosynthetic process
amine metabolic process
carbohydrate binding
pattern binding
polysaccharide binding
chitin binding
chitinase activity
peptidase activity, acting on L-amino acid peptides
endopeptidase activity
serine-type endopeptidase activity
serine-type peptidase activity
serine hydrolase activity
ligand-dependent nuclear receptor activity
steroid hormone receptor activity
FAD binding
sequence-specific DNA binding
extracellular region
B
Enrichement analysis: -6 hrs, down-regulated (p<0.05)
Parent terms
% Sequences
0
1
2
3
4
5
6
7
8
BP
calcium-dependent cell-matrix adhesion
membrane protein ectodomain proteolysis
MF
structural constituent of cuticle
transferase activity, transfering glycosyl groups
calcium-dependent cell-matrix adhesion
membrane protein ectodomain proteolysis
structural constituent of cuticle
transferase activity, transfering glycosyl groups

Figure 3-18. Enriched GO terms at the time of HCS. Sets of significantly up- and down-regulated genes detected for the stage at time of HCS were tested for the enrichment of GO terminologies. (Fisher's Exact Test corrected for multiple testing, $p<0.05$). Enriched terms were detected only in both the set of up-regulated **(A)** and the set of down-regulated **(B)** genes. The set of up-regulated and down-regulated genes contained 398 and 263 Blast2go annotated genes, respectively. The reference set was composed of the entire set of 8,831 genes that were annotated in this study. Shown are the significant GO terminologies arranged by the GO categories biological process (BP), molecular function (MF) and cellular component (CC). Directed acyclic graphs were used to display more general unifying terms in each category. The percentage of sequences in each enriched GO category are shown for test (blue) and reference (black) sets.

Figure 3-18

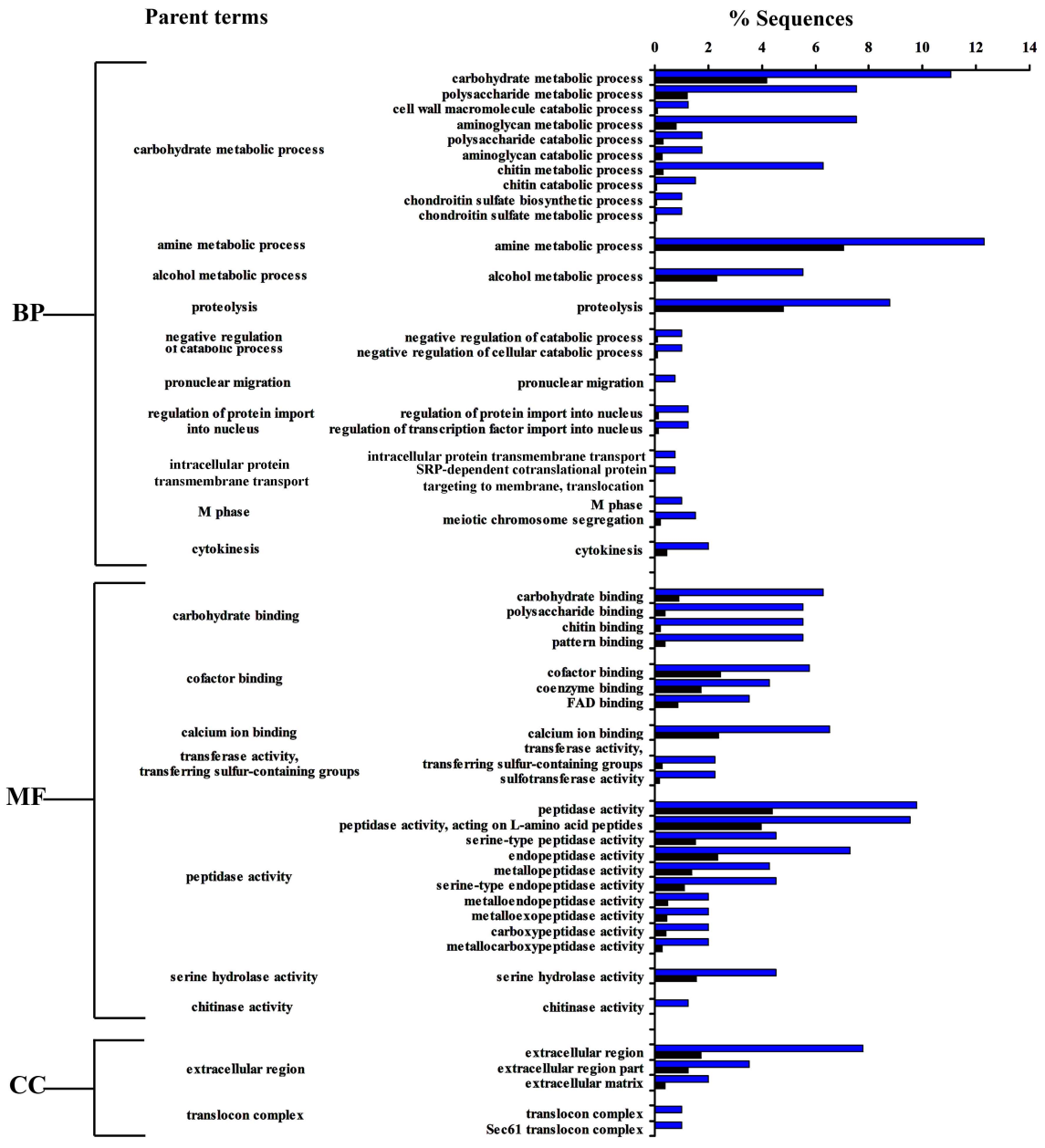
A Enrichment analysis: HCS, up-regulated (p<0.05)
Parent terms
% Sequences
0
2
4
6
8
10
12
14
BP
MF
CC
carbohydrate metabolic process
amine metabolic process
alcohol metabolic process
proteolysis
negative regulation of catabolic process
pronuclear migration
regulation of protein import into nucleus
intracellular protein transmembrane transport
M phase
cytokinesis
carbohydrate binding
cofactor binding
calcium ion binding
transferase activity, transferring sulfur-containing groups
peptidase activity
serine hydrolase activity
chitinase activity
extracellular region
translocon complex
carbohydrate metabolic process
polysaccharide metabolic process
cell wall macromolecule catabolic process
aminoglycan metabolic process
polysaccharide catabolic process
aminoglycan catabolic process
chitin metabolic process
chitin catabolic process
chondroitin sulfate biosynthetic process
chondroitin sulfate metabolic process
amine metabolic process
alcohol metabolic process
proteolysis
negative regulation of catabolic process
negative regulation of cellular catabolic process
pronuclear migration
regulation of protein import into nucleus
regulation of transcription factor import into nucleus
intracellular protein transmembrane transport
SRP-dependent cotranslational protein targeting to membrane, translocation
M phase
meiotic chromosome segregation
cytokinesis
carbohydrate binding
polysaccharide binding
chitin binding
pattern binding
cofactor binding
coenzyme binding
FAD binding
calcium ion binding
transferase activity, transferring sulfur-containing groups
sulfotransferase activity
peptidase activity
peptidase activity, acting on L-amino acid peptides
serine-type peptidase activity
endopeptidase activity
metallopeptidase activity
serine-type endopeptidase activity
metalloendopeptidase activity
metalloexopeptidase activity
carboxypeptidase activity
metallocarboxypeptidase activity
serine hydrolase activity
chitinase activity
extracellular region
extracellular region part
extracellular matrix
translocon complex
Sec61 translocon complex

Figure 3-18 (Cont'd)

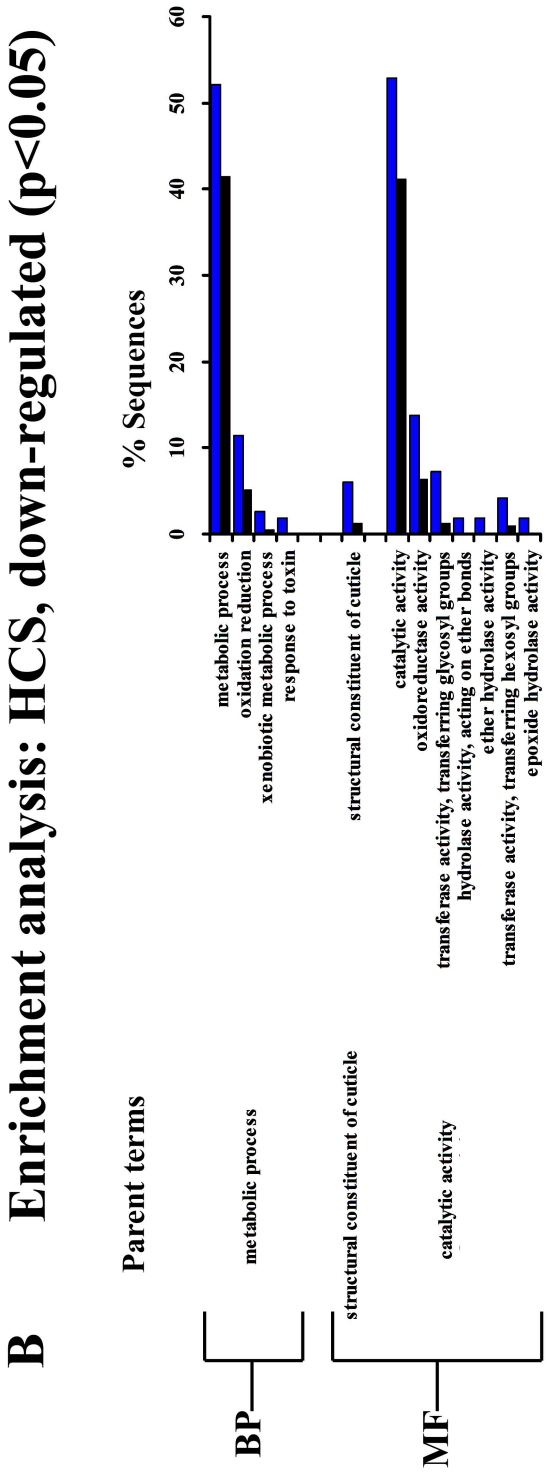

Figure 3-19. Enriched GO terms at HCS +18 hrs. Sets of significantly up- and down-regulated genes detected for the stage HCS +18 hrs were tested for the enrichment of GO terminologies. (Fisher's Exact Test corrected for multiple testing, $p<0.05$). Enriched terms were detected only in both the set of up-regulated **(A)** and the set of down-regulated **(B)** genes. The set of up-regulated and down-regulated genes contained 422 and 109 Blast2go annotated genes, respectively. The reference set was composed of the entire set of 8,831 genes that were annotated in this study. Shown are the significant GO terminologies arranged by the GO categories biological process (BP), molecular function (MF) and cellular component (CC). Directed acyclic graphs were used to display more general unifying terms in each category. The percentage of sequences in each enriched GO category are shown for test (blue) and reference (black) sets.

Figure 3-19

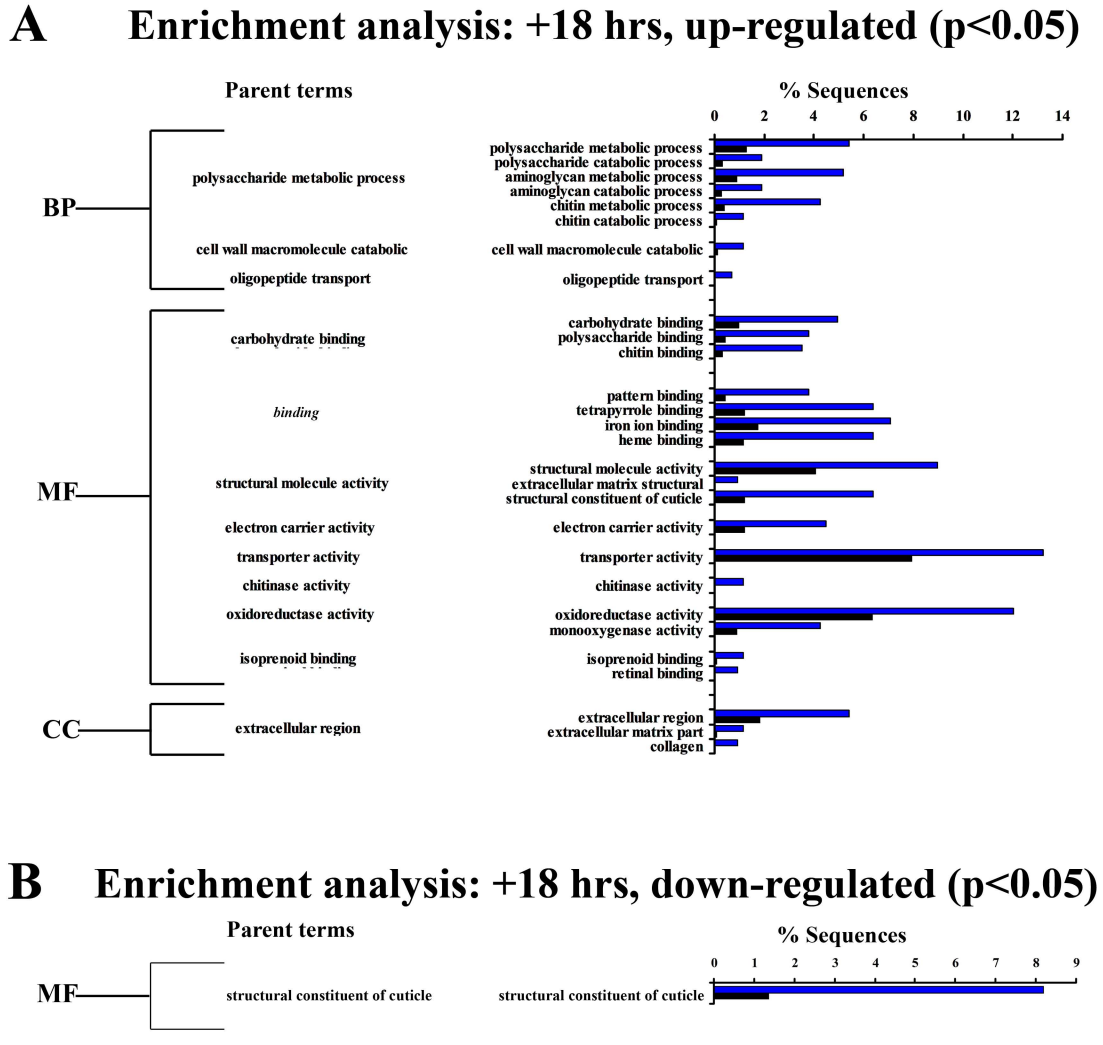
A
Enrichment analysis: +18 hrs, up-regulated (p<0.05)
Parent terms
% Sequences
0
2
4
6
8
10
12
14
BP
MF
CC
polysaccharide metabolic process
cell wall macromolecule catabolic
oligopeptide transport
carbohydrate binding
binding
structural molecule activity
electron carrier activity
transporter activity
chitinase activity
oxidoreductase activity
isoprenoid binding
extracellular region
polysaccharide metabolic process
polysaccharide catabolic process
aminoglycan metabolic process
aminoglycan catabolic process
chitin metabolic process
chitin catabolic process
cell wall macromolecule catabolic
oligopeptide transport
carbohydrate binding
polysaccharide binding
chitin binding
pattern binding
tetrapyrrole binding
iron ion binding
heme binding
structural molecule activity
extracellular matrix structural
structural constituent of cuticle
electron carrier activity
transporter activity
chitinase activity
oxidoreductase activity
monooxygenase activity
isoprenoid binding
retinal binding
extracellular region
extracellular matrix part
collagen
B
Enrichment analysis: +18 hrs, down-regulated (p<0.05)
Parent terms
% Sequences
0
1
2
3
4
5
6
7
8
9
MF
structural constituent of cuticle
structural constituent of cuticle

Figure 3-20. Enriched GO terms at HCS -48 hrs. Sets of significantly up- and down-regulated genes detected for the stage HCS -48hrs were tested for the enrichment of GO terminologies. (Fisher's Exact Test corrected for multiple testing, $p<0.05$). Enriched terms were detected only in both the set of up-regulated **(A)** and the set of down-regulated **(B)** genes. The set of up-regulated and down-regulated genes contained 205 and 79 Blast2go annotated genes, respectively. The reference set was composed of the entire set of 8,831 genes that were annotated in this study. Shown are the significant GO terminologies arranged by the GO categories biological process (BP), molecular function (MF) and cellular component (CC). Directed acyclic graphs were used to display more general unifying terms in each category. The percentage of sequences in each enriched GO category are shown for test (blue) and reference (black) sets.

Figure 3-20

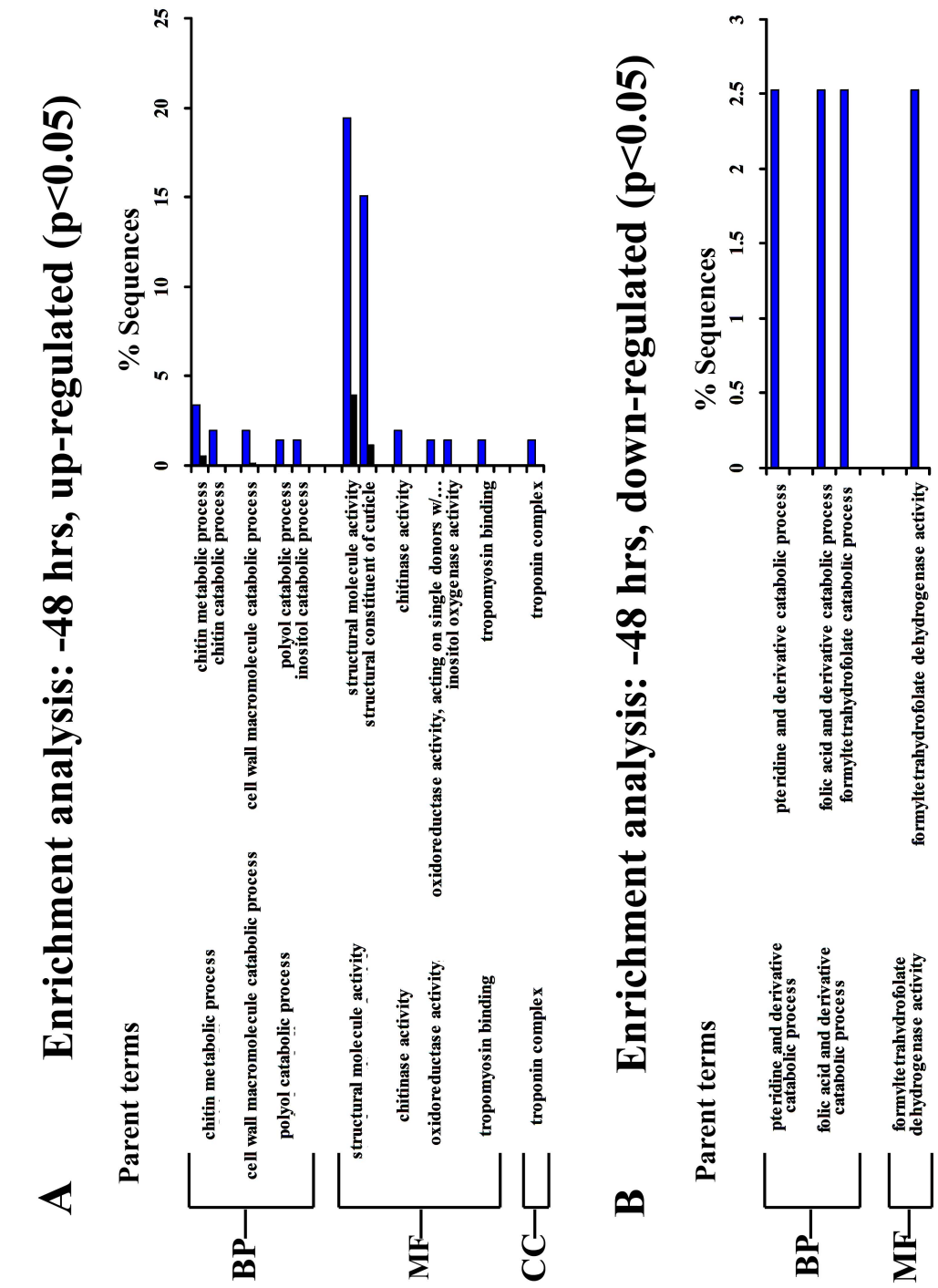
A
Enrichment analysis: -48 hrs, up-regulated (p<0.05)
Parent terms
% Sequences
0
5
10
15
20
25
BP
MF
CC
chitin metabolic process
cell wall macromolecule catabolic process
polyol catabolic process
structural molecule activity
chitinase activity
oxidoreductase activity
tropomyosin binding
troponin complex
chitin metabolic process
chitin catabolic process
cell wall macromolecule catabolic process
polyol catabolic process
inositol catabolic process
structural molecule activity
structural constituent of cuticle
chitinase activity
oxidoreductase activity, acting on single donors w/...
inositol oxygenase activity
tropomyosin binding
troponin complex
B
Enrichment analysis: -48 hrs, down-regulated (p<0.05)
Parent terms
% Sequences
0
0.5
1
1.5
2
2.5
3
BP
MF
pteridine and derivative catabolic process
folic acid and derivative catabolic process
formyltetrahydrofolate dehydrogenase activity
pteridine and derivative catabolic process
folic acid and derivative catabolic process
formyltetrahydrofolate catabolic process
formyltetrahydrofolate dehydrogenase activity

Figure 3-21. Transcription factors and transcription factor regulation. Shown is a list of putative transcription factors and transcription factor regulators that are differentially expressed (absolute fold change over 2-fold) during at least one developmental stage. SilkDB gene ID's are shown, along with $\log_2$fold changes at stages relative to HCS (-18 hrs, -12 hrs, -6 hrs, time of HCS, +18 hrs and -48 hrs). All fold changes are shown, but significant fold-changes (>2 or <0.5, $p<0.1$) are colored in (A, B) red (significantly up-regulated) or (B, C) blue (significantly down-regultated). Blast2go descriptions are also provided. Each of the corresponding SilkDB proteins were reciprocally blasted (blastx) using FlyBase, and FlyBase gene ID's belonging to orthologs, along with their descriptions (when available). Reciprocal blasting in NCBI (using *M. sexta* gene subset) was also used to identify putative *M. sexta* orthologs, and NCBI accession numbers and descriptions are also provided, when available.

Figure 3-21

A

B. mori Gene ID	-18	-12	-6	HCS	18	-48	BLAST2GO sequence description	RB (*D. mel*)	*D. melantogaster* sequence description	RB (*M. sext*)
BGIBMGA013421	2.2	3.6	4.8	3.8	2.8	1.6	isoform c	CG14029	vrille	
BGIBMGA009687	1.5	4.7	7.9	6.1	1.9	0.0	hormone receptor 3			
BGIBMGA000988	1.1	2.3	2.7	2.8	-0.8	-0.5	zinc finger transcription factor	CG6824	ovo	
BGIBMGA004355	1.2	1.7	2.3	2.5	-1.0	-0.6	zinc finger	CG12212	pebbled	
BGIBMGA004584	2.9	3.1	3.9	1.8	0.6	3.1	glis family zinc finger 1	CG4677	lame duck	
BGIBMGA008843	2.2	2.3	2.2	1.8	0.0	2.1	sister of odd and bowl	CG3242	sister of odd and bowl	
BGIBMGA003233	1.6	0.1	1.2	1.5	-0.1	1.9	gbx homeobox protein	CG1650	unplugged	
BGIBMGA006400	1.5	0.4	-1.0	-0.1	0.1	-0.5	homeotic protein proboscipedia	CG31481	proboscipedia	
BGIBMGA006638	1.4	0.6	1.5	-1.4	0.6	1.5	calcitonin gene-related peptide-rec..	CG4875	Receptor component protein	
BGIBMGA005669	1.1	0.1	0.4	0.0	-0.7	-0.6	forkhead box j protein			
BGIBMGA013412	1.3	0.9	1.1	-0.2	0.9	0.6	mediator of rna polymerase ii transcript..	CG1793	Mediator complex subunit 26	
BGIBMGA011052	0.7	1.2	1.6	1.7	1.5	-0.1	pftaire-interacting factor 1a	CG42599	PIF-1A	
BGIBMGA003624	0.5	1.5	1.4	2.7	3.2	0.9	isoform a	CG13188	no name	
BGIBMGA007888	1.0	2.6	5.1	4.8	3.1	0.4	hormone receptor 4	CG16902	Hr4	AF288088.1
BGIBMGA009688	0.6	3.2	6.2	4.9	1.5	-0.2	hormone receptor 3	CG33183	Hormone receptor-like in 46; DHR3	X74566.1
BGIBMGA000305	0.9	1.6	2.1	2.7	0.8	0.6	mesenchymal stem cell protein dscd75	CG4666	no name	
BGIBMGA003895	0.5	1.4	2.4	1.3	0.0	-0.2	ecdysone-induced protein 78c	CG18023	Ecdysone-induced protein 78C	
BGIBMGA000874	0.9	2.2	2.9	1.6	-1.4	-0.5	CREB	CG7450	CREB	
BGIBMGA006839	0.6	1.5	2.1	1.2	-0.9	-0.6	ecdysone-induced protein 75b	CG8127	Ecdysone-induced protein 75B	S60738.1
BGIBMGA014069	0.4	1.4	1.8	1.7	0.4	-0.4	isoform d	CG42599	no name; aka PIF-1A	
BGIBMGA010185	0.5	0.9	1.4	1.3	1.6	0.0	trachealess	CG42865	trachealess	
BGIBMGA002551	0.4	1.1	1.7	0.5	-0.1	0.0	zinc finger	CG1322	Zn finger homeodomain 1	
BGIBMGA012028	0.6	3.1	3.3	2.2	-Inf	2.1	pentatricopeptide repeat protein 1	CG4611	no name	
BGIBMGA000639	0.8	1.6	1.4	0.8	-0.3	-0.5	iroquois-class homeodomain protein irx	CG10601	mirror	
BGIBMGA010929	0.7	1.6	-0.4	-0.7	0.5	-0.2	class b basic helix-loop-helix protein	CG17100	clockwork orange	
BGIBMGA001148	1.6	3.1	2.3	0.2	0.6	2.1	lethal of scute			
BGIBMGA010667	0.6	0.7	1.3	1.1	0.6	1.2	tata-box-binding protein			
BGIBMGA000670	-0.5	0.9	1.6	0.3	-0.5	0.0	nuclear receptor			
BGIBMGA001460	0.5	0.8	1.1	0.7	0.0	-0.3	CREB			

Figure 3-21 (Cont'd)

A (con't)

B. mori Gene ID	-18	-12	-6	HCS	18	-48	BLAST2GO sequence description	RB (*D. mel*)	*D. melantogaster* sequence description	RB (*M. sext*)
BGIBMGA007914	0.1	0.8	1.2	0.1	0.7	0.1	nuclear hormone receptor ftz-f1 beta	CG8676	Hormone receptor-like in 39	
BGIBMGA003623	0.4	1.3	1.5	2.4	2.9	-0.1	isoform a	CG13188	no name	
BGIBMGA003625	0.5	0.3	0.8	2.0	2.2	0.5	isoform a			
BGIBMGA006392	2.2	2.3	1.6	3.9	3.9	0.5	antennapedia protein	CG1028	Antennapedia	AAB39545.1
BGIBMGA006272	-1.4	-1.7	1.8	2.5	-1.4	-1.5	37-kda protease	CG4386	no name	
BGIBMGA000716	-0.8	-0.5	0.5	0.2	2.6	0.5	nuclear hormone receptor (ftz-f1 alpha)	CG4059	ftz transcription factor 1	AF288089.1
BGIBMGA003436	0.6	-1.3	0.0	-Inf	2.6	-1.0	gc-rich sequence dna-binding factor			
BGIBMGA003494	0.6	0.5	0.7	1.0	1.5	0.5	viral a-type inclusion protein repeat			
BGIBMGA003938	-0.6	-0.8	-0.2	0.6	2.7	0.0	transcription factor ts			
BGIBMGA003939	0.6	0.0	-0.1	0.6	3.3	0.4	e74-like factor 3			
BGIBMGA000498	0.2	-0.8	-0.1	0.5	0.9	1.4	circadian locomoter output cycles kaput			
BGIBMGA000838	NA	NA	Inf	Inf	NA	Inf	forkhead box protein	CG12632	forkhead domain 3F	
BGIBMGA001000	NA	NA	Inf	NA	Inf	Inf	lethal of scute			
BGIBMGA002652	1.0	1.5	1.3	2.0	1.0	1.5	centromeric protein	CG18304	no name	
BGIBMGA003556	1.0	0.7	1.0	0.3	0.4	1.3	general transcription factor 3c polypeptic	CG8950	no name	
BGIBMGA006899	0.8	0.8	0.9	0.8	0.6	1.2	e2f transcription factor 4			
BGIBMGA008390	0.2	0.0	-0.7	0.2	1.1	1.3	helix-loop-helix protein delilah	CG5441	delilah	
BGIBMGA010118	0.6	0.6	0.5	0.7	0.4	1.7	atp synthase subunit s-like protein	CG4042	no name	

B

B. mori Gene ID	-18	-12	-6	HCS	18	-48	BLAST2GO sequence description	RB (*D. mel*)	*D. melantogaster* sequence description	RB (*M. sext*)
BGIBMGA007970	-0.5	-0.5	-1.1	-1.2	1.1	0.0	transcription factor e74	CG32180	Ecdysone-induced protein 74EF	AY170859.1
BGIBMGA013687	-Inf	-Inf	-Inf	-Inf	3.4	-2.0	ccaat enhancer binding protein	CG4354	slow border cells	
BGIBMGA010184	0.0	0.5	0.9	0.9	1.4	-0.9	bm trachealess			
BGIBMGA011397	0.1	0.5	0.5	0.6	1.2	0.3	uncharacterized protein c11orf9-like prot	CG3328	no name	

Figure 3-21 (Cont'd)

C

B. mori Gene ID	-18	-12	-6	HCS	18	-48	BLAST2GO sequence description	RB (*D. mel*)	*D. melantogaster* sequence description	RB (*M. sext*)
BGIBMGA005771	-1.0	-1.1	-1.1	-1.1	0.2	-0.1	scm-like with four mbt domains 1			
BGIBMGA002995	-Inf	-Inf	-0.5	-Inf	-1.2	0.5	t-box transcription factor tbx20			
BGIBMGA010300	-1.2	-0.2	-2.9	-3.2	0.2	-0.9	pou class transcription factor 1			
BGIBMGA001001	-1.4	-1.1	-2.0	-1.7	-0.5	-0.8	lethal of scute	CG3839	lethal of scute	
BGIBMGA003159	-0.7	-1.1	-1.9	0.5	0.5	0.0	ubiquitin conjugating enzyme 7 interact..			
BGIBMGA004750	-0.1	-1.5	-1.5	-2.8	0.1	0.4	isoform b			
BGIBMGA008838	-0.5	-2.2	-1.8	-1.3	-1.9	-0.9	isoform a	CG11160	no name	
BGIBMGA003174	-0.7	-3.3	-1.6	-0.2	-Inf	-0.7	t-box protein			
BGIBMGA009798	-0.4	-Inf	-1.4	-2.8	-Inf	-0.1	homeobox protein engrailed			
BGIBMGA007968	-1.8	-3.7	-2.0	-1.8	0.4	-0.1	transcription factor e74 isoform a			
BGIBMGA003176	0.3	-Inf	-1.6	0.2	-1.0	-1.0	cg11617 cg11617-pa	CG11617	no name	
BGIBMGA004895	-1.1	-2.0	-0.4	0.1	-0.9	-0.6	cg6913	CG6913	48 related 3	
BGIBMGA003172	-2.0	-1.7	-Inf	-3.4	-Inf	-1.5	t-box transcription factor			
BGIBMGA013390	-0.1	-0.7	-2.0	-1.6	-1.1	-0.2	isoform f			
BGIBMGA003874	-0.2	-0.5	-1.2	-1.1	0.1	0.0	par domain protein	CG17888	PAR-domain protein 1	
BGIBMGA012680	0.1	-0.2	-1.1	-1.7	0.1	0.0	four and a half lim domains			
BGIBMGA003998	-0.2	0.4	-1.3	-0.8	0.0	-0.7	sorting nexin			
BGIBMGA003160	0.1	0.2	-0.3	-1.3	-1.9	-0.1	zinc finger protein	CG18783	Kruppel homolog 1	
BGIBMGA005390	-0.4	-0.9	-0.1	-2.2	-1.8	0.1	hairy	CG6494	hairy	
BGIBMGA007140	-0.9	-0.5	-0.8	-1.1	-0.3	-0.4	cryptochrome 1	CG3772	cryptochrome	
BGIBMGA009644	-0.4	-2.7	-1.4	-Inf	-Inf	-0.1	transcription factor	CG9015	engrailed	
BGIBMGA012517	-0.3	-0.2	-0.9	-1.4	-0.8	0.0	b-cell cll lymphoma 6 member b	CG34346	maternal gene required for meiosis	
BGIBMGA012004	0.0	0.2	-0.2	-0.7	-1.2	-0.6	diminutive	CG10798	diminutive	
BGIBMGA002964	-0.7	-0.3	0.1	-0.3	-2.7	-0.6	probable nuclear hormone receptor hr38	CG1864	Hormone receptor-like in 38	
BGIBMGA002109	-0.7	-0.5	0.4	0.0	-0.2	-Inf	set and mynd domain-containing	CG1868	no name	
BGIBMGA004050	-0.4	0.2	-1.2	-1.6	-0.4	-1.2	mucoepidermoid carcinoma translocated	CG6064	TORC	
BGIBMGA006182	-0.8	-0.8	-0.8	-0.6	-0.5	-1.1	transcription factor glial cells missing	CG12245	glial cells missing	
BGIBMGA008718	0.0	-0.2	-0.6	-0.4	0.0	-1.5	polymerase iii (dna directed) polypeptide	CG5147	no name	
BGIBMGA011356	-0.1	-0.6	-0.1	-0.8	-1.0	-1.9	homeobox protein dbx			
BGIBMGA013554	-1.3	-1.0	-0.4	-1.1	-1.0	-1.9	transcription factor	CG10034	traffic jam	

Figure 3-22. Transcription factor expression profiles. Shown are the expression profiles of 10 "classic" ecdysone cascade transcription factors that were identified as being significantly differentially expressed during at least one developmental stage. For each gene, $\log_2$fold change is plotted for each of the 6 developmental time-points sampled. All fold change is relative to expression levels at -30 hrs relative to HCS (mid-intermolt feeding-stage larvae). Shown are the expression levels at -48 hrs relative to HCS, -18 hrs, -12 hrs, -6 hrs, time of HCS, and 18 hrs following HCS (~9-12 hrs prior to the completion of ecdysis). SilkDB gene ID's are provided for each profile. Gene names (right of each profile) were determined using Blast2go, SilkDB, FlyBase and NCBI (*M. sexta* subset) databases. Gene names listed were confirmed using reciprocal blasts (rb). (Rb) with available, and characterized, *M. sexta* sequences took precedence. When gene names could not be confirmed by (rb), they were labeled with (?). Above are the average 1 hr fractions of quiescence (n=8) measured for 4th instar larvae in chapter 2. Shown is the profile from -48 to +18 hrs relative to HCS. E=early inter-molt stage, R=predicted rise of ecdysteroids, P=predicted peak of ecdysteroids, F=predicted fall of ecdysteroids, L=late molt when ecdysteroid levels of low. Predicted ecdysteroid levels are based on Langelan et al 2000.

Figure 3-22

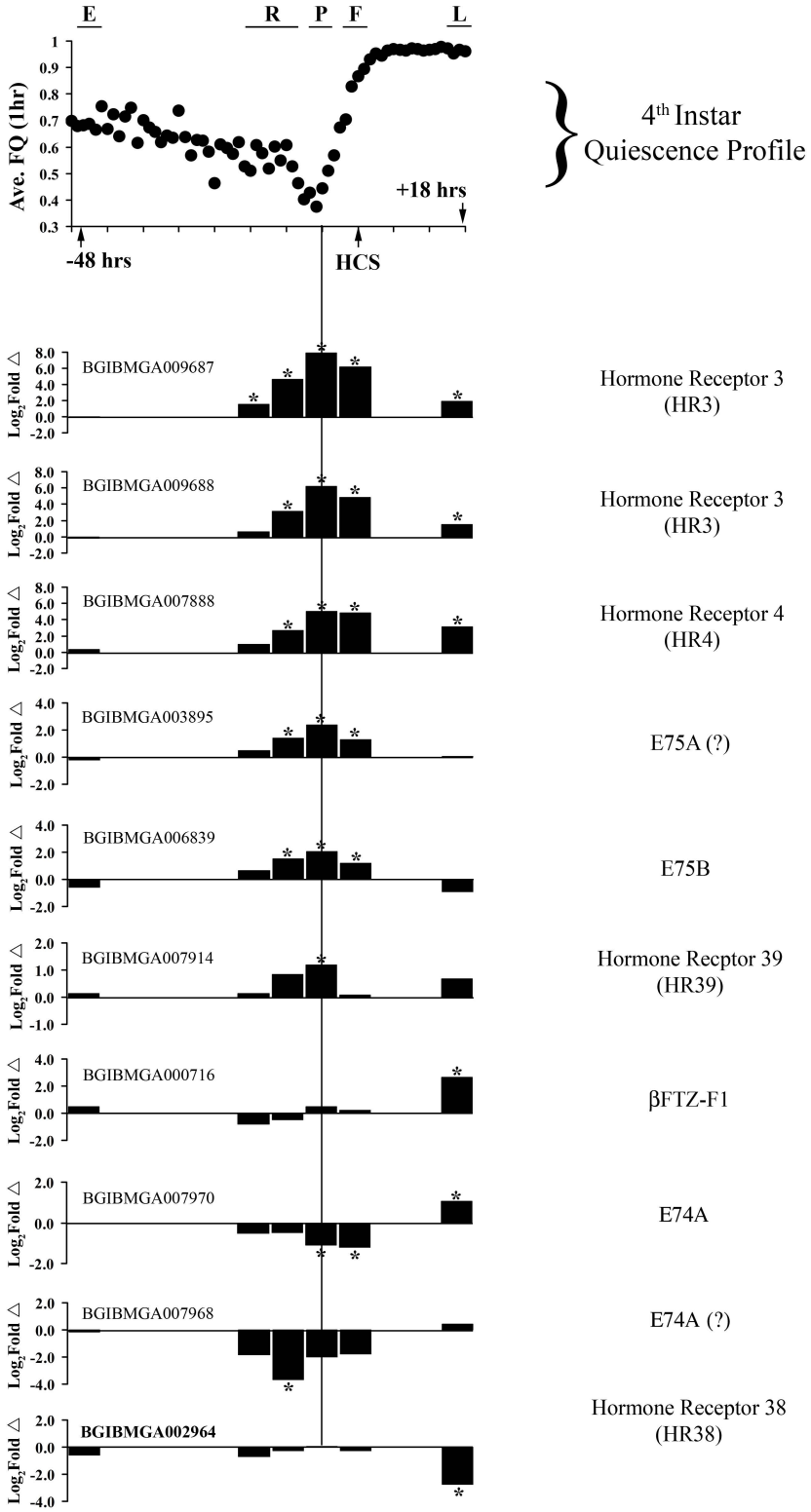
E
R
P
F
L
Ave. FQ (1hr)
+18 hrs
-48 hrs
HCS
4th Instar Quiescence Profile
BGIBMGA009687
Hormone Receptor 3 (HR3)
BGIBMGA009688
Hormone Receptor 3 (HR3)
BGIBMGA007888
Hormone Receptor 4 (HR4)
BGIBMGA003895
E75A (?)
BGIBMGA006839
E75B
BGIBMGA007914
Hormone Recptor 39 (HR39)
BGIBMGA000716
βFTZ-F1
BGIBMGA007970
E74A
BGIBMGA007968
E74A (?)
BGIBMGA002964
Hormone Receptor 38 (HR38)
Log2Fold Δ

Figure 3-23. STEM analysis. Above is a screen shot showing the 1,250 distinct expression profiles generated by the STEM algorithm (maximum unit change between time-points=2). Significant profiles are shaded, and similar profiles (correlation coefficient >0.7) are of the same shade. The input file contained the profiles of the 1,461 genes that showed significant differential expression during at least one of the sampled developmental stages. (This set of genes excludes the 383 genes that showed infinite fold changes). 34 significant profiles were detected (Bonferonni FDR <0.05).

Figure 3-23

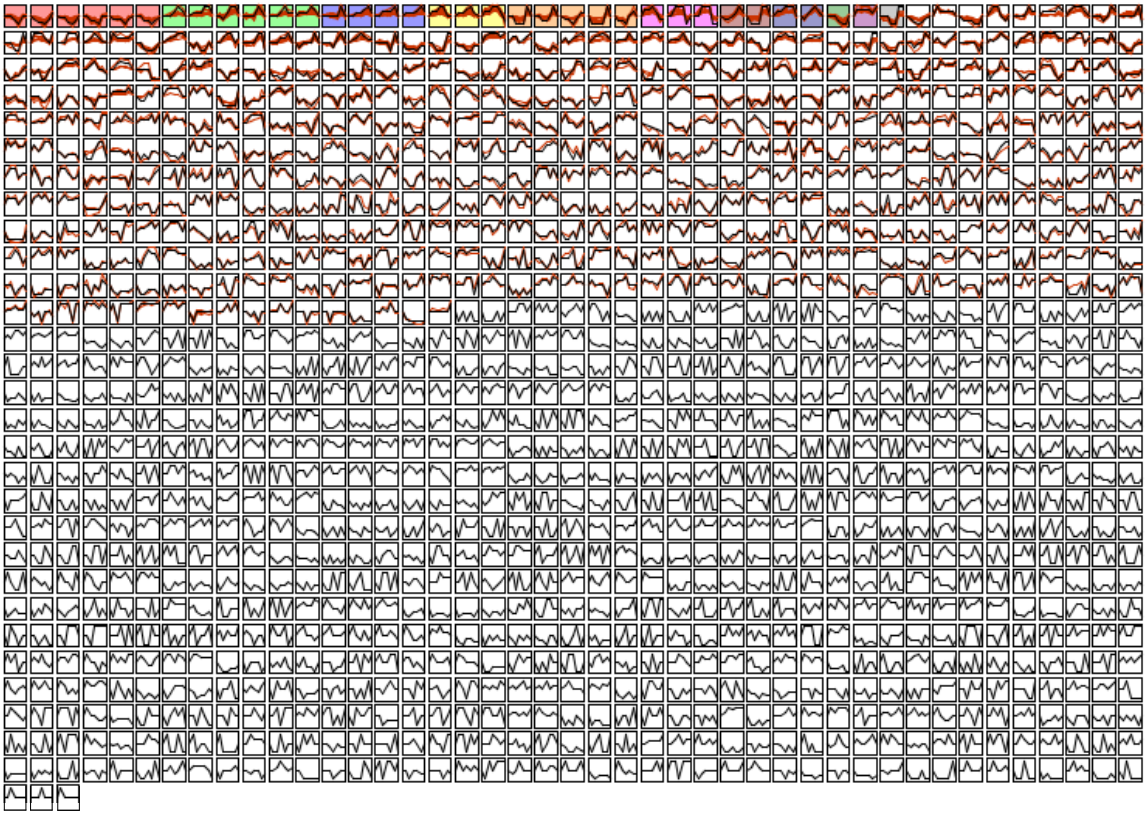

Figure 3-24. A close-up of the 34 significant expression profiles detected by STEM analysis. For each cluster, p-values are listed in the lower left, and profile # (from screen-shot) is listed in the upper right corner. Similar profiles are of the same shade, and form a total of 11 clusters (Clusters 0-10).

Figure 3-24

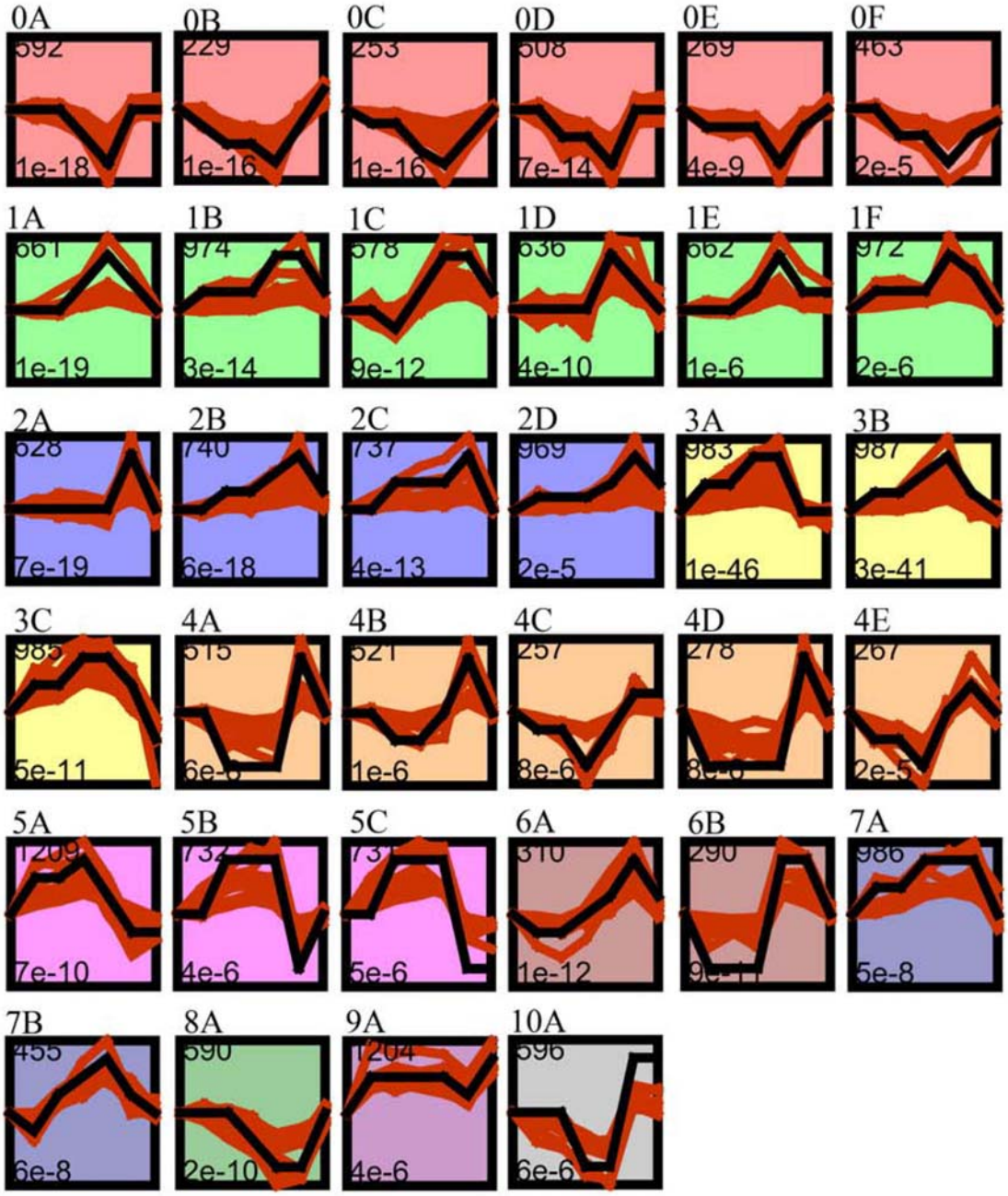
0A
592
1e-18
0B
229
1e-16
0C
253
1e-16
0D
508
7e-14
0E
269
4e-9
0F
463
2e-5
1A
661
1e-19
1B
974
3e-14
1C
578
9e-12
1D
536
4e-10
1E
662
1e-6
1F
972
2e-6
2A
628
7e-19
2B
740
6e-18
2C
737
4e-13
2D
969
2e-5
3A
983
1e-46
3B
987
3e-41
3C
985
5e-11
4A
515
6e-6
4B
521
1e-6
4C
257
8e-6
4D
278
4E
267
2e-5
5A
1209
7e-10
5B
732
4e-6
5C
737
5e-6
6A
310
1e-12
6B
290
7A
986
5e-8
7B
455
6e-8
8A
590
2e-10
9A
1204
4e-6
10A
596
6e-6

Figure 3-25. 11 clusters generated by STEM analysis. For each cluster, the expression profiles of all genes were plotted (as log_2fold changes) along with the average fold change (black squares). Developmental stage (relative to the time of HCS) is plotted in the order: -30 hrs (reference stage, fold-change=0), -18 hrs, -12 hrs, -6 hrs, time of HCS, +18 hrs and -48 hrs. The number of genes assigned to each cluster is as follows: Cluster 0 (n=95); Cluster 1 (n=87); Cluster 2 (n=90); Cluster 3 (n=82); Cluster 4 (n=47); Cluster 5 (n=29); Cluster 6 (n=27); Cluster 7 (n=21); Cluster 8 (n=12); Cluster 9 (n=9); Cluster 10 (n=8). Enriched GO terminologies were found for Clusters 0, 2, 3 and 4.

Figure 3-25

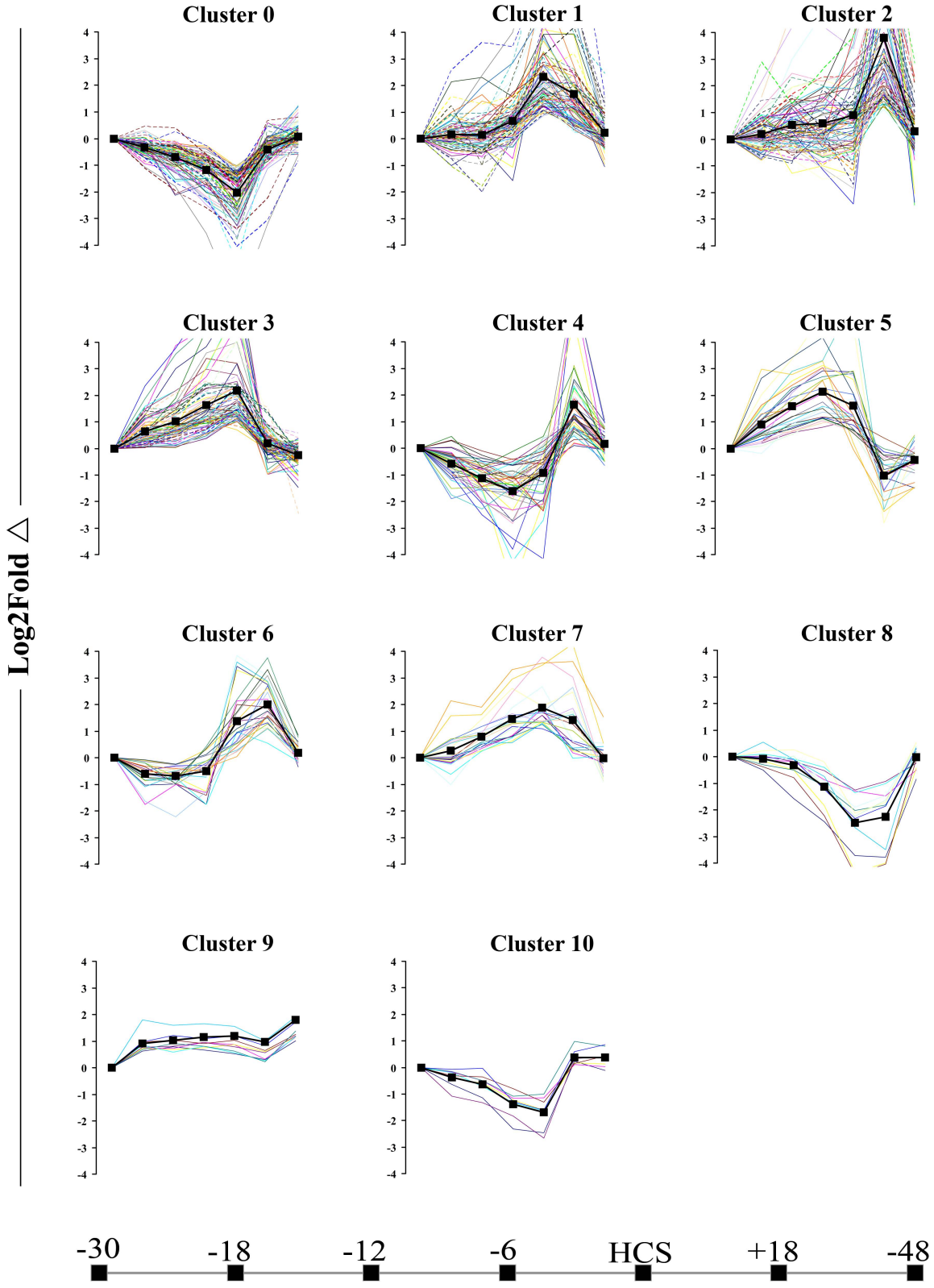
Cluster 0
Cluster 1
Cluster 2
Cluster 3
Cluster 4
Cluster 5
Cluster 6
Cluster 7
Cluster 8
Cluster 9
Cluster 10
Log2Fold △
-30
-18
-12
-6
HCS
+18
-48

Table 3-3. Enriched GO terminologies for Clusters C0, C2, C3, and C4. For each cluster, assigned gene-sets were tested for the enrichment of GO terminologies using the GOSSIP package integrated into Blast2go (Fisher's exact test, FDR <0.05). The set of 8,831 annotated genes were used as a reference set. For each cluster, enriched GO terminologies are listed in the order of significance.

Table 3-3

A

(Cluster 0) Enriched GO terms	FDR	#Seq
epoxide hydrolase activity	1.5E-04	4
ether hydrolase activity	1.5E-04	4
hydrolase activity, acting on ether bonds	5.2E-04	4
oxidoreductase activity	6.5E-04	19
metabolic process	1.1E-03	57
catalytic activity	1.4E-03	56
oxidation reduction	1.8E-03	16
response to toxin	3.4E-03	4
xenobiotic metabolic process	7.4E-03	5
heme binding	3.0E-02	7
tetrapyrrole binding	3.1E-02	7
monooxygenase activity	4.6E-02	6

B

(Cluster 2) Enriched GO terms	FDR	#Seq
carbohydrate binding	1.1E-02	7
chitin binding	1.1E-02	5
chitinase activity	1.5E-02	3
chitin metabolic process	1.6E-02	5
cationic amino acid transmembrane transporter activity	1.8E-02	2
pattern binding	1.8E-02	5
polysaccharide binding	1.8E-02	5
chitin catabolic process	1.8E-02	3
metallopeptidase activity	1.8E-02	7
polyamine transport	3.7E-02	2
cell wall macromolecule catabolic process	3.7E-02	3

Table 3-3 (Cont'd)

C

(Cluster 3) Enriched GO terms	FDR	#Seq
translocon complex	8.3E-06	4
Sec61 translocon complex	8.3E-06	4
SRP-dependent cotranslational protein targeting to membrane, translocation	2.2E-04	3
intracellular protein transmembrane transport	5.6E-04	3
serine-type endopeptidase activity	3.8E-03	7
endopeptidase activity	7.2E-03	9
negative regulation of autophagy	7.2E-03	3
Golgi cisterna membrane	1.2E-02	2
mitotic spindle organization	1.2E-02	5
negative regulation of catabolic process	1.2E-02	3
regulation of autophagy	1.2E-02	3
negative regulation of cellular catabolic process	1.2E-02	3
serine-type peptidase activity	1.2E-02	7
serine hydrolase activity	1.2E-02	7
organelle organization	2.3E-02	12
spindle organization	2.5E-02	5
microtubule cytoskeleton organization	2.7E-02	6
regulation of cellular catabolic process	3.3E-02	3
cell division	3.3E-02	6
cytokinesis	3.3E-02	4
cytoskeletal part	3.3E-02	9
regulation of catabolic process	4.7E-02	3
Golgi membrane	4.7E-02	3

D

(Cluster 4) Enriched GO terms	FDR	#Seq
cGMP biosynthetic process	2.8E-02	3
guanylate cyclase activity	2.8E-02	3
nucleoside monophosphate biosynthetic process	2.8E-02	4
cGMP metabolic process	2.8E-02	3
nucleoside monophosphate metabolic process	2.8E-02	4
GTP metabolic process	2.8E-02	3
heme binding	2.8E-02	5
tetrapyrrole binding	3.3E-02	5
cyclase activity	4.1E-02	3
cyclic nucleotide biosynthetic process	4.2E-02	3

Table 3-4. Heavily annotated GO terminologies for the 11 detected clusters. For each of the 11 clusters detected by STEM analysis, heavily annotated GO terminologies were detected by calculating node scores using Blast2go. Only the top 10 GO terminologies (most annotated nodes) for the categories biological process (BP), molecular function (MF) and cellular component (CC) are listed. Prior to selection, GO terminologies were filtered by level so that only GO terminologies from level 3 or below are shown.

Table 3-4

(C0) N=95

MF			BP			CC		
Graph Level	**GO Term**	**#Seq**	**Graph Level**	**GO Term**	**#Seq**	**Graph Level**	**GO Term**	**#Seq**
3	oxidoreductase activity	19	3	oxidation reduction	16	3	cell part	43
4	heme binding	7	4	transport	20	4	membrane	26
3	hydrolase activity	19	5	transmembrane transport	11	5	cytoplasm	18
3	transferase activity	15	3	primary metabolic process	31	6	integral to membrane	10
5	metal ion binding	15	3	cellular metabolic process	25	4	intracellular part	20
4	cation binding	17	3	establishment of localization	22	5	cytoplasmic part	11
4	monooxygenase activity	6	3	response to chemical stimulus	8	5	intrinsic to membrane	11
6	transition metal ion binding	11	5	ion transport	11	4	membrane part	11
4	transferase activity, transferring glycosyl groups	6	6	cation transport	7	7	mitochondrion	6
4	coenzyme binding	5	3	biosynthetic process	16	4	intracellular	20

(C1) N=87

MF			BP			CC		
Graph Level	**GO Term**	**#Seq**	**Graph Level**	**GO Term**	**#Seq**	**Graph Level**	**GO Term**	**#Seq**
3	protein binding	13	3	multicellular organismal development	15	3	cell part	45
7	zinc ion binding	6	5	transmembrane transport	8	4	membrane	27
6	transition metal ion binding	10	4	transport	16	6	integral to membrane	10
3	oxidoreductase activity	8	3	primary metabolic process	28	4	intracellular part	22
4	cation binding	13	3	anatomical structure development	13	4	intracellular	25
5	metal ion binding	11	4	anatomical structure morphogenesis	10	5	intrinsic to membrane	12
6	serine-type endopeptidase activity	4	4	system development	12	5	cytoplasm	15
6	FAD binding	4	5	signal transduction	5	5	intracellular organelle	17
5	chitin binding	4	4	regulation of cellular process	14	4	intracellular organelle part	12
7	ATP binding	4	6	chitin metabolic process	5	5	cytoplasmic part	12

Table 3-4 (Cont'd)

(C2) N=90

MF			BP			CC		
Graph Level	**GO Term**	**#Seq**	**Graph Level**	**GO Term**	**#Seq**	**Graph Level**	**GO Term**	**#Seq**
3	protein binding	9	4	transport	16	3	cell part	32
3	oxidoreductase activity	10	3	primary metabolic process	31	4	membrane	20
5	peptidase activity, acting on L-amino acid peptides	9	5	proteolysis	10	6	integral to membrane	9
6	transition metal ion binding	11	3	establishment of localization	17	4	intracellular	14
4	cation binding	16	3	oxidation reduction	7	5	intrinsic to membrane	10
6	metallopeptidase activity	7	3	macromolecule metabolic process	21	4	membrane part	12
5	metal ion binding	13	4	protein metabolic process	11	3	protein complex	7
3	hydrolase activity	18	3	multicellular organismal development	10	5	cytoplasm	6
7	zinc ion binding	5	4	lipid metabolic process	7	5	plasma membrane	4
5	chitin binding	5	3	cellular metabolic process	15	4	intracellular part	8

(C3) N=82

MF			BP			CC		
Graph Level	**GO Term**	**#Seq**	**Graph Level**	**GO Term**	**#Seq**	**Graph Level**	**GO Term**	**#Seq**
7	ATP binding	8	5	proteolysis	9	3	cell part	42
3	protein binding	14	3	primary metabolic process	25	4	membrane	22
6	serine-type endopeptidase activity	7	3	organelle organization	14	5	cytoplasmic part	20
3	hydrolase activity	20	4	mitotic cell cycle	8	3	protein complex	17
6	endopeptidase activity	9	3	cell cycle	9	4	intracellular part	32
6	adenyl ribonucleotide binding	8	4	microtubule cytoskeleton organization	7	5	cytoplasm	23
5	metal ion binding	10	4	protein metabolic process	13	5	intracellular organelle	29
5	serine-type peptidase activity	7	4	transport	14	4	intracellular organelle part	21
7	zinc ion binding	4	5	mitotic spindle organization	5	6	intracellular membrane-bounded organelle	20
	calcium ion binding	4	3	macromolecule metabolic process	20	6	integral to membrane	9

Table 3-4 (Cont'd)

(C4) N=47

MF			BP			CC		
Graph Level	**GO Term**	**#Seq**	**Graph Level**	**GO Term**	**#Seq**	**Graph Level**	**GO Term**	**#Seq**
4	heme binding	5	3	oxidation reduction	5	3	cell part	18
6	transition metal ion binding	9	3	primary metabolic process	19	6	integral to membrane	7
7	zinc ion binding	4	3	multicellular organismal development	5	6	intracellular membrane-bounded organelle	7
5	metal ion binding	10	3	cellular metabolic process	14	5	cytoplasmic part	6
3	nucleic acid binding	5	6	purine base metabolic process	4	5	intrinsic to membrane	7
3	tetrapyrrole binding	5	3	small molecule metabolic process	9	4	membrane	9
4	guanylate cyclase activity	3	8	GTP metabolic process	3	4	intracellular part	8
3	oxidoreductase activity	5	5	signal transduction	3	7	nucleus	3
7	iron ion binding	5	7	cGMP biosynthetic process	3	5	intracellular organelle	7
3	nucleotide binding	2	5	cellular amino acid metabolic process	3	4	intracellular	9

(C5) N=29

MF			BP			CC		
Graph Level	**GO Term**	**#Seq**	**Graph Level**	**GO Term**	**#Seq**	**Graph Level**	**GO Term**	**#Seq**
4	cation binding	7	3	primary metabolic process	15	3	cell part	11
5	metal ion binding	4	5	proteolysis	4	5	cytoplasm	6
7	zinc ion binding	3	5	cellular amino acid metabolic process	2	3	protein complex	4
4	DNA binding	3	3	cellular metabolic process	9	8	transcription factor complex	3
7	metalloendopeptidase activity	3	5	signal transduction	3	4	membrane	4
5	sequence-specific DNA binding	3	4	protein metabolic process	5	6	nucleoplasm part	3
3	protein binding	4	3	macromolecule metabolic process	11	4	intracellular part	8
3	ion binding	7	6	salivary gland cell autophagic cell death	3	5	cytoplasmic part	4
6	endopeptidase activity	4	3	cell adhesion	3	6	lipid particle	2
6	transition metal ion binding	3	4	regulation of cellular process	5	5	plasma membrane	2

Table 3-4 (Cont'd)

(C6) N=27

MF			BP			CC		
Graph Level	**GO Term**	**#Seq**	**Graph Level**	**GO Term**	**#Seq**	**Graph Level**	**GO Term**	**#Seq**
4	cation binding	10	3	primary metabolic process	10	4	membrane	5
6	calcium ion binding	4	3	cellular metabolic process	6	3	cell part	7
5	metal ion binding	8	5	proteolysis	3	6	integral to membrane	2
7	zinc ion binding	3	3	biosynthetic process	4	5	intrinsic to membrane	2
3	ion binding	10	4	cellular biosynthetic process	3	5	cytoplasm	1
6	transition metal ion binding	4	8	glycosaminoglycan catabolic process	2	5	proteinaceous extracellular matrix	1
7	beta-N-acetylhexosaminidase activity	2	6	amino sugar metabolic process	2	8	transcription factor complex	1
4	pyridoxal phosphate binding	2	6	limb morphogenesis	2	4	membrane part	2
5	peptidase activity, acting on L-amino acid peptides	3	5	transmembrane transport	2	4	intracellular part	2
5	carboxy-lyase activity	2	8	globoside metabolic process	2	6	nucleoplasm part	1

(C7) N=21

MF			BP			CC		
Graph Level	**GO Term**	**#Seq**	**Graph Level**	**GO Term**	**#Seq**	**Graph Level**	**GO Term**	**#Seq**
6	calcium ion binding	3	6	serine family amino acid metabolic process	4	6	integral to membrane	3
7	ATP binding	3	3	cellular metabolic process	8	3	cell part	9
3	protein binding	3	5	cellular amino acid metabolic process	5	8	transcription factor complex	2
7	protein serine/threonine kinase activity	3	4	regulation of cellular process	6	3	protein complex	3
5	metal ion binding	3	5	cell cycle phase	3	5	intrinsic to membrane	3
5	sequence-specific DNA binding	2	7	protein amino acid phosphorylation	3	6	intracellular membrane-bounded organelle	4
5	kinase activity	4	3	primary metabolic process	7	4	intracellular	6
4	DNA binding	2	7	meiosis	2	4	membrane	4
6	adenyl ribonucleotide binding	3	5	signal transduction	3	5	intracellular organelle	5
3	signal transducer activity	2	6	M phase	3	7	nucleus	3

Table 3-4 (Cont'd)

(C8) N=12

MF			BP			CC		
Graph Level	**GO Term**	**#Seq**	**Graph Level**	**GO Term**	**#Seq**	**Graph Level**	**GO Term**	**#Seq**
3	transferase activity	4	3	oxidation reduction	2	4	membrane	2
3	oxidoreductase activity	2	5	proteolysis	2	3	cell part	3
6	serine-type endopeptidase activity	2	3	regulation of biological process	3	4	extracellular space	1
6	endopeptidase activity	2	4	protein metabolic process	3	8	transcription factor complex	1
5	serine-type peptidase activity	2	4	innate immune response	2	6	nucleoplasm part	1
8	protein tyrosine phosphatase activity	1	4	regulation of immune system process	2	3	protein complex	1
3	transcription factor activity	1	4	defense response	2	3	extracellular region part	1
3	protein binding	1	3	primary metabolic process	3	7	nuclear lumen	1
4	transferase activity, transferring glycosyl groups	1	7	protein amino acid dephosphorylation	1	6	intracellular organelle lumen	1
3	lipid binding	1	5	negative regulation of cellular process	1	4	intracellular organelle part	1

(C9) N=9

MF			BP			CC		
Graph Level	**GO Term**	**#Seq**	**Graph Level**	**GO Term**	**#Seq**	**Graph Level**	**GO Term**	**#Seq**
3	protein binding	2	3	cellular metabolic process	5	3	protein complex	2
3	nucleic acid binding	2	4	regulation of cellular process	1	5	cytoplasm	2
8	protein tyrosine phosphatase activity	1	5	cellular protein metabolic process	2	7	prefoldin complex	1
4	unfolded protein binding	1	7	protein amino acid dephosphorylation	1	8	transcription factor complex	1
6	aminoacyl-tRNA hydrolase activity	1	6	translation	1	4	intracellular part	2
4	chaperone binding	1	5	regulation of cell cycle	1	6	nucleoplasm part	1
4	iron-sulfur cluster binding	1	7	iron-sulfur cluster assembly	1	6	cytosolic part	1
3	nucleotide binding	1	6	tyrosine metabolic process	1	3	cell part	2
3	transcription factor activity	1	5	organ morphogenesis	1	4	intracellular	2
7	phosphoprotein phosphatase activity	1	9	regulation of transcription involved in G1/S-phase of mitotic cell cycle	1	6	cytosol	1

Table 3-4 (Cont'd)

(C10) N=8

MF			BP			CC		
Graph Level	**GO Term**	**#Seq**	**Graph Level**	**GO Term**	**#Seq**	**Graph Level**	**GO Term**	**#Seq**
4	cation binding	4	6	salivary gland cell autophagic cell death	1	7	nucleus	2
5	metal ion binding	3	7	regulation of transcription	1	5	cytoplasm	1
6	calcium ion binding	2	3	circadian rhythm	1	8	transcription factor complex	1
4	DNA binding	1	6	nucleotide catabolic process	1	5	plasma membrane	1
4	hydrolase activity, acting on ester bonds	1	7	mitosis	1	3	cell part	2
5	hydrolase activity, hydrolyzing O-glycosyl compounds	1	5	DNA endoreduplication	1	4	intracellular part	2
5	sequence-specific DNA binding	1	4	cell cycle process	1	6	intracellular membrane-bounded organelle	2
5	protein homodimerization activity	1	3	primary metabolic process	3	6	nucleoplasm part	1
3	nucleotide binding	1	5	nuclear division	1	4	membrane	1
3	transcription factor activity	1	6	regulation of nucleobase, nucleoside, nucleotide and nucleic acid metabolic process	1	3	protein complex	1

Figure 3-26. GPCRs and NT-gated ion channels. Twenty-seven putative receptors were identified as significantly up- or down-regulated during at least one stage of development. Provided is the list of *B. mori* genes (SilkDB), and their log_2fold expression profiles. All values represent fold-change relatative to HCS -30 hrs. **(A)** Red shade indicates significant up-regulation (>2-fold, $p<0.1$) and **(B)** blue shade indicates significant down-regulation (<0.5-fold, $p<0.1$). For each gene, log_2fold is ordered relative to the time of HCS, except for the early inter-molt stage (HCS -48hrs), which is shown last for comparison. Blast2go descriptions are provided. Also provided is a list of *Drosophila* orthologs (with FlyBase ID's and descriptions) when reciprocal blasting yielded positive results.

Figure 3-26

A

Gene ID	-18	-12	-6	HCS	18	-48	Sequence description (B2G)	*D. mel (RB)*	*D. melan.* description
BGIBMGA007240	2.7	3.2	3.3	2.5	5.9	1.0	neurotransmitter gated ion channel	CG7589	*no desc.*
BGIBMGA011935	1.0	1.8	2.4	0.5	1.4	0.0	g protein coupled receptor	*NRB*	*NA*
BGIBMGA008039	1.9	2.8	3.0	2.0	1.9	2.1	tachykinin receptor 1 (agap002824-pa)	CG6515	Tachykinin-like receptor
BGIBMGA011934	0.9	1.4	1.9	0.8	1.0	-0.9	g protein coupled receptor	*NRB*	*NA*
BGIBMGA002513	0.0	inf	inf	inf	inf	0.0	cg14257 cg14257- partial	CG14257	*no desc.*
BGIBMGA012465	0.3	0.5	0.2	2.0	2.1	1.3	viral a-type inclusion protein	*NRB*	*NA*
BGIBMGA005507	-0.6	-2.9	-2.2	-2.9	2.0	0.5	g protein-coupled receptor	*NRB*	*NA*
BGIBMGA011527	0.0	inf	0.0	0.0	inf	0.0	glutamate ionotropic kainate 2	*NRB*	*NA*
BGIBMGA000697	0.4	0.3	0.7	0.9	0.6	1.2	g-protein coupled receptor	CG18314	DopEcR
BGIBMGA002249	-0.1	0.1	-0.6	0.2	-0.3	1.1	class a rhodopsin-like GPCR	*NRB*	*NA*
BGIBMGA008273	0.9	1.2	-0.4	-1.2	-1.6	-0.6	dopamine invertebrate	*NRB*	*NA*

Figure 3-26 (Cont'd)

B

Gene ID	-18	-12	-6	HCS	18	-48	Sequence description (B2G)	*D. mel (RB)*	*D. melan.* description
BGIBMGA012730	-2.9	-Inf	-2.5	-3.2	-Inf	-1.3	hypocretin receptor 1	*NRB*	*NA*
BGIBMGA010037	-0.6	-1.4	-1.5	0.1	-0.3	-0.3	prostaglandin e2 receptor ep4 subtype	CG7497	*no desc.*
BGIBMGA002442	-1.0	-0.6	-2.9	-0.7	-1.0	0.0	neuropeptide y receptor (npy-r) (pr4 rec)	*NRB*	*NA*
BGIBMGA006593	-0.6	-1.1	-0.7	-1.7	0.1	0.1	adenosine receptor	*NRB*	*NA*
BGIBMGA006596	-0.8	-0.2	-1.3	-1.7	0.4	-0.2	adenosine a2 receptor	CG9753	Adenosine receptor
BGIBMGA011918	-0.2	-0.8	-1.1	-1.4	-0.6	0.1	g-protein coupled receptor	CG12796	*no desc.*
BGIBMGA008802	-0.6	-1.0	-0.8	-0.3	-0.7	0.0	bombesin receptor subtype-3	CG14593	CCHamide-2 receptor
BGIBMGA009039	-0.1	-1.3	-0.8	0.4	-0.4	-0.7	bombesin receptor subtype-3	CG30106	CCHamide-1 receptor
BGIBMGA009470	-0.4	-2.3	-0.5	0.2	-0.7	-0.4	glutamate ionotropic kainate 3 (glur7)	*NRB*	*NA*
BGIBMGA006361	-2.1	0.7	0.5	0.1	-0.1	0.9	neuropeptide receptor a33	*NRB*	*NA*
BGIBMGA000843	-0.6	-0.4	-0.8	-1.7	-0.3	-0.2	neurotransmitter gated ion channel	CG12344	*no desc.*
BGIBMGA001531	0.5	0.0	0.3	-2.4	-0.4	0.2	corazonin receptor	CG10698	GRHRII
BGIBMGA003036	-0.3	-0.4	-0.7	-1.1	-0.4	-0.4	isoform c	CG31660	poor gastrulation
BGIBMGA004625	-0.3	-0.2	-0.4	-1.2	-0.1	0.0	metabotropic glutamate receptor 4	CG31116	Chloride channel-a
BGIBMGA009499	-1.2	-1.0	-0.5	-0.1	-Inf	0.4	neuropeptide receptor a27	*NRB*	*NA*
BGIBMGA007492	0.1	-0.1	0.0	-0.5	-0.1	-1.1	class d atypical GPCR	*NRB*	*NA*

Figure 3-27. Neurotransmitter and neuropeptide systems. 14 differentially-expressed genes were identified as coding for either peptide neurotransmitters or enzymes associated with neurotransmitter metabolic pathways. Provided is the list of *B. mori* genes (SilkDB), and their log_2fold expression profiles. All values represent fold-change relatative to HCS -30 hrs. **(A)** Red shade indicates significant up-regulation (>2-fold, $p<0.1$) and **(B)** blue shade indicates significant down-regulation (<0.5-fold, $p<0.1$). For each gene, log_2fold is ordered relative to the time of HCS, except for the early inter-molt stage (HCS -48 hrs), which is shown last for comparison. Blast2go descriptions are provided. Also provided is a list of *Drosophila* orthologs (with FlyBase ID's and descriptions) when reciprocal blasting yielded positive results.

Figure 3-27

A

Gene ID	-18	-12	-6	HCS	18	-48	Sequence description (B2G)	*D. mel (RB)*	*D. melan.* description
BGIBMGA002077	0.7	1.3	1.7	1.9	2.6	-0.3	tan	CG12120	tan
BGIBMGA011086	inf	inf	inf	inf	inf	inf	partner of burs	CG15284	partner of burs
BGIBMGA002958	-0.2	-0.5	-0.5	1.1	1.1	0.4	aromatic amino acid decarboxylase	CG10697	Dopa decarboxylase
BGIBMGA003199	-0.2	-0.3	-0.2	1.1	1.4	0.6	dopa decarboxylase protein	CG10697	Dopa decarboxylase
BGIBMGA010779	-0.2	-0.4	-1.1	4.1	3.9	-0.5	domon domain-containing protein	CG14681	*no desc.*
BGIBMGA002971	0.4	0.6	0.9	1.1	0.2	0.4	zinc transporter	CG10449	Catecholamines up
BGIBMGA011926	Inf	Inf	Inf	Inf	Inf	Inf	bombyxin c-1 precursor	*NRB*	*NA*
BGIBMGA013957	-0.1	0.1	0.5	1.0	3.8	-0.2	moxd1-like protein 2	CG12781	nahoda
BGIBMGA003762	0.8	0.2	0.8	-0.4	0.2	1.2	n-acetylserotonin o-methyltransferase-lik	CG9515	*no desc.*

B

Gene ID	-18.0	-12.0	-6.0	HCS	18.0	-48.0	Sequence description (B2G)	*D. mel (RB)*	*D. melan.* description
BGIBMGA002938	-0.4	-0.7	-1.0	-1.8	0.1	0.5	nitric oxide synthase	*NRB*	*NA*
BGIBMGA008538	-0.5	-0.9	-1.7	-3.1	-0.6	0.0	arylalkylamine n-acetyltransferase	CG3318	Dopamine N acetyltransferase
BGIBMGA001235	-0.6	-0.5	-1.2	-1.7	-0.2	-0.1	gtp cyclohydrolase i isoform a	CG9441	Punch
BGIBMGA002922	-0.3	-0.7	-1.0	0.2	-0.3	-0.1	white	CG2759	white
BGIBMGA001149	0.7	-Inf	-1.0	-0.8	-1.0	-2.0	yellow protein	CG3757	yellow

Figure 3-28. Dopamine (DA)-related metabolic pathways. Shown are the metabolic pathways leading to DA neurotransmitter synthesis, melanin and sclerotization (adapted from True 2003). Differentially expressed genes are labeled in red (up-regulated) and blue (down-regulated). Names for *Drosophila* orthologs (verified using reciprocal blasts) are used to identify the genes. Actual expression levels (relative to developmental timing) are shown in Figure 3-27.

Figure 3-28

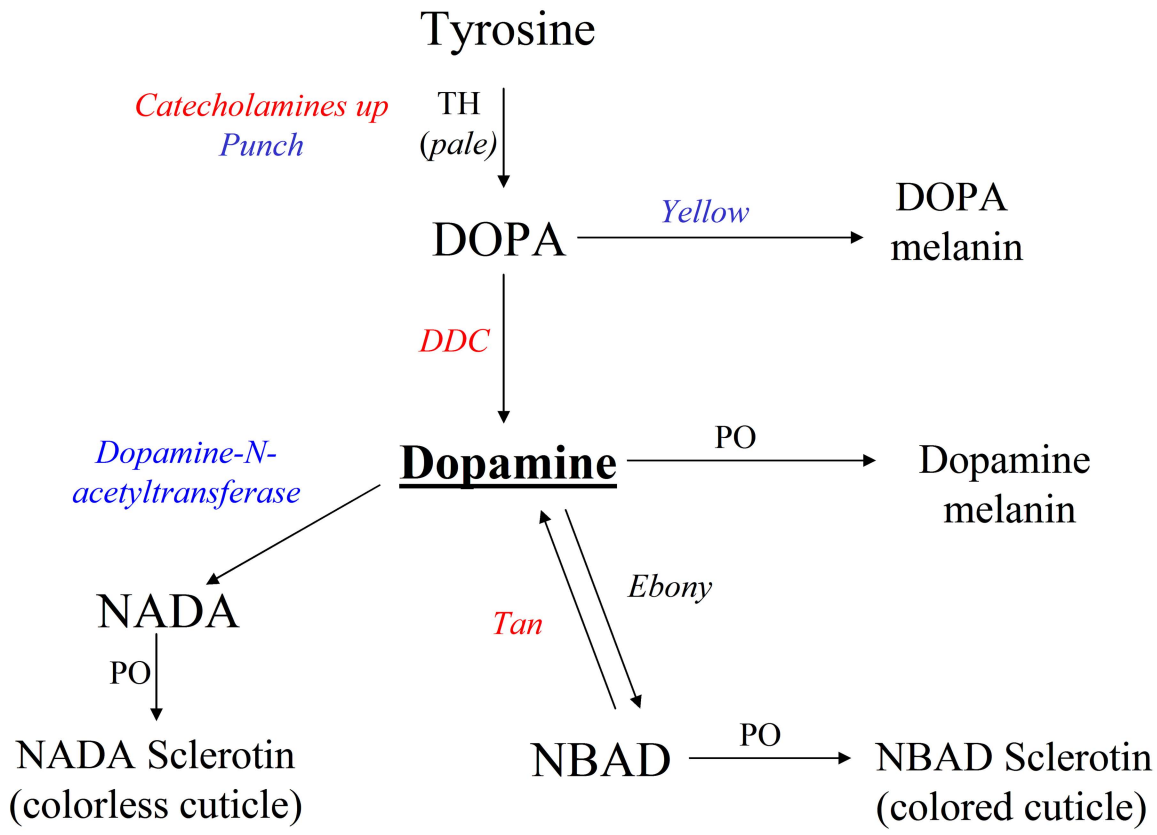
Tyrosine
Catecholamines up
Punch
TH
(pale)
DOPA
Yellow
DOPA
melanin
DDC
Dopamine-N-
acetyltransferase
Dopamine
PO
Dopamine
melanin
NADA
Tan
Ebony
PO
NADA Sclerotin
(colorless cuticle)
NBAD
PO
NBAD Sclerotin
(colored cuticle)

Figure 3-29. Ion channels and ion channel regulators. 14 differentially-expressed genes were identified as coding for either ion channels or ion channel-regulating proteins. Provided is the list of *B. mori* genes (SilkDB) and their log_2fold expression profiles. All values represent fold-change relative to HCS -30hrs. **(A)** Red shade indicates significant up-regulation (>2-fold, $p<0.1$) and **(B)** blue shade indicates significant down-regulation (<0.5-fold, $p<0.1$). For each gene, log_2fold is ordered relative to the time of HCS, except for the early inter-molt stage (HCS -48 hrs), which is shown last for comparison. Blast2go descriptions are provided. Also provided is a list of *Drosophila* orthologs (with FlyBase ID's and descriptions) when reciprocal blasting yielded positive results.

Figure 3-29

A

Gene ID	-18	-12	-6	HCS	18	-48	Sequence description (B2G)	*D. mel (RB)*	*D. melan.* description
BGIBMGA003640	0.3	0.6	1.1	1.3	-0.1	0.2	dihydropyridine-sensitive l-type ca2+ ch.	CG12295	straightjacket
BGIBMGA002286	0.4	0.3	0.9	1.9	1.5	1.1	t family of potassium channels protein	CG34396	*no desc.*
BGIBMGA001166	0.4	0.4	0.7	1.5	0.8	0.6	transient rec. pot. cation channel painless	CG15860	painless
BGIBMGA000577	0.0	0.2	-0.1	-0.1	2.2	0.3	cyclic-nucleotide-gated cation channel	CG7779	Cyclic-nucleotide-gated ion channel protein
BGIBMGA002131	-0.2	-0.1	-0.9	-0.8	-0.3	1.1	transient receptor potential isoform f	CG5751	Transient receptor potential A1
BGIBMGA007008	0.0	1.0	1.0	0.2	-0.4	1.5	voltage-dependent t-type calcium chan.	*NRB*	*NA*
BGIBMGA009560	0.5	-0.1	-0.3	0.3	-0.1	1.0	potassium channel interacting protein	*NRB*	*NA*

B

Gene ID	-18	-12	-6	HCS	18	-48	Sequence description (B2G)	*D. mel (RB)*	*D. melan.* description
BGIBMGA013345	-1.4	-0.4	-0.5	-0.2	-2.2	0.4	ca	*NRB*	*NA*
BGIBMGA013356	-0.8	-0.5	-1.7	-1.4	-0.5	-0.6	voltage-gated potassium channel	*NRB*	*NA*
BGIBMGA001881	0.0	-0.5	-1.1	-0.9	0.1	0.1	potassium sodium hyperpolarization-activated cyclic nucleotide-gated channel	*NRB*	*NA*
BGIBMGA007070	-0.1	0.2	0.2	-1.3	-1.4	0.1	inwardly rectifying k+	CG4370	Inwardly rectifying potassium channel 2
BGIBMGA001376	-0.3	-0.1	-0.9	-1.4	-0.3	-0.5	protein quiver ame: full=protein sleepless	CG33472	quiver
BGIBMGA008375	-0.7	-0.4	-1.0	-2.3	-1.4	0.1	open rectifier k	CG1615	Open rectifier K+ channel
BGIBMGA014186	-0.7	-1.0	-0.8	-2.7	-0.5	0.2	transient receptor potential chan. pyrexia	CG17142	*NA*

Figure 3-30. Epidermal growth factor (EGF) and insulin signaling. 9 differentially-expressed genes were identified as coding for proteins annotated with descriptions and/or GO terminologies relating them to EGF or insulin signaling. Provided is the list of *B. mori* genes (SilkDB) and their log_2fold expression profiles. All values represent fold-change relative to HCS -30 hrs. **(A)** Red shade indicates significant up-regulation (>2-fold, $p<0.1$) and **(B)** blue shade indicates significant down-regulation (<0.5-fold, $p<0.1$). For each gene, log_2fold is ordered relative to the time of HCS, except for the early inter-molt stage (HCS -48 hrs), which is shown last for comparison. Blast2go descriptions are provided. Also provided is a list of *Drosophila* orthologs (with FlyBase ID's and descriptions) when reciprocal blasting yielded positive results.

Figure 3-30

A

Gene ID	-18	-12	-6	HCS	18	-48	Sequence description (B2G)	*D. mel (RB)*	*D. melan.* description
BGIBMGA008174	0.9	2.6	2.6	2.9	2.2	1.1	insulin-related peptide binding protein	CG15009	Ecdysone-inducible gene L2
BGIBMGA004550	0.4	0.9	1.1	1.2	-0.6	-0.5	epidermal growth factor receptor kinase substrate 8	CG4276	arouser
BGIBMGA007045	-0.6	0.2	0.8	2.0	0.0	0.1	insulin receptor tyrosine kinase substrate	CG32082	*no desc.*
BGIBMGA002855	-Inf	1.9	-Inf	3.2	-Inf	-Inf	protein rhomboid	CG17212	rhomboid-6
BGIBMGA004551	-Inf	1.3	2.3	1.6	-Inf	0.0	epidermal growth factor receptor kinase substrate 8	*NRB*	*NA*
BGIBMGA006209	0.3	0.7	0.8	1.2	-0.1	-0.2	sec61 protein translocation complex beta subunit	CG10130	Sec61β
BGIBMGA011926	Inf	Inf	Inf	Inf	Inf	Inf	bombyxin c-1 precursor	*NRB*	*NA*

B

Gene ID	-18	-12	-6	HCS	18	-48	Sequence description (B2G)	*D. mel (RB)*	*D. melan.* description
BGIBMGA010766	-1.3	-0.4	-1.6	-1.9	-0.2	-2.4	protein star	CG4385	Star
BGIBMGA011826	-0.5	-0.1	-0.4	-1.5	-0.6	-0.4	ataxin 1-like	CG4547	Ataxin 1

Figure 3-31. Enrichment analysis of overlapping gene sets: an across-species comparison. A comparison was made between differentially expressed genes in our study with differentially expressed genes in a microarray-based study that examined the transcriptome of *B. mori* brains during pupal development (Gan *et al*., 2011). 231 genes overlapped between studies, and the 161 successfully annotated genes were used for enrichment analysis using the GOSSIP package integrated into BLAST2GO (Fisher's Exact Test corrected for multiple testing, $p<0.05$). 10 enriched GO categories were detected, and they are listed in the order of significance.

Figure 3-31

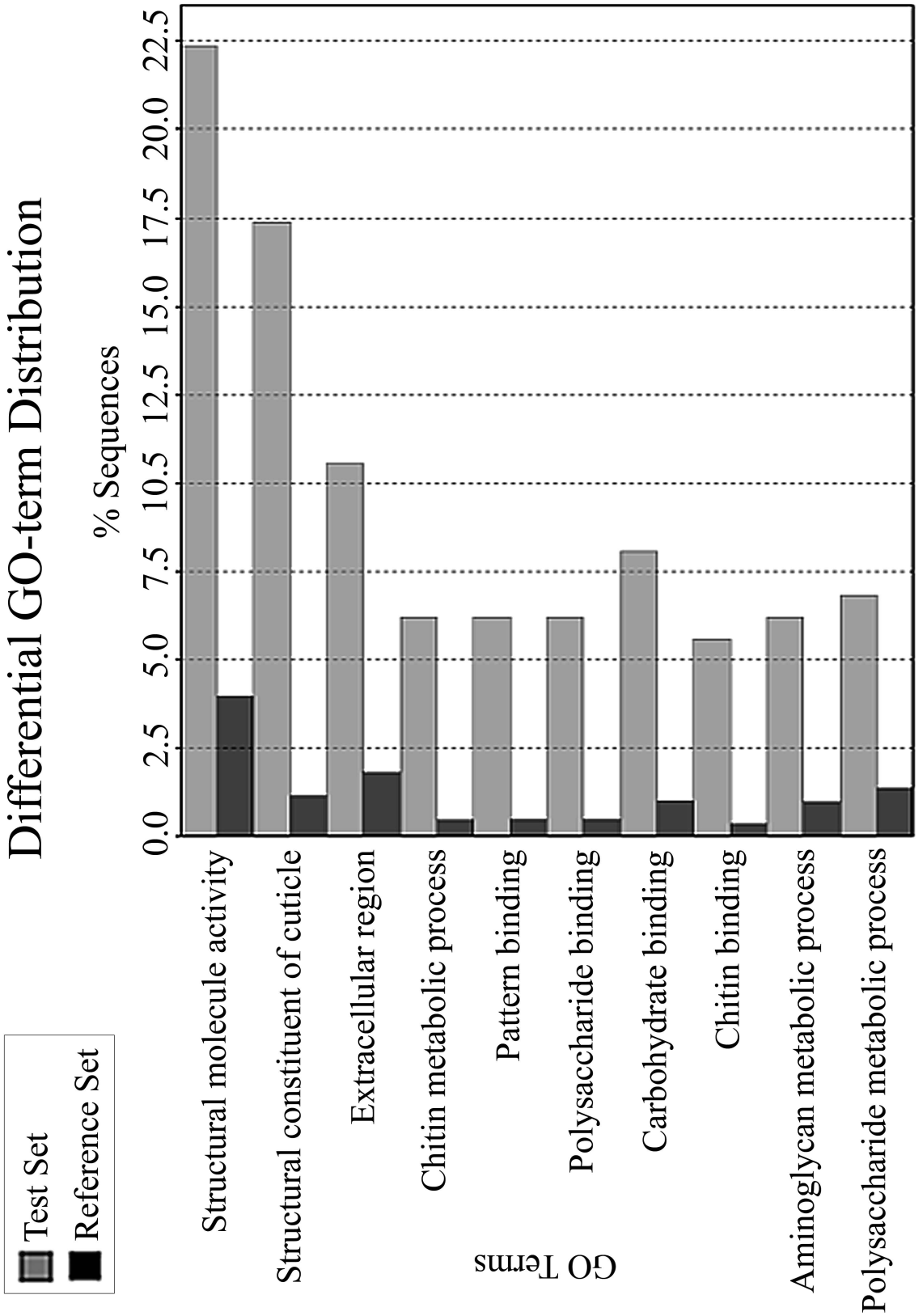
Differential GO-term Distribution
% Sequences
0.0
2.5
5.0
7.5
10.5
12.5
15.0
17.5
20.0
22.5
Test Set
Reference Set
Structural molecule activity
Structural constituent of cuticle
Extracellular region
Chitin metabolic process
Pattern binding
Polysaccharide binding
Carbohydrate binding
Chitin binding
Aminoglycan metabolic process
Polysaccharide metabolic process
GO Terms

Concluding Remarks

Although it has long been known that the larval behavioral repertoire of *Manduca sexta* includes a significant amount of behavioral quiescence, our study is the first to characterize this behavior. Quiescence is accompanied by increased arousal thresholds and is rapidly-reversible during both the intermolt and molting periods, thereby resembling sleep-like states of adult insects. An unexpected finding was that molting larvae are able to retain the ability to locomote and to respond to noxious stimuli in a way that is very similar to that observed for feeding-stage larvae. We propose that the presence of rapidly-reversible reduced responsiveness during prolonged molting periods confers a selective advantage in the natural environment. Apolysis is accompanied by morphological changes that for the duration of the molt-sleep prevent ingestion of food. Decreased behavioral drive coupled with retention of the ability to respond to a changing environment would both conserve energy and allow for protection from threatening conditions, thereby increasing viability.

Deprivation of quiescence during the molt was not followed by quiescence-rebound and did not alter developmental timing, and activity levels were normal for intermolt larvae that were deprived of quiescence during the preceding molting period. But long-term effects of quiescence deprivation during the molt on development and nervous system function were not addressed in this study. For now, the function of the molt-sleep seems to be a purely behavioral one, at least during the larval stage transitions. This contrasts with the robust quiescence rebound that follows deprivation during the inter-molt feeding period. One possible interpretation of these observations is that

functional circuitries or metabolic processes for which sleep during the feeding stage is important are either shut down or not engaged during the molt-sleep period.

The correlation of molt-sleep onset with the predicted peak of molting hormones suggests either direct or indirect actions of steroid hormones. Illumina sequencing of the brain transcriptome demonstrates differential-expression of hundreds of genes prior to and during onset of the molt-sleep. Many identified transcripts are associated with neurotransmitter systems, ion channels and other gene products that might potentially underlie the modulation of larval arousal state. Whether or not ecdsyteroids are acting peripherally or centrally to bring about these changes awaits future studies that test the effects of hormones on isolated nervous systems. It will also be important to expand transcriptome profiling to include other regions of the CNS, such as the subesophageal, thoracic and abdominal ganglia. In this study, we were limited to the time-course study of one tissue, and we chose to profile the larval brain (supraesophageal ganglion) due to the presence of structures implicated in the modulation of sleep-wake arousal in the adult fly. However, control of behavior and processing of sensory information are distributed in other areas of the nervous system such as the subesophageal ganglion, for example, which is a control center important for generation of feeding behavior and locomotion. Division of labor between different ganglia likely reflects across-ganglion differences in gene expression, in which a particular gene may be up-regulated in one ganglion while simultaneously down-regulated in another. Therefore, separate profiling of different ganglia is important so as to not obscure detection of differentially-expressed genes. Future studies might also include the separate profiling of different brain regions.

Successful profiling of the *M. sexta* brain transcriptome demonstrates the usefulness of RNA-seq technology in the study of organisms for which a genome is not known. One barrier that confronts many biologists who might want to take advantage of these high throughput technologies is the requirement of a strong background in computer programming and bioinformatics. Researchers who might benefit from techniques such as Illumina sequencing may not have access to the type of expertise required for the initial processing and subsequent downstream analysis of this type of data. At present, the number of institutions and companies that offer services such as Illumina sequencing is expanding. As next-generation technologies become increasingly available, new user-friendly analysis programs such as BLAST2GO are also likely to become more available, enabling biologists working on non-model organisms to use these high-throughput technologies to generate and to test new hypotheses.

Appendix

Partial cloning of a putative *Manduca sexta* dopamine *D2-like* receptor

Degenerate primers were designed from regions of high homology using a ClustalX (www.clustal.org) alignment of previously identified insect D2-like dopamine receptors (*Drosophila melanogaster, Apis mellifera, Bombyx mori,* and *Triboleum castaneum*) (Banks 2010). Nested PCR with two sets of primers was used to eliminate nonspecific DNA fragments amplified with the degenerate primers. The following degenerate primers were used for PCR, round-1: 5´-GTNTAYTTYCARGTNAAYGG-3´, and 5´-TCNGGRTTRAADATNGTRTA, and the cycling parameters were 1x 3min@95°C, 40x (20sec@95°C, 20sec@gradient 40-50°C, 1min@72°C), 1x 10min@72°C). The following degenerate primers were used for PCR, round-2: 5´-ATHTTYAAYYTIGTNGCNAT-3´, and 5´-TCNGGRTTRAADATNGTRTA-3´, with cycling parameters 1x 3min@95°C, 15x (20sec@95°C, 20sec@60°C, 1min@72°C), 25x (20sec@95°C, 20sec@45°C, 1min@72°C), 1x 10min@72°C. PCR products were run on a 1% agarose gel w/ ethidium bromide and compared to standards (1kb plus; Invitrogen). For PCR reactions that showed a specific ~1kb band, the remaining product was purified using QuickClean 5M Purification Kit (GenScript) and submitted for Sanger (BigDye) sequencing (Applied Biosystems) at the Genomics Core of the University of California, Riverside. The identity of the resulting 1012 base pair (bp) nucleotide sequence was confirmed using BLASTx alignment against protein sequences in the Genbank and Silkworm Genome databases. The nucleotide and amino acid sequences are provided in

Appendix Figure-1A/B. ClustalX aligments of the translated amino acid sequences to the known D2-like receptor sequences from other insects is shown in Appendix Figure-2A/B.

Appendix Figure A1. Putative *M. sexta* D2-like dopamine receptor. Shown are **(A)** the partial (1012 bp) nucleotide sequence, and **(B)** the partial amino acid (B) sequence of a putative *M. sexta* D2-like dopamine receptor.

Appendix Figure A-1

Appendix Figure A2. ClustalX boxshade alignments of the partial putative *M. sexta* D2-like dopamine receptor with known D2-like sequences from other insect species. (A) Blastx alignments in SilkDB and GeneBank using default parameters show top hits and high sequence similarities to other D2-like receptors: *Bombyx mori* (SilkDB protein ID BGIBMGA008272; Identities=78%, Expect=e-147), *Drosophila melanogaster* (GeneBank Accession NP 001014759.1; Identities=51%, Expect=e-64), *Anopheles gambia* (GeneBank Accession XP 313744.3; Identities=54%, Expect=e-68). *Apis mellifera* (GeneBank Accession NP 001014983.1; Identities=51%, Expect=e-54). **(B)** Clustalx boxshade aligment of *M. sexta* and *B. mori* (BGIBMGA008282) sequence.

Appendix Figure A-2